

SEISMIC STABILITY EVALUATIONS OF CHESBRO, LENIHAN, STEVENS CREEK, AND UVAS DAMS (SSE2)

PHASE A: STEVENS CREEK AND LENIHAN DAMS

LENIHAN DAM

ENGINEERING ANALYSES (REPORT No. LN-4)

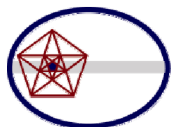
Prepared for

SANTA CLARA VALLEY WATER DISTRICT

5750 Almaden Expressway

San Jose, CA 95118

November 2012



TERRA / GeoPentech
a Joint Venture

TABLE OF CONTENTS

SECTION 1	INTRODUCTION	1-1
1.1	General.....	1-1
1.2	Purpose and Scope of Engineering Analyses.....	1-1
1.3	Organization of Document.....	1-2
SECTION 2	SUMMARY OF SITE CHARACTERIZATION	2-1
2.1	General.....	2-1
2.2	Geometry of Dam Embankment and Dam Foundation	2-1
2.2.1	Dam Embankment	2-1
2.2.2	Dam Foundation	2-2
2.3	Physical and Index Properties of Embankment Materials	2-2
2.4	Engineering Properties of Embankment Materials	2-3
2.5	Ground Motions	2-4
SECTION 3	SEEPAGE ANALYSES.....	3-1
3.1	General.....	3-1
3.2	Piezometer Measurements at Lenihan Dam	3-2
3.3	Results of Seepage Analyses	3-2
3.3.1	Section Chosen for Analyses	3-2
3.3.2	Results of Analyses for Section F-F'.....	3-3
SECTION 4	STATIC STABILITY AND PSEUDO-STATIC YIELD ACCELERATION	4-1
4.1	General.....	4-1
4.2	Input Parameters	4-1
4.3	Results of Analyses.....	4-2
SECTION 5	SEISMIC DEFORMATION ANALYSES.....	5-1
5.1	General.....	5-1
5.2	Analysis Methodology	5-1
5.2.1	Overview.....	5-1
5.2.2	Analysis Platform and Soil Model.....	5-1
5.3	Analysis Section, Pore Pressures, and Discretization	5-2
5.3.1	Analysis Section	5-2
5.3.2	Pore Pressures.....	5-3
5.3.3	Discretization of Analysis Section.....	5-3
5.4	Material Properties.....	5-3
5.4.1	Material Properties.....	5-3
5.5	Loma Prieta and MCE Ground Motions	5-4
5.6	Loma Prieta Case History	5-5
5.6.1	Loma Prieta Event at the Site	5-5
5.6.2	Key Results from Loma Prieta Case History Analysis	5-5
5.6.3	Summary of Loma Prieta Case History	5-7
5.7	Seismic Deformation Evaluation under MCE Ground Motions	5-7
5.7.1	Results of Seismic Deformation Analyses.....	5-7
5.7.2	Evaluation of Cracking Potential	5-10

TABLE OF CONTENTS

SECTION 6	SUMMARY AND CONCLUSIONS	6-1
6.1	General	6-1
6.2	Site Characterization, Material Properties and Monitoring Data.....	6-1
6.3	Seepage Analyses.....	6-1
6.4	Static Stability and Pseudo-Static Yield Accelerations	6-2
6.5	Seismic Deformation Analyses.....	6-2
6.6	Conclusions.....	6-3
6.7	Recommendations.....	6-3
SECTION 7	REFERENCES	7-1

Tables

2-1	Material Classification Summary
2-2	Summary of Engineering Properties
2-3	Results of Permeability Tests
3-1	Summary of Permeability Values
5-1	Summary of Engineering Properties used in Analyses
5-2A	Characteristics of Selected Earthquake Records for Stanford-Monte Vista Event
5-2B	Characteristics of Selected Earthquake Records for San Andreas Event
5-3	Summary of Calculated Deformations

Figures

2-1	Regional Site Location Map
2-2	Footprint and Section Locations
2-3	Cross-Sections A-A' and B-B'
2-4	Three-Dimensional View of Foundation Surface
2-5	Cross-Sections with Foundation Surface
2-6	Maximum Cross Section B-B'
2-7	Modulus Reduction and Damping Ratio Curves
2-8	Characteristics of Kobe E/Q, Nishi-Akashi (FN) Matched Record
2-9	Characteristics of Loma Prieta E/Q, LGPC (FN) Matched Record
2-10	Characteristics of Northridge E/Q, Sylmar (FN) Matched Record
2-11	Characteristics of Manjil E/Q, Abbar (FN) Matched Record
2-12	Characteristics of Chi Chi E/Q, TCU065 (FN) Matched Record

TABLE OF CONTENTS

2-13	Characteristics of Landers E/Q, Lucerne (FN) Matched Record
3-1	Partial Plan Showing Locations of Existing Piezometers
3-2	Sections A-A' and B-B' with Measured Piezometric Levels
3-3	Section F-F' with Measured Piezometric Levels
3-4	Comparison of Measured to Modeled Total Heads, Section F-F'
4-1	Pore Pressures at Full Reservoir Level
4-2	Computed Undrained Shear Strength
4-3	Static FS and Pseudo-Static Yield Acceleration
5-1	Idealized Section and FLAC Discretized Mesh
5-2	Comparison of Modulus Reduction and Damping Ratio Curves
5-3	FLAC Input Motion – Loma Prieta Earthquake
5-4	Response Spectra for Evaluation Motions – SA & SMV
5-5	Loma Prieta Damage Map
5-6A	Comparison of Response Spectra at Dam Crest
5-6B	Comparison of Computed and Measured Response
5-7	Loma Prieta Event - Displacement Contours
5-8	Comparison of Computed Response Spectra at Crest
5-9	Comparison of SA, SMV and LPE Response Spectra
5-10	Case SA2-Landers, FLAC and QUAD4MU Response Spectra
5-11	Case SA2-Landers, Displacement Contours
5-12	Case SA2-Landers, Displacement Vectors
5-13	Case SA2-Landers, Shear Strain Contours
5-14	Case SA2-Landers, Deformation Time History
5-15	Results of Full Newmark Analysis
5-16	Horizontal Stretching of Upstream Embankment

Appendices

A	Loma Prieta Case History
B	Detailed Results of FLAC Analyses

1.1 GENERAL

In May 2010, the Santa Clara Valley Water District (District) retained Terra / GeoPentech (TGP), a joint venture of Terra Engineers, Inc. and GeoPentech, Inc., to complete seismic stability evaluations of Chesbro, Lenihan, Stevens Creek and Uvas Dams. These evaluations were required by the Division of Safety of Dams (DSOD) in June 2008 as part of their Phase III screening process of the State's dams located in highly seismic environments. The evaluations are also a vital part of the District's Dam Safety Program (DSP). Phase A of the project includes work on Stevens Creek and Lenihan Dams and has a planned completion date of 2012. Phase B of the project includes work on Chesbro and Uvas Dams and is scheduled to begin in 2012 and to finish by the end of 2013. The general scope of the project consists of the field, laboratory, and office studies required to evaluate the seismic stability of the four referenced dams.

This document contains the results of our engineering analyses at James J. Lenihan Dam (Lenihan Dam) based on the results of our site characterization at the dam that is documented in Report No. LN-3 (Terra/GeoPentech, 2011b). A summary of the relevant information contained in Report No. LN-3 is included hereinafter for completeness but the reader should refer the referenced report for details of the site characterization, material properties, and site-specific ground motions.

1.2 PURPOSE AND SCOPE OF ENGINEERING ANALYSES

The purpose of the engineering analyses is to evaluate the seismic stability of the dam during the Maximum Credible Earthquake (MCE) and assess the seismic deformations of the structure as a result of the MCE. To that end, the scope of the analyses included the following:

1. seepage analyses to establish total heads and pore-water pressures associated with steady state seepage;
2. static and pseudo-static stability analyses; and
3. non-linear dynamic analyses of seismic deformations.

In addition to the evaluation of the seismic response of the dam to the MCE, the non-linear deformation analyses also included an evaluation of the seismic performance of the dam during the Loma Prieta earthquake of 1989 using the motion recorded at the left abutment of the dam as the input ground motion. A preliminary evaluation of the dam during this event was completed before the additional investigations for the primary purpose of identifying data gaps and supporting the work plan for additional site investigations and laboratory testing (Terra/GeoPentech, 2011a). The performance of the dam during the Loma Prieta earthquake was re-analyzed as part of the study presented herein using the material properties established during the site characterization effort. The Loma Prieta event provides an opportunity to assess the reasonableness of the results of the seismic evaluation during the MCE based on the quantitative and observational seismic performance data collected at the dam during and after the Loma Prieta event.

1.3 ORGANIZATION OF DOCUMENT

This document contains seven sections, including this introduction. Section 2.0 provides a summary of the relevant information derived from the site characterization effort documented in Report No. LN-3. Section 3.0 documents the results of the seepage analyses and Section 4.0 presents the results of the static stability analyses and the pseudo-static yield accelerations. Section 5.0 describes the methodology used in the seismic deformation analyses and discusses the results of these analyses. Section 6.0 provides a summary of the key findings of the seismic stability evaluation of the dam and conclusions. Section 7.0 is a list of references.

There are two appendices to the report. Appendix A contains the results of the evaluation of the dam during the Loma Prieta earthquake and Appendix B contains details of the results of the non-linear seismic deformations analyses.

2.1 GENERAL

This section provides a summary of the information and data contained in Report No. LN-3 on Site Characterization, Material Properties, and Ground Motions (Terra/GeoPentech, 2011b) that are most relevant to the engineering analyses of the dam. This summary is included herein for completeness and ease of reference but the reader is referred to Report No. LN-3 for additional details.

Lenihan Dam is located in Santa Clara County, California, about 1 mile south of the City of Los Gatos, as shown on Figure 2-1. The dam is an earthfill structure that was constructed across Los Gatos Creek in 1952. The dam impounds Lexington Reservoir, which has a maximum capacity of 19,044 acre-feet at the spillway elevation of 653 feet¹.

Appurtenant structures include a concrete-lined ogee type spillway located in the left abutment and an outlet tunnel through the right abutment connected to an inclined inlet structure in the reservoir, on the upstream side of the right abutment, and to an outlet structure that allows reservoir water to discharge into Los Gatos Creek approximately 150 feet beyond the toe of the dam. The outlet tunnel and inclined inlet structure were completed in 2009 and replaced the original outlet pipe that generally followed the preconstruction thalweg of Los Gatos Creek beneath the dam. The original outlet pipe was filled with grout and abandoned in place in 2009.

2.2 GEOMETRY OF DAM EMBANKMENT AND DAM FOUNDATION

2.2.1 Dam Embankment

Figure 2-2 is an aerial photograph of Lenihan Dam that shows the outline of the embankment, and the locations of two transverse sections (at Stations 14+10 and 15+95) that are representative of dam zoning and conditions near the center of the valley. The sections are shown on Figure 2-3. Lenihan Dam was constructed as a compacted earth dam with upstream and downstream shells, core and drainage zones. The core is further divided into the upper core and lower core to reflect significant differences in material properties above and below elevation 590 feet. The dam is about 195 feet high as measured from the lowest point in the foundation beneath the axis to the crest, and about 207 feet high as measured from the lowest point of the downstream toe to the crest.

Following the Loma Prieta Earthquake, it was determined that the crest of the dam had settled about 2.3 feet since construction because of a combination of long-term consolidation and seismically-induced deformation from the earthquake. The crest was subsequently raised by up to 4.5 feet, and the spillway chute walls raised by up to 6 feet, during the 1996-1997 freeboard restoration project. Thus, the crest is currently at nominal elevation 673 feet and is about 40 feet wide, 830 feet long, and cambered. In general, the upstream face is inclined at 5.25 to 5.5 Horizontal to 1 Vertical (5.25 to 5.5H:1V). The downstream slope is inclined at 2.5 to 3H:1V. The concrete-lined, un-gated ogee crest spillway is located on the left abutment, with a nominal spillway crest elevation of 653 feet.

¹ Unless otherwise noted in this document, all elevations are referenced to NAVD88 vertical datum.

2.2.2 Dam Foundation

Lenihan Dam was constructed on Franciscan Complex bedrock, without a foundation seepage cutoff or grout curtain. Regional geologic mapping by the USGS (McLaughlin et al, 2001) shows the majority of the dam site being underlain by Franciscan mélange, with an area of more massive sandstone occurring at the upper end of the spillway and under the left upstream side of the dam. The mélange typically consists of intensely fractured to crushed shale that encases blocks of harder sandstone and greenstone, some of which are up to several hundred feet in length, with lesser blocks of serpentinite and chert. The area of more massive sandstone that occurs at the upper end of the spillway on the left abutment includes some interbedded shale.

Our detailed review of a number of maps and reports documenting the conditions in the foundation area that existed prior, during, and after construction of the dam, led us to the conclusion that, for all practical purposes, the compacted dam embankment is founded directly on bedrock and that no alluvium or colluvium soils are present beneath the dam. However, the rock surface on which the dam is founded is complex.

Figure 2-4 provides a three-dimensional perspective as shaded relief of that bedrock surface. The right side of the valley has a typical, relatively uniform slope but there is a massive rock knob under the upstream portion of the embankment on the left side of the valley. This irregular geometry is further illustrated by the cross-sections contained in Figure 2-5.

The results of in-situ permeability (packer) tests performed in the rock foundation by a number of investigators (RLVA, 1999a and 1999b; Frame and Volpe, 2001; and Geomatrix, 2006) indicate that the calculated permeability of the rock ranged from 0 (i.e., no flow) to 4.7×10^{-4} cm/sec. Our review of these data (including the field test data sheets) led us to conclude that 10^{-6} cm/sec or less probably represents a typical permeability coefficient for the sheared shale mélange matrix comprising significant portions of the foundation. For the most part, the higher calculated permeability coefficients (up to about 10^{-4} cm/sec) occurred within masses of harder and shallower rock (e.g., sandstone, greenstone, etc.) that are more likely to be open fractured, with an attendant higher hydraulic conductivity than the sheared mélange matrix (crushed shale) surrounding the blocks.

2.3 PHYSICAL AND INDEX PROPERTIES OF EMBANKMENT MATERIALS

As noted in Section 2.2.1, Lenihan Dam was constructed as an earthfill embankment consisting of various zones. Figure 2-6 is a generalized configuration of the dam through the maximum section (section B-B' on Figure 2-2) including the idealized limits of each zone based on construction records. These zones consist of the following:

- Zone 1 – Upstream Shell;
- Zone 2U – Upper Core;
- Zone 2L – Lower Core;
- Zone 3 – Drain; and
- Zone 4 – Downstream Shell.

The predominant soil classifications for each of the zones are also listed on Figure 2-6. Table 2-1 is a summary of the material classification and index properties.

The upstream shell and upper core materials were obtained from the Franciscan Complex mélange just upstream of the upstream toe of the dam and their physical/index properties are similar. These materials are generally classified as gravelly clayey sand (SC) to sandy clays (CL) (for the upstream shell) and gravelly clayey sands (SC) to clayey gravel (GC) (for the upper core).

The materials forming the lower core were derived from clayey alluvial/colluvial fan deposits that occurred at the mouth of Limekiln Canyon just south of the boat ramp on the upstream right abutment. These materials are generally classified as highly plastic sandy clays (CH) to highly plastic silty sands-sandy silts (SM-MH). The downstream shell consists mainly of gravelly clayey sands (SC) to clayey gravels (GC) obtained from the spillway excavation. There is no classification information available on the drain materials. However, construction records indicate that limited amounts of materials for the drain were obtained from on-site borrow areas but that most of the materials were procured from off-site commercial quarries.

2.4 ENGINEERING PROPERTIES OF EMBANKMENT MATERIALS

Seismic stability and non-linear deformation analyses require the following material properties: unit weight, effective stress friction angle, undrained strength, undrained stress-strain-strength relationship, and dynamic properties (i.e., shear-wave velocity, shear modulus reduction, and damping ratio curves). In addition, the permeabilities of the various materials are required as input to the seepage analyses that provide estimates of pore pressures that are necessary to calculate the initial effective stresses within the dam for input into the engineering analyses of seismic deformations.

Table 2-2 provides a summary of the engineering properties selected for each of the zones of the dam except for the shear modulus reduction and damping ratio curves that are shown on Figure 2-7. The derivation of these properties from the existing data is discussed in detail in Report No. LN-3 (Terra/GeoPentech, 2011b). The Zone 3 drain materials should be predominantly sand or sand and gravel mixes but no classification or engineering property information is available for these materials from previous studies. Thus, the Zone 3 materials have been assigned the same stiffness and strength as the Zone 4 materials for the engineering analyses of stability and seismic deformations.

Volpe (RLVA, 1999a) summarized all the data available on soil permeability of the embankment materials and interpreted the data to estimate horizontal and vertical permeability of the various zones of the dam, except for Zone 3 – Drain. This information is summarized in Table 2-3 and is used as the starting point for the seepage analyses. No data are available on the permeability of the Zone 3 drain materials. However, from an engineering perspective, they are essentially free draining compared to the very low permeabilities of the other embankment zones provided the drain materials are continuous. However, the continuity and effectiveness of the inclined drain is of concern and this drain may not function as intended. This issue is considered further in the seepage analyses discussed in Section 3.0.

2.5 GROUND MOTIONS

Earthquake ground motions from the controlling events on the Stanford-Monte Vista, Berrocal, and San Andreas faults were considered to develop site-specific ground motions for the seismic stability evaluation of the dam. These input ground motions were developed in terms of response spectral values and candidate acceleration time histories to be used in developing time histories that are compatible with the specified response spectral values.

Key elements in the development of these site specific ground motions are as follows:

1. Lenihan Dam is classified as a "high consequence" dam by DSOD, based on a DSOD Hazard Classification Total Class Weight of 30.
2. The two seismogenic faults controlling the seismic hazard at the dam are the Stanford-Monte Vista and San Andreas faults. The Maximum Credible Earthquake (MCE) on the Stanford-Monte Vista fault is a magnitude 6.9 event that has a peak ground acceleration of 1.05 g and is located at a distance of 5.5 km from the dam. The MCE on the San Andreas fault is a magnitude 7.9 event that has a peak ground acceleration of 0.73 g and is located at a distance of 2.1 km from the dam. The Stanford-Monte Vista event controls the shaking condition at the site for periods of 1 second or less for the lower magnitude earthquake scenario. The San Andreas event has a larger earthquake magnitude and controls the shaking condition at the site for periods larger than about 1 second.
3. The V_{S30} for the foundation of the dam was calculated based on OYO shear wave velocity data collected at two locations beneath the dam and one location within close proximity of the dam. A site-specific V_{S30} of 1,260 m/sec was determined based on these measurements and used in the development of the design response spectra for the Stanford-Monte Vista and San Andreas events.
4. Three seed time histories were selected for the Stanford-Monte Vista event and adjusted to match the target response spectra. The spectrally-matched time histories are shown on Figures 2-8 to 2-10. It should be noted that the Arias Intensity values of the three selected ground motions exceed the best estimate of Arias Intensity provided by the Watson-Lamprey and Abrahamson relationship with 84th percentile ground motion inputs.
5. Seed time histories for the San Andreas event were selected through a multi-step screening of the PEER Ground Motion Database because of the relatively small number of high quality ground motion records from stations that are very close to ruptures of very large magnitude earthquakes. The selection process screened all 3,551 records in the Database and yielded eight records with values of Arias Intensity and significant duration similar to those of the San Andreas event. These eight records, as well as the Denali TAPS record, were chosen and evaluated, and three final seed time histories were selected. The final three selected seed time histories were then adjusted to match the target response spectra. The spectrally-matched time histories are shown on Figures 2-11 to 2-13. As for the Stanford-Monte Vista event, the Arias Intensity values of the three ground motions exceed the best estimate of Arias Intensity provided by the Watson-Lamprey and Abrahamson relationship with 84th percentile ground motion inputs.

3.1 GENERAL

Analyses of seepage through an earth dam provide information on the distribution of total head and pore-water pressure, gradients, and flow rates within the dam. The pore-water pressures within the dam under steady state seepage conditions for a full reservoir are used to calculate effective stresses, which are then combined with the effective-stress-strength parameters and soil unit weights to calculate the Factor of Safety of the dam under steady state seepage conditions. The effective stresses within the dam are also used to estimate the undrained shear strength of the clayey embankment soils. These undrained shear strengths are used in limiting equilibrium stability analyses to calculate the Factor of Safety of the dam for undrained loading combined with steady state seepage (and other loading conditions), and to calculate the yield acceleration of the embankment under pseudo-static earthquake loading. These undrained shear strengths are also an important input parameter for the non-linear analyses of the permanent deformations caused by earthquake loading. The static and pseudo-static stability analyses are described in Section 4 and the seismic deformation analyses are discussed in Section 5.

Our approach for the seepage analyses includes the following steps:

1. Develop a finite element model for the dam and dam foundation that includes the geometry of the dam and the various internal zones and other important features within the dam; assign values of permeability (for both horizontal and vertical flow) to all the materials; and establish boundary conditions.
2. Use the model to calculate total heads throughout the dam and foundation and compare calculated total heads from the model to measured total heads from piezometers.
3. Based on comparisons of calculated to measured total heads, make reasonable adjustments in the material properties and boundary conditions to improve the agreement between calculated and measured total heads.
4. Use the final model results to make a best estimate of the distribution of total heads and pore pressures within the dam and use this information to calculate effective stresses and undrained shear strengths of the embankment materials for use in stability analyses and seismic deformation analyses, as described above.

The PLAXIS finite element computer program was used for the seepage analyses. PLAXIS is the brand of the Software and the name of the company that develops and supports the software (www.plaxis.nl). PLAXIS offers a suite of finite element computer programs for geotechnical applications that include static and dynamic deformation analyses and analyses of seepage and consolidation. The seepage analyses for this study are based on a two-dimensional plane-flow finite element model.

Section 3.2 summarizes the history of piezometer measurements at Lenihan Dam and the maximum measured piezometric levels that were used to validate the seepage model. Section 3.3 presents the results of the seepage analyses.

3.2 PIEZOMETER MEASUREMENTS AT LENIHAN DAM

The following is a history of piezometer installations at Lenihan Dam:

1. Two pneumatic piezometers (now abandoned) and three open well piezometers were installed in 1975 and three additional pneumatic piezometers (now abandoned) were installed in 1979 (Wahler, 1982).
2. Twenty-two “permanent” piezometers were installed in 1998 to monitor piezometric levels adjacent to the outlet pipe; these piezometers were abandoned when the outlet pipe was grouted in 2009.
3. Thirty-two vibrating wire piezometers were installed in two phases during 1999 and 2001: 23 piezometers in the dam embankment, 2 within the bedrock foundation beneath the dam, and 7 within the bedrock at the right abutment.

The locations of the currently existing piezometers are shown on Figure 3-1; the locations of Sections A-A', B-B' and F-F' are also shown on this figure. As discussed in Section 2.2, Sections A-A' and B-B' are representative of dam zoning and conditions near the center of the valley. These sections were heavily instrumented with piezometers. Section F-F' follows the alignment of the original creek bed and the alignment of the original outlet pipe (that was grouted closed in 2009). Maximum piezometer levels (i.e. measured total heads at full reservoir level) from the vibrating wire piezometer data within the embankment are shown on Figure 3-2 for sections A-A' and B-B'. Figure 3-3 shows the locations of embankment piezometers projected onto Section F-F' and also shows the maximum piezometric levels measured in piezometers installed in the soil surrounding the original outlet pipe.

The maximum piezometer levels shown in these figures were used to validate the results of the PLAXIS seepage analyses.

3.3 RESULTS OF SEEPAGE ANALYSES

3.3.1 Section Chosen for Analyses

The maximum section of the dam is Section B-B' and previous work has shown that this section is the critical section for stability analyses and seismic deformation analyses. However, the axis of the dam is oriented at an angle of about 65° from the thalweg of Los Gatos Creek and 2-dimensional seepage analyses for Section B-B' would be problematic because the base of the dam crosses Los Gatos Creek and runs uphill on the downstream side of the creek. More importantly, the water that is collected by the French Drain at this section must flow out of the model and this cannot be modeled given the assumptions of two-dimensional planar flow. Section A-A' was also considered for the analyses but found to be inappropriate because of the same plane-flow limitations as Section B-B' and because of the limited height of the dam along this section. As a result, we concluded that Section F-F' which follows the original thalweg of Los Gatos Creek was the most appropriate section because it most closely satisfies the assumption of plane flow. In addition, modeling of seepage along Section F-F' allows explicit consideration of the measured piezometric levels along the alignment of the original outlet pipe.

The results from the analyses of Section F-F' can then be “rotated” back to determine the distribution of total heads along a transverse section and applied to Section B-B'.

3.3.2 Results of Analyses for Section F-F'

More than 10 cases were considered in order to develop boundary conditions and material properties that best represent the values of measured piezometric levels at Section F-F' and provide converged solutions. Convergence is an issue because of the need to iterate to find the correct location of the phreatic surface within the dam.

Five of the cases investigated how to model flow conditions along the original outlet pipe in order to best match the measured piezometric levels along the pipe. The construction reports for the pipe were reviewed as part of this work and it was found that the zone along the pipeline where there was relatively small amounts of head loss upstream of the center of the dam corresponded to areas where the pipe was probably constructed in relatively hard limestone. It was also found that the zone along the pipe from the centerline of the dam to 100 feet downstream of the centerline of the dam where the majority of the head loss has been observed to take place corresponds to areas where the pipe was probably constructed in relatively soft shale. Based on this, the pipe backfill was included in the model and the permeability of the pipe backfill from the centerline of the dam to 100 feet downstream of the centerline of the dam was modeled as 200 times smaller than the permeability of the backfill upstream and downstream of this zone. Having modeled the conditions along the pipe, the remaining cases considered various combinations of permeability for the various embankment zones.

Table 3-1 summarizes the permeability values used in the final PLAXIS model for Section F-F' and compares the final values used in the model to the values estimated by Volpe (1999a) and the initial estimates of permeability made by TGP at the start of our seepage analyses. Volpe (1999a) estimated that the horizontal soil permeability for the embankment materials would be 10 times higher than the vertical soil permeability. Analyses of flow through dams by TGP has shown that the horizontal permeability for compacted clayey fill dams is at least 20 times the vertical permeability and we have used that ratio in our analyses. The upstream shell of the dam and the upper core material came from the same borrow area and are clays of low plasticity that have similar physical and index properties; consequently we have assigned the same permeability to these materials. The lower core material is from a different borrow area and is comprised of a clay of high plasticity and has a lower permeability. The downstream shell materials were primarily obtained from the spillway excavation and were initially estimated by TGP to be twice more permeable than the upper core and upstream shell materials. As shown on Table 3-1, the final values of permeability for the embankment materials are similar to the initial TGP estimates. The only difference is that the downstream shell was found to be best modeled using a permeability that is the same as the upper core and upstream shell, rather than twice the permeability of these materials.

As shown in Table 3-1, we found that using a permeability of the inclined drainage blanket that is the same as that of the downstream shell materials gave the best agreement between calculated and measured total heads. This is consistent with the discussion in Section 5.5.6 of Report No. LN-3 that concluded that the drain may not function as intended because of the way it was constructed.

The permeability of the rock blanket drain was modeled using a horizontal permeability that was 100 times greater than the permeability of the downstream shell and a vertical permeability that was 2,000 times greater than the vertical permeability of the downstream shell. The permeability of the rock drain used in the PLAXIS model may be less than the actual permeability of the materials but is high enough to allow the rock drain to behave as a free draining material while avoiding numerical problems associated with having values of permeability of adjacent soil layers that are drastically different.

Finally, as shown in Table 3-1, the permeability of the pipe backfill was modeled as 20 feet per year (ft/ yr) within the portion of the pipe where the backfill is limestone and 0.10 ft/yr in the portion of the pipe where the backfill is shale. These values compare to permeabilities of the shell materials and underlying rock of 0.05 ft/yr.

Figure 3-4 compares the measured to modeled total heads for the final PLAXIS analysis at Section F-F'. Contours of calculated total heads within the embankment are shown and the values from the contour lines can be compared to the measured maximum piezometric levels at the various piezometer locations. The agreement between calculated total heads and measured piezometric levels is generally good, typically within 10 to 15 feet. The maximum difference between calculated total head and measured piezometric level was found for the piezometer located within the downstream portion of the lower core at about elevation 520 feet where the measured piezometric level of 532 feet compares to a calculated total head of 560 feet. The fact that the calculated value is higher than the measured value at this location means that the calculated values are more conservative from the perspective of the evaluation of seismic deformations and stability.

Figure 3-4 also compares calculated total heads along the outlet pipe to measured piezometric heads along the pipe. The agreement is good and shows that the measured total heads along the pipe are most likely due to differences in permeability of the backfill surrounding the pipe and/or local variations in bedrock conditions.

The use of the calculated total heads and associated pore-water pressures to estimate the undrained strengths of the embankment materials is discussed in Section 4 - Static Stability and Pseudo-Static Yield Acceleration.

4.1 GENERAL

The cross-section of Lenihan Dam at the maximum section (Section B-B' on Figure 3-2) is the critical section for static stability analyses and for calculating the yield acceleration from pseudo-static stability analyses. The static stability and yield accelerations have been calculated using circular failure surfaces that were analyzed by the Simplified Bishop Method of Slices with the computer program Galena (www.galenasoftware.com). Galena is a powerful and relatively easy to use slope stability program that was developed and is supported by Clover Technology. This software is used for geotechnical and mining applications by licensed users located in over 70 countries around the world. The following cases have been analyzed and are reported herein.

Case	Type of Analyses	Material Properties	Factor of Safety	Yield Acceleration
Full Reservoir – D/S Slope	Static	Drained	X	
Full Reservoir – U/S Slope	Static	Drained	X	
Full Reservoir – D/S Slope	Static	Undrained	X	
Full Reservoir – U/S Slope	Static	Undrained	X	
Rapid Drawdown – U/S Slope	Static	Undrained	X	
Full Reservoir – D/S Slope	Pseudo-Static	Undrained		X
Full Reservoir – U/S Slope	Pseudo-Static	Undrained		X
Loma Prieta – D/S Slope	Pseudo-Static	Undrained		X
Loma Prieta – U/S Slope	Pseudo-Static	Undrained		X

The Loma Prieta cases correspond to the reservoir level at the time of the Loma Prieta earthquake which was about 10 feet above the upstream toe of the dam; i.e., at about the same level as the rapid drawdown case.

4.2 INPUT PARAMETERS

The input for the slope stability analyses includes:

1. the geometry of the dam and the internal zones within the dam, and the total unit weights of the materials within the various zones of the dam;
2. for drained analyses, the reservoir level, and the pore-water pressures and effective stress strength parameters for the various zones of the dam; and
3. for undrained analyses, the reservoir level and the undrained shear strengths for the various zones of the dam.

SECTION 4.0

STATIC STABILITY AND PSEUDO-STATIC YIELD ACCELERATION

The engineering properties for the various materials were discussed in Section 2 and are summarized in Table 2-2.

The undrained shear strength of the various embankment materials is a function of the vertical effective stress acting on the soil at any particular location within the dam. The vertical effective stress is calculated from the vertical total stress and the pore-water pressure within the dam.

Figure 4-1 shows the geometry of the maximum section of the dam and contours of pore-water pressures within the dam for steady state seepage analyses based on the seepage analyses presented in Section 3. The vertical total stress within the dam was calculated as part of the FLAC analyses presented in Section 5. The vertical total stress was then combined with the pore-water pressures to calculate the vertical effective stress, and the undrained shear strength was calculated from the vertical effective stress. Figure 4-2 shows contours of undrained shear strength within the dam corresponding to steady state seepage under full reservoir. The vertical effective stresses and corresponding undrained shear strengths will be higher for steady state seepage conditions under lower reservoir levels but this increase in strength would take a long time to occur because of the low permeability of the soils. Consequently, we have used the undrained strength corresponding to steady state seepage under full reservoir level for all undrained loading conditions in order to be reasonably conservative.

4.3 RESULTS OF ANALYSES

The distribution of total heads within the dam shown in Figure 3-4 and the distribution of undrained shear strengths shown in Figure 4-2 are not simple from a modeling perspective for limiting equilibrium analyses. Nevertheless, the Galena slope stability program is capable of closely modeling them. For the drained analyses, the total heads (or piezometric levels) were modeled by dividing the upstream shell, core, and downstream shell into 5, 9, and 8 horizontal layers, respectively, and by specifying a piezometric line for each layer to define the distribution of total heads. For the undrained analyses, the distribution of undrained shear strength was modeled by defining materials where the average undrained shear strength varied in increments of 500 pounds per square foot (lb/ft²) within each of the dam zones. A total of 29 materials were required to achieve this modeling.

The calculated Factor of Safety or Yield Acceleration for the various cases analyzed are summarized below.

Case	Type of Analyses	Material Properties	Factor of Safety	Yield Acceleration
Full Reservoir – D/S Slope	Static	Drained	2.06	NA
Full Reservoir – U/S Slope	Static	Drained	4.47	NA
Full Reservoir – D/S Slope	Static	Undrained	1.97	NA
Full Reservoir – U/S Slope	Static	Undrained	4.00	NA
Rapid Drawdown – U/S Slope	Static	Undrained	2.60	NA

SECTION 4.0 STATIC STABILITY AND PSEUDO-STATIC YIELD ACCELERATION

Case	Type of Analyses	Material Properties	Factor of Safety	Yield Acceleration
Full Reservoir – D/S Slope	Pseudo-Static	Undrained	NA	0.23g
Full Reservoir – U/S Slope	Pseudo-Static	Undrained	NA	0.33g
Loma Prieta – D/S Slope	Pseudo-Static	Undrained	NA	0.23g
Loma Prieta – U/S Slope	Pseudo-Static	Undrained	NA	0.28g

The locations of the critical circular failure surfaces associated with these cases are shown on Figure 4-3.

These results show that the Factors of Safety for static loading are all significantly greater than the minimum factors of safety recommended by the US Army Corps of Engineers (2003) for static loading conditions; i.e., 1.5 for downstream slope with steady state seepage under full reservoir and 1.3 for rapid drawdown. The yield accelerations were used for Newmark-type analyses, as discussed in Section 5.

5.1 GENERAL

This section documents the results of the seismic deformation evaluation of Lenihan Dam under the postulated evaluation ground motions that represent the Maximum Credible Earthquake (MCE). The seismic deformation evaluation focuses on seismically-induced permanent deformations of the dam embankment particularly in the crest area that could lead to a loss of freeboard and the formation of cracks.

Following this introduction, Section 5.2 describes the methodology and approach used in the evaluation; Section 5.3 discusses the cross-section used in the analyses; Section 5.4 summarizes the material properties; and Section 5.5 presents the ground motions for the Loma Prieta earthquake and the MCE evaluation ground motions as well as the corresponding analysis input time histories. Section 5.6 discusses the key results from the evaluation of the Loma Prieta case history that provides a site-specific empirical basis for the current evaluation and Section 5.7 is a summary of the results of the seismic deformation evaluation of the dam under the MCE evaluation ground motions.

There are two appendices associated with this section. Appendix A provides some additional details on the work completed for the Loma Prieta case history as used in this evaluation, and Appendix B contains detailed graphical results of the FLAC (Itasca, 2008) seismic deformation analyses performed as part of the evaluation.

5.2 ANALYSIS METHODOLOGY

5.2.1 Overview

The seismic deformation of the dam under the MCE ground motions was evaluated using FLAC (Itasca, 2008). However, a documented case history of the dam during and following the 1989 Loma Prieta earthquake exists for Lenihan Dam (RLVA, 1990). Therefore, this case history was evaluated first to develop an overall understanding of the seismic behavior of the dam in terms of major contributing factors, and to provide a level confidence that the developed model reasonably captures the important aspects of the dam response. Specifically, the Loma Prieta case history was used to tie the following to a site-specific empirical basis: the general methodology adopted for the use of FLAC in the evaluation, the reasonably conservative assignment of undrained shear strengths, and the surface cracking potential.

5.2.2 Analysis Platform and Soil Model

The computer program FLAC (Fast Lagrangian Analysis of Continua) was used in the evaluation. FLAC is a two-dimensional explicit finite difference program for geotechnical and other applications developed by Itasca (2008). An analysis section is divided into zones and nodal points in a way analogous to the finite element method. FLAC uses the Lagrangian formulation of momentum equations (Newton's second law of motion) and, thereby, inherently accounts for the mass conservation law and allows elements with fixed masses to translate, rotate, or deform in space. The analysis input motion is specified at the base of the analysis

section (elevation 400 feet, as shown on Figure 5-1), incorporating the effects of a compliant boundary representing the bedrock in the analysis.

The calculation loop in FLAC has two main alternating components: zone (or element) calculations and nodal point calculations. In the zone calculations, the current velocities and displacements of nodal points are used to compute the strain increments in the zone formed by these nodes; these strain increments, in turn, are used to compute the stress increments of the zone. With the new state of stress, the out-of-balance force can be computed and then used to calculate the incremental displacements of the nodes.

Various stress-strain models are available in FLAC. For the evaluation documented herein the Mohr-Coulomb model and the elastic model in FLAC were used in the analyses. Details of these models are provided by Itasca (2008). For all the results presented here, the elastic model was used for the bedrock and, depending on the analysis, either the Mohr-Coulomb model or the elastic model was used for all the other materials. In particular, the Mohr-Coulomb model was used for the embankment materials in the non-linear seismic deformation analyses.

The Mohr-Coulomb model consists of elastic-perfectly-plastic stress-strain relationships. Therefore, the materials are elastic before yielding. To make the elastic portion of the analysis reasonable, we perform an equivalent-linear analysis using the computer program QUAD4MU (Tan, 2003) on a two-dimensional model of the dam to obtain the strain-compatible modulus and damping values for the postulated shaking conditions. The analysis results from QUAD4MU provide the basis for the strain-compatible shear modulus and damping values to be used in the elastic portion of the Mohr-Coulomb model in the FLAC analyses. The "perfectly-plastic" portion of the Mohr-Coulomb model is specified as the appropriate undrained shear strength of the material. As discussed later, the appropriate undrained shear strengths are assigned considering various contributing factors including laboratory test results and the results of our analyses of the Loma Prieta case history.

5.3 ANALYSIS SECTION, PORE PRESSURES, AND DISCRETIZATION

5.3.1 Analysis Section

Figure 2-6 shows the idealized section of the dam selected for the analyses, identified as Section B-B'. The location of this section is shown on the plan insert contained in Figure 2-6. The generalized embankment zones and material types are also tabulated on Figure 2-6.

Section B-B' was chosen for the analyses because it is the maximum section and also because the bedrock surface along this section is irregular with a significant bedrock "knoll" at the upstream side of the core beneath the embankment as shown on Figure 2-6; the inset on Figure 2-6 shows the complexity of the bedrock contours beneath the dam embankment. The Loma Prieta case history suggests that the shape of the bedrock surface probably affects the seismic response of the dam. Note that the selected analysis section is relatively free to deform in the steeper downstream direction but the presence of the bedrock knoll below the upstream section needs to be considered to evaluate the potential for seismically-induced surficial cracking (as was observed during the Loma Prieta event). Thus, in providing conclusions based on the seismic deformation analyses, one needs to consider this complexity of the bedrock topography.

5.3.2 Pore Pressures

The location of the phreatic surface and the distribution of pore water pressures within the embankment just before the earthquake shaking need to be specified in the seismic deformation analyses. The reservoir is postulated to be full at elevation 653 feet during the MCE that is defined by the postulated evaluation ground motions. The pore water pressure distribution associated with this reservoir level has been estimated by the seepage analyses presented in Section 3.0. Figure 4-1 shows the pore water pressure contours within the dam used in the stability analyses and seismic deformation analyses.

The reservoir level during the Loma Prieta event was at elevation 550 feet. However, given the uncertainty in estimating the pore pressure conditions then and the very low permeability values of the embankment materials, we made the reasonably conservative assumption that the effective stress conditions (and associated undrained shear strengths) in the embankment at the time of the Loma Prieta event were similar to the effective stress state established for the reservoir level at 653 feet. This assumption is similar to the assumption for a rapid drawdown analysis.

5.3.3 Discretization of Analysis Section

Figure 5-1 shows the further idealized analysis section and the same section discretized into a finite difference mesh for use in the FLAC analyses. The mesh shown on this figure was generated to: (1) set up appropriate dynamic wave propagation in the system; (2) control kinematic constraints provided by the linear zones (or elements) used in FLAC; and (3) control numerical problems introduced by element shapes.

Although not shown on Figure 5-1, the bedrock was also discretized for the sole purpose of providing a compliant base that would appropriately and adequately allow the incoming seismic waves and absorb the outgoing seismic waves. The numbers shown in various zones of the dam on Figure 5-1 correspond to the zone numbers identified on Figure 2-6.

5.4 MATERIAL PROPERTIES

5.4.1 Material Properties

The material properties used in the analyses are documented in Section 2.0 and summarized in Table 2-2. They include: unit weight; small-strain shear modulus (shear wave velocity, V_s , or maximum shear modulus, G_{max}); shear modulus reduction and damping ratio curves; and shear strength. The shear wave velocity of the bedrock is also listed in Table 2-2. The shear modulus reduction and damping ratio curves are discussed in Section 2.0. The material properties used in the evaluation were the same for all cases analyzed. For the seismic deformation analyses, we have assigned the Zone 3 materials the same stiffness and strength as the Zone 4 materials (see Figure 5-1).

The shear modulus reduction and damping curves used (Section 2.0) are confining pressure-independent relationships by Vucetic and Dobry (1991). Figure 5-2 compares confining-pressure-dependent shear modulus reduction and damping curves based on Darendeli (2001) with those based on Vucetic and Dobry (1991) for the two end-member materials in the

evaluation (the third material has an in-between PI of 17). Figure 5-2 shows that the relationships by Vucetic and Dobry (1991) in this case provide damping values and shear modulus reduction curves that are generally comparable to those by Darendeli (2001) in appropriate confining pressure ranges. The use of the adopted relationships is considered adequate based on this observation combined with the relatively low embankment height of the dam.

The primary embankment loading conditions due to seismic shaking are reasonably represented by direct simple shear (DSS) loading. Thus, for the seismic deformation analyses, undrained shear strengths measured under DSS loading conditions are of interest. As presented in Report No. LN-3 (Terra/GeoPentech, 2011b), our test data indicate that the DSS undrained shear strengths of the compacted clay soils at Lenihan Dam are typically 60 percent of the undrained shear strengths measured in triaxial compression (TXC) tests. Therefore, the TXC shear strengths should be multiplied by 0.6 to obtain estimates of DSS shear strengths. However, because all the DSS tests were conducted using a static loading rate (5 percent per hour), some adjustment in the static shear strengths for the rate of loading effects needs to be made for the seismic deformation analyses. Such adjustments should also reflect some cyclically-induced softening effects. As discussed in Section 5.6, the final assignment of undrained shear strengths was based on these considerations and the Loma Prieta case history. As discussed later, the final outcome was to multiply the TXC undrained shear strengths by 0.84.

5.5 LOMA PRIETA AND MCE GROUND MOTIONS

The input ground motion representing the 1989 Loma Prieta earthquake ground motions at the site used in the case history analyses is the transverse component of the three-component ground motions recorded at the left abutment and shown on Figure 5-3; see Appendix A for further details. As discussed in Appendix A, the applicability of this input motion to the section being analyzed is one of the main sources of uncertainty associated with the Loma Prieta case history analysis.

The evaluation ground motions that represent the MCE are discussed in Report No. LN-3 (Terra/GeoPentech, 2011b) and summarized in Section 2.5. The earthquake ground motions for the Stanford-Monte Vista event and the ground motion associated with the San Andreas event used in the seismic deformation evaluation of the dam are shown in terms of response spectra at 5 percent damping on Figure 5-4. The following six ground motions were selected and used in developing time histories that are compatible with the response spectral values shown on Figure 5-4:

1. Earthquake Records for Stanford-Monte Vista Event
 - a. Kobe Earthquake, Nish-Akashi Station, 1/16/1995
 - b. Loma Prieta Earthquake, LGPC Station, 10/18/1989
 - c. Northridge Earthquake, Sylmar-Olive View Med. FF Station, 1/17/1994
2. Earthquake Records for San Andreas Event
 - a. Chi-Chi Earthquake, TCU065 Station, 9/20/1999
 - b. Landers Earthquake, Lucerne Station, 6/28/1992

c. Manjil Earthquake, Abbar Station, 11/03/1990

Further details of these ground motions are provided in Tables 5-1A and 5-1B for the Stanford-Monte Vista event and the San Andreas event, respectively. The above six records adjusted to the spectral values shown on Figure 5-4 are presented on Figures 2-8 to 2-13.

5.6 LOMA PRIETA CASE HISTORY

5.6.1 Loma Prieta Event at the Site

The Loma Prieta earthquake occurred on October 17, 1989, along a branch of the San Andreas Fault. The epicenter of this magnitude 6.9 event was located about 13 miles (20 km) from Lenihan Dam. The effects of the Loma Prieta earthquake on Lenihan Dam were investigated by the District and R.L. Volpe & Associates (RLVA, 1990) in the days following the event as part of an overall investigation of District dams affected by the earthquake. The observed damage at the dam was documented in a report by RLVA (RLVA, 1990).

Following the Loma Prieta earthquake, the dam was found to have sustained about 10 inches of crest settlement at the maximum section and a maximum of about 3 inches of lateral movement downstream. As shown in Figure 5-5, localized cracking was observed on the upstream face, the downstream face and both abutments of the dam. Also, about six weeks after the earthquake, a wet area was observed below the footpath near the right abutment although no flow was reportedly emanating from this area (RLVA, 1990).

5.6.2 Key Results from Loma Prieta Case History Analysis

Appendix A presents the results of the evaluation of the Loma Prieta case history. As discussed in this appendix, the Loma Prieta case history evaluation indicates that the adopted methodology consisting of FLAC seismic deformation analyses using the Mohr-Coulomb soil model combined with the corresponding QUAD4MU equivalent linear analysis provides a reasonable and possibly somewhat conservative assessment of the seismic performance of the dam. Figure 5-6A compares three response spectra of calculated acceleration time histories and one response spectrum of recorded acceleration time history all at the crest. The results associated with QUAD4MU (equivalent linear) and FLAC equivalent linear (Mohr-Coulomb without yielding) analyses are similar as can be seen on Figure 5-6A; and the results associated with the FLAC Mohr-Coulomb (the same as the FLAC equivalent linear, but with yielding included) analysis and the recorded spectrum (from the Loma Prieta event) are also similar. All four response spectra shown on Figure 5-6A are in fact similar in a first-order sense.

The FLAC Mohr-Coulomb and the recorded portions of the results shown on Figure 5-6A are shown on Figure 5-6B in terms of amplification function (ratio of the crest response spectral value to the input response spectral value at the same period shown as a function of the period). The amplification functions of the recorded motion and the FLAC Mohr-Coulomb calculated results are very similar for periods of 0.25 to 1.0 seconds but differ somewhat at higher and lower periods.

Note on Figure 5-6B that the crest response spectrum calculated using FLAC Mohr-Coulomb is somewhat lower than the response spectrum of the recorded crest motion for periods greater than 1 second. The undrained shear strength used in the FLAC Mohr-Coulomb model shown on Figure 5-6B is 0.84 times the TXC undrained shear strength, which implies a factor of 1.4 increase for the combined effects of the rate of loading and cyclically-induced softening after accounting for the TXC to DSS conversion using a factor of 0.6 (i.e., $0.84 = 0.6 \times 1.4$). The agreement between FLAC Mohr-Coulomb and the measured response shown on Figure 5-6B could be improved, but to do so would require that the 1.4 factor to be increased. Given the literature information on the rate of loading effects and possible cyclically-induced softening effects, it was considered prudent to use a factor of 1.4 and not to increase it further.

The reasonably conservative nature (in the sense of calculating possibly higher seismic shear deformation in the MCE evaluation analyses) of the undrained shear strength assignment discussed in the previous paragraph is illustrated on Figure 5-7 by the contours of end-of-shaking permanent seismic displacements calculated using the Loma Prieta recorded input motion. A comparison of Figure 5-7 to Figure 5-5 indicates that the computed horizontal crest displacement is higher than the horizontal crest displacement observed for a nearby crest monument, i.e., 0.4 feet versus 0.1 feet. Note that the computed value of 0.4 feet is higher than the largest observed horizontal seismic displacement value of 0.25 feet at Station 14+00 (see Figure 5-5).

However, Figure 5-7 also shows that the computed crest settlement was only about 0.2 feet while Figure 5-5 indicates that the nearby crest monument settled during, or almost immediately following, the earthquake by about 0.5 feet relative to the abutments (for a total of 0.8 feet). This difference is quite small, particularly when all the uncertainties are considered (see Appendix A); shear modulus softening due to pore pressure build-up or cyclically-induced volumetric strain are among the many possible explanations for this discrepancy. As discussed in Appendix A, we propose accounting for this discrepancy during the MCE evaluation analyses in a reasonable way by considering the gravity induced settlement of the crest due to embankment softening caused by seismically-induced pore water pressures in the embankment materials. Our evaluation indicated that the settlement difference of 0.3 feet ($0.5 - 0.2$) can be captured by about 10 to 20 percent softening of the shear modulus in the embankment. In this regard, it is interesting to note the following:

1. as indicated on Figure 5-5, a wet area was observed following the Loma Prieta event (RLVA, 1990), possibly indicating pore water pressure increases;
2. some piezometers registered pore pressure increase following the Loma Prieta event (RLVA, 1998); and
3. as indicated on Figure 5-7, our analysis showed higher deformation in the general vicinity of the wet area reported by RLVA (1990).

The surface cracking potential is discussed in Section 5.7. However, we note here that the cracking potential discussion in that section is in part based on the longitudinal cracks observed below the upstream side of the crest following the Loma Prieta event (see Figure 5-5). These shallow cracks were considered to have been initiated by the presence of the bedrock knoll beneath the embankment as indicated by our analysis of the Loma Prieta case history in Appendix A.

5.6.3 Summary of Loma Prieta Case History

As discussed above, the Loma Prieta case history provides a site-specific empirical basis that:

1. confirms the reasonableness of the overall approach based on FLAC with the Mohr-Coulomb soil model combined with the QUAD4MU equivalent linear analysis;
2. shows that the undrained shear strengths assigned to the embankment materials are reasonably conservative; and
3. indicates the surface cracking pattern was possibly a result of high seismic shaking together with the bedrock topography.

5.7 SEISMIC DEFORMATION EVALUATION UNDER MCE GROUND MOTIONS

5.7.1 Results of Seismic Deformation Analyses

This section presents the selected results of the seismic deformation analysis using the evaluation input motions that have been used to represent the MCE. The FLAC analyses were performed using the Mohr-Coulomb model (with the undrained shear strengths set at 0.84 the TXC undrained shear strengths) combined with the corresponding QUAD4MU equivalent linear analysis to set the shear modulus and damping values in the Mohr-Coulomb model; this is the same model described in the previous sections and confirmed by the Loma Prieta case history evaluation (Appendix A).

The FLAC seismic deformation analyses were performed using the positive and negative polarities for each of the six input ground motions (or a total of 12 cases). The results of these analyses are summarized in Table 5-2 in terms of crest, upstream, and downstream horizontal and vertical permanent seismic displacements at the end of shaking. For each ground motion, the critical polarity case (i.e., the case that led to larger crest displacements) was selected. The graphical presentation of these results is provided in Appendix B. Each selected case is identified by "SAx" and "SMVx" for the San Andreas and Stanford-Monte Vista events, respectively, where "x" is an integer from 1 through 3 corresponding to each of the three time histories for the two events. Where appropriate, each case is further identified by the seed time history as well; for example, "SA2 Landers" corresponds to the critical polarity case for the San Andreas event represented by the adjusted acceleration time history based on the Landers earthquake record.

As can be seen in Table 5-2, the calculated horizontal crest displacements range from 0.1 to 1.1 feet downstream and the calculated vertical displacements (settlements) range from 0.1 to 0.3 feet [note that vertical settlements are shown as negative values in Table 5-2, as per footnote (2)]. At mid-height of the upstream slope the calculated horizontal displacements range from 0.5 feet downstream to 1.1 feet upstream and the calculated vertical displacements are up (i.e., heave) and range from 0.2 to 0.7 foot. At mid-height of the downstream slope the calculated horizontal displacements range from 0.7 to 2.8 feet downstream and the calculated vertical displacements are all up and range from 0.1 to 0.4 feet.

The calculated crest displacements listed in Table 5-2 for the MCE are only slightly higher than those calculated for the Loma Prieta case history (0.4 feet horizontal displacement and 0.2 feet settlement). As explained further below, the reason for this somewhat unexpected finding is that the spectral accelerations at the fundamental period of the dam are about the same for the MCE and the Loma Prieta event.

Figure 5-8 compares the calculated response spectra (at 5 percent damping) for the horizontal acceleration time histories at the crest produced by FLAC for all six selected cases, as well as the Loma Prieta case history. In general, these response spectra are strikingly similar, even for the Loma Prieta ground motion. Figure 5-9 compares the response spectra of the input motions (SA, SMV, and Loma Prieta); the differences among response spectra of the three input motions are significant. The overall similarity of the calculated seismic displacements and seismic responses may be in part due to the similarity of the spectral values of the input motions in the period range near the fundamental period of the embankment. The QUAD4MU and Equivalent Linear FLAC analyses indicate that the fundamental period of the dam embankment under these shaking conditions is about 1 second, and as can be seen on Figure 5-9, the response spectral values of the Loma Prieta ground motion for this site are in fact slightly higher than those of the MCE evaluation ground motions in the vicinity of 1 second.

The analysis results for the SA2 Landers input motion gave the highest crest displacement and are presented herein as example results. The results of all six critical cases are presented graphically in Appendix B.

Figure 5-10 compares the response spectra of acceleration time histories computed for the SA2 Landers case at four points (i.e., the crest, the mid-heights of the upstream and downstream slopes, and the top of the lower core) using both QUAD4MU and FLAC. This figure indicates that the seismic responses induced by the SA2 Landers input motion appear reasonable for the purposes of calculating the seismic displacements.

Figure 5-11 shows the seismic displacement contours for the SA2 Landers case; seismic displacement vectors with numbers corresponding to the computed seismic displacements in feet are shown for three points (i.e., the crest and the mid-heights of the upstream and downstream slopes). The calculated seismic displacement values are not large, but there is a general trend of seismically-induced movements in a downstream direction. All the seismic displacement vectors shown appear reasonable and consistent with this trend except perhaps the upward movement of the upstream point. This is at least in part caused by the presence of the knoll beneath the embankment in that area as discussed under the cracking potential subsection below.

Figure 5-12 shows the seismic displacement vectors; Figure 5-13 shows the contours of computed permanent maximum shear strains at the end of shaking; and Figure 5-14 shows time histories of seismic displacements at the three selected points on the surface of the embankment, all for the SA2 Landers case. The combination of the results shown on Figures 5-11 through 5-14 provides an appreciation of the computed seismic deformations within the embankment for this case.

The seismic displacements at the end of shaking in the crest area (and elsewhere) computed in the evaluation analyses are small and highly unlikely to lead to a significant loss of freeboard. However, the Loma Prieta experience indicates that these undrained shear-induced seismic

displacements should be increased in the vertical direction. For the Loma Prieta event the additional settlement of the crest was 0.5 feet. The similarity of computed seismic response and computed seismically- induced displacements among the San Andreas (SA) and Stanford-Monte Vista (SMV) events and the Loma Prieta event indicates that the additional settlement expected for the SA and SMV events would not be substantially different from that associated with the Loma Prieta experience. It is noted that for near-normally consolidated clayey embankments the effect of the shaking duration is considered secondary when compared to the effects of the shaking level and yielding. Nevertheless, for the purpose of the evaluation, an additional crest settlement of 1 foot is postulated herein (and will be added to the calculated crest settlement from the FLAC analyses) to account for the "softening" effects. The combined results are considered to be consistent with the empirical database of seismic performance of embankments by Swaisgood (2003) when appropriate site specific considerations are superimposed.

A full Newmark-type analysis (Newmark, 1965 and Barneich et al., 1996) was run for the controlling ground motion which was found to be the Landers scaled time history for the San Andreas event. Figure 5-15 summarizes the results of this analysis. The magnitude and time history of block displacement from the full Newmark-type analysis are in the same range as the crest displacements from the FLAC analyses shown on Figure 5-14.

Simplified Newmark-type analyses were also used to estimate displacements from the SA and SMV events at the site. The yield acceleration of the sliding mass identified in the static stability analyses (0.23 g) was used in conjunction with the target response spectral values to estimate seismic deformation using the procedure presented by Bray and Travasarou (2007). The Bray and Travasarou approach was carried out using the degraded natural period and spectral acceleration at the degraded natural period of the embankment as determined in the QUAD4MU analysis. The results for both the SMV and SA events are tabulated below. The seismic deformation was also estimated using the methodology presented by Makdisi and Seed (1978). For this approach, the maximum acceleration of the sliding mass, k_{max} , was estimated based on the maximum acceleration at the crest determined by the QUAD4MU response analysis. The estimated displacements for each event are tabulated below; both the average and the range of values are reported for the Makdisi and Seed method.

Seismic Displacement Method	Stanford-Monte Vista Event	San Andreas Event
Bray and Travasarou Simplified Method (T_d from QUAD4MU)	0.5 feet	1.1 feet
Makdisi-Seed Simplified Method (k_{max} from QUAD4MU)	0.2 feet (0.1 to 0.6 feet)	1.1 feet (0.6 to 2.2 feet)

The estimates from these simplified Newmark-type methods also fall within the range of displacements estimated using FLAC.

5.7.2 Evaluation of Cracking Potential

The computed results of seismic displacement values listed in Table 5-2 are not large and are very unlikely to lead to significant longitudinal or transverse cracks in the embankment.

However, as stated previously, the Loma Prieta case history indicate some shallow longitudinal cracks below the upstream crest that were likely a result of high shaking combined with the presence of a rock knoll beneath the embankment in those areas (Section 5.6 and Appendix A).

Figure 5-16 shows the percentage stretching of soil columns in the upstream knoll area when the seismically-induced displacements at the end of shaking are compared to the corresponding initial values. The results shown on Figure 5-15 cover all the six selected evaluation cases and the Loma Prieta case history. Note on Figure 5-15 the location of the soil column was guided by the seismic displacement vector plot, as indicated by the SA1 Chi Chi example in the inset.

It is clear from Figure 5-16 that the Loma Prieta event likely caused the most stretching of the soil columns of any of the cases considered because the reservoir level was down at the time of the event. On the basis of these results, we conclude that the likelihood of similar cracks forming from the MCE evaluation event is considered low. Shallow cracks did form in this area during the Loma Prieta event (Figure 5-5); however, this area was above reservoir level during the Loma Prieta event, making it easier to form cracks, but would be below reservoir level for the MCE evaluation events making it difficult to form cracks. Furthermore, even if some cracks form, they would likely be shallow longitudinal cracks of limited extent, and not more serious than the cracking observed during the Loma Prieta event.

6.1 GENERAL

The purpose of the engineering analyses documented in this report is to evaluate the seismic performance and safety of Lenihan Dam during the Maximum Credible Earthquake. The report reviews previous findings related to site characterization, material properties and monitoring data; and then presents the results of seepage analyses, static stability analyses and pseudo-static yield accelerations, and seismic deformation analyses. A brief summary of each of these topics is presented below, followed by our conclusions and recommendations regarding the seismic safety evaluation of the dam.

6.2 SITE CHARACTERIZATION, MATERIAL PROPERTIES AND MONITORING DATA

The key findings related to site characterization, material properties and monitoring data are as follows:

1. The geometry of the valley where the dam was constructed is complex. The right side of the valley (looking downstream) has relatively uniform side slopes but the left side of the valley is characterized by a large knob of bedrock that underlies the upstream portion of the dam.
2. The dam is founded directly on bedrock – no alluvial or colluvial soils were left in place beneath the embankment.
3. With the exception of internal drainage zones, all embankment materials are well-compacted soils with varying amounts of sand and gravel in a clay matrix, and have very low permeabilities.
4. The drained and undrained shear strengths of the embankment materials are well-defined by extensive laboratory testing.
5. There are no liquefiable materials within the dam or the dam foundation.
6. The distribution of groundwater heads within the embankment and along the original outlet pipe is well defined by a large number of piezometers.
7. The vertical and lateral movements of the dam have been documented continually since the end of construction.
8. The dam experienced relatively minor damage during the Loma Prieta earthquake and measurements of permanent seismic displacements due to the earthquake are available as well as measurements of acceleration time histories from three seismographs, two located on the dam crest and one located on the left abutment.

6.3 SEEPAGE ANALYSES

Seepage analyses are used to define the distribution of groundwater heads and pore-water pressures under operating reservoir levels. These pore-water pressures allow effective stresses within the various embankment zones to be defined and, in turn, allow the calculation of undrained shear strengths based on these effective stresses.

The finite element seepage analyses showed good agreement between measured piezometric levels and calculated total heads and provide a reliable basis for defining pore-water pressures for stability and seismic deformation analyses.

6.4 STATIC STABILITY AND PSEUDO-STATIC YIELD ACCELERATIONS

The Factor of Safety for steady state seepage under full reservoir level is 2.1 and the Factor of Safety for rapid drawdown conditions is 2.6; these values exceed the minimum required values of 1.5 and 1.3, respectively, specified by the US Army Corps of Engineers (2003).

The yield accelerations from pseudo-static loading of the dam are as follows:

Loading Condition	Slope	Yield Acceleration
Full Reservoir and Steady State Seepage	Downstream	0.23g
	Upstream	0.33g
Loma Prieta Reservoir Level and Rapid Drawdown	Downstream	0.23g
	Upstream	0.28g

6.5 SEISMIC DEFORMATION ANALYSES

The measured performance of Lenihan Dam during the Loma Prieta earthquake provides an unusual and extremely valuable opportunity to develop a site-specific empirical basis that:

1. confirms the reasonableness of the overall approach based on FLAC with the Mohr-Coulomb soil model combined with the QUAD4MU equivalent linear analysis;
2. shows that the undrained shear strengths assigned to the embankment materials are reasonably conservative; and
3. indicates that the surface cracking pattern was possibly a result of high shaking combined with the bedrock topography.

The results of the FLAC analyses for the six evaluation ground motions that represent the Maximum Credible Earthquake indicate that the permanent seismic deformations of the dam are only slightly higher than the deformations measured during the Loma Prieta event. The overall similarity of the calculated seismic displacements and seismic responses may be in part due to the similarity of the spectral values of the input motions in the period range near the fundamental period of the embankment. The QUAD4MU and Equivalent Linear FLAC analyses indicate that the fundamental period of the embankment under these shaking conditions is about 1 second and the response spectral values of the Loma Prieta ground motion for this site are in fact slightly higher than those of the MCE evaluation ground motions for a period in the vicinity of 1 second.

To test the reasonableness of the seismic deformation estimates resulting from the FLAC analyses, both simplified Newmark-type analyses and a full Newmark-type analysis were used to estimate displacements based on yield accelerations and the MCE evaluation ground motions.

The estimates from these Newmark-type methods fall within the range of displacements estimated using FLAC and confirm the reasonableness of the FLAC results.

The results of the seismic deformation analyses indicate the following:

1. For the evaluation of the potential for the loss of freeboard, one can conservatively use a vertical crest settlement of about 1-1/2 feet and a horizontal downstream movement of about 1 foot. The estimated crest settlement includes the estimated vertical movement from the FLAC analyses plus an additional allowance of about 1 foot to account for earthquake-induced vertical movements that may be underestimated by the FLAC analyses.
2. The seismic deformations of the embankment elsewhere should be relatively small, but some locally larger seismic deformations (less than a few feet) may be possible. However, it is highly unlikely that these locally larger seismic deformations will affect the integrity of the dam.
3. Because the values of seismically-induced displacements from the MCE evaluation events are relatively small, the likelihood of significant cracks forming in the crest and other areas is considered very low. Furthermore, even if some cracks form, they would likely be shallow longitudinal cracks of limited extent, and not more serious than the cracking observed during the Loma Prieta event.

6.6 CONCLUSIONS

The engineering analyses described herein indicate that Lenihan Dam will perform well when subjected to the evaluation ground motions that represent the Maximum Credible Earthquake. Maximum crest settlements of about 1 ½ feet and horizontal downstream movement of about 1 foot have been estimated. The likelihood of significant cracks forming in the crest and other areas is considered very low. As a result, we have concluded that no seismic remedial measures are necessary at Lenihan Dam.

6.7 RECOMMENDATIONS

We recommend that piezometric levels, vertical and lateral movements, and seepage flows continue to be monitored and evaluated to assure the continued safe operation of the dam. We also recommend that the condition of the dam be inspected immediately following future earthquakes to check that movements and cracking are consistent with those expected based on our engineering analyses.

- Barneich, J.A., Beikae, M., Luebbbers, M., and Osmun, D., 1996 (July), Seismic Deformation Analysis of Eastside Reservoir Dams, The Sixteenth USCOLD Annual Meeting and Lecture.
- Bray, J.D. and Travarasrou, T., 2007, Simplified Procedure for Estimating Earthquake-Induced Deviatoric Slope Displacements, *Journal of Geotechnical and Geoenvironmental Engineering*, ASCE, 133 (4).
- Darendeli, M.B., 2001, Development of a New Family of Normalized Modulus Reduction and Material Damping Curves, PhD Dissertation, University of Texas at Austin.
- Frame, P.A. and Volpe, R.L., 2001 (October), Santa Clara Valley Water District (SCVWD) Phase B Instrumentation Project Basic Data Report.
- Geomatrix Consultants, 2006, Final Geologic and Geotechnical Data Report, Lenihan Dam Outlet Modification Project.
- Harza Engineering Company, 1997 (January), GEFDYN Verification of Lexington Dam, Draft Report, prepared for Tennessee Valley Authority.
- Idriss, I. M., 2003, Personal communication.
- Itasca, 2008, FLAC, version 6.0, Itasca Consulting Group Inc., Minneapolis.
- Makdisi, F. and Seed, H., 1978, Simplified Procedure for Estimating Dam and Embankment Earthquake-Induced Deformations, *Journal of Geotechnical Engineering*, ASCE, 104 (7).
- McLaughlin, R.J., Oppenheimer, D., Helley, E.J., and Sebrier, M., 1992, The Lexington fault zone: a north-south link between the San Andreas fault and range front fault system, Los Gatos, California: *Geologic Society of America Abstracts with Programs*, v. 24, no. 5, p. 69.
- Newmark, N.M., 1965, Effects of earthquakes on dams and embankments, *Geotechnique*, London, Vol. 15, No. 2, pp. 139-160.
- Swaigood, S.R., 2003, Embankment dam deformations caused by earthquakes, 2003 Pacific Conference on Earthquake Engineering.
- Tan, P., 2003, Addendum to User's Manual for QUAD4M for updates to the QUAD4MU version.
- Terra / GeoPentech, 2011a (April), Seismic Stability Evaluations of Chesbro, Lenihan, Stevens Creek, and Uvas Dams, Phase A: Stevens Creek and Lenihan Dams, Lenihan Dam, Work Plan for Site Investigations and Laboratory Testing (Report No. LN-1), prepared for Santa Clara Valley Water District.
- Terra / GeoPentech (TGP), 2011b (November), Seismic Stability Evaluations of Chesbro, Lenihan, Stevens Creek, and Uvas Dams, Phase A: Stevens Creek and Lenihan Dams, Lenihan Dam, Site Characterization, Material Properties and Ground Motion (Report No. LN-3), prepared for Santa Clara Valley Water District.
- US Army Corps of Engineers, 2003, EM 1110-2-1902 Engineer Manual – Slope Stability.

- Volpe, R.L. and Associates (RLVA), 1990, Investigation of SCVWD Dams Affected by Loma Prieta Earthquake of October 17, 1989, Report to Santa Clara Valley Water District.
- Volpe, R.L. and Associates (RLVA), 1998, Instrumentation Design and Review, Lenihan Dam, Draft Report to Santa Clara Valley Water District.
- Volpe, R.L. and Associates (RLVA), 1999a, Lenihan Dam Outlet Investigation, Vol. 1 – Final Engineering Report.
- Volpe, R.L. and Associates (RLVA), 1999b, Lenihan Dam Outlet Investigation, Vol. 2 – Basic Data Report.
- Vucetic, M. and Dobry, R., 1991, Effect of Soil Plasticity on Cyclic Response, Journal of Geotechnical Engineering Division, ASCE, Vol. 117, No. 1, pp.89-107.
- Wahler Associates, 1982, Final Report on Seismic Safety Evaluation of Lexington Dam.

TABLES

TABLE 2-1
MATERIAL CLASSIFICATION SUMMARY

Zone ²	Idealized Material Description	Generalized USCS Classification	In-Situ Conditions ³			Gradation ³				Atterberg Limits ³	
			Dry Unit Weight, γ_d (pcf)	Moisture Content, W_c (%)	Compaction (%) ⁴	Gravel (%)	Sand (%)	Fines (%)	Clay Fraction, -2μ (%)	Liquid Limit LL	Plasticity Index PI
1	Upstream Shell	SC, CL	119.3 (95.2 - 132.3)	15.0 (10.3 - 26.5)	95 (76 - 106)	27 (0 - 43)	34 (3 - 44)	39 (19 - 97)	21 (12 - 44)	33 (30 - 39)	15 (6 - 24)
2U	Upper Core (Above El. 590 ft)	SC, GC	119.6 (108.0 - 131.5)	11.9 (6.0 - 17.7)	95 (81 - 112)	33 (3 - 58)	35 (23 - 48)	31 (16 - 53)	17 (13 - 30)	37 (30 - 48)	17 (14 - 29)
2L	Lower Core (Below El. 590 ft)	CH, SM-MH	99.9 (89.7 - 111.2)	24.1 (17.8 - 37.1)	101 (91 - 113)	6 (0 - 29)	15 (3 - 43)	79 (29 - 97)	42 (16 - 53)	62 (43- 70)	35 (15- 48)
4	Downstream Shell	SC, GC	124.3 (100.6 - 143.3)	11.9 (6.2 - 19.9)	89 (72 - 102)	32 (13 - 56)	38 (16 - 60)	30 (15 - 63)	17 (11- 26)	33 (22 - 46)	15 (6 - 29)

Notes:

1. Data in this table are averages with minimum and maximum values in parentheses. No data is available for Drain Material (Zone 3).
2. See Figure 2-6.
3. In-situ conditions, gradation and Atterberg limits are summarized based on laboratory testing performed by Wahler (1981), Geomatrix (1996), Harza (1997), RLVA (1999), Frame and Volpe (2001), and Terra / GeoPentech (2011c).
4. Per D1557 modified, 20,000 ft-lbs.

TABLE 2-2
SUMMARY OF ENGINEERING PROPERTIES

Zone	Moist Unit Weight (pcf) γ_t	Effective Friction Angle ⁽¹⁾ ϕ'	Triaxial Undrained Strength Parameter ⁽²⁾ S_u/σ_{vc}'	Stress-Strain Strength Relationship ⁽³⁾ E_{u50} / S_u	Shear Wave Velocity, V_s ⁽⁴⁾ (ft/sec)	
					K (ft/sec)	n
1	138	37.5 °	$e^{[-0.22 \cdot \ln(\sigma_{vc}') + 0.12]}$	140	1305	0.25
2U	132	35.5 °	$e^{[-0.20 \cdot \ln(\sigma_{vc}') - 0.01]}$	180	1190	0.25
2L	124	25.5 °	$e^{[-0.27 \cdot \ln(\sigma_{vc}') - 0.15]}$	170	680	0.25
4	140	35 °	$e^{[-0.21 \cdot \ln(\sigma_{vc}') - 0.12]}$	180	1550	0.25

Notes:

⁽¹⁾ Effective Friction Angle, ϕ' (with no cohesion)

⁽²⁾ σ_{vc}' in ksf; minimum S_u for all soils = 2.0 ksf

⁽³⁾ Stress-Strain Strength Relationship

E_{u50} = Undrained Secant Modulus at 50% S_u

⁽⁴⁾ Shear Wave Velocity, V_s

$V_s = K \cdot (\sigma_{vc}'/p_a)^n$ where K is in ft/sec

TABLE 2-3
RESULTS OF PERMEABILITY TESTS

Material	Measured Permeability, cm/sec			Estimated Permeability, cm/sec (RLVA, 1999a)	
	Triaxial Test	1-Dimensional Consolidation	Field CPT	Horizontal	Vertical
Upstream Shell	1.7 x 10 ⁻⁸ 3.3 x 10 ⁻⁸ 2.9 x 10 ⁻⁹	2.0 x 10 ⁻⁹	3.7 x 10 ⁻⁸ 7.3 x 10 ⁻⁷ 7.2 x 10 ⁻⁷ 7.9 x 10 ⁻⁸ 7.3 x 10 ⁻⁹	5 x 10 ⁻⁸	5 x 10 ⁻⁹
Upper Core	1.7 x 10 ⁻⁸	2.5 x 10 ⁻⁸	2.4 x 10 ⁻⁸ 1.0 x 10 ⁻⁸ 1.1 x 10 ⁻⁸ 1.0 x 10 ⁻⁸	1 x 10 ⁻⁸	1.0 x 10 ⁻⁹
Lower Core	6.6 x 10 ⁻⁹ 4.5 x 10 ⁻⁹ 5.3 x 10 ⁻⁹ 8.1 x 10 ⁻⁹ 4.4 x 10 ⁻⁹ 1.1 x 10 ⁻⁹	5.0 x 10 ⁻⁸ 2.5 x 10 ⁻⁹	1.2 x 10 ⁻⁸ 5.7 x 10 ⁻⁹ 2.4 x 10 ⁻⁸	1 x 10 ⁻⁸	5 x 10 ⁻⁹
Downstream Shell	3.1 x 10 ⁻⁶			1 x 10 ⁻⁷	1 x 10 ⁻⁷
Foundation	3.3 x 10 ⁻⁹				

Data from RLVA (1999a)

TABLE 3-1
SUMMARY OF PERMEABILITY VALUES

Material	Volpe (1999) Estimate		Initial TGP Estimate		Final TGP Estimate	
	k_h, ft/yr	k_y, ft/yr	k_h, ft/yr	k_y, ft/yr	k_h, ft/yr	k_y, ft/yr
Upstream Shell	0.05	0.005	0.05	0.0025	0.05	0.0025
Upper Core	0.01	0.001	0.05	0.0025	0.05	0.0025
Lower Core	0.01	0.001	0.01	0.0005	0.01	0.0005
Downstream Shell	0.1	0.1	0.1	0.005	0.05	0.0025
Inclined Drain	-	-	100	100	0.05	0.0025
Rock Blanket	-	-	1000	1000	5	5
Bedrock	-	-	0.05	0.05	0.05	0.05
Pipe Backfill - Limestone	-	-	-	-	20	1
Pipe Backfill - Shale	-	-	-	-	0.10	0.0025

TABLE 5-1A
CHARACTERISTICS OF SELECTED EARTHQUAKE RECORDS
FOR STANFORD-MONTE VISTA EVENT

No.	Earthquake Event	Recording Station	Style of Faulting ⁽¹⁾	Magnitude (Mw)	Closest Distance (km)	NEHRP Site Class/V _{s30}	Highest Usable Period (sec)	Event Date
1	Kobe	Nishi-Akashi	SS	6.9	7.1	C/609	8	1/16/1995
2	Loma Prieta	LGPC	RV/OBL	6.9	3.9	C/478	8	10/18/1989
3	Northridge	Sylmar-Olive View Med. FF	RV	6.7	5.3	C/440	8.3	1/17/1994

TABLE 5-1B
CHARACTERISTICS OF SELECTED EARTHQUAKE RECORDS
FOR SAN ANDREAS EVENT

No.	Earthquake Event	Recording Station	Style of Faulting ⁽¹⁾	Magnitude (Mw)	Closest Distance (km)	NEHRP Site Class/V _{s30}	Highest Usable Period (sec)	Event Date
1	Chi-Chi	TCU065	RV/OBL	7.6	0.7	D/305	13.3	9/20/1999
2	Landers	Lucerne	SS	7.3	2.2	C/684	10.0	6/28/1992
3	Manjil	Abbar	SS	7.4	12.6	C/724	7.7	11/03/1990

TABLE 5-2
SUMMARY OF CALCULATED DEFORMATIONS

Case ⁽¹⁾	Input GM	Polarity	Crest Displacement ⁽²⁾		Upstream Slope ⁽³⁾		Downstream Slope ⁽³⁾		Critical ⁽⁴⁾
			Horiz (ft)	Vert (ft)	Horiz (ft)	Vert (ft)	Horiz (ft)	Vert (ft)	
SA1	Chi Chi Scaled Input Motion	Normal	0.8	-0.2	-0.4	0.7	2.8	0.3	Yes
	Chi Chi Scaled Input Motion	Negative	0.4	-0.2	-1.1	0.5	2.6	0.4	No
	Landers Scaled Input Motion	Normal	0.1	-0.2	-0.7	0.2	0.7	0.1	No
SA2	Landers Scaled Input Motion	Negative	1.1	-0.3	0.4	0.3	1.5	0.1	Yes
	Manjil Scaled Input Motion	Normal	0.4	-0.1	-0.5	0.4	1.5	0.1	No
SA3	Manjil Scaled Input Motion	Negative	0.4	-0.1	-0.7	0.4	1.5	0.1	Yes
SMV1	Kobe Scaled Input Motion	Normal	0.7	-0.2	-0.3	0.5	2.0	0.2	Yes
	Kobe Scaled Input Motion	Negative	0.4	-0.1	-0.9	0.4	1.7	0.2	No
	Loma Prieta Scaled Input Motion	Normal	0.2	-0.1	-0.7	0.4	1.3	0.2	No
SMV2	Loma Prieta Scaled Input Motion	Negative	0.6	-0.2	-0.5	0.4	1.5	0.2	Yes
SMV3	Northridge Scaled Input Motion	Normal	0.9	-0.2	0.5	0.3	1.7	0.1	Yes
	Northridge Scaled Input Motion	Negative	0.1	0.1	-0.8	0.2	0.8	0.2	No

Notes:

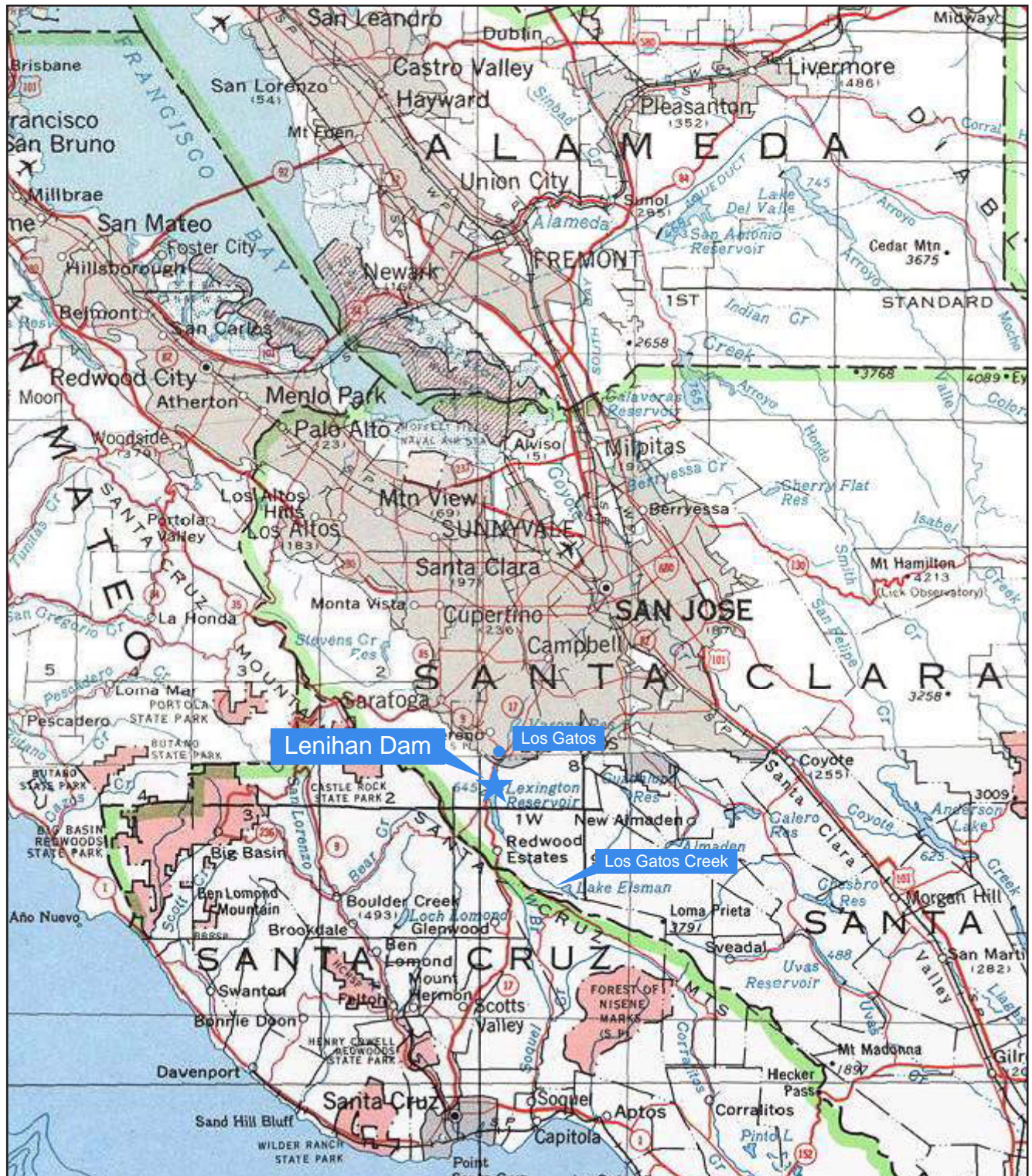
⁽¹⁾ Only the critical case between normal and negative polarity is assigned a Case Number.

⁽²⁾ Negative vertical displacement indicates settlement.

⁽³⁾ Positive horizontal displacement indicated movement towards downstream.

⁽⁴⁾ The critical case between the two polarities was chosen based on the magnitude of the calculated crest displacements.

FIGURES



0 5 10 15 20 miles

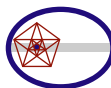
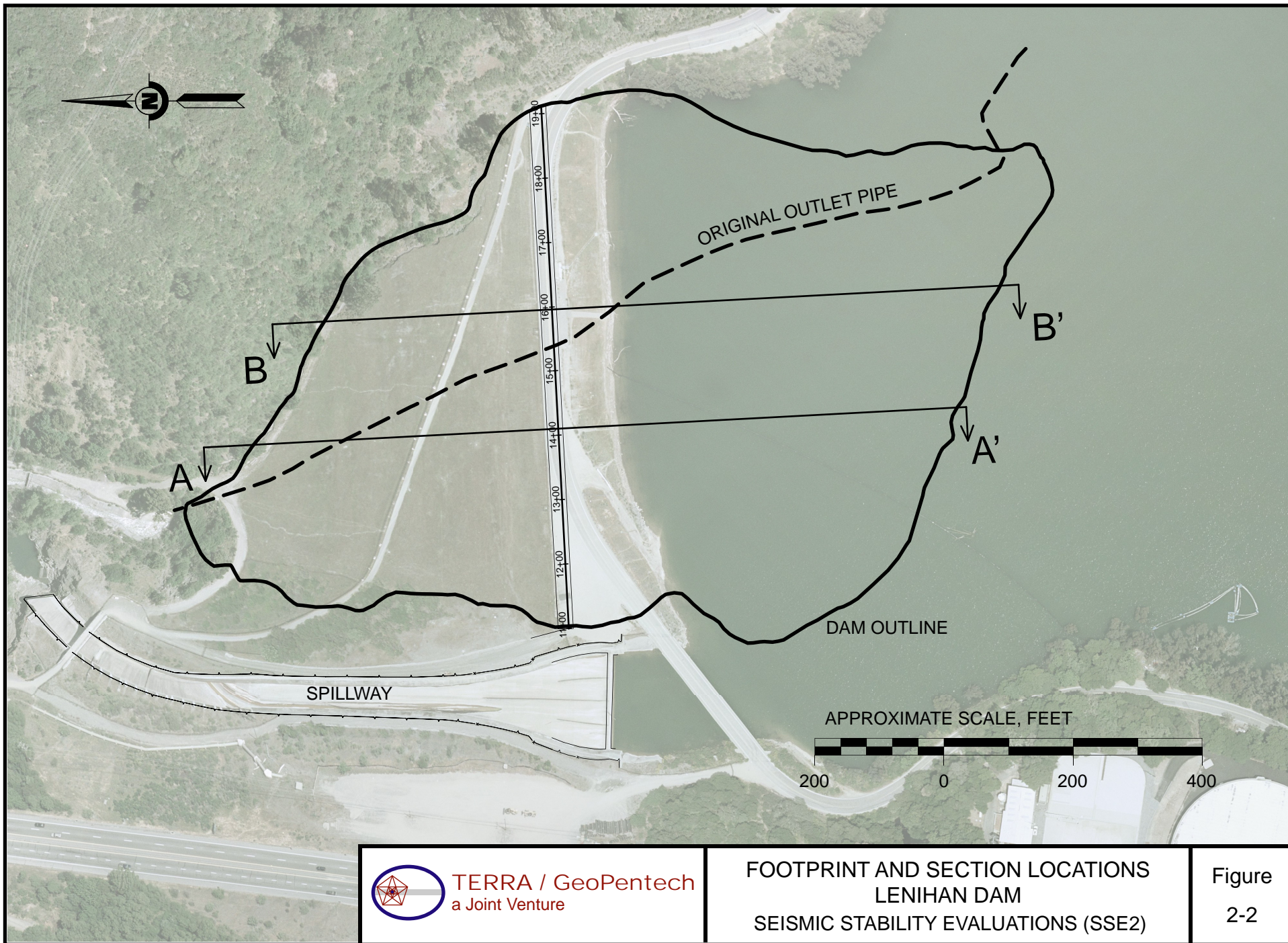
Note: Base map printed from USGS 1:24,000 scale topographic maps by TOPO! © 2003 National Geographic.



TERRA / GeoPentech
a Joint Venture

**REGIONAL SITE LOCATION MAP
LENIHAN DAM
SEISMIC STABILITY EVALUATIONS (SSE2)**

**Figure
2-1**

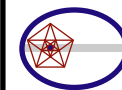
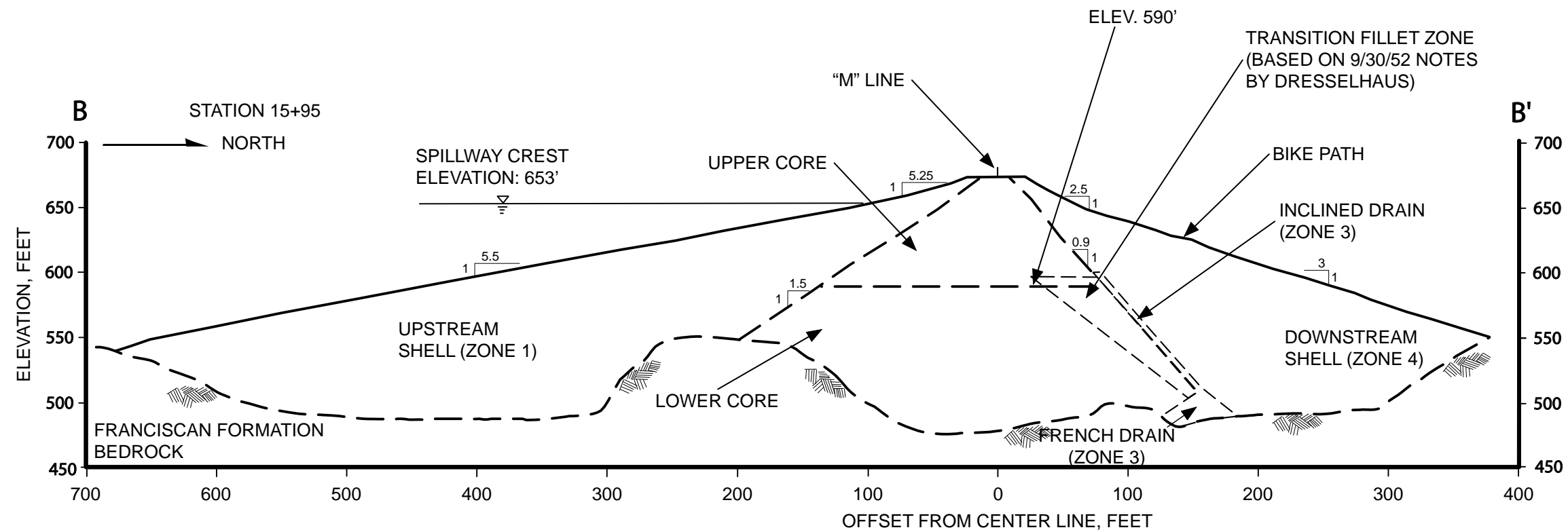
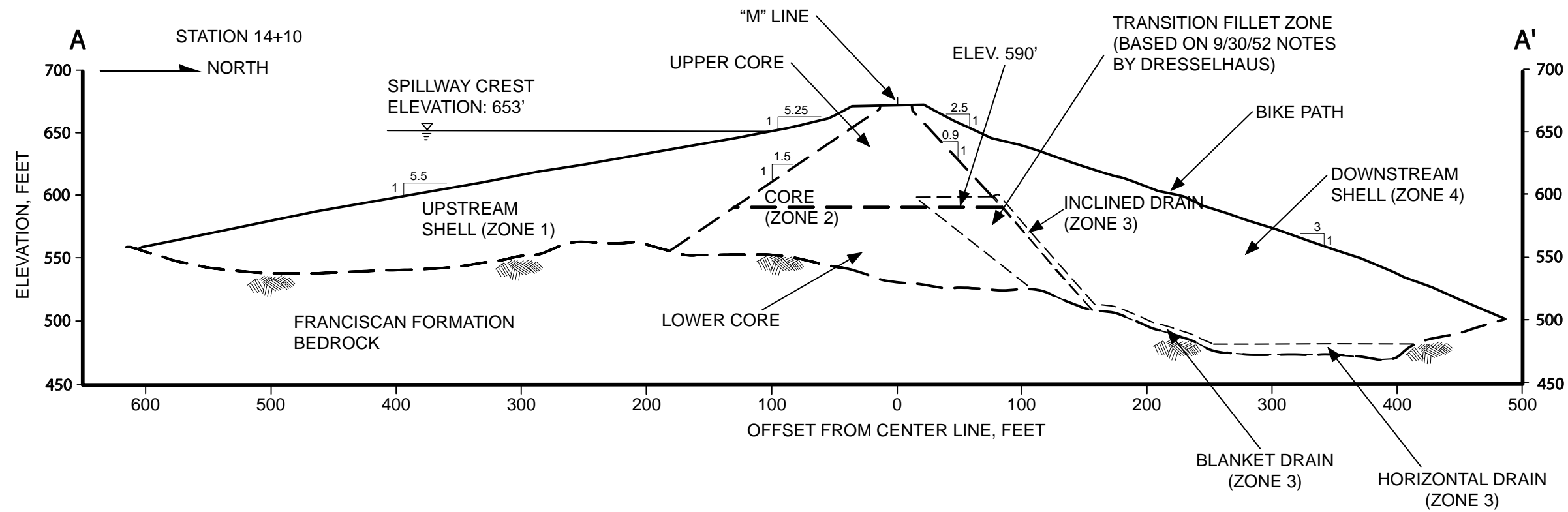


TERRA / GeoPentech
a Joint Venture

**FOOTPRINT AND SECTION LOCATIONS
LENIHAN DAM
SEISMIC STABILITY EVALUATIONS (SSE2)**

**Figure
2-2**

Rev. 0 03/16/2012 SSE2-R-4LN

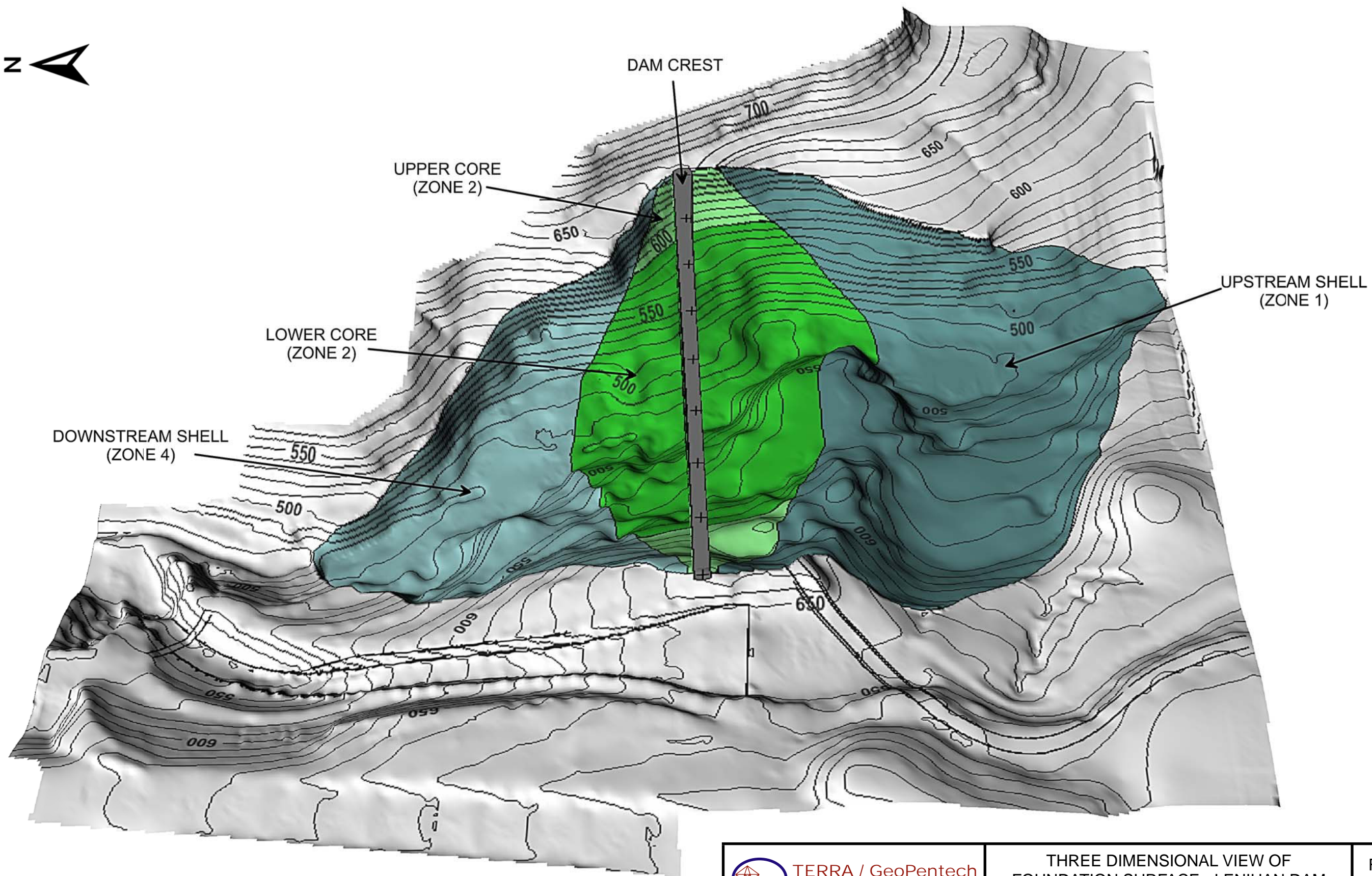


TERRA / GeoPentech
a Joint Venture

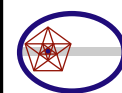
CROSS SECTIONS A-A' AND B-B'
LENIHAN DAM
SEISMIC STABILITY EVALUATIONS (SSE2)

Figure
2-3

0' 100' 200' 300' 400'



Note:
1. Contacts of various dam zones with foundation surface are shown.

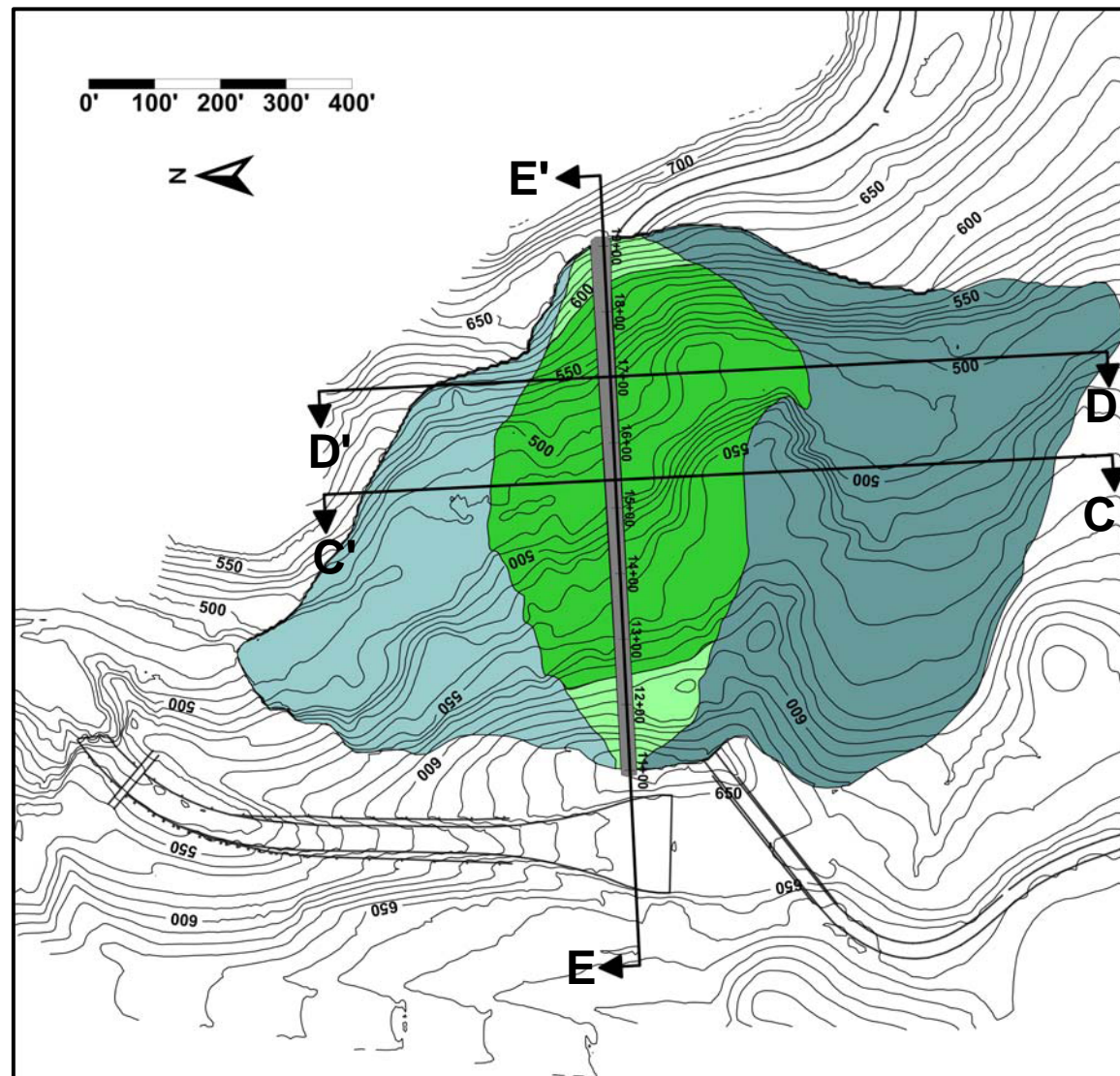


TERRA / GeoPentech
a Joint Venture




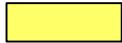


THREE DIMENSIONAL VIEW OF
FOUNDATION SURFACE - LENIHAN DAM
SEISMIC STABILITY EVALUATIONS (SSE2)

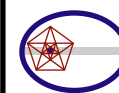
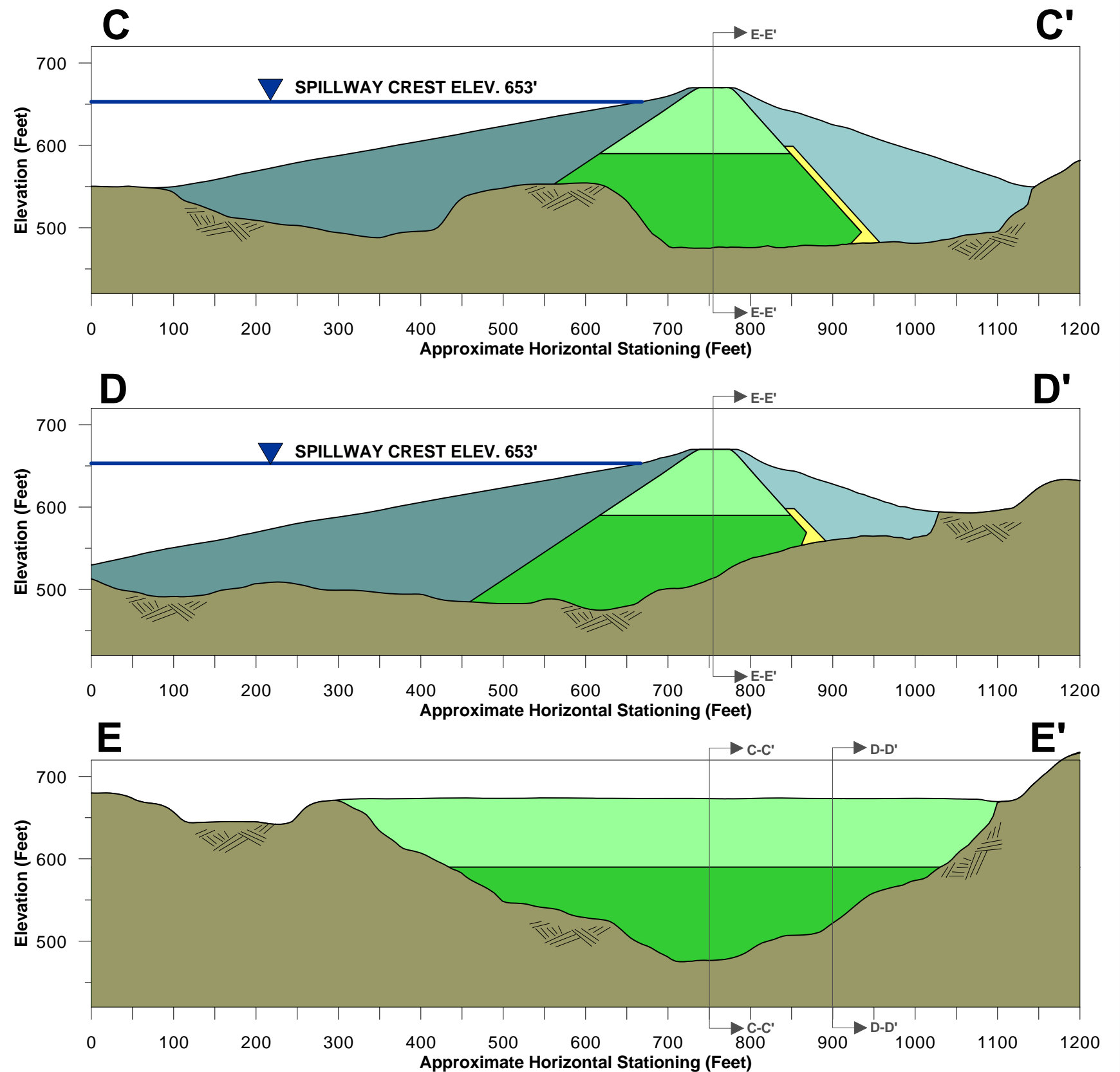
Figure
2-4

CROSS SECTION LOCATION MAP



LEGEND

-  Upstream Shell (Zone 1)
-  Lower Core (Zone 2, Below El. 590)
-  Upper Core (Zone 2, Above El. 590)
-  Drain Zone (Zone 3)
-  Downstream Shell (Zone 4)
-  Franciscan Complex Bedrock



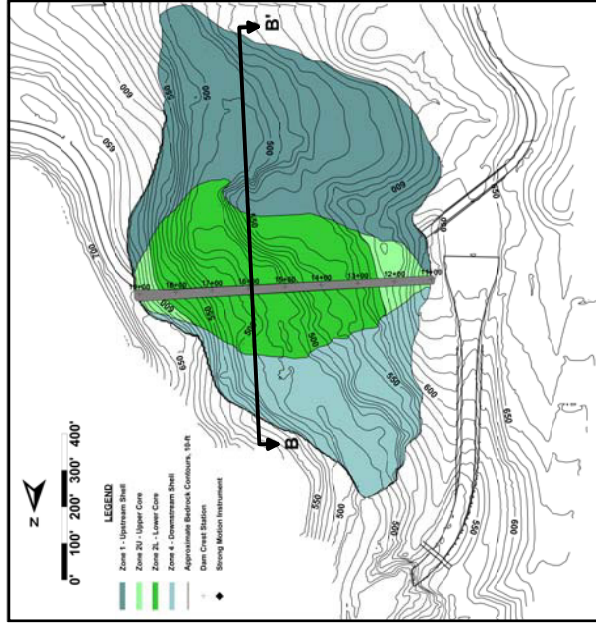
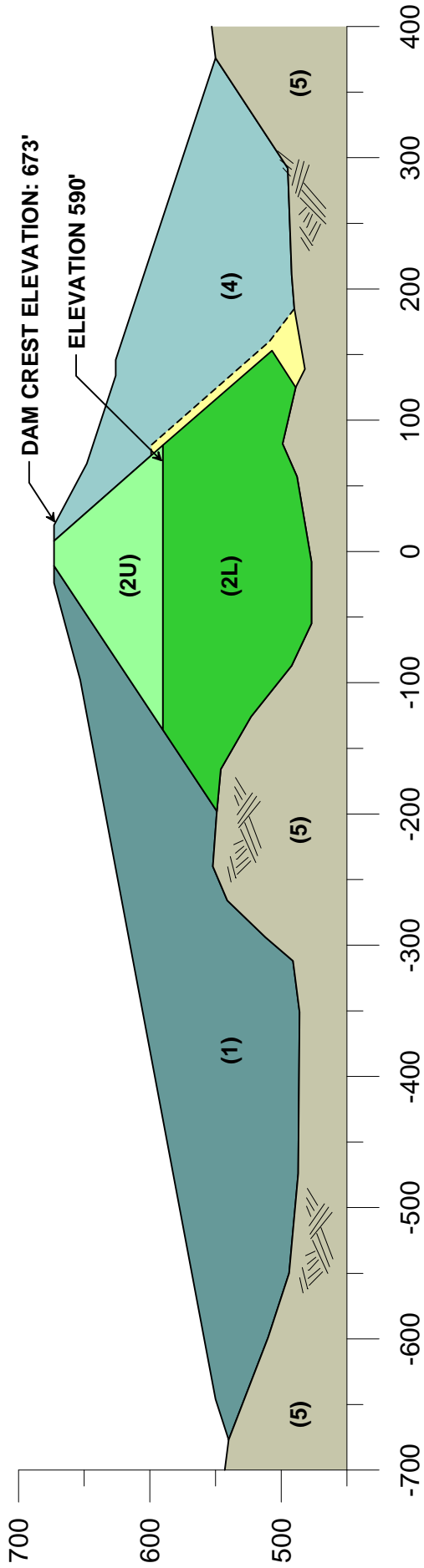
TERRA / GeoPentech
a Joint Venture

CROSS SECTIONS WITH FOUNDATION
SURFACE - LENIHAN DAM
SEISMIC STABILITY EVALUATIONS (SSE2)

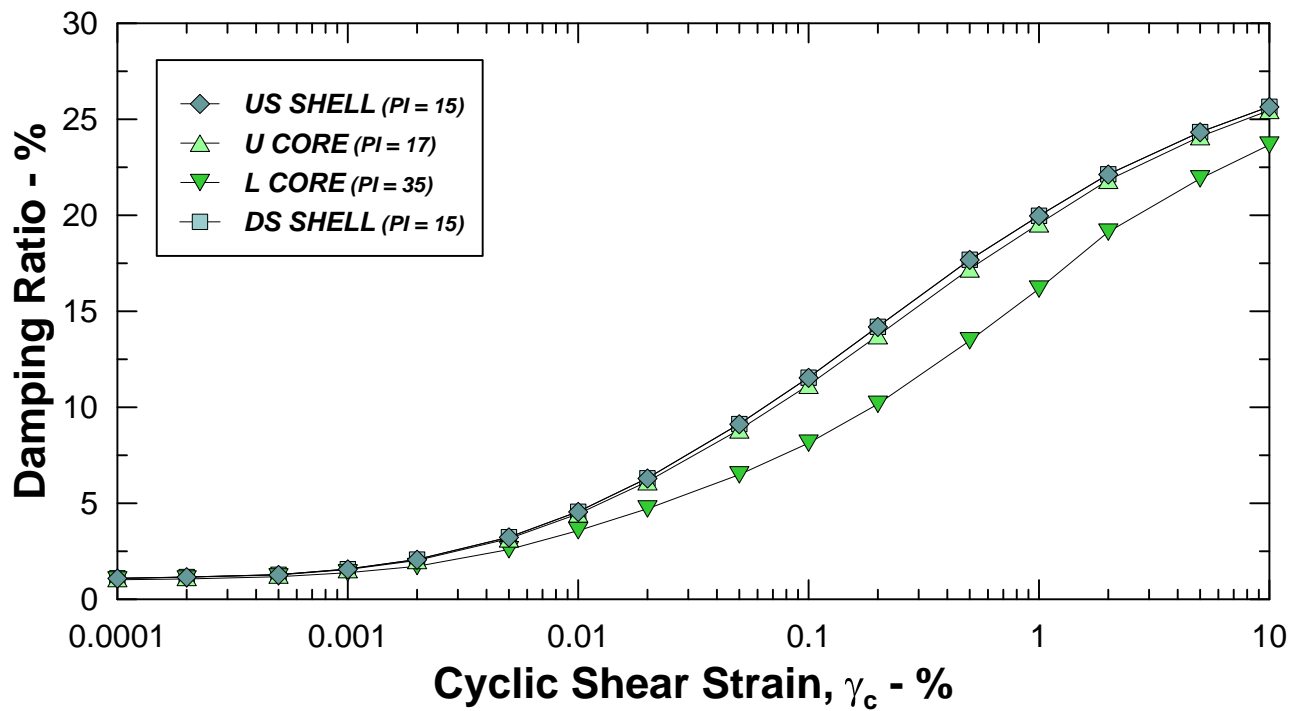
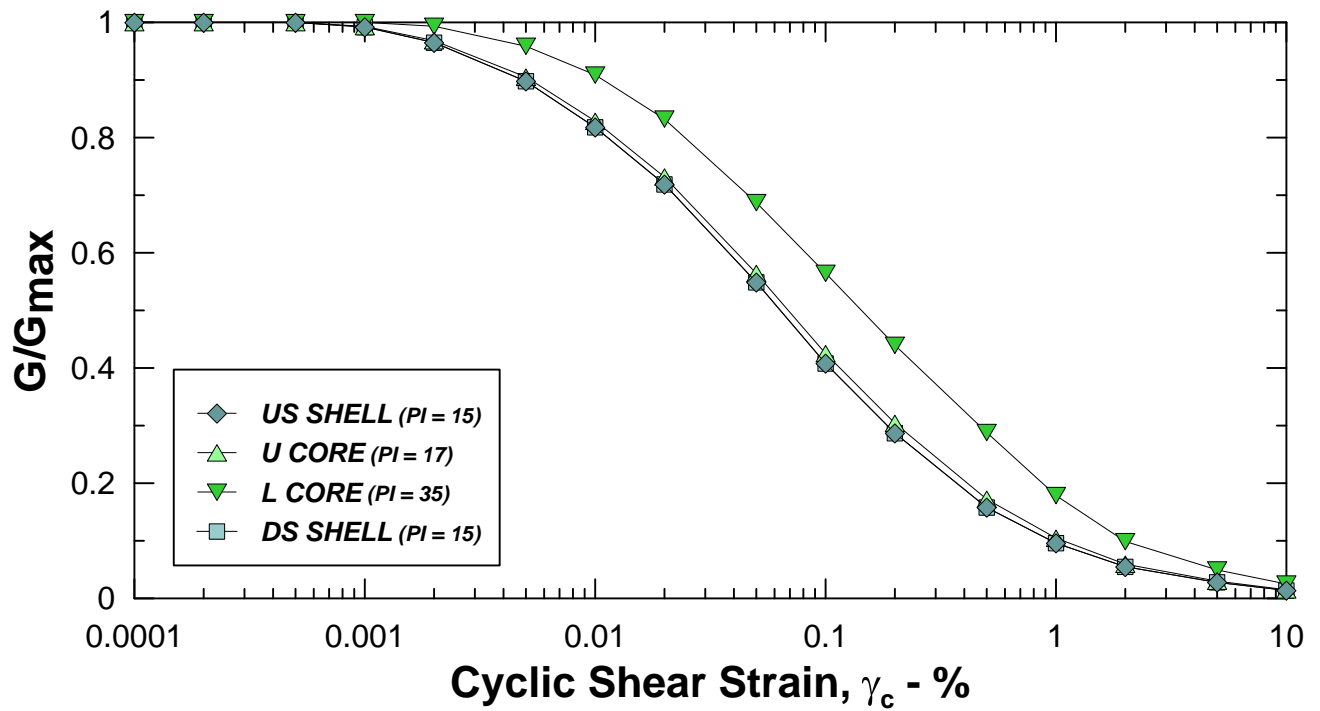
Figure
2-5

B

B'



Zone	Color Code	Material Description	Predominant Soil Classification
1		Upstream Shell	Gravely Clayey Sands (SC) to Sandy Clays (CL)
2U		Upper Core (Above El. 590)	Gravely Clayey Sands (SC) to Clayey Gravels (GC)
2L		Lower Core (Below El. 590)	Sandy Highly Plastic Clays (CH) to Silty Sands-Sandy Highly Plastic Silts (SM/MH)
3		Drain Material	N/A
4		Downstream Shell	Gravely Clayey Sands (SC) to Clayey Gravels (GC)
5		Bedrock	Franciscan Complex



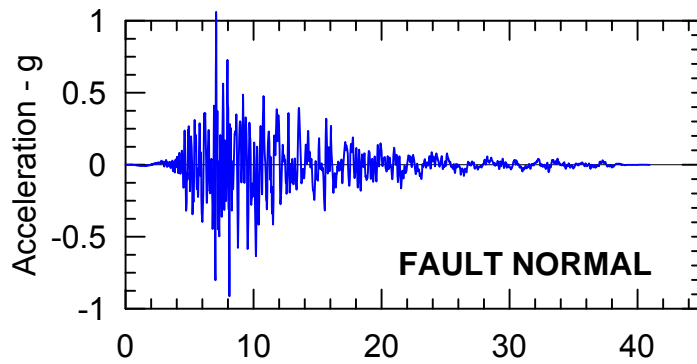
Note: Modulus reduction and damping ratio curves are based on Vucetic and Dobry, 1991



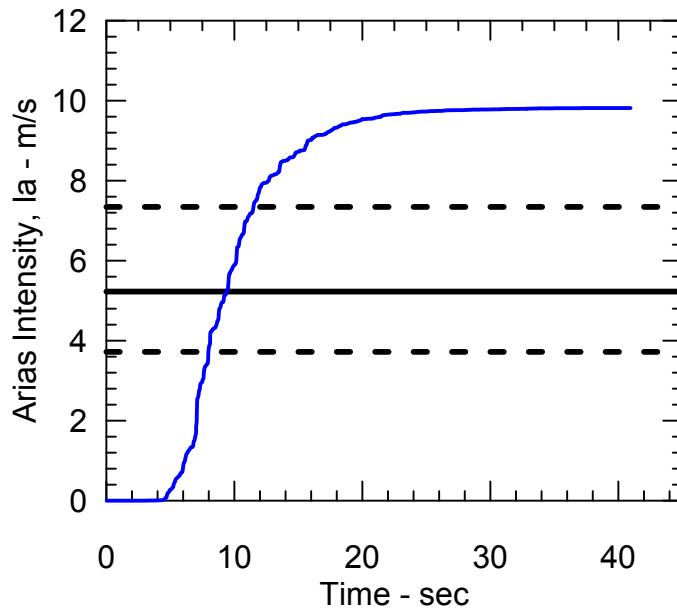
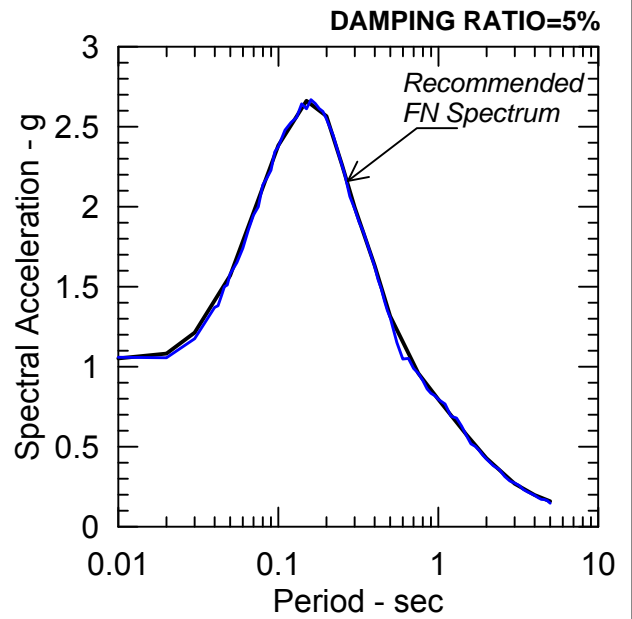
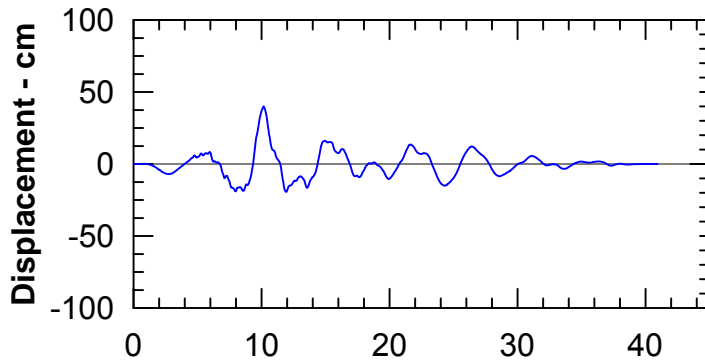
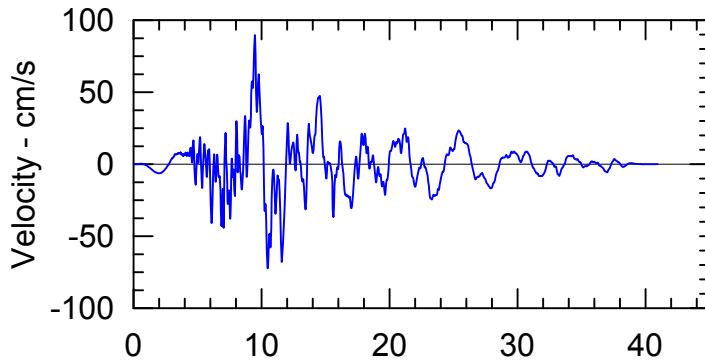
TERRA / GeoPentech
a Joint Venture

MODULUS REDUCTION AND DAMPING
RATIO CURVES - LENIHAN DAM
SEISMIC STABILITY EVALUATIONS (SSE2)

Figure
2-7



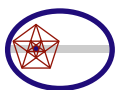
**Kobe - Nishi-Akashi
Strike Slip Event
Rotated to Fault Normal
Spectrally Matched to SMV**

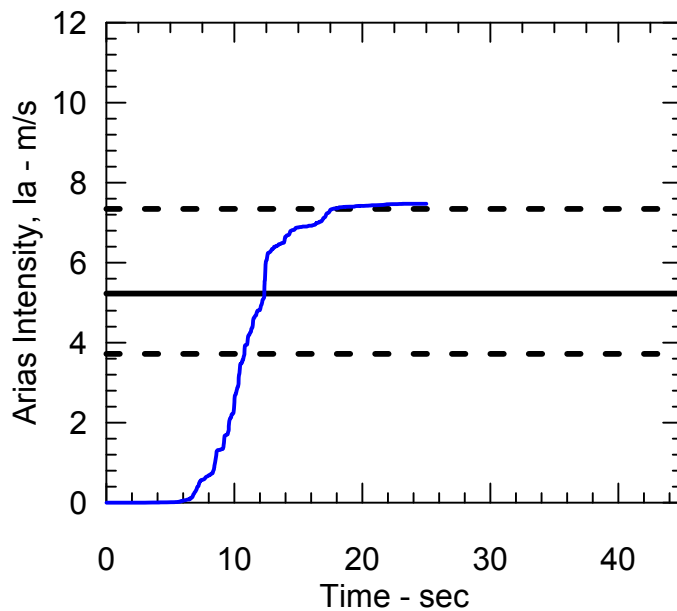
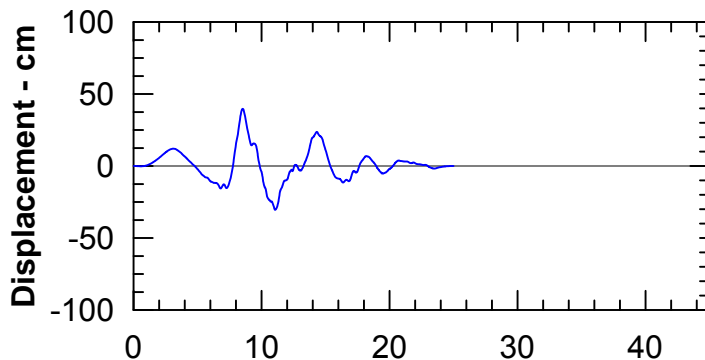
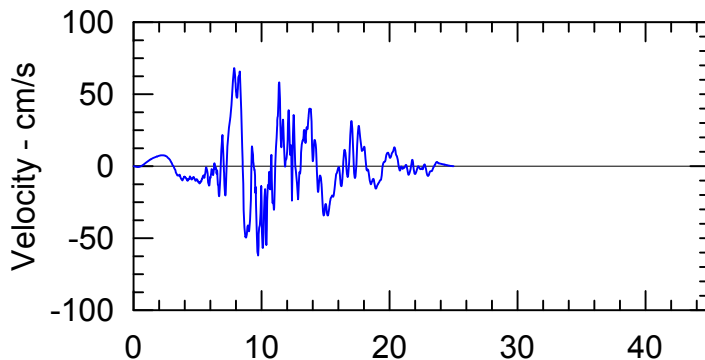
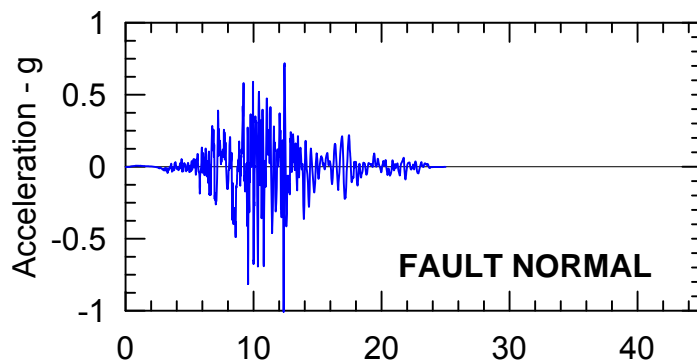


Watson-Lamprey I_a plus σ

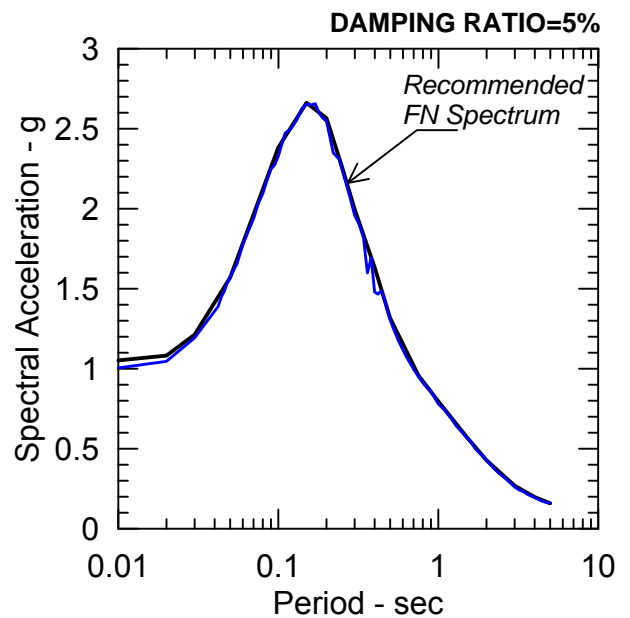
I_a from Watson-Lamprey (2007)
@84th Percentile [5.2 m/s]

Watson-Lamprey I_a minus σ





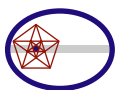
***Loma Prieta - LGPC
Reverse Oblique Event
Rotated to Fault Normal
Spectrally Matched to SMV***

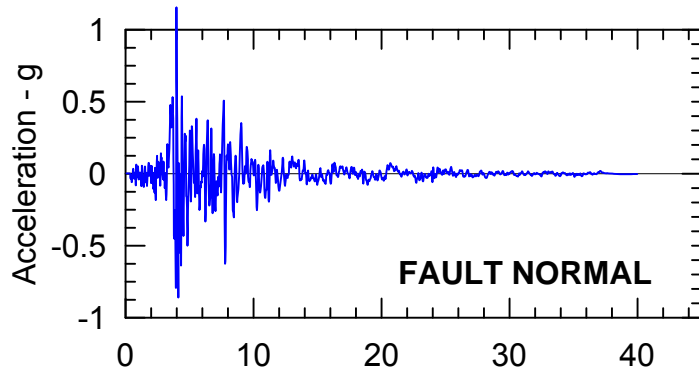


Watson-Lamprey I_a plus σ

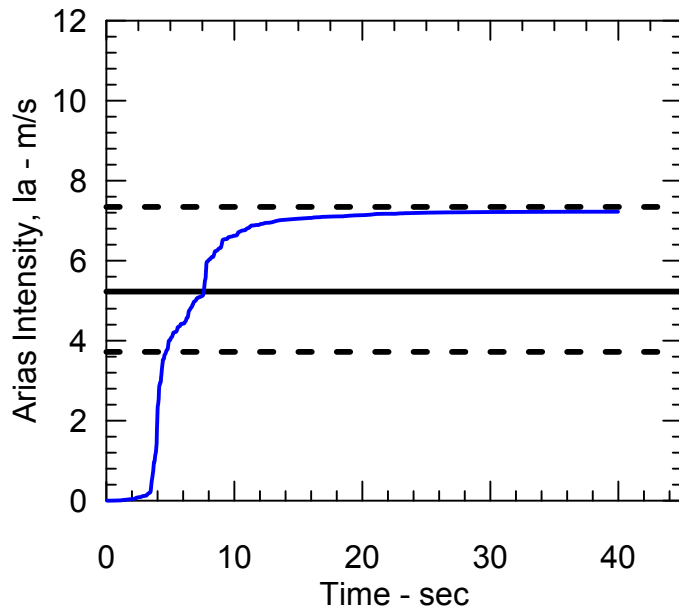
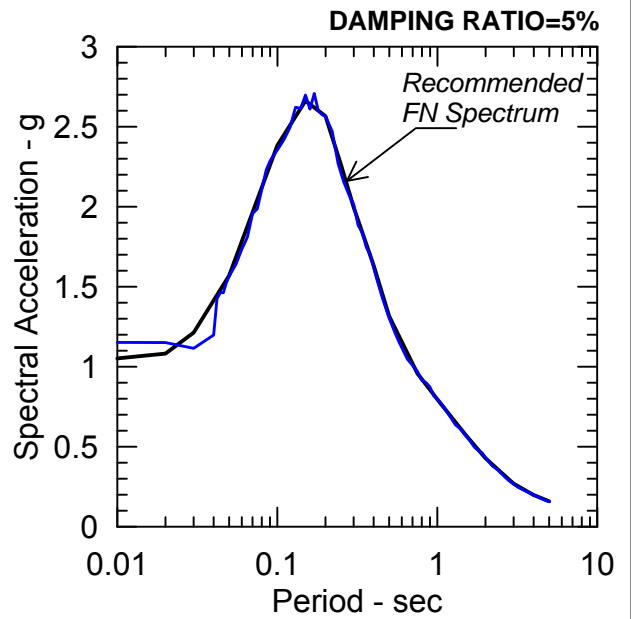
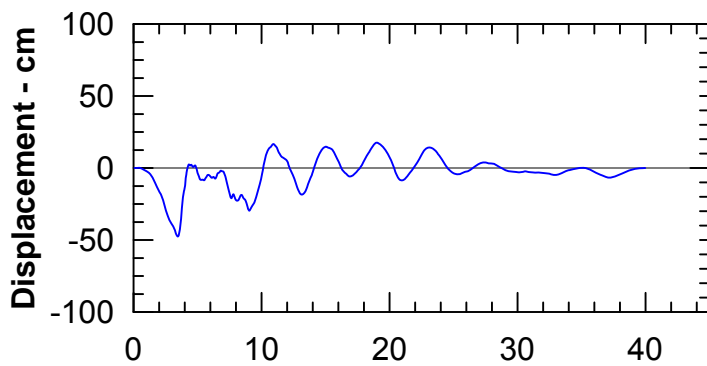
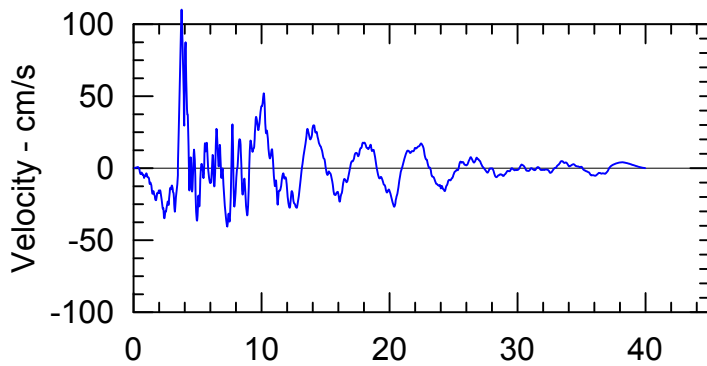
I_a from Watson-Lamprey (2007)
@84th Percentile [5.2 m/s]

Watson-Lamprey I_a minus σ

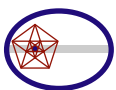


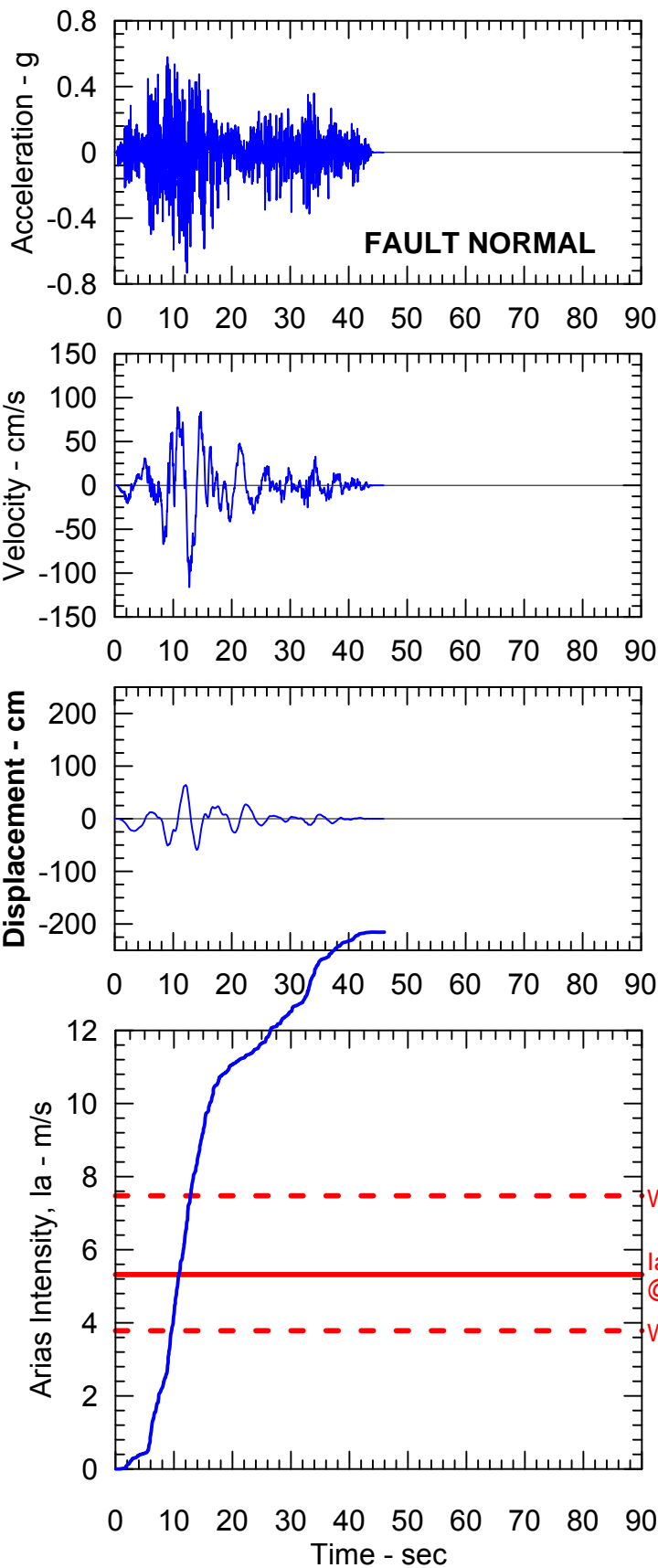


**Northridge - Sylmar
Reverse Event
Rotated to Fault Normal
Spectrally Matched to SMV**

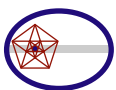
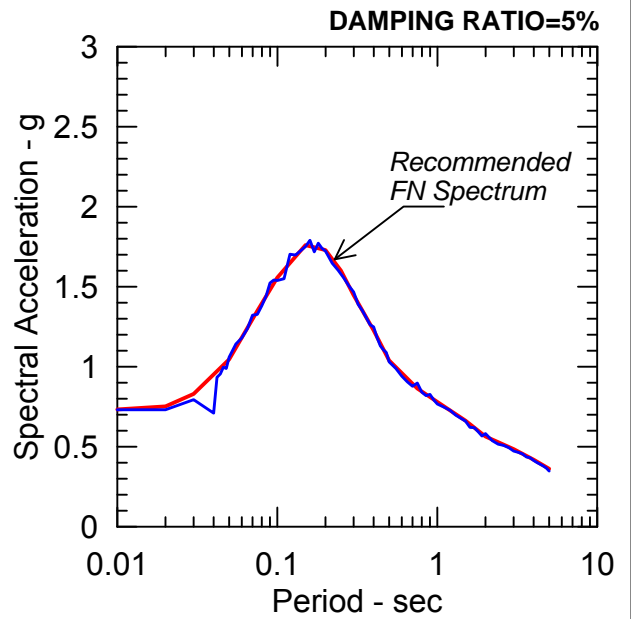


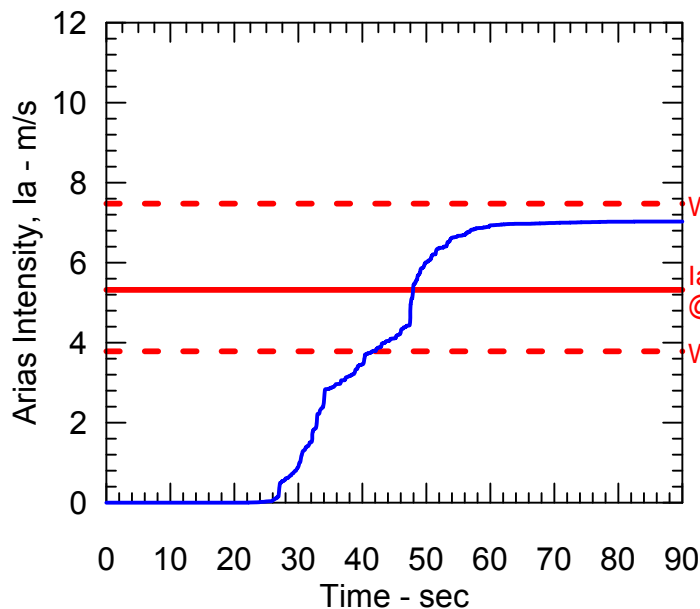
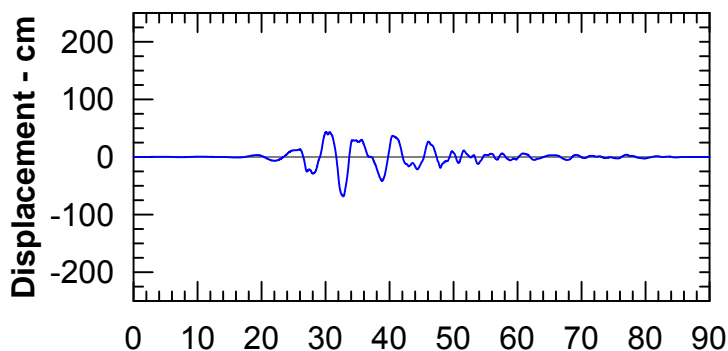
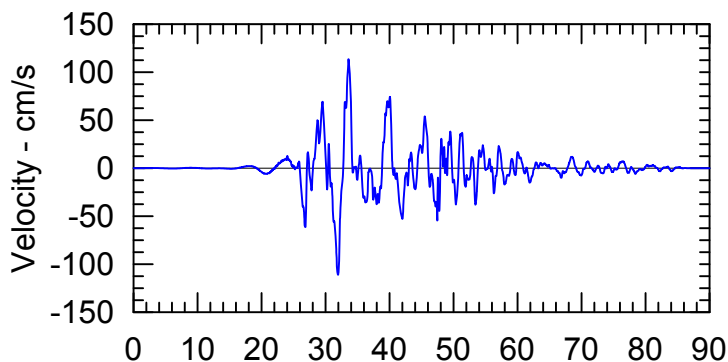
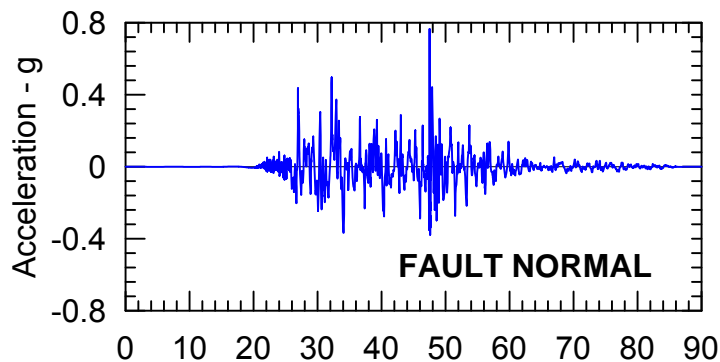
Watson-Lamprey Ia plus σ
Ia from Watson-Lamprey (2007)
@84th Percentile [5.2 m/s]
Watson-Lamprey Ia minus σ



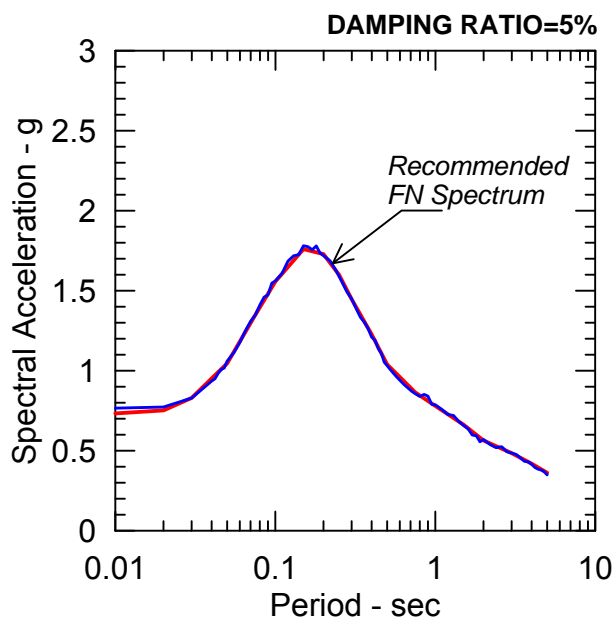


**Manjil - Abbar
Strike Slip Event
Rotated to Fault Normal
Spectrally Matched to SA**



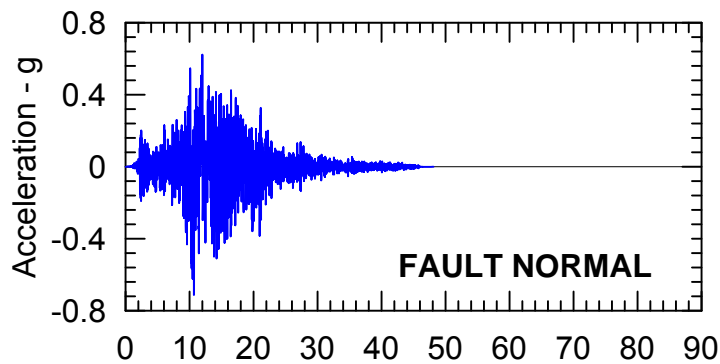


Chi Chi - TCU065
Reverse-Oblique Event
Rotated to Fault Normal
Spectrally Matched to SA

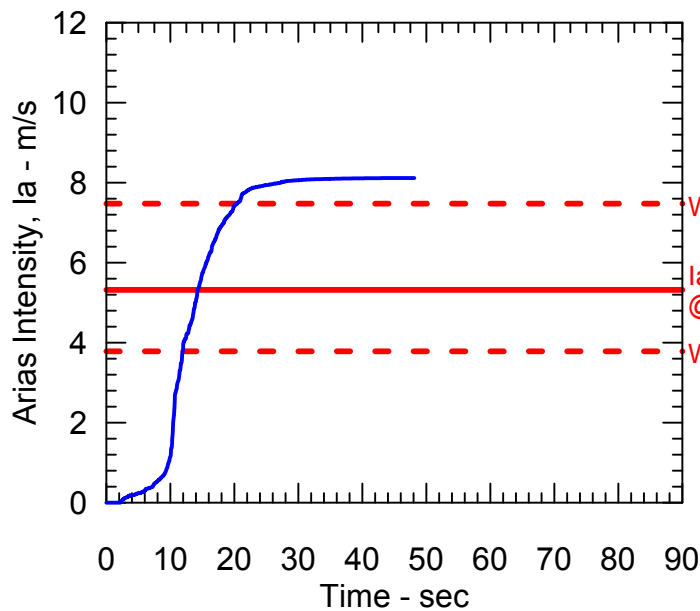
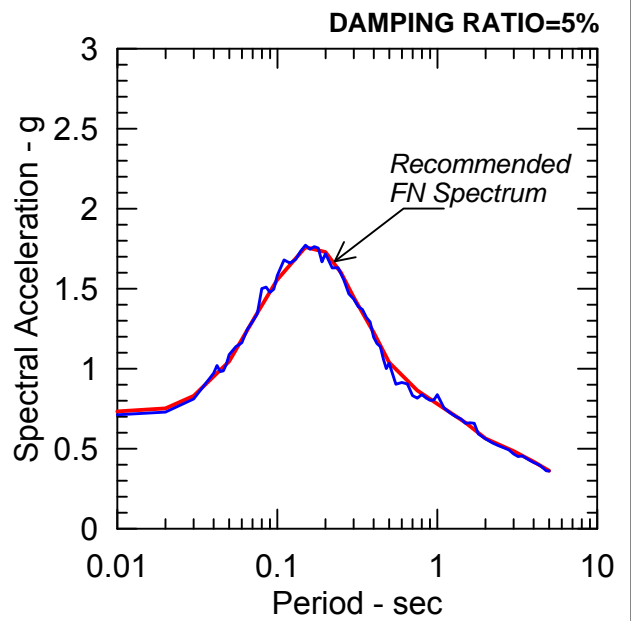
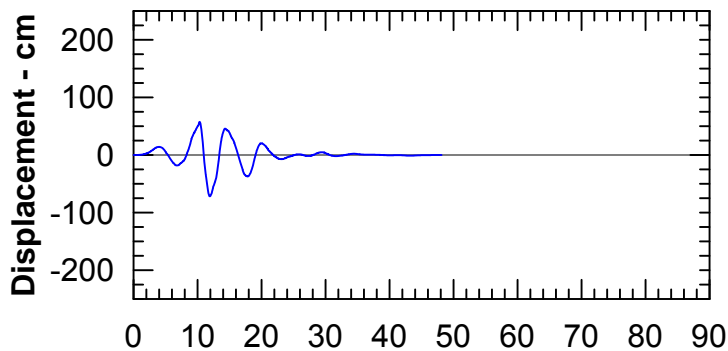
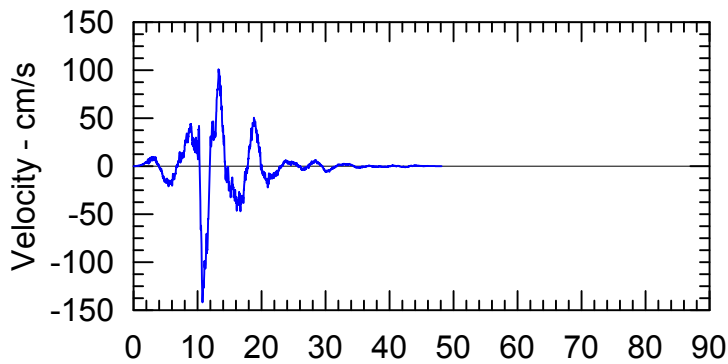


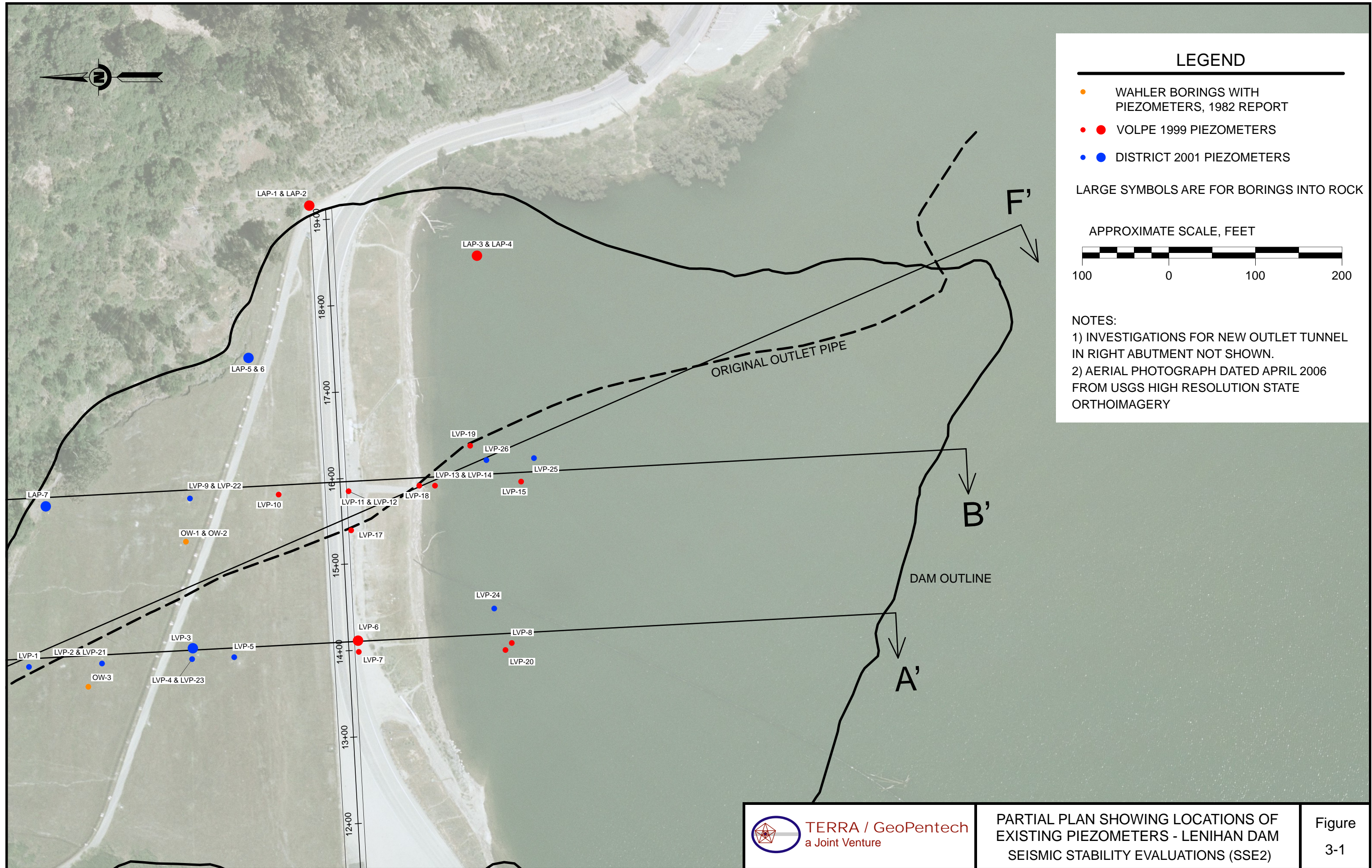
Watson-Lamprey I_a plus σ
 I_a from Watson-Lamprey (2007)
 @84th Percentile [5.3 m/s]
 Watson-Lamprey I_a minus σ

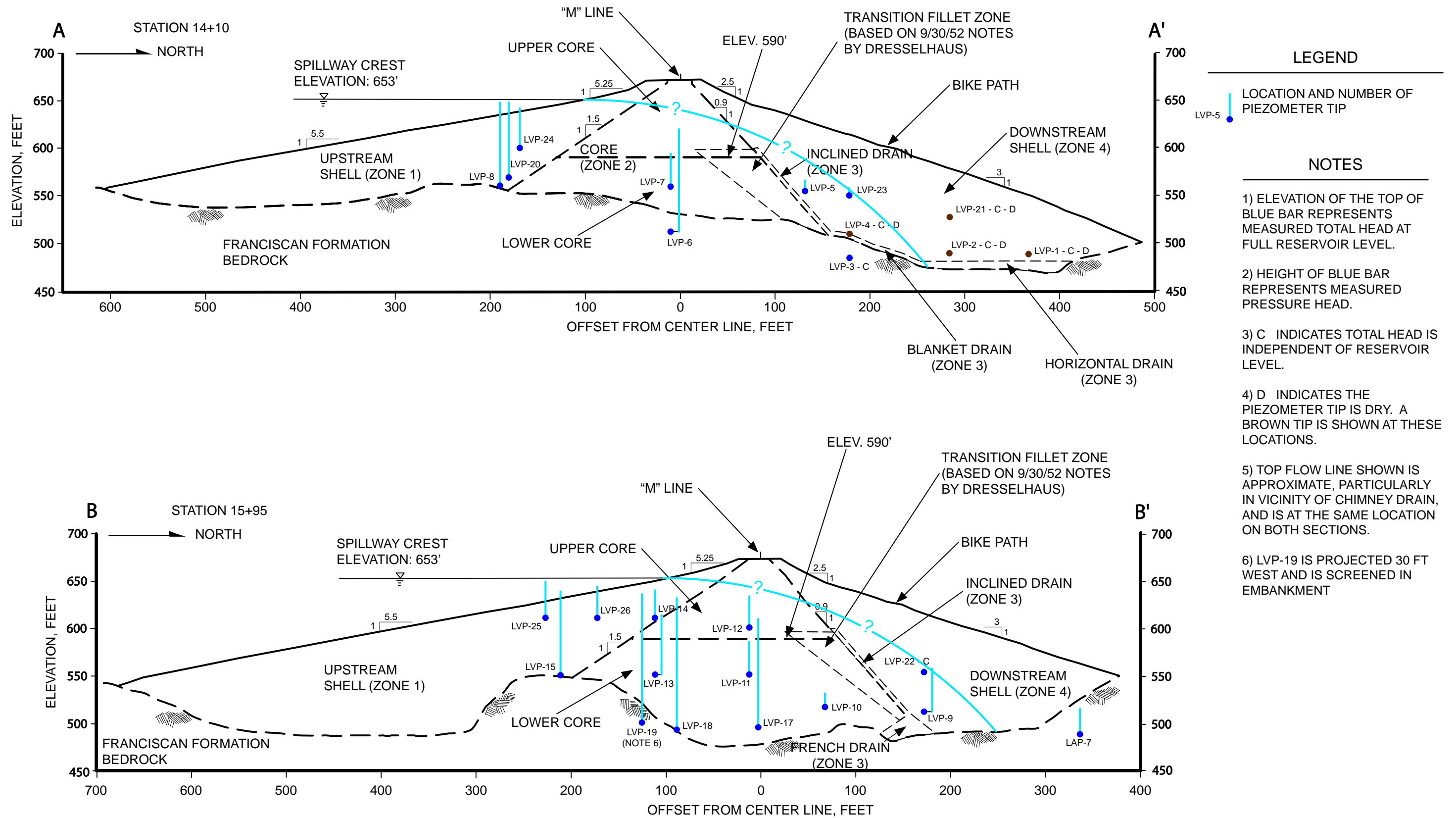


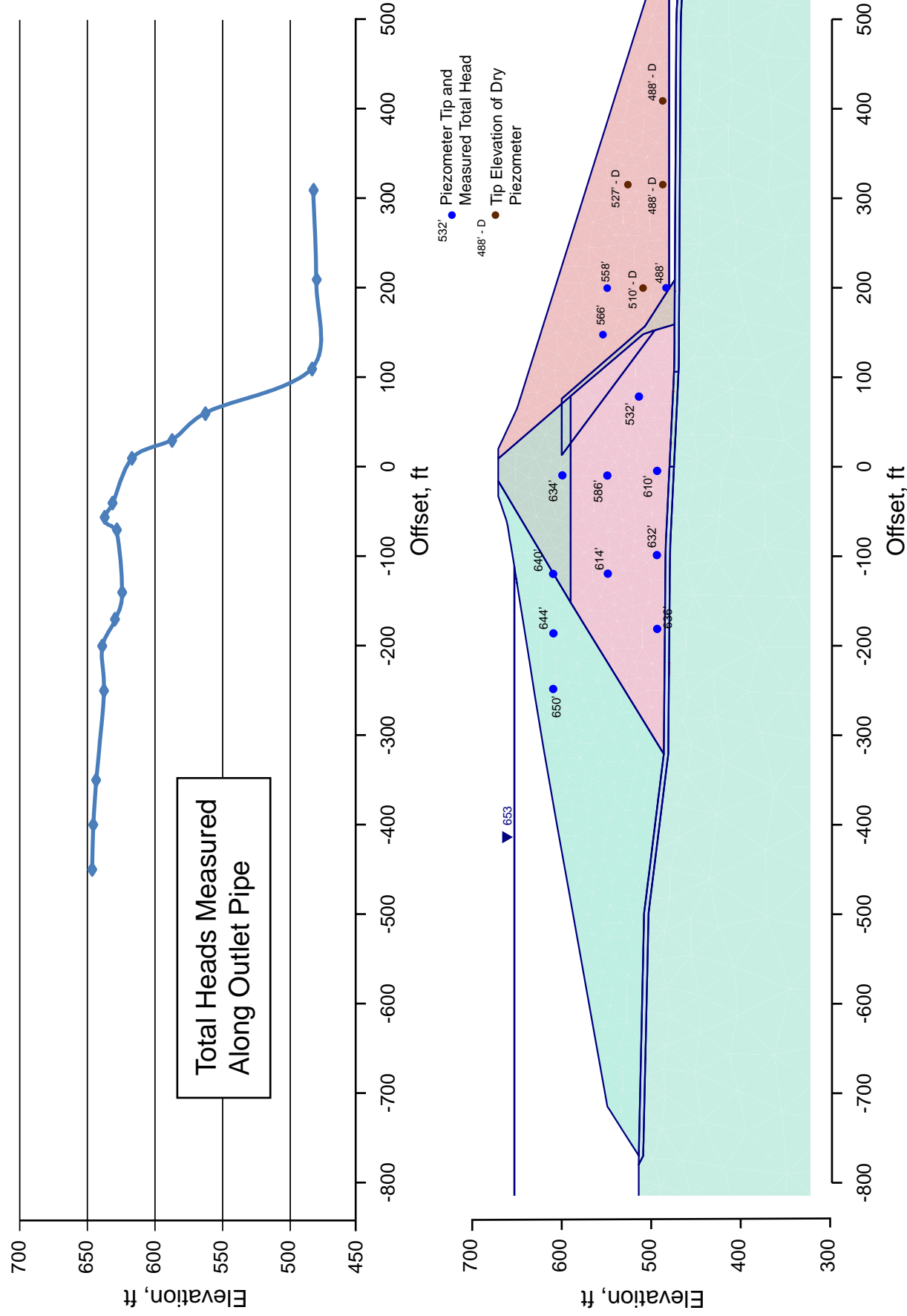


***Landers - Lucerne
Strike Slip Event
Rotated to Fault Normal
Spectrally Matched to SA***



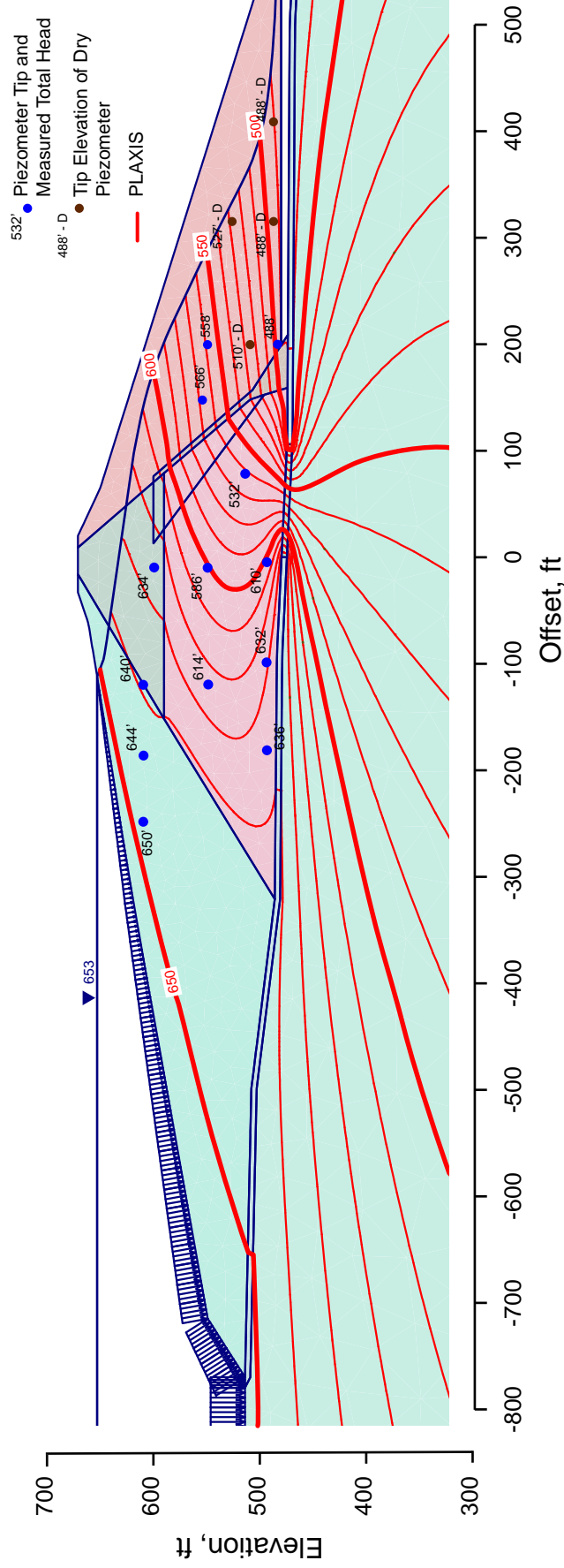
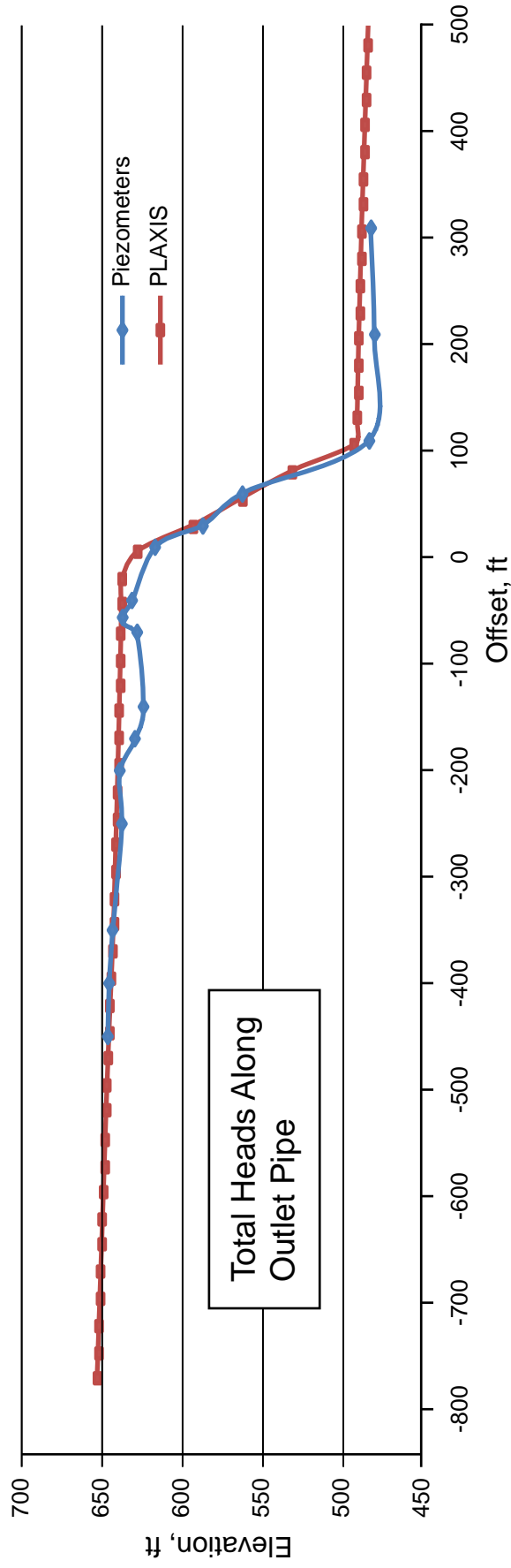






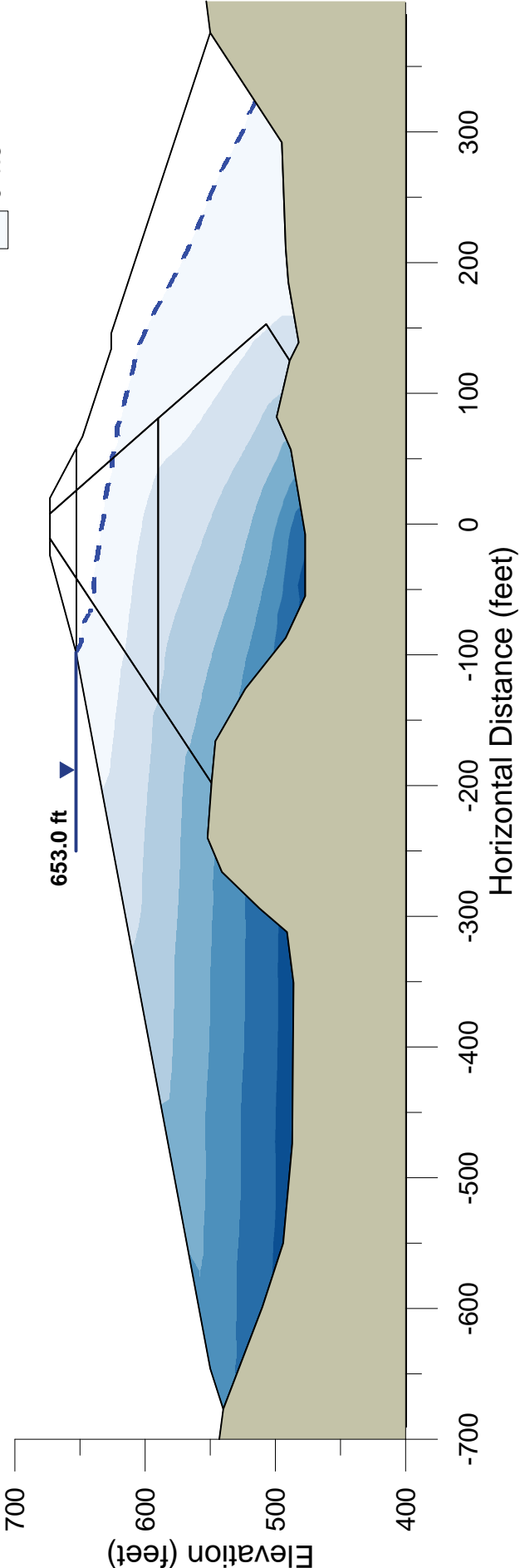
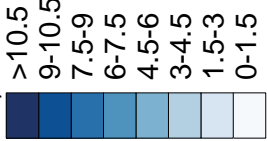
SECTION F-F' WITH MEASURED PIEZOMETRIC LEVELS - LENIHAN DAM
SEISMIC STABILITY EVALUATIONS (SSE2)

Figure 3-3



COMPARISON OF MEASURED TO MODELED
TOTAL HEADS, SECTION F-F' - LENIHAN DAM
SEISMIC STABILITY EVALUATIONS (SSE2)

Pore Pressure
(ksf)

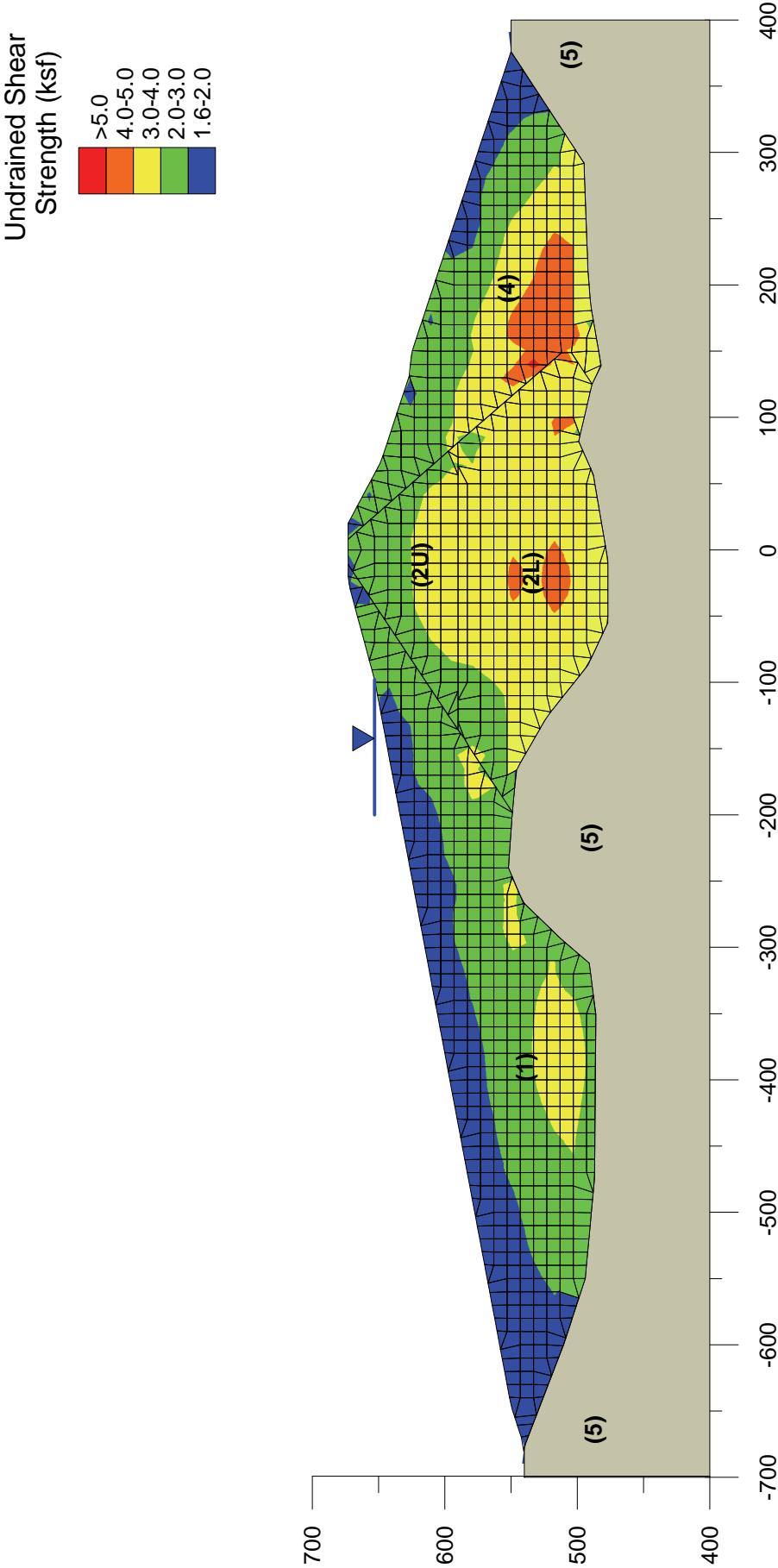


Pore Pressure Contours from PLAXIS Seepage Analyses



PORE PRESSURES AT FULL RESERVOIR
LEVEL - LENIHAN DAM
SEISMIC STABILITY EVALUATIONS (SSE2)

Figure
4-1

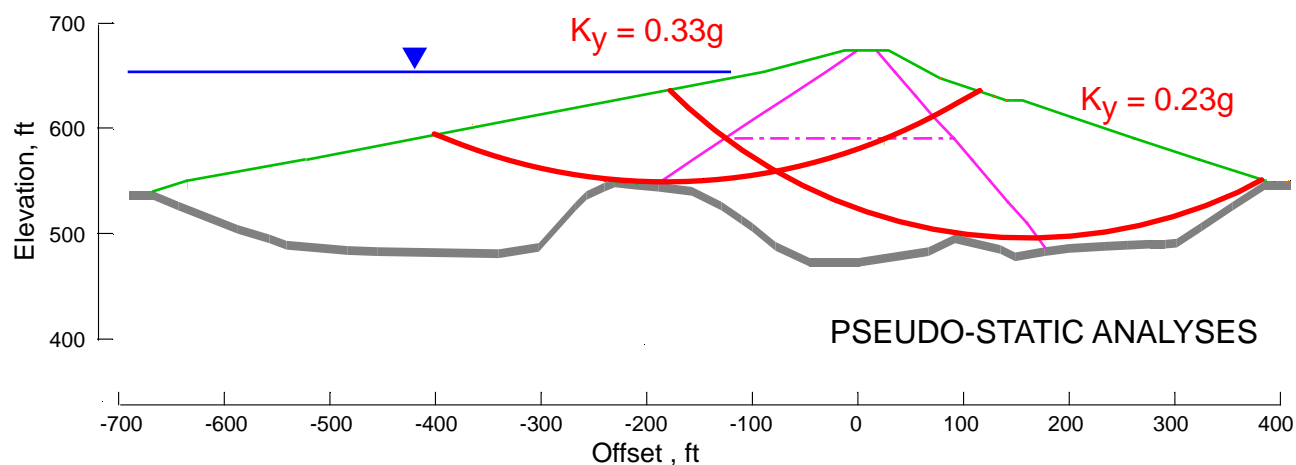
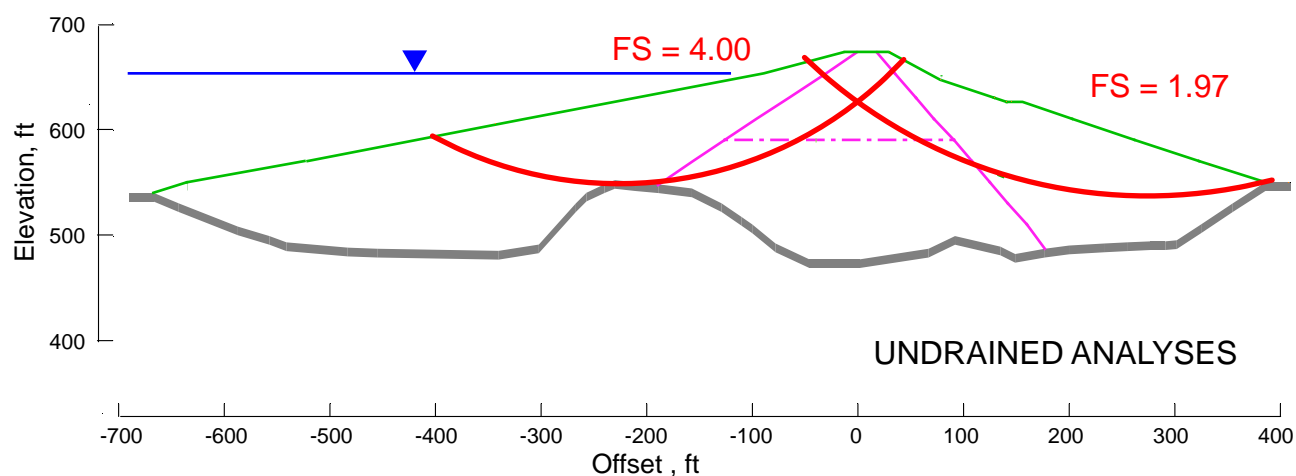
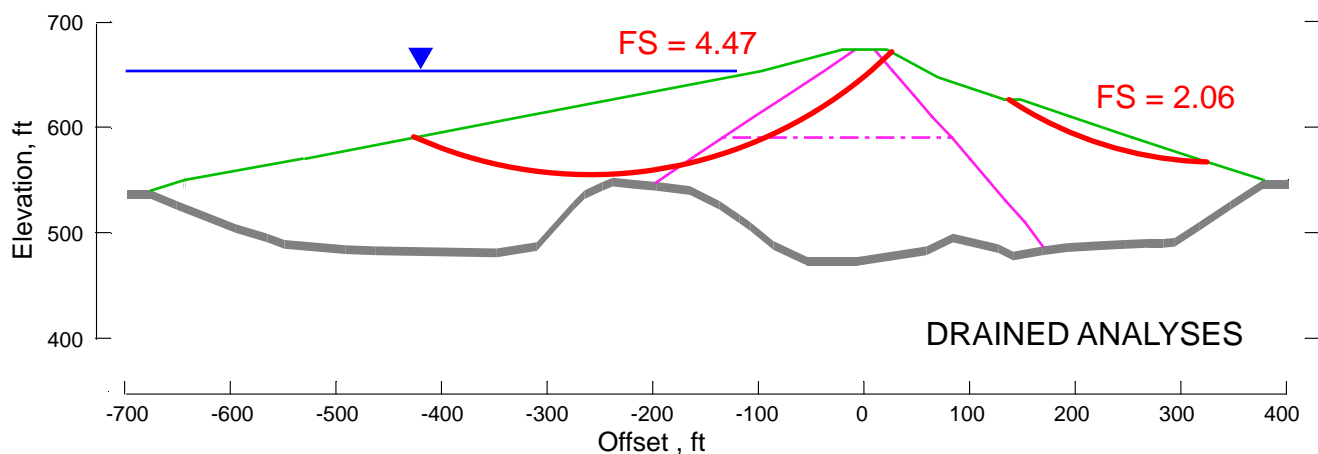


Note: Undrained shear strength based on effective stresses for steady state seepage and 84 percent of triaxial compression undrained strengths to account for DSS loading and strain rate effects.



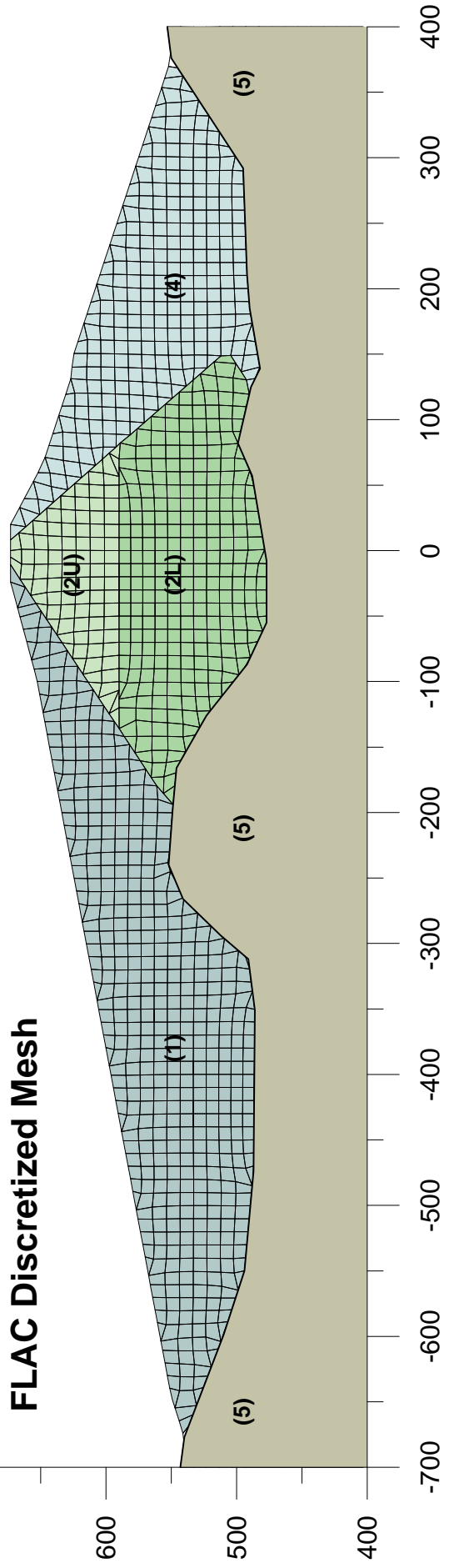
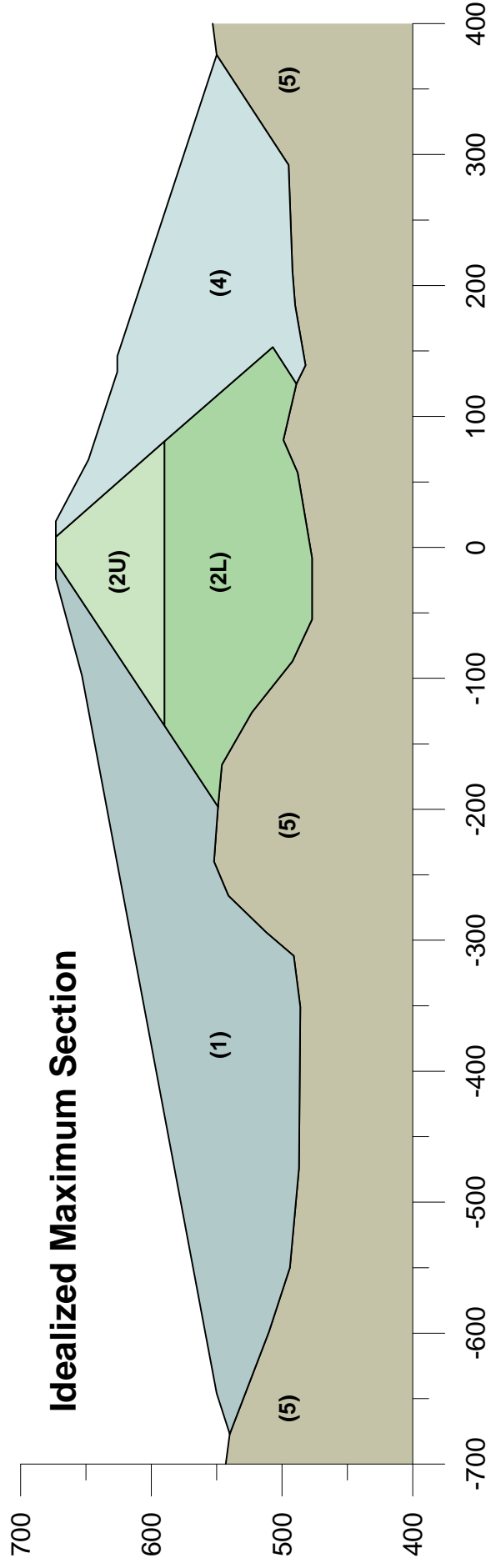
COMPUTED UNDRAINED SHEAR STRENGTH
LENIHAN DAM
SEISMIC STABILITY EVALUATIONS (SSE2)

Figure
4-2

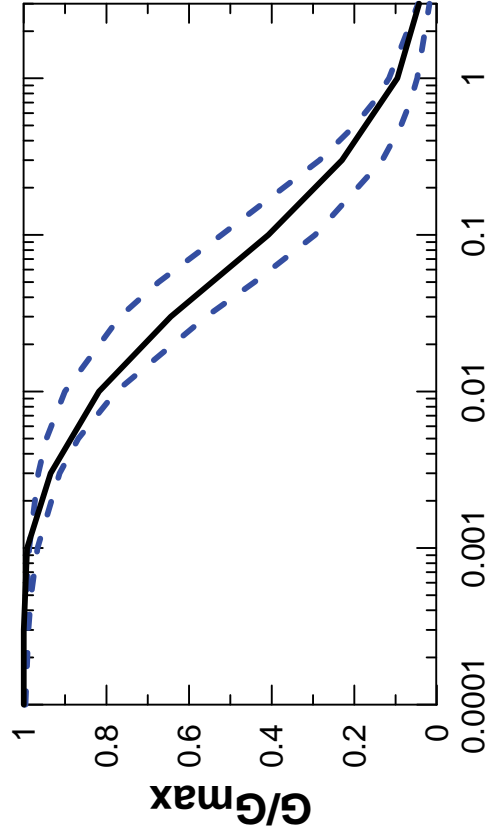


FS = Factor of Safety
 K_y = Yield Acceleration

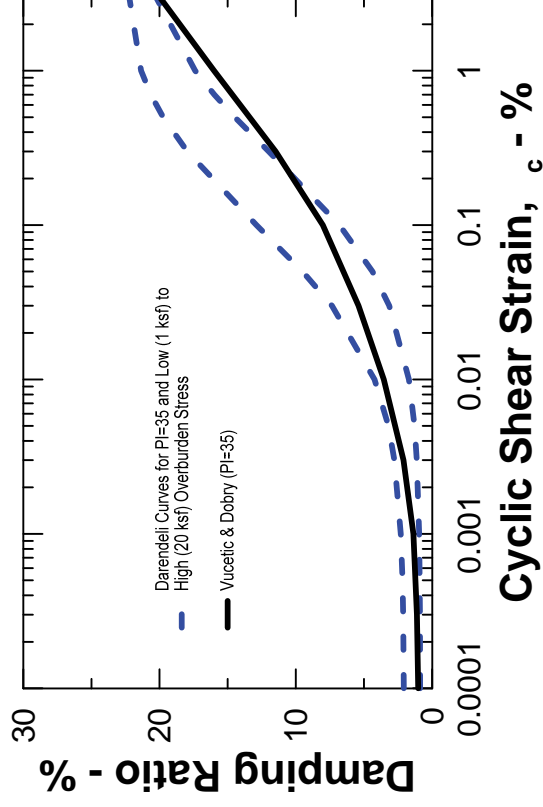
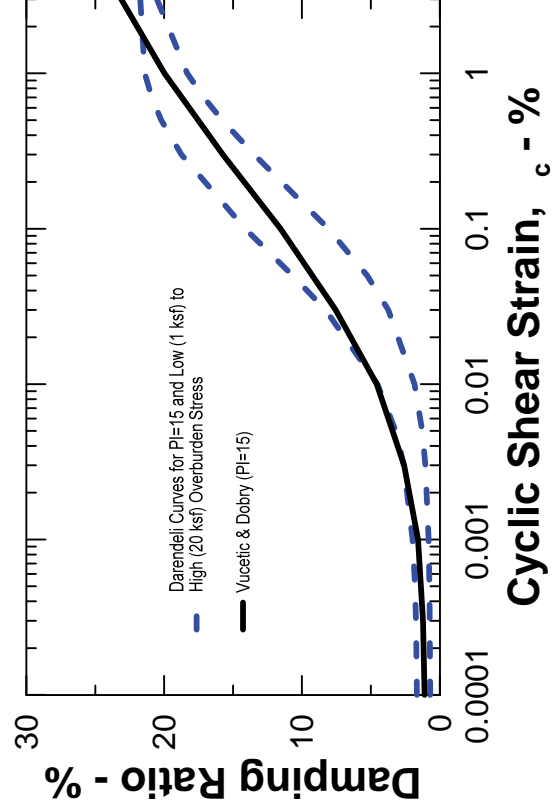
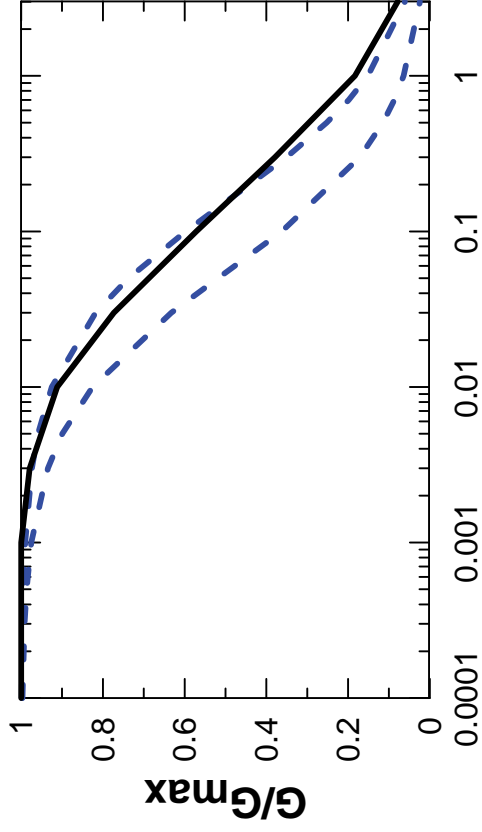


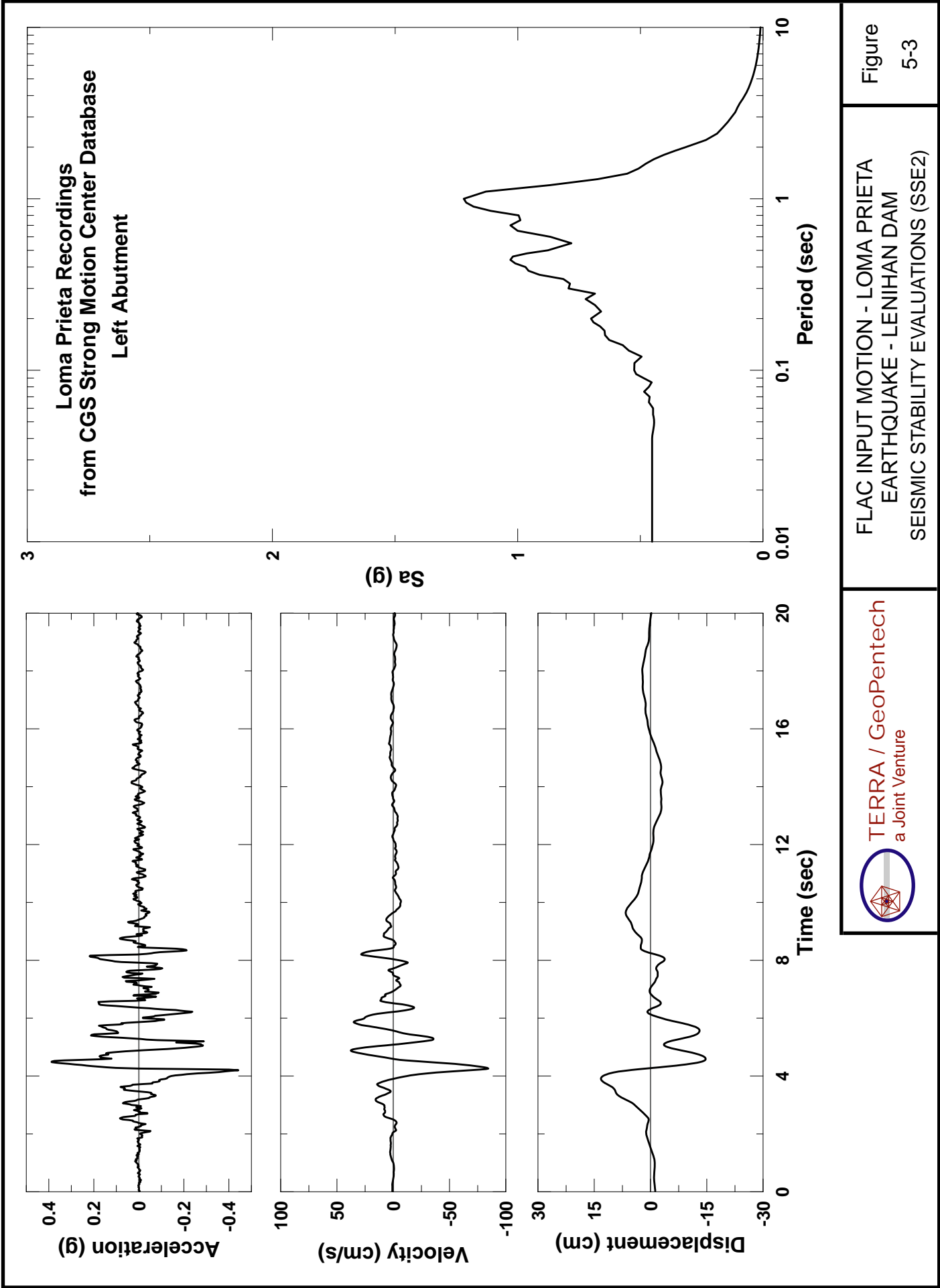


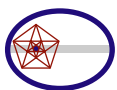
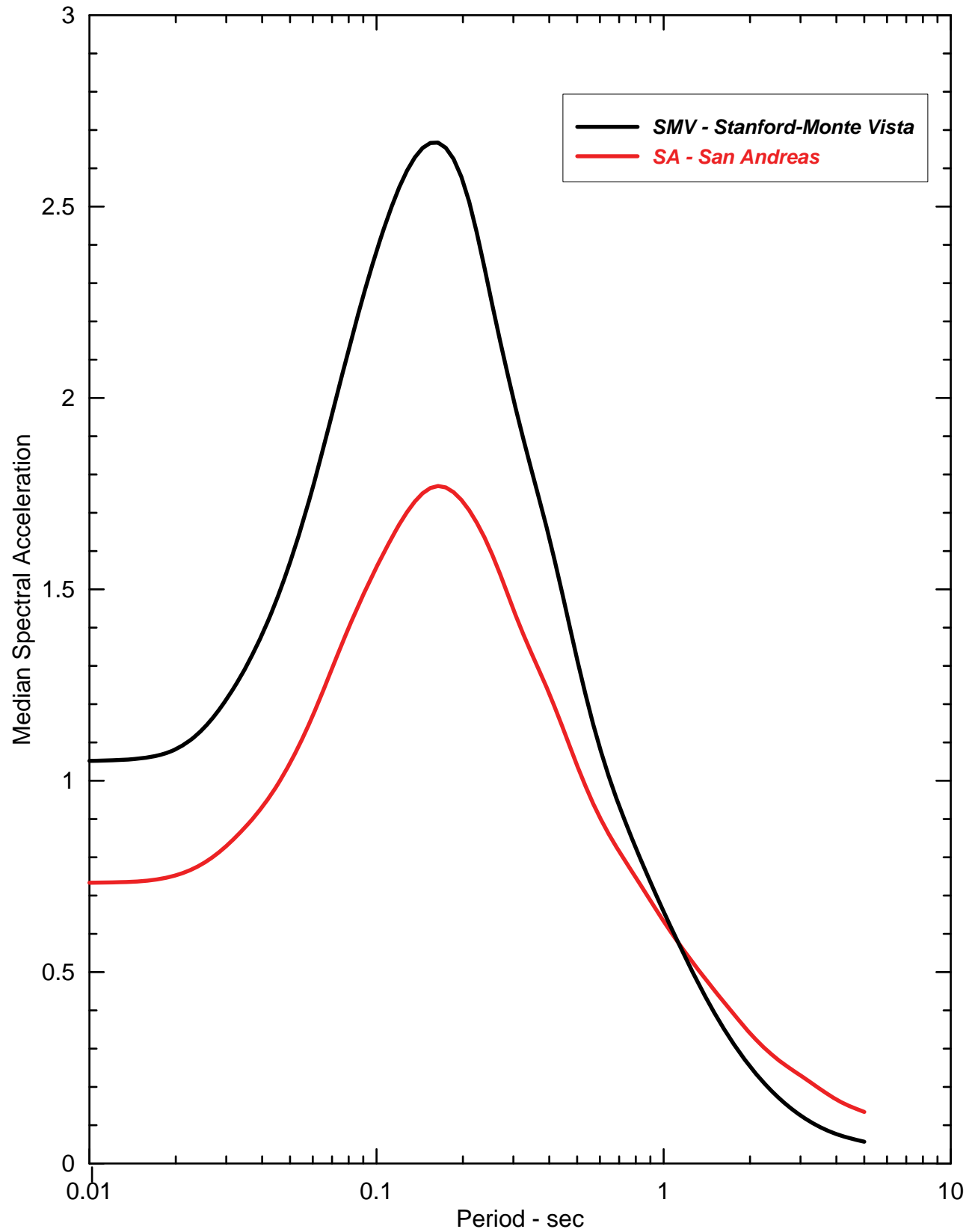
PI=15



PI=35







Deformation from Survey Measurement

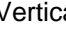
Crest Station	Horizontal Change* (Between 7/11/89 and 10/18/89)	Vertical Change (Between 7/11/89 and 10/18/89)
11+00	0.03 ft	-0.15 ft
13+00	0.21 ft	-0.61 ft
14+00	0.25 ft	-0.74 ft
15+00	0.18 ft	-0.85 ft
16+00	0.10 ft	-0.78 ft
17+00	-0.01 ft	-0.63 ft
18+00	-0.12 ft	-0.46 ft
19+00	-0.12 ft	-0.35 ft

*Positive indicates downstream movement, negative indicates upstream movement.

Wet Area Observed on Downstream Face²

Limits of Embankment

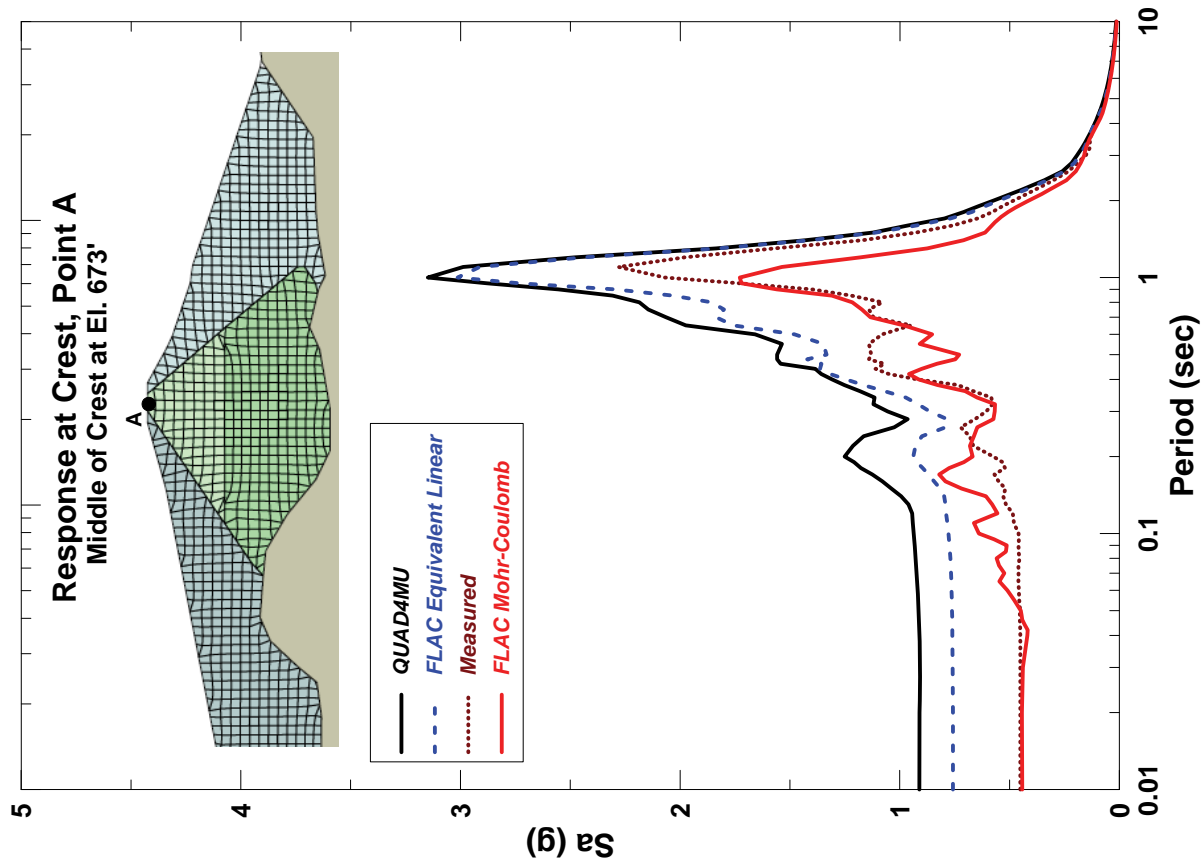
LEGEND

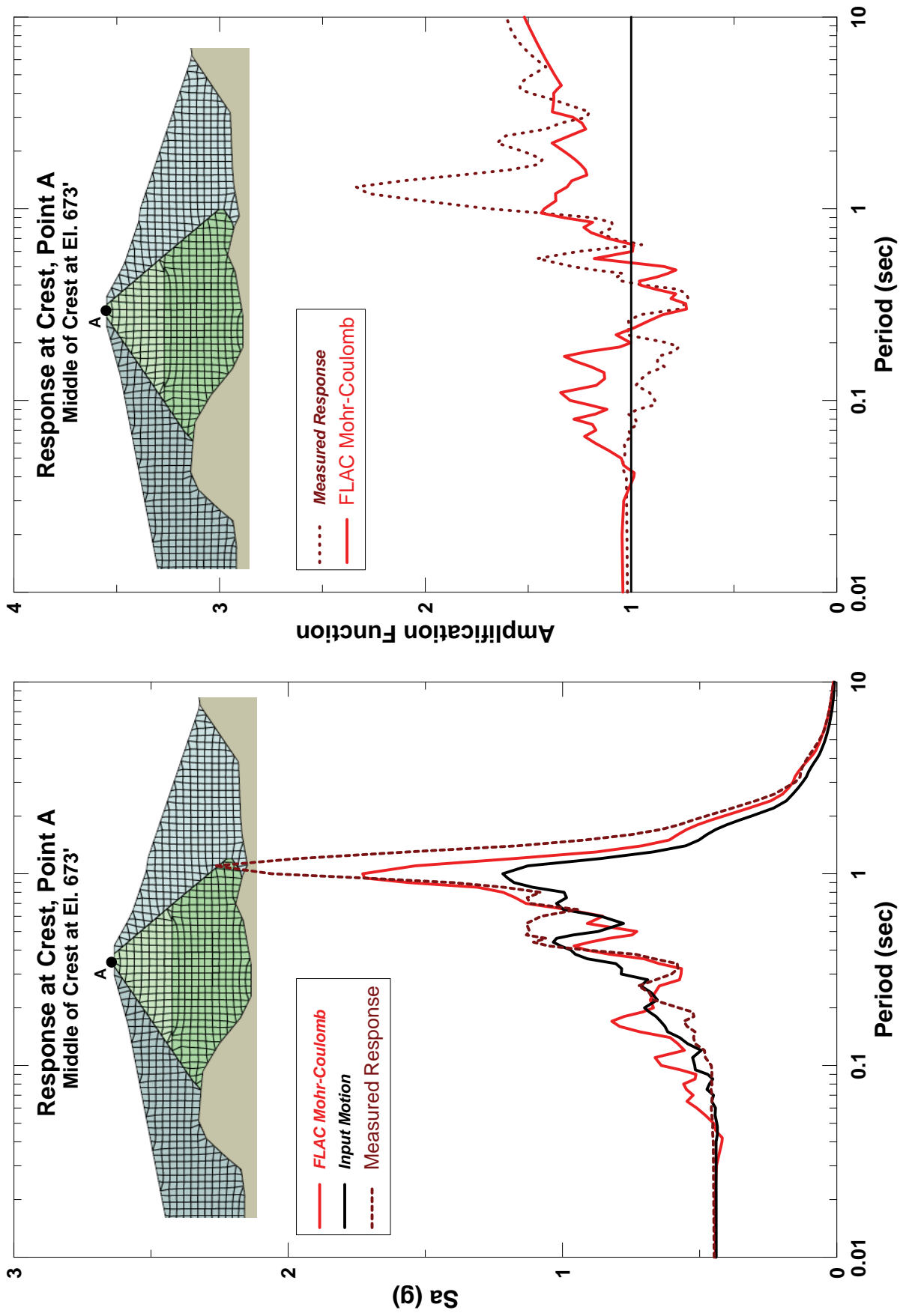
- Zone 1 - Upstream Shell
- Zone 2U - Upper Core
- Zone 2L - Lower Core
- Zone 4 - Downstream Shell
- Approximate Bedrock Contours, 10-ft
- Approximate Crack Location ¹
- Horizontal Movement (Magnitude: 1"=.25')
- Vertical Movement (Magnitde:  = .8')
- Dam Crest Station
- Strong Motion Instrument



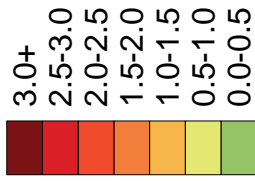
Notes:

- 1. Approximate locations of cracks derive from Investigation of SCVWD Dams Affected by the Loma Prieta Earthquake of October 17, 1989 (RLVA, 1990).
- 2. Wet area speculated to be due to previously installed drill hole casing backfilled with pea gravel acting as a relief well for groundwater in the bedrock fracture system in response to the increased pressure induced by the shaking conditions. This hypothesis is documented in RLVA, 1990.





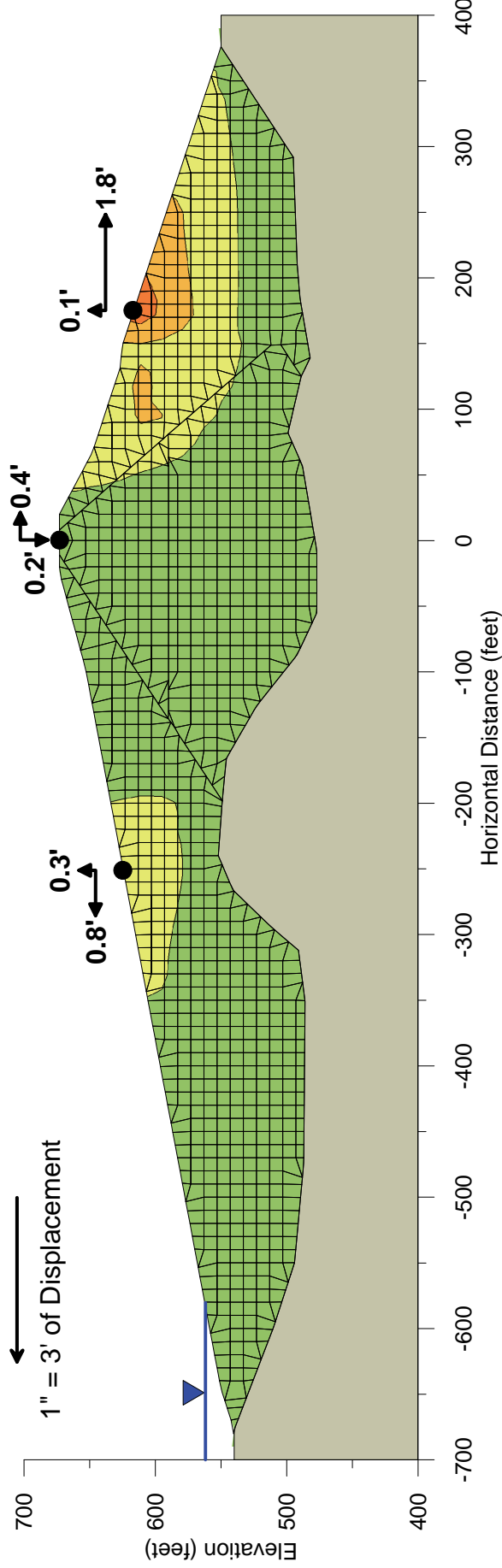
Displacement Scale (ft)



Vector Scale

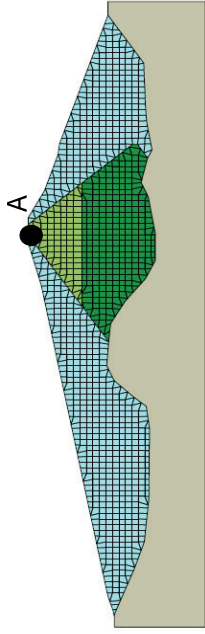
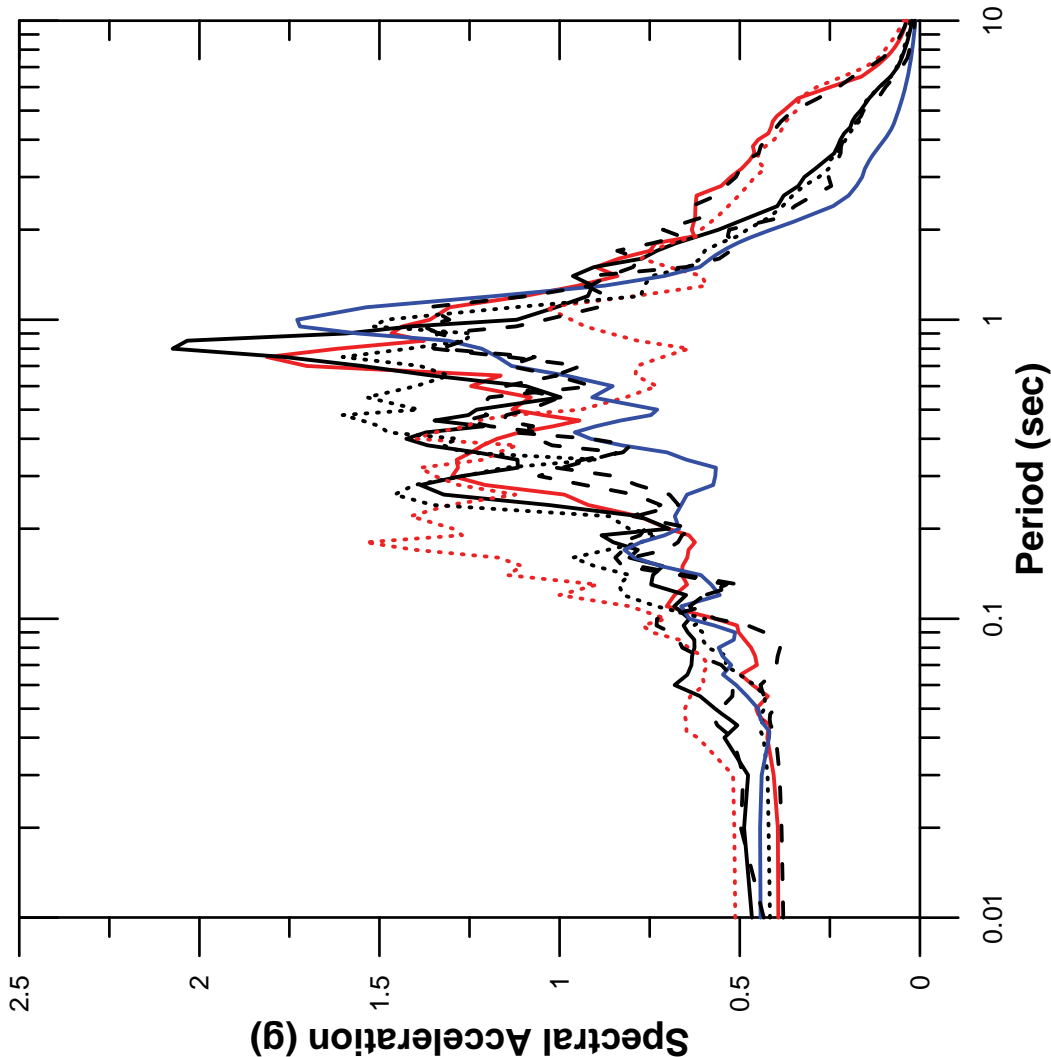


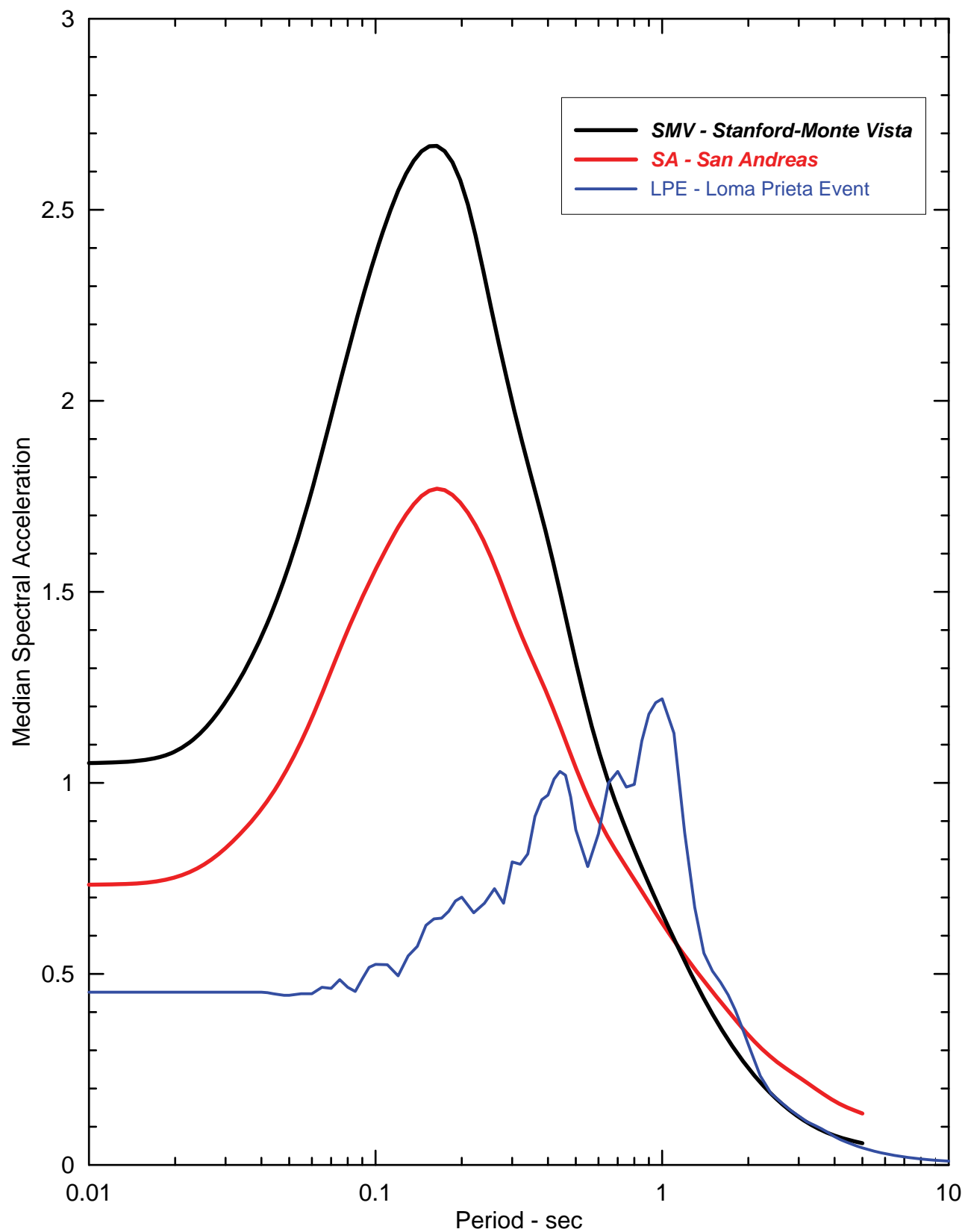
1" = 3' of Displacement

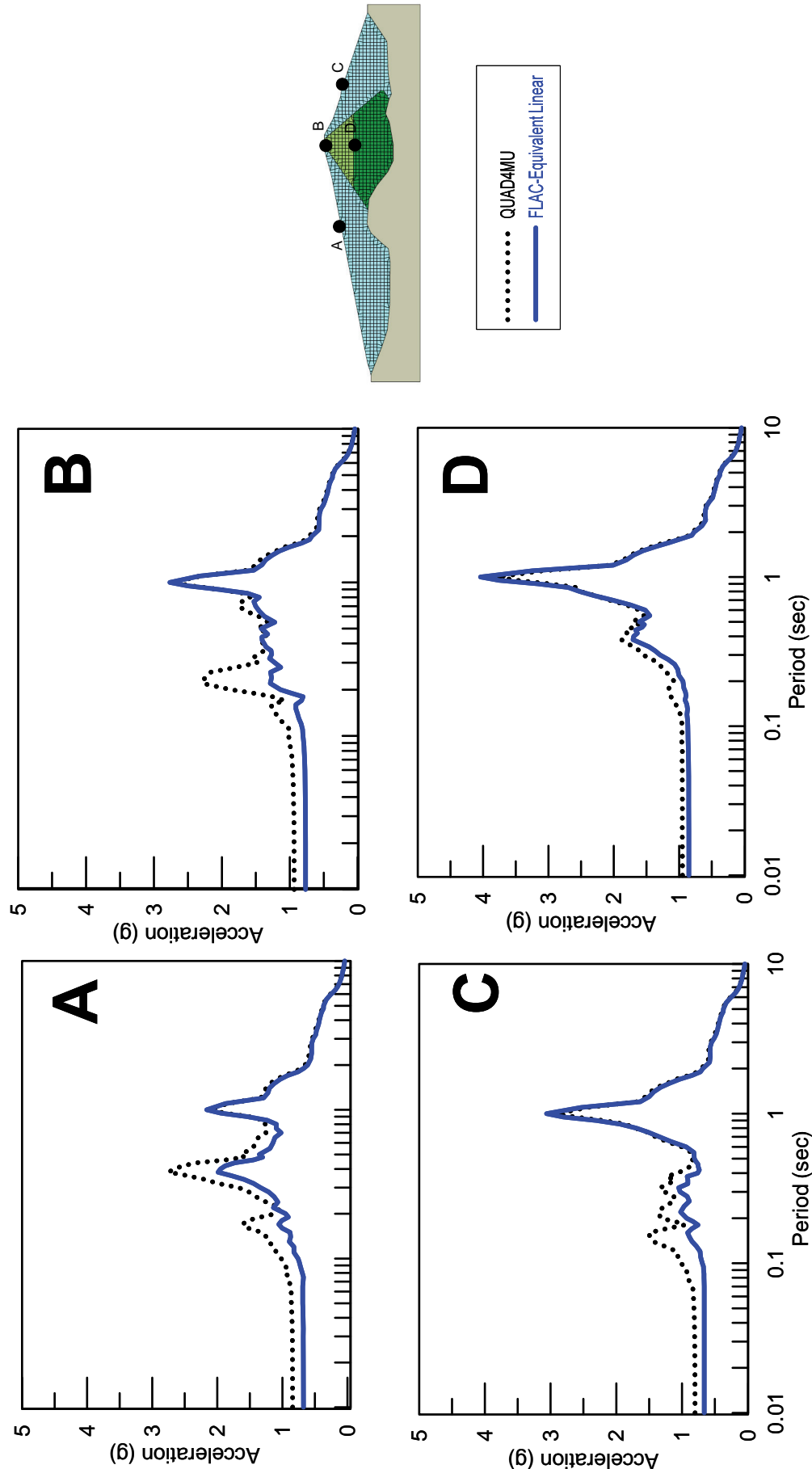


Note: Permanent seismic displacement at the end of shaking, values in feet.

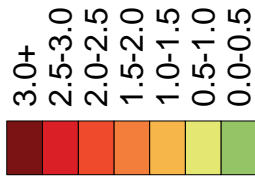
Acceleration Response Spectra of Crest







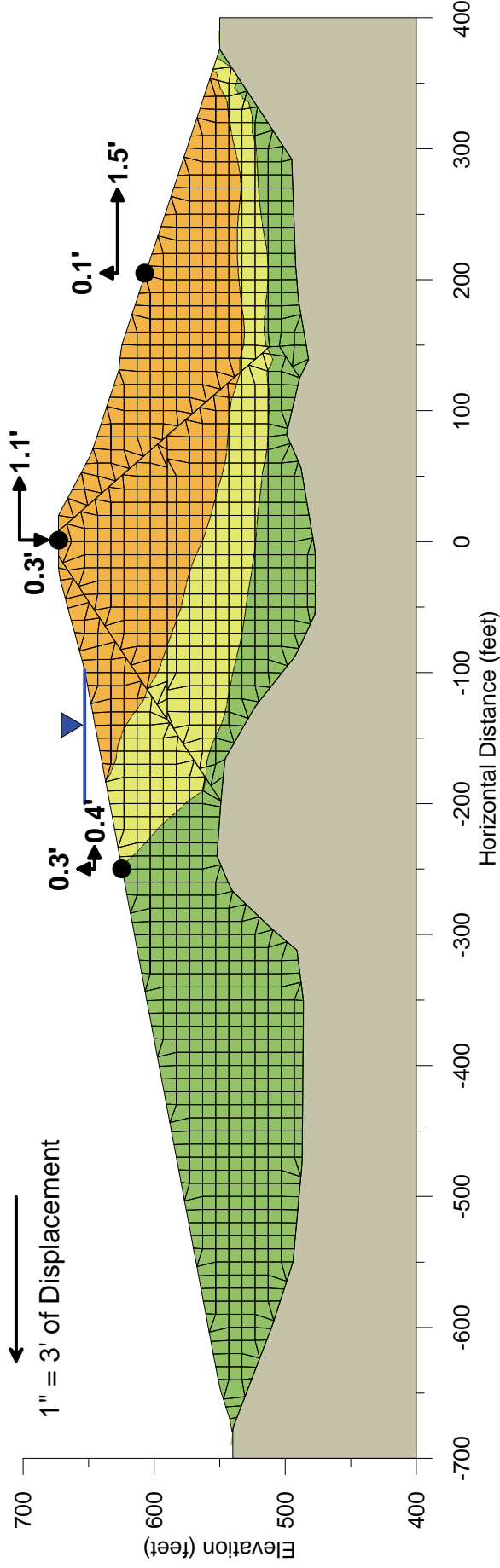
Displacement Scale (ft)



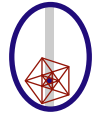
Vector Scale



1" = 3' of Displacement



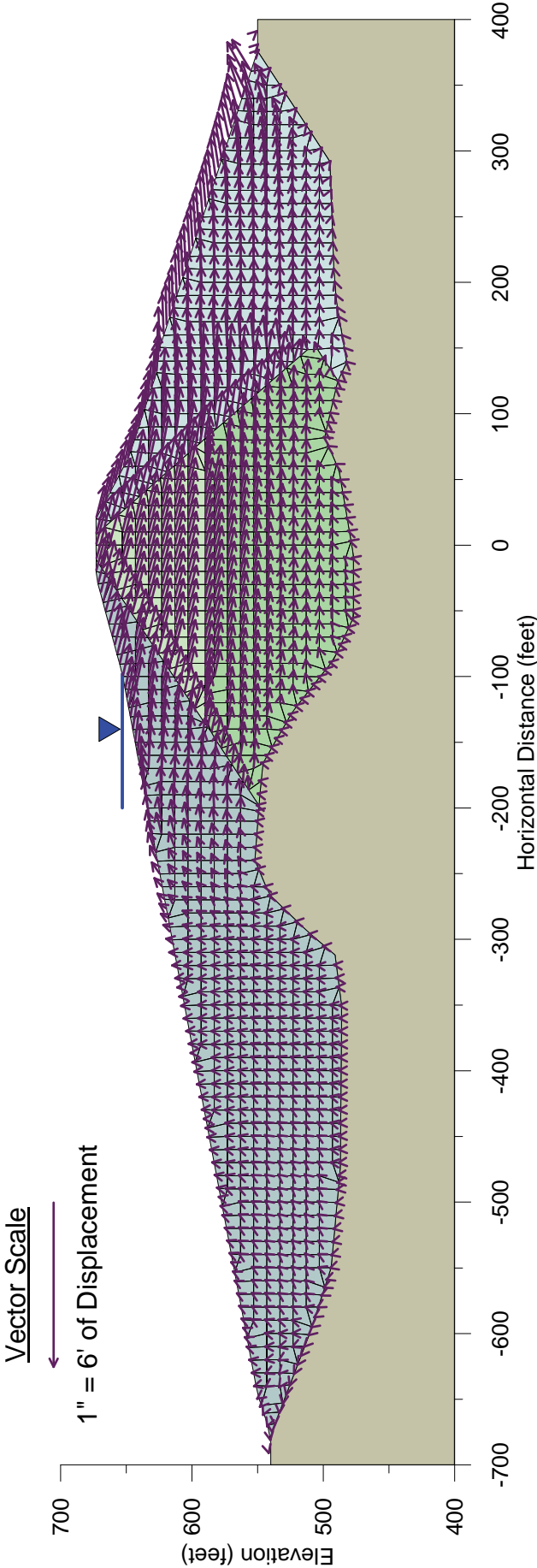
Note: Permanent seismic displacement at the end of shaking, values in feet.



TERRA / GeoPentech
a Joint Venture

CASE SA2 - LANDERS, DISPLACEMENT
CONTOURS - LENIHAN DAM
SEISMIC STABILITY EVALUATIONS (SSE2)

Figure
5-11

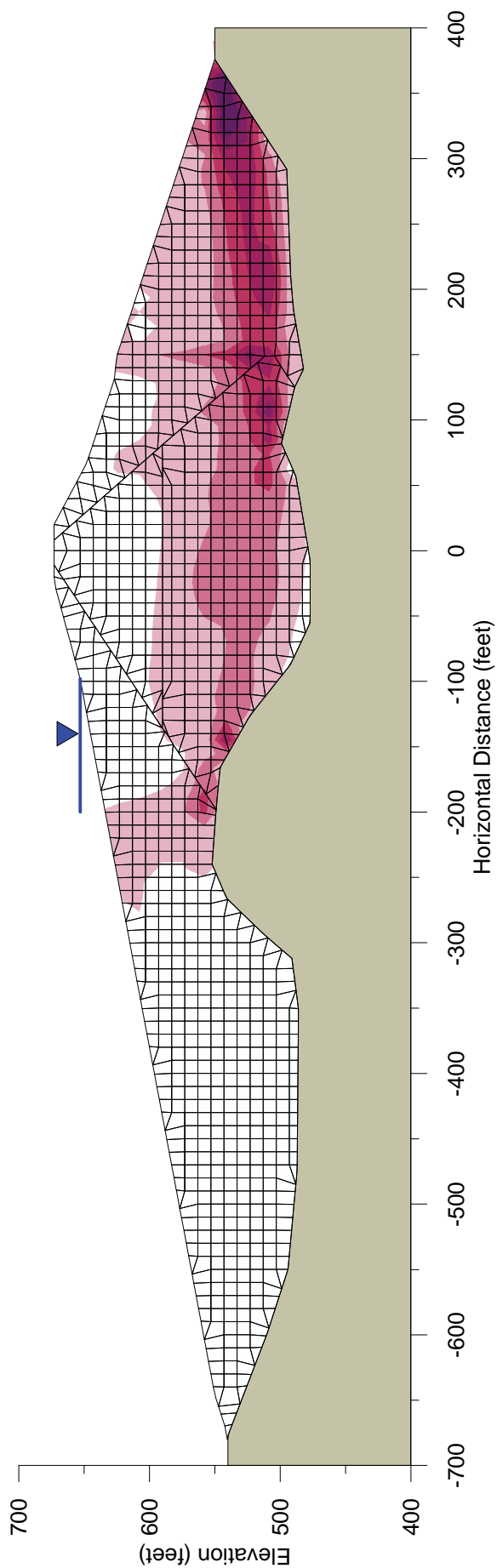
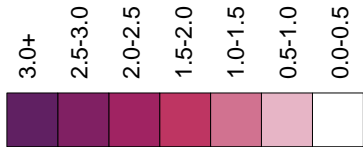


Note: Permanent seismic displacement at the end of shaking.

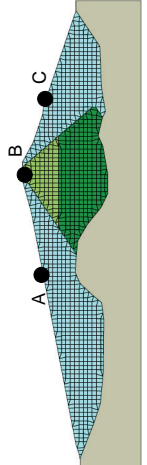
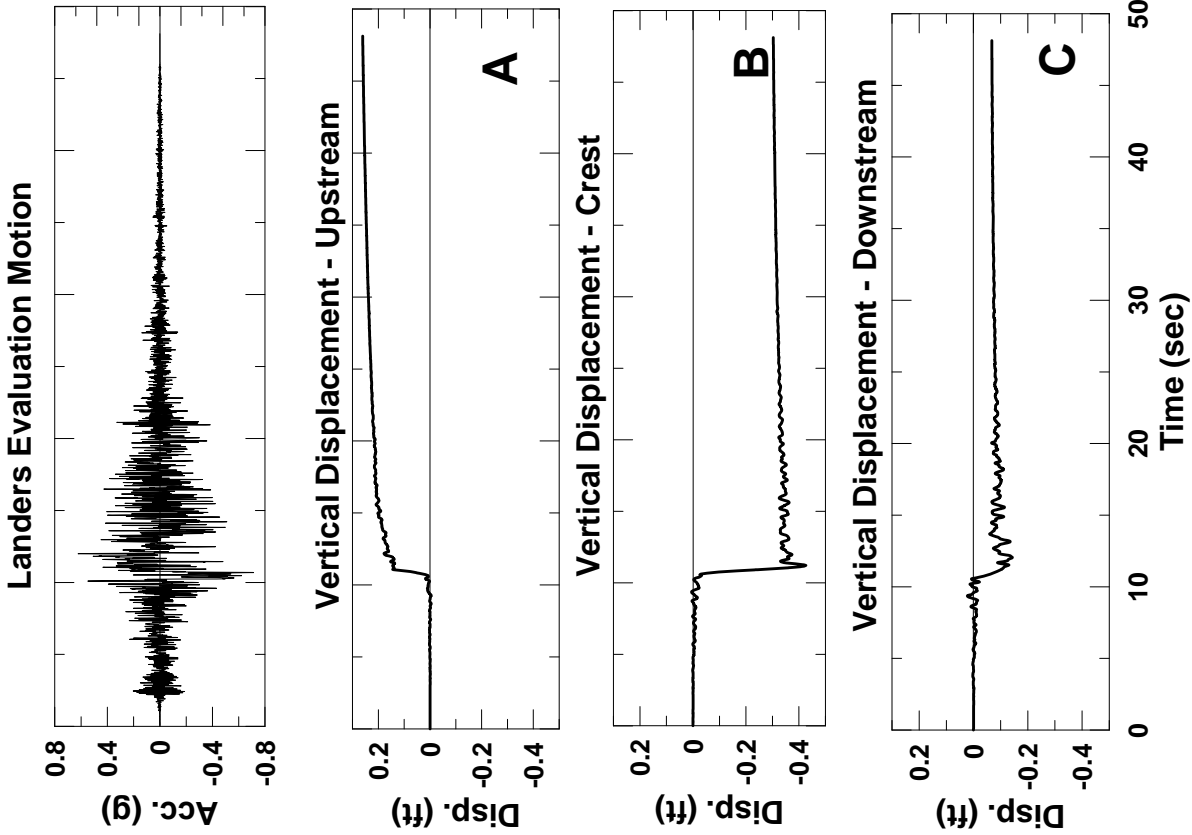


CASE SA2 - LANDERS, DISPLACEMENT
VECTORS - LENIHAN DAM
SEISMIC STABILITY EVALUATIONS (SSE2)

Shear Strain Scale (%)



Note: Shear strain at the end of shaking.

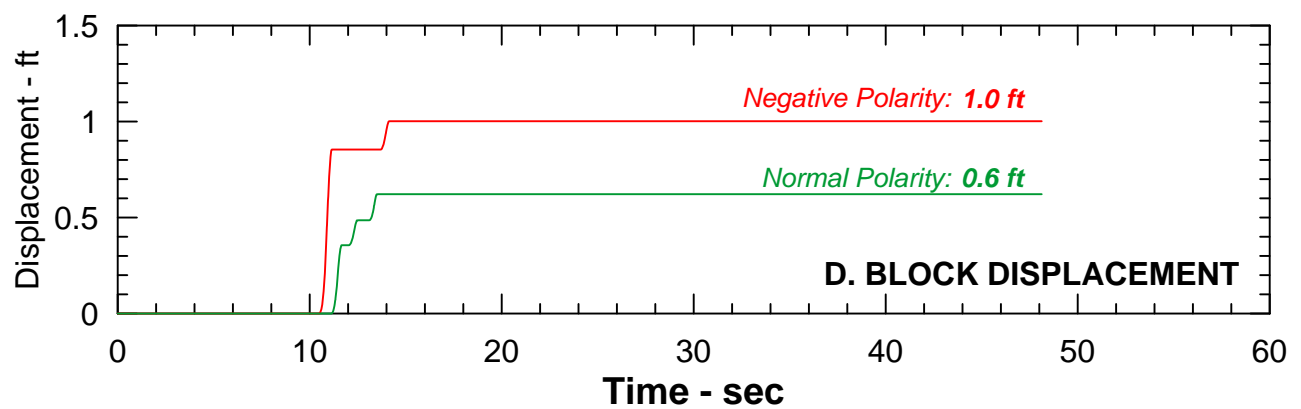
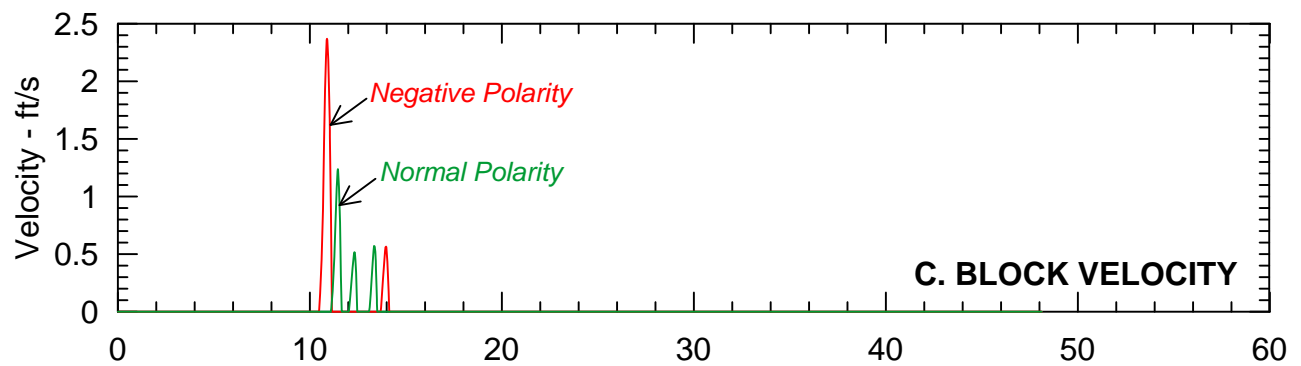
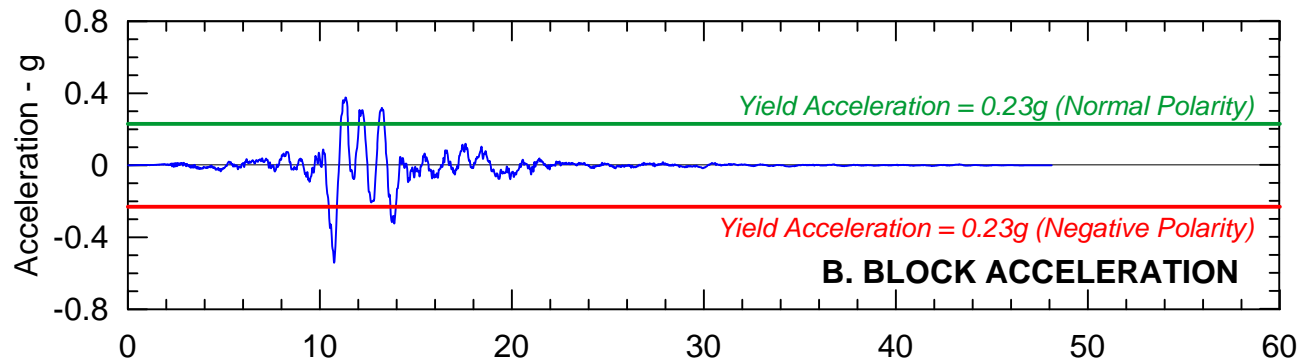
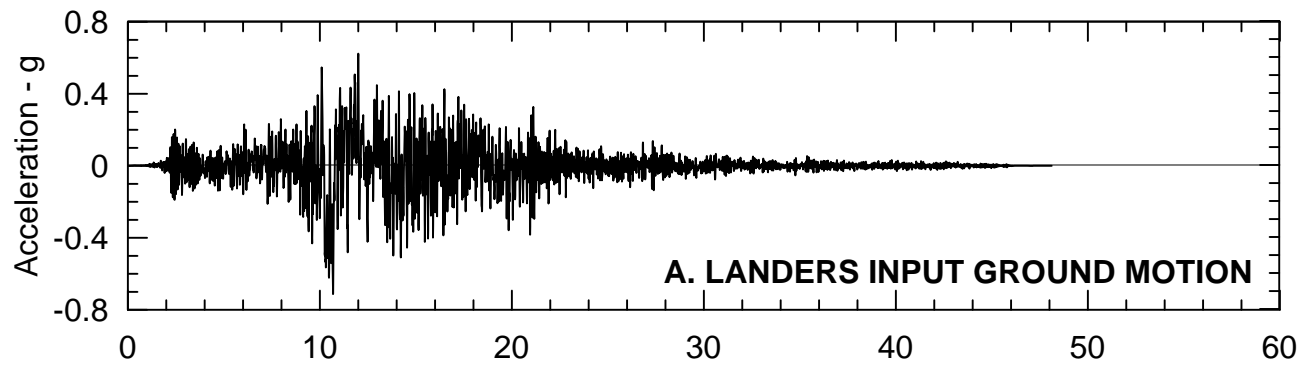


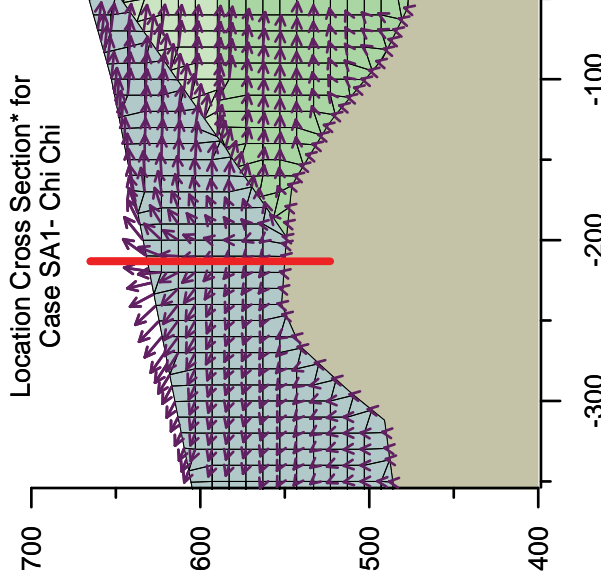
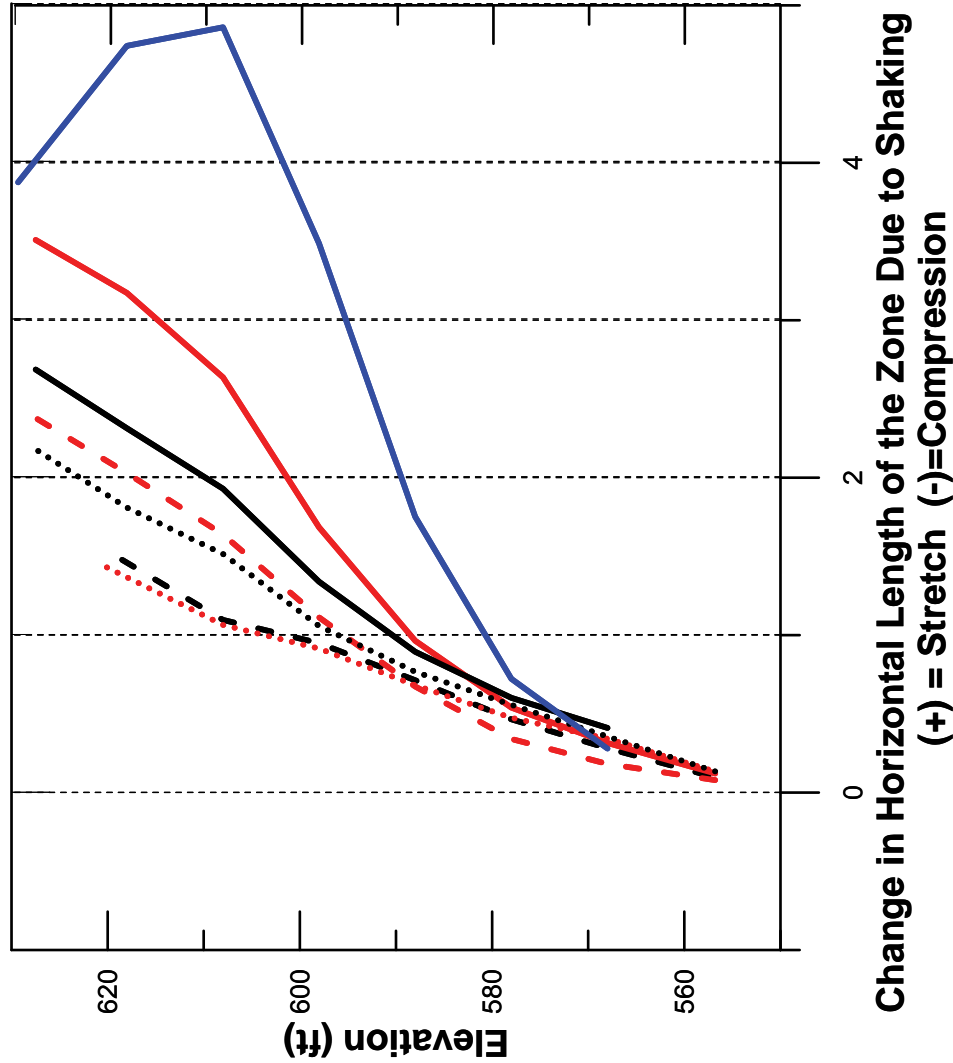


TERRA / GeoPentech
a Joint Venture

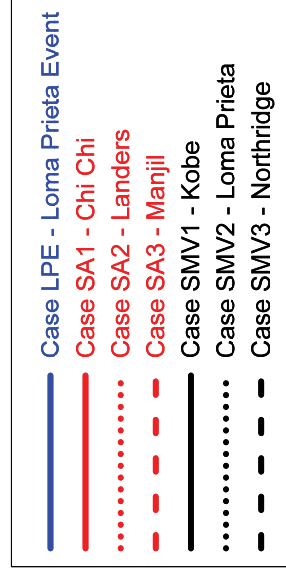
CASE SA2 - LANDERS, DEFORMATION TIME HISTORY - LENIHAN DAM
SEISMIC STABILITY EVALUATIONS (SSE2)

Figure
5-14





* Cross section for calculation of the stretch is selected to correspond to the section with maximum stretch, as shown in the sketch below.



APPENDIX A

TABLE OF CONTENTS

A.1	INTRODUCTION	A-1
A.2	METHODOLOGY AND APPROACH	A-1
A.3	LOMA PRIETA EVENT AT THE SITE	A-3
A.4	ANALYSIS PLATFORM AND SOIL MODELS	A-3
A.5	ANALYSIS SECTION.....	A-4
A.6	MATERIAL PROPERTIES	A-5
A.7	INPUT MOTION	A-5
A.8	RESULTS OF ANALYSES	A-5
A.8.1	Seismic Response and Input Motion.....	A-6
A.8.2	Seismic Deformation Analyses.....	A-7
A.8.3	Surface Cracks	A-7
A.9	DISCUSSION AND CONCLUSIONS	A-8

Figures

A-1	Loma Prieta Damage Map
A-2	Crest Section with Strong-Motion Instrument Locations
A-3	Loma Prieta Time Histories
A-4	Loma Prieta Response Spectra
A-5	Idealized Maximum Cross Section
A-6	Pore Pressures at Full Reservoir Level
A-7	Idealized Section and FLAC Discretized Mesh
A-8	FLAC Input Motion – Loma Prieta Earthquake
A-9	Comparison of FLAC and QUAD4MU Response Spectra
A-10	Comparison of Response Spectra at Crest
A-11	Comparison of Computed and Measured Response
A-12	Loma Prieta Event - Displacement Contours
A-13	Loma Prieta Event - Displacement Vectors
A-14	Loma Prieta Event - Shear Strain Contours
A-15	Loma Prieta Event – Deformation Time History
A-16	Loma Prieta Event – Crest Point Deformation Time History
A-17	Horizontal Stretching of Upstream Embankment

A.1 INTRODUCTION

This appendix presents the evaluation of the Loma Prieta case history for Lenihan Dam so that the evaluation of the seismic deformations of the dam under the evaluation ground motions that represent the MCE and are discussed in the main text can be tied to a site-specific empirical basis that:

1. confirms the reasonableness of the overall approach based on FLAC with the Mohr-Coulomb soil model combined with the QUAD4MU equivalent linear analysis;
2. shows that the undrained shear strengths assigned to the embankment materials are reasonably conservative; and
3. indicates that the observed surface cracking potential is probably a result of high shaking combined with the bedrock topography.

During the Loma Prieta earthquake, the seismic response of Lenihan Dam was recorded by three accelerographs (two on the dam crest and one on the abutment), which indicated peak ground accelerations of about 0.4g. In addition, some quantitative and observational seismic performance data were collected at the dam during and after the Loma Prieta event. The data and observations related to the Loma Prieta event provided an opportunity to "calibrate" the FLAC-based seismic deformation model for use in the seismic deformation evaluation of the dam embankment under the postulated evaluation earthquake shaking conditions. It also facilitated the refinement of material properties and input parameters used in the analyses. The analysis results for the Loma Prieta case history are presented here and are compared to observed performance data to obtain confidence that the developed seismic deformation model reasonably captures the important aspects of the dam performance, and also to refine the strength parameters to be used for seismic deformation analyses.

A.2 METHODOLOGY AND APPROACH

Section B-B' shown on Figure A-1, the maximum section of the dam, was used in the Loma Prieta evaluation. The input motion was postulated to be the transverse component of the abutment ground motions recorded during the 1989 Loma Prieta earthquake. The zoning and material properties described in Section 2.0 were used as the initial inputs.

The Loma Prieta evaluation included a two-dimensional equivalent linear analysis using the computer programs QUAD4MU (Tan, 2003) and FLAC (Itasca, 2008). The equivalent linear seismic response computed by QUAD4MU was compared to the results obtained from the equivalent linear analysis with FLAC as well as to the seismic response of the dam that was recorded during the Loma Prieta event. The seismic deformations were then calculated using the Mohr-Coulomb soil model available in FLAC and were compared to the observed patterns and values of seismic deformations recorded during the event.

The uncertainties involved in the characterization of the dam and in the selection of the input ground motions, as well as the uncertainty inherent to the two-dimensional FLAC model analysis, were considered in performing the evaluation and interpreting the results.

The seismic performance of dams results from the interaction of many factors (including some unknown factors and some factors that may appear relatively minor) that all contribute to uncertainty. However, for this evaluation, the following first-order effects have been identified as the major components of epistemic uncertainties:

1. Input Motion

- a. The incoming seismic energy into a dam can be quite variable along the contact surface between the embankment and the bedrock foundation; this may be particularly true when the bedrock materials covered by the dam consist of both "soft" rock and "hard" rock as may be the case for Lenihan Dam (Terra/GeoPentech, 2011b). In addition, the bedrock topography at the site is quite variable. Therefore, an appropriate "single-point" input motion for use in the seismic analysis of a two-dimensional section for a past event ideally should reflect the combined effects of all these uncertainties.
- b. Ground motions were recorded at two locations on the dam and one location on the left abutment during the Loma Prieta earthquake. The only candidate input motions recorded at the site are the three-component time histories at the left abutment and it is unclear whether these input motions are appropriate for the chosen analysis section, or any other sections. The applicability of these input motions to the section being analyzed is the main source of uncertainty associated with the input ground motions.

2. Seismic Response

- a. Given an appropriate input motion, the first-order seismic behavior of the dam is controlled by the seismic response of the structure. The seismic response of the dam can be represented using, for example, the response spectra resulting from the seismic event at various points on the dam.
- b. The main source of uncertainty regarding the seismic response of the dam is associated with the dynamic properties of the embankment materials (shear wave velocity and associated small-strain shear modulus, shear modulus reduction curves, and damping ratio curves) and how the values of these properties are distributed throughout the embankment.

3. Seismic Deformation

- c. Given appropriate input motion and seismic response, the first-order seismic deformation behavior of the dam is controlled by how the materials yield at various points within the dam, and, therefore, how permanent strains accumulate during the seismic event.
- d. The main source of uncertainty in the seismic deformation is the shear strength of the materials in the dam and how the shear strength values are distributed throughout the dam.

The case history evaluation should focus on the major issues discussed above and assess how comfortable one feels about these issues and about one's ability to control, in a practical way, the epistemic uncertainties. In this regard, too much focus on "matching" the recorded data by "manipulating" some details of the analyses (which could lead to getting the right answer for the wrong reasons) without gaining an overall appreciation of the key lessons a given case history has to offer would not be fruitful. Thus, the Loma Prieta case history evaluation documented

herein is aimed at developing an overall understanding of the seismic behavior of the dam and providing a level of confidence that the developed model reasonably captures the important aspects of the seismic response of the dam rather than obtaining a close match of calculated to recorded motions or deformations.

The following sections provide a summary of the effects of the Loma Prieta event at the site and a description of the computer program FLAC and of its application in the Loma Prieta case history evaluation.

A.3 LOMA PRIETA EVENT AT THE SITE

The Loma Prieta earthquake occurred on October 17, 1989, along a branch of the San Andreas fault. The epicenter of this event was located about 13 miles (20 km) from Lenihan Dam. The effects of the Loma Prieta earthquake on Lenihan Dam were investigated by the District and R.L. Volpe & Associates (RLVA) in the days following the event as part of an overall investigation of District dams affected by the earthquake. The relatively minor observed damage at the dam was documented in a report by RLVA (1990).

Following the Loma Prieta earthquake, the dam was found to have sustained about 10 inches of crest settlement at the maximum section and a maximum of about 3 inches of lateral movement downstream, in addition to some localized cracking that was primarily longitudinal. Also, about six weeks after the earthquake, a wet area was observed below the footpath near the right abutment although no flow was reportedly emanating from this area (RLVA, 1990). The observed seismic displacements and the locations of the observed cracks and wet area are summarized on Figure A-1. This figure also shows the locations of the three strong-motion instruments at the site and the section selected for the analyses (Section B-B').

Three sets of three-component ground motions were recorded during the earthquake at two locations on the crest and one at the left abutment, as shown on Figure A-1. Figure A-2 is a longitudinal cross section along the dam axis used to illustrate the location of the abutment recording station relative to the embankment and the surrounding topography.

The dam parallel, dam transverse, and vertical acceleration time histories for the three recording locations are shown on Figures A-3; the response spectra at 5 percent damping corresponding to these acceleration time histories are shown on Figure A-4. As shown on Figure A-3, the peak horizontal ground accelerations at all locations are similar and in the range of 0.34g to 0.45g. However, as shown on Figure A-4, the spectral accelerations at the crest, when compared to those at the abutment, show a significant amplification at about a period of about 1 second. This is especially the case at the right crest location, which is close to the maximum section of the dam used in the analyses. Also, the peak vertical accelerations and spectra values are in general much lower than the corresponding horizontal values.

A.4 ANALYSIS PLATFORM AND SOIL MODELS

The computer program FLAC (Fast Lagrangian Analysis of Continua) was used as the main analysis tool for this evaluation. FLAC is a two-dimensional explicit finite difference program for geotechnical and mining applications that was developed by Itasca (2008). An analysis section is divided into zones (or elements) and nodal points in a way analogous to the finite

element method. FLAC uses the Lagrangian formulation of momentum equations (Newton's second law of motion) and, thereby, inherently accounts for the mass conservation law and allows elements with fixed masses to translate, rotate, or deform in space. The analysis input motion was specified at the base of the analysis section (elevation 400 ft), incorporating the effects of a compliant boundary representing the bedrock in the evaluation.

The calculation loop in FLAC has two main alternating components: zone (or element) calculations and nodal point calculations. In the zone calculations, the current velocities and displacements of nodal points are used to compute the strain increments in the zone formed by these nodes; these strain increments, in turn, are used to compute the stress increments of the zone. With the new state of stress, the out-of-balance force can be computed and then used to calculate the incremental displacements of the nodes.

Various stress-strain models are available in FLAC. For the evaluation documented herein the Mohr-Coulomb model and the elastic model were used in the analyses. Details of these models are provided by Itasca (2008). For all the results presented here, the elastic model was used for the bedrock and, depending on the analysis, the Mohr-Coulomb or elastic model was used for all the other materials.

The Mohr-Coulomb model consists of elastic-perfectly-plastic stress-strain relationships. Therefore, the materials are elastic before yielding. To make the elastic portion of the analysis reasonable, we perform an equivalent-linear analysis using the computer program QUAD4MU to obtain the strain-compatible modulus and damping values for the shaking conditions. The analysis results from QUAD4MU provide the basis for the strain-compatible shear modulus and Rayleigh damping values to be used in the elastic portion of the Mohr-Coulomb model in the FLAC analyses.

A.5 ANALYSIS SECTION

Figure A-5 shows the section of the dam selected for the analyses. The plan location of this section is shown on Figure A-1 as well as on the inset in Figure A-5. The generalized embankment zones and material types established in Report No. LN-3 (Terra/GeoPentech, 2011b) are also tabulated on Figure A-5.

Section B-B' was chosen for the analyses because it is the maximum section and also because the bedrock surface along the section is irregular with a significant bedrock "knoll" at the upstream side of the core as shown on Figure A-5; the shape of the bedrock surface may affect the seismic response of the dam.

One of the inputs to the analysis is the location of the phreatic surface and distribution of the pore water pressure just before the shaking. The pore-water pressure distribution for the steady state seepage conditions corresponding to the full level at elevation 653 feet was presented in Section 3.0. Figure A-6 shows the pore-water pressure contours within the dam based on this analysis. Section 4.0 describes how the undrained shear strength of the clayey embankment soils was calculated for the case of steady state seepage under full reservoir.

The reservoir level during the Loma Prieta event was at elevation 550 feet. Because of the lower reservoir level the effective stresses and associated undrained shear strengths of the soils will be somewhat higher than those for steady state seepage under full reservoir but, the amount of

increase in effective stress is expected to be relatively small because of the very low permeability of the embankment soils and the long time required for consolidation. Consequently, we made the reasonably conservative assumption that the undrained shear strengths for the embankment at the time of the Loma Prieta event can be represented by those corresponding to the reservoir level of elevation 653 feet.

Figure A-7 shows the further idealized analysis section and the same section discretized into a finite difference mesh for use in the FLAC analyses. The mesh shown on Figure A-7 was generated to: (1) ensure appropriate dynamic wave propagation in the system; (2) control kinematic constraints provided by the linear elements used in FLAC; and (3) control numerical problems introduced by element shapes.

Although not shown on Figure A-7, the bedrock was also discretized for the sole purpose of providing a compliant base that would appropriately and adequately allow the incoming seismic waves and absorb the outgoing seismic waves. The numbers shown in various zones of the dam on Figure A-7 correspond to the zone numbers identified on Figure A-5.

A.6 MATERIAL PROPERTIES

The material properties used in the analyses are documented in Section 2.0 and summarized in Table A-1. They include: unit weight; small-strain shear modulus (shear wave velocity, V_s , or maximum shear modulus, G_{max}); shear modulus reduction and damping ratio curves; and shear strength. The shear modulus reduction and damping ratio curves were discussed in Section 2.0.

A.7 INPUT MOTION

The input motion representing the 1989 Loma Prieta earthquake ground motions at the site that was used in the analyses is the transverse component of the three-component ground motions recorded at the left abutment (Figures A-1 and A-2). The selected acceleration time history and response spectrum for this input motion are identified by a dashed rectangle on Figures A-3 and A-4. The horizontal component of the input motion is presented on Figure A-8 in terms of acceleration, velocity, displacement time histories, and associated response spectrum at 5 percent damping.

As discussed, the use of the abutment time history as an input motion at the base of the dam necessarily results in potentially significant uncertainty. One previous study (Harza, 1997) indicated that the response of the dam might have affected the abutment recording. As can be inferred from Figures A-1 and A-2, the topographic high at the left abutment could also have affected the recorded ground motions at that location and the variability of the rock conditions beneath the embankment could be even more important than the geometric effects.

Nevertheless, it was decided to use the as-recorded motion shown on Figures A-3 and A-8 for this evaluation because it was measured on rock "near" the dam.

A.8 RESULTS OF ANALYSES

The following sections present the results of the analyses performed for the Loma Prieta evaluation. The seismic response of the dam as calculated by QUAD4MU and FLAC is

discussed first and then the results of two FLAC seismic deformation analyses are presented and discussed.

A.8.1 Seismic Response and Input Motion

Two dimensional "equivalent-linear" response analyses of the analysis cross-section were performed using QUAD4MU and FLAC. The resulting response spectra of the horizontal component of the response (at 5 percent damping) at the crest and at the top of the Lower Core zone are plotted on Figure A-9. The response spectra at the ground surface (Point A on the crest) and at the top of the Lower Core (Point B) are shown on the left and right sides of the figure, respectively. Also shown on the left side of Figure A-9 is the 5 percent damping response spectrum of the transverse component of the recording from the Loma Prieta earthquake at the crest station close to the analysis section; i.e., the "Right Crest" station identified on Figure A-2.

The response spectra calculated by the QUAD4MU and FLAC equivalent linear analyses are very similar at Points A and B indicating that the shear modulus and damping values used in the FLAC model are reasonable when compared to the QUAD4MU results in terms of seismic response.

Figure A-9 shows that the response spectra from the two-dimensional QUAD4MU and FLAC equivalent linear analyses at Point A are quite similar in general shape to that from the recording; however, the recorded motion shows somewhat less amplification than the calculated results up to a period of about 1 second.

Figure A-10 shows that the response spectra from the two-dimensional non-linear FLAC analyses at Point A are quite similar in general shape to that from the recording; however, the recorded motion shows somewhat more amplification than the calculated results, particularly at period of about 1 second.

Figure A-11 compares the 5 percent damping response spectra corresponding to the input motion (i.e., the transverse abutment record from the Loma Prieta earthquake) to (a) the computed response spectrum of the horizontal motion at Point A from the non-linear FLAC analyses and (b) the transverse motion recorded at the crest near the analysis section. The same information in terms of the ratios of the crest surface horizontal motion response spectral values (computed or measured) divided by the input response spectral value at the same period are also plotted on Figure A-11. These plots can be viewed as "response spectral amplification functions". The results shown on Figure A-11 indicate that the measured and calculated responses of the dam are quite comparable for periods between 0.25 and 1.0 seconds.

There are some differences between the measured and calculated response spectra and amplification functions. It may be desirable at some level to reduce these differences. However, there is no practical way of discerning in any quantitative manner what is contributing to what and causing these differences. As mentioned before, one potential source of these differences is the input motion. However, trying to reduce the uncertainty in the input motion from the Loma Prieta event for the purpose of the seismic deformation analyses would not be fruitful because additional data on input motions are not available and because of issues related to variable bedrock and incoming seismic energy.

A.8.2 Seismic Deformation Analyses

Figures A-12, A-13, and A-14 document the results of the FLAC analysis with the Mohr-Coulomb soil model. Figure A-12 show the seismic displacement contours in the embankment at the end of shaking. The computed vertical and horizontal seismic displacement values and directions at the crest of the dam and mid-slopes of the downstream and upstream shells are also shown as vector components. Figure A-13 shows the end-of-shaking seismic displacement vectors, describing the general pattern of seismic deformations. Figure A-13 should be considered for seismic deformation patterns only; an exaggerated scale is used to plot the displacement vectors for clarity of presentation and that exaggerated scale may provide a somewhat unrealistic sense of the calculated overall seismic deformations. Figures A-14 shows color-coded contour intervals of computed shear strains at the end of shaking.

Figure A-15 documents the calculated horizontal and vertical time histories of displacements at selected points. This figure indicates that the seismic displacements take place during the strong shaking portion of the input motion and stabilize after that.

Figure A-16 documents the calculated horizontal and vertical time histories of displacements at the crest. These results indicate that the calculated crest displacements consist of about 0.2 feet of settlement and 0.4 feet of horizontal movement in the downstream direction.

The measured horizontal displacement at the crest during the Loma Prieta event ranged from 0.12 feet upstream to 0.25 feet downstream, with 0.1 feet downstream movement at the location of the analysis cross section (see Figure A-1). The calculated value of the horizontal displacement (i.e., 0.4 feet) is slightly higher than the measured values, but this difference is relatively small (in the order of inches).

The measured vertical displacement at the crest during Loma Prieta event ranged from 0.15 feet to 0.85 feet, with 0.78 feet of settlement at the location of the analysis cross section (see Figure A-1). The calculated value of the vertical settlement (i.e. 0.2 feet) is lower than the measured values.

A.8.3 Surface Cracks

Observations after the Loma Prieta earthquake (RLVA, 1990) also documented cracks at the upstream face of the dam as well near the dam abutments. The pattern of the displacements calculated by our analysis (see Figure A-13) is consistent with this observation. This pattern indicates the "rock knoll" beneath the upstream shell is likely affecting the displacement patterns in such a way that is consistent with the formation of longitudinal cracks above this knoll, as has been observed (see Figure A-1). Figure A-17 documents the magnitude of stretching of the soil zones over the knoll. These results indicate that the soil zones in this area may have been susceptible to cracking, as was observed after the earthquake, due to seismically-induced reduction in horizontal confining pressures. It is noted that the calculated location of the cracks is slightly upstream compared to the field observations; this may be due to the two-dimensional nature of the analysis.

A.9 DISCUSSION AND CONCLUSIONS

The results presented herein indicate that, overall, the calculated response of the dam is in reasonably good agreement with the observed response during the Loma Prieta event. The displacement patterns, response spectra at the crest, and magnitude of displacements are generally in adequate agreement with the measured values. The differences between the measured and calculated values can be attributed to epistemic uncertainties such as input motion, material properties, and three dimensional effects, among others.

Note on Figure A-11 that the crest response spectrum calculated using the FLAC Mohr-Coulomb model is somewhat lower than the response spectrum of the recorded crest motion. The undrained shear strength used in the FLAC Mohr-Coulomb model is 0.84 times the shear strength for triaxial compression (TXC) loading, which implies a factor of 1.4 increase for the combined effects of the rate of loading and cyclically induced softening after accounting for the TXC to Direct Simple Shear (DSS) conversion using a factor of 0.6 (i.e., $0.84 = 0.6 \times 1.4$). The agreement between the FLAC Mohr-Coulomb model and the measured response shown on Figure A-11 can be improved, but to do so would require that the 1.4 factor be increased. Given the literature information on the rate of loading effects and possible cyclically-induced softening effects, it was considered prudent to use a factor of 1.4 and not to increase it further.

The reasonably conservative nature (in the sense of calculating possibly higher seismic shear deformation in the MCE evaluation analyses) of the undrained shear strength assignment discussed in the previous paragraph is shown on Figure A-12. A comparison of Figure A-12 to Figure A-1 indicates that the computed horizontal crest displacement is higher than the horizontal crest displacement observed for a nearby crest monument, i.e., 0.4 feet versus 0.1 feet. Note that the computed value of 0.4 feet is higher than the largest observed horizontal seismic displacement value of 0.25 feet at Station 14+00 (see Figure A-1).

Figure A-12 also shows that the computed crest settlement was only about 0.2 feet while Figure A-1 indicates that the nearby crest monument settled during, or almost immediately following, the earthquake by about 0.8 feet. Many factors could have contributed to this difference, which is not very large particularly when all the uncertainties are considered as discussed earlier. However, one of the potential causes of this difference could be the effects of gravity load as the cyclic softening of the embankment takes place; this process is not reflected in our analysis. To investigate this effect further, a simplified analysis has been performed. In this simplified analysis, the static vertical settlement of the crest due to gravity loads was calculated for different levels of reduction in shear modulus, where the modulus reduction was applied uniformly throughout the dam.

Our analysis indicated that the settlement difference of 0.6 feet ($0.8 - 0.2$) can be captured by approximately 20 percent additional softening of the shear modulus in the embankment, which was considered reasonable.

In conclusion, we have found that the evaluation of the Loma Prieta case history presented in this appendix can be used in the seismic deformation evaluation of the Lenihan Dam under the evaluation ground motions to provide a site-specific empirical basis that:

1. confirms the reasonableness of the overall approach based on FLAC with the Mohr-Coulomb soil model combined with the QUAD4MU equivalent linear analysis;

2. shows that the undrained shear strengths assigned to the embankment materials are reasonably conservative; and
3. indicates that the observed surface cracking is probably a result of high shaking combined with the bedrock topography.

TABLE A-1
SUMMARY OF ENGINEERING PROPERTIES USED IN ANALYSIS

Zone	Moist Unit Weight (pcf) γ_t	Effective Friction Angle ⁽¹⁾ ϕ'	Triaxial Undrained Strength Parameter ⁽²⁾ S_u/σ_{vc}'	Dynamic Properties ⁽³⁾		
				V_s		G/G _{max} and Damping Ratio
				K (ft/sec)	n	
1	138	37.5 °	$e^{[-0.22 \cdot \ln(\sigma_{vc}') + 0.12]}$	1305	0.25	Vucetic & Dobry (PI=15)
2U	132	35.5 °	$e^{[-0.20 \cdot \ln(\sigma_{vc}') - 0.01]}$	1190	0.25	Vucetic & Dobry (PI=17)
2L	124	25.5 °	$e^{[-0.27 \cdot \ln(\sigma_{vc}') - 0.15]}$	680	0.25	Vucetic & Dobry (PI=35)
4	140	35 °	$e^{[-0.21 \cdot \ln(\sigma_{vc}') - 0.12]}$	1550	0.25	Vucetic & Dobry (PI=15)

Notes:

⁽¹⁾ Effective Friction Angle, ϕ' (with no cohesion)

⁽²⁾ σ_{vc}' in ksf; minimum S_u for all soils = 2.0 ksf; Multiply by 0.84 for conversion to Direct Simple Shear strength (See Section 5.2.5)

⁽³⁾ Dynamic Properties, V_s (shear wave velocity), G/G_{max} (shear modulus) and Damping Ratio

$$V_s = K \cdot (\sigma_{vc}'/p_a)^n \text{ where } K \text{ is in ft/sec}$$

FIGURES

Deformation from Survey Measurement


Crest Station	Horizontal Change* (Between 7/11/89 and 10/18/89)	Vertical Change (Between 7/11/89 and 10/18/89)
11+00	0.03 ft	-0.15 ft
13+00	0.21 ft	-0.61 ft
14+00	0.25 ft	-0.74 ft
15+00	0.18 ft	-0.85 ft
16+00	0.10 ft	-0.78 ft
17+00	-0.01 ft	-0.63 ft
18+00	-0.12 ft	-0.46 ft
19+00	-0.12 ft	-0.35 ft

*Positive indicates downstream movement, negative indicates upstream movement.

Wet Area Observed on Downstream Face²

Limits of Embankment

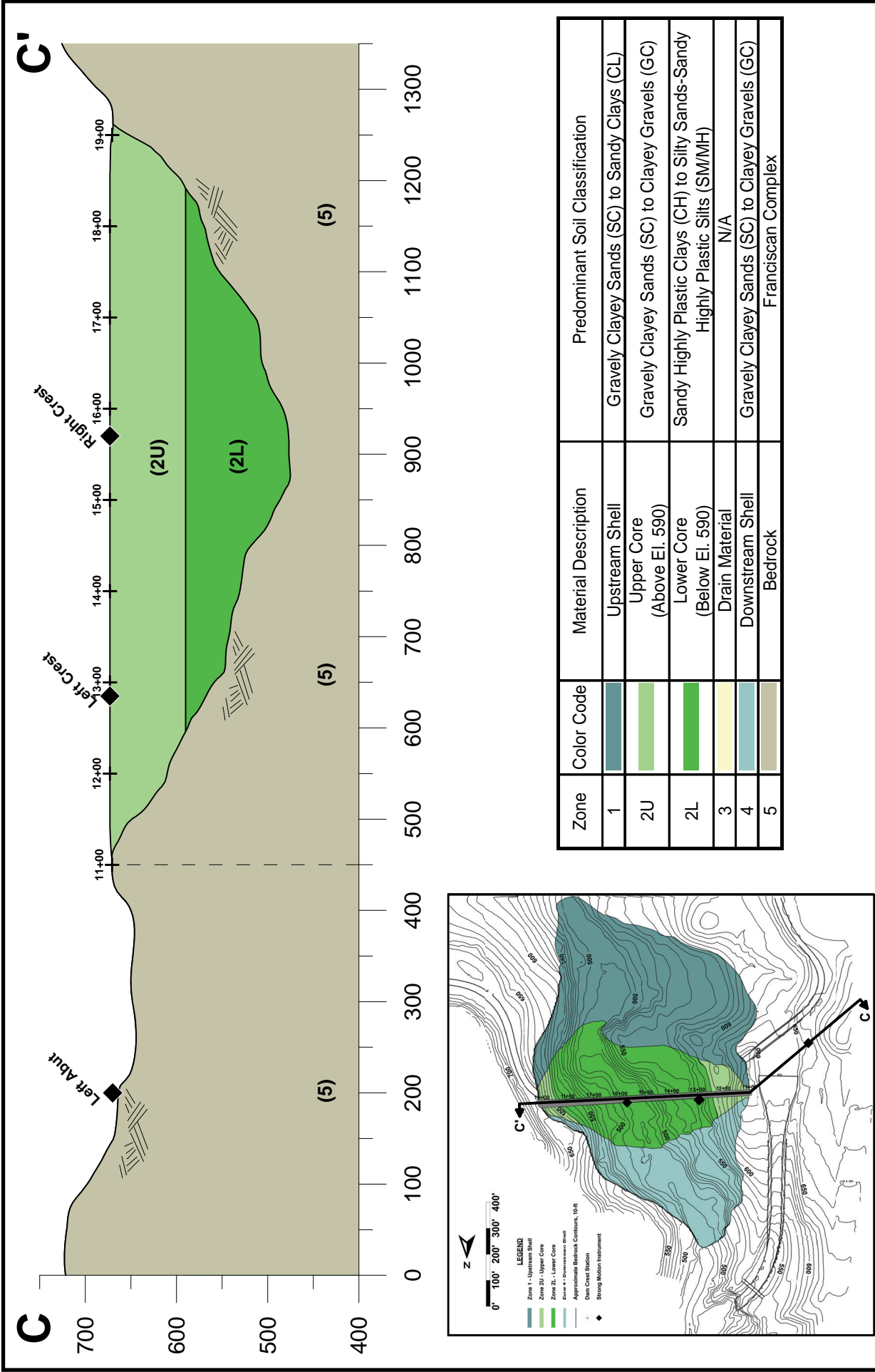
LEGEND

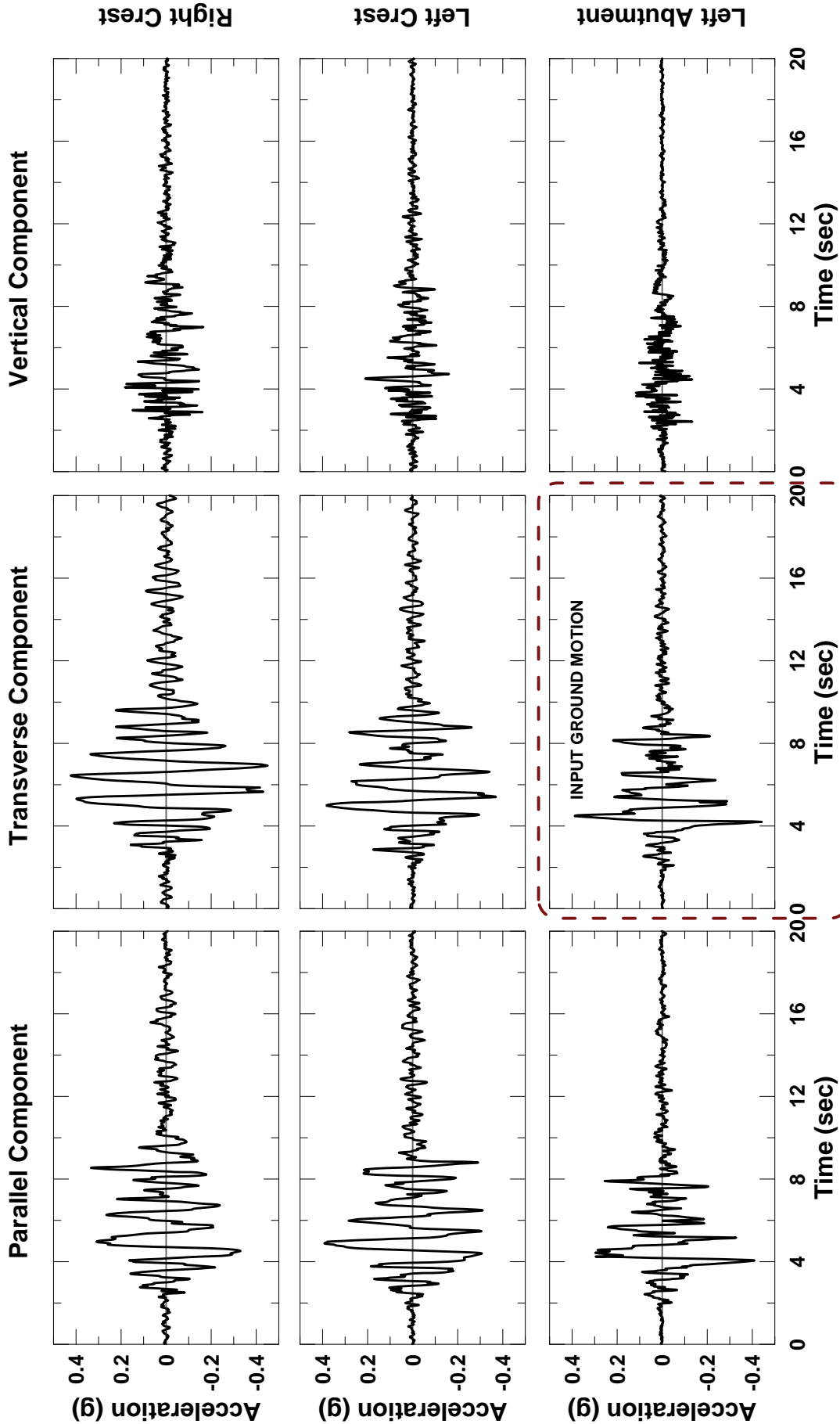
- Zone 1 - Upstream Shell
- Zone 2U - Upper Core
- Zone 2L - Lower Core
- Zone 4 - Downstream Shell
- Approximate Bedrock Contours, 10-ft
- Approximate Crack Location ¹
- Horizontal Movement (Magnitude: 1"=.25')
- Vertical Movement (Magnitde:  = .8')
- Dam Crest Station
- Strong Motion Instrument



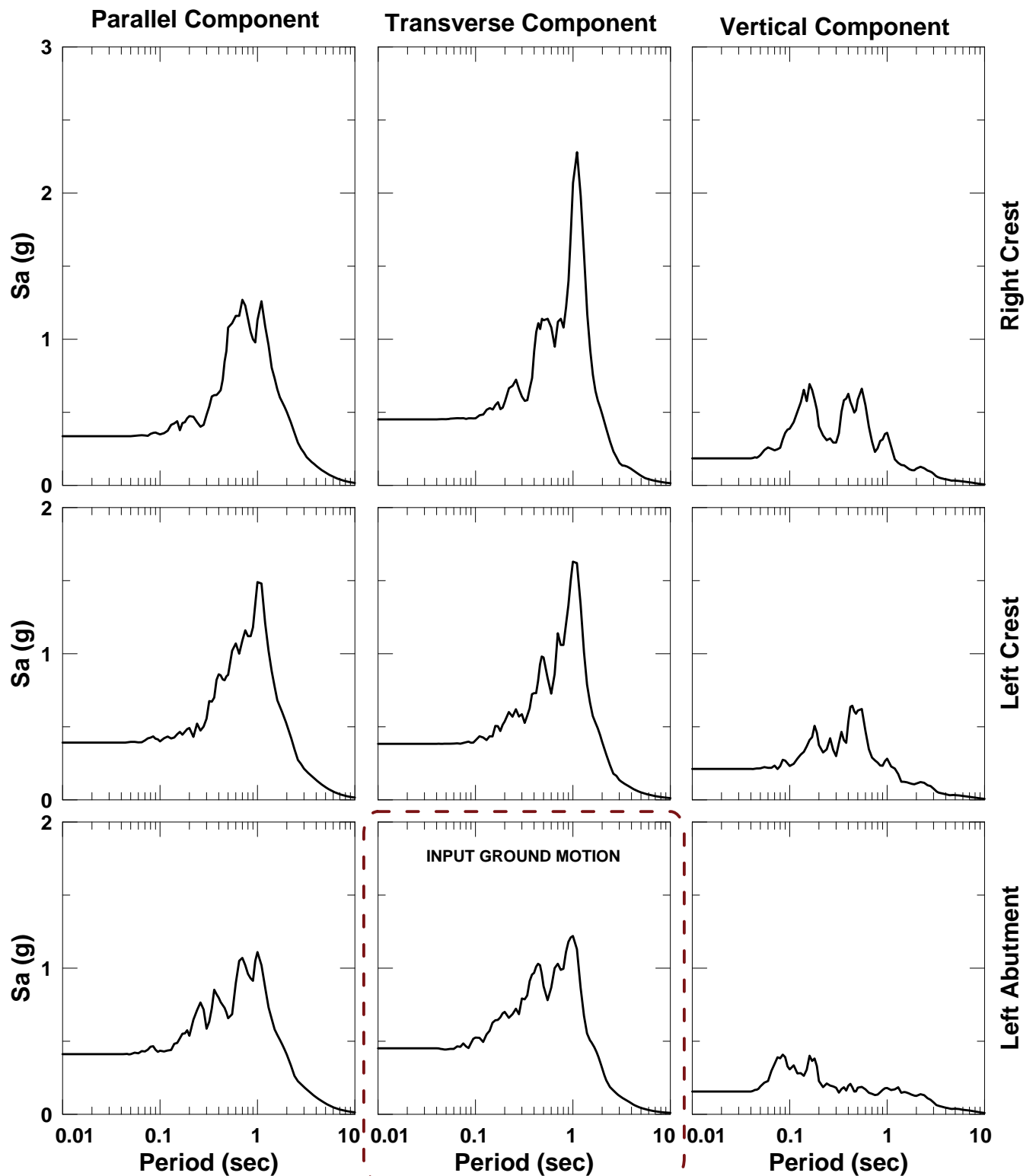
Notes:

- 1. Approximate locations of cracks derive from Investigation of SCVWD Dams Affected by the Loma Prieta Earthquake of October 17, 1989 (RLVA, 1990).
- 2. Wet area speculated to be due to previously installed drill hole casing backfilled with pea gravel acting as a relief well for groundwater in the bedrock fracture system in response to the increased pressure induced by the shaking conditions. This hypothesis is documented in RLVA, 1990.





Acceleration Time Histories of
Loma Prieta Recordings from CGS Strong Motion Center Database

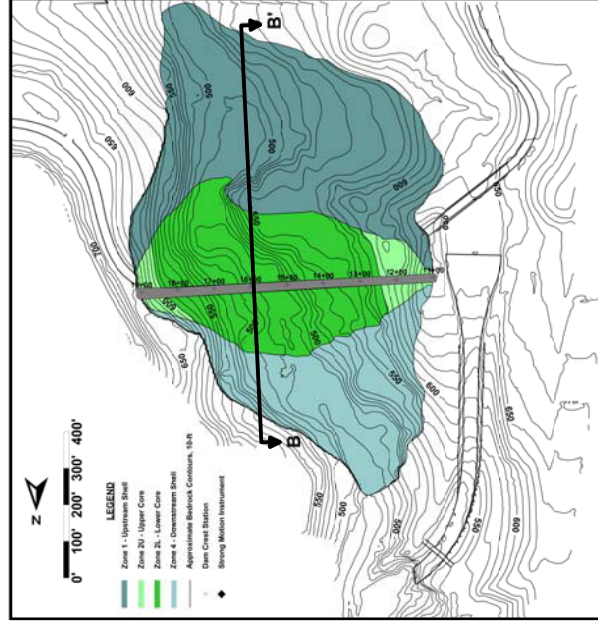
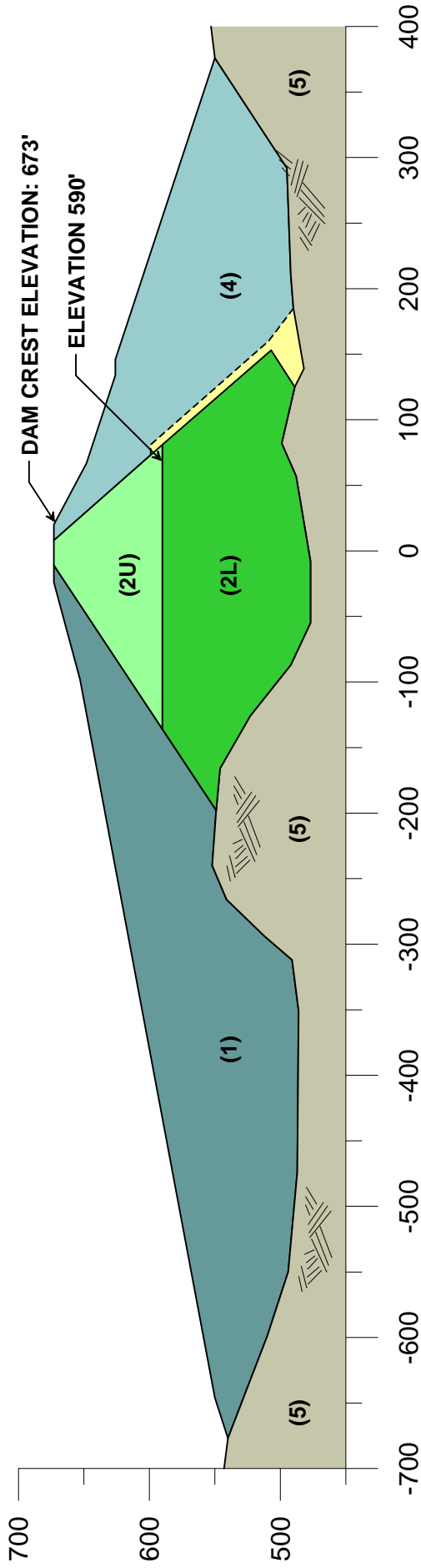


**Acceleration Response Spectra (5% Damped) of
Loma Prieta Recordings from CGS Strong Motion Center Database**



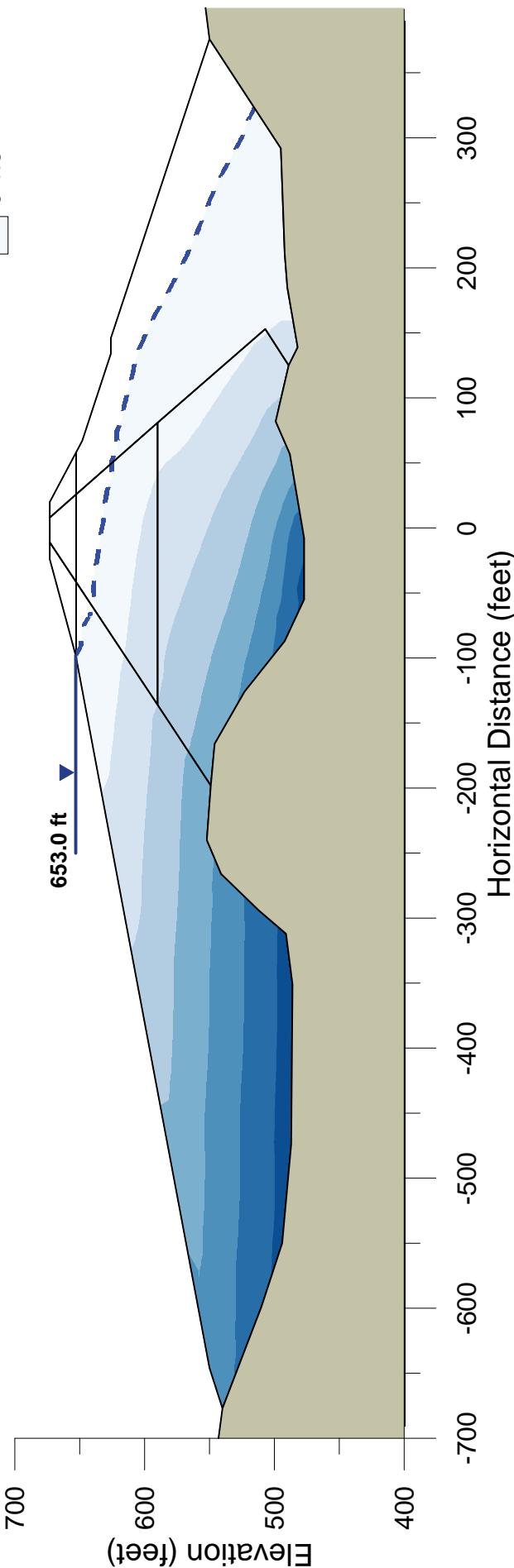
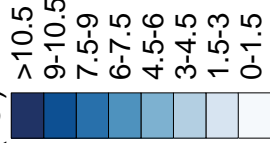
B

B'



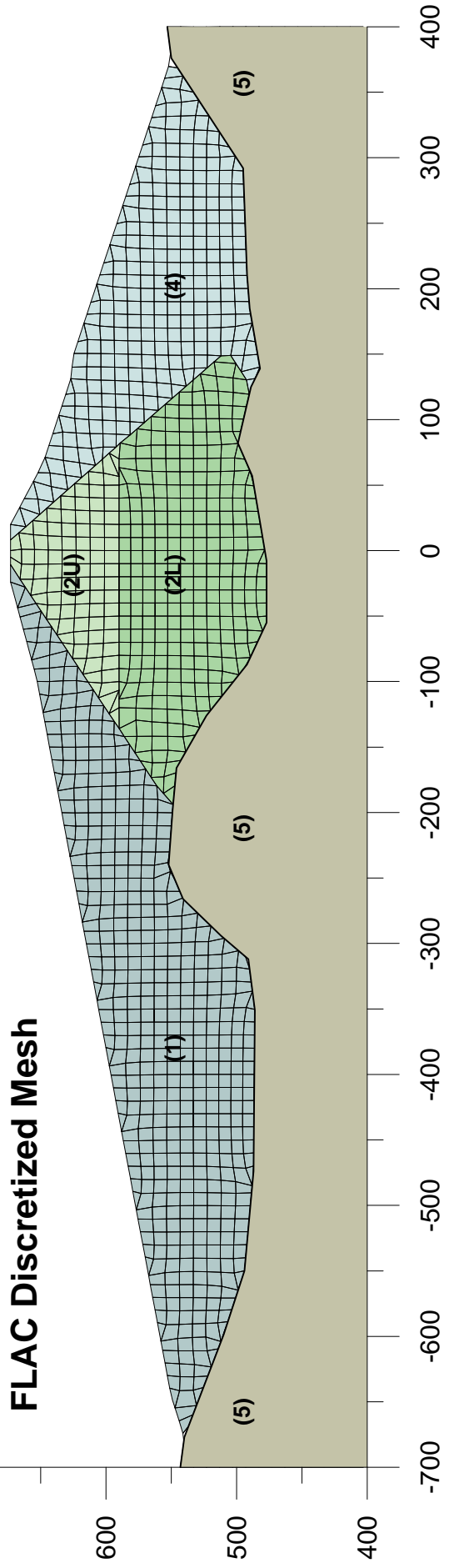
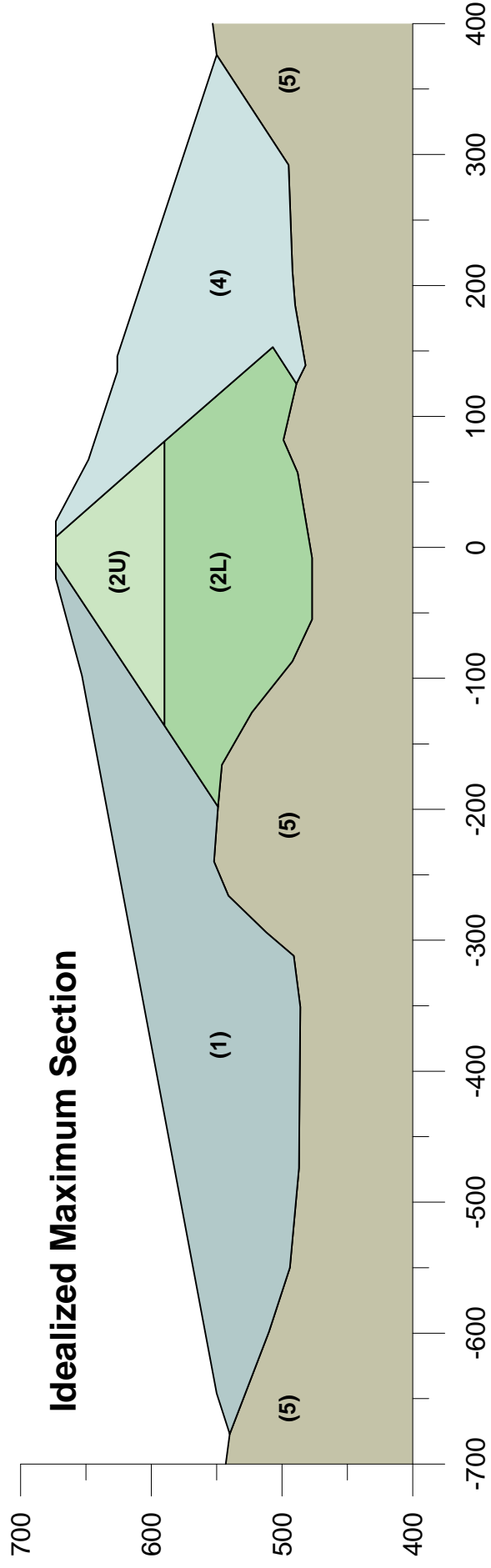
Zone	Color Code	Material Description	Predominant Soil Classification
1		Upstream Shell	Gravely Clayey Sands (SC) to Sandy Clays (CL)
2U		Upper Core (Above El. 590)	Gravely Clayey Sands (SC) to Clayey Gravels (GC)
2L		Lower Core (Below El. 590)	Sandy Highly Plastic Clays (CH) to Silty Sands-Sandy Highly Plastic Silts (SM/MH)
3		Drain Material	N/A
4		Downstream Shell	Gravely Clayey Sands (SC) to Clayey Gravels (GC)
5		Bedrock	Franciscan Complex

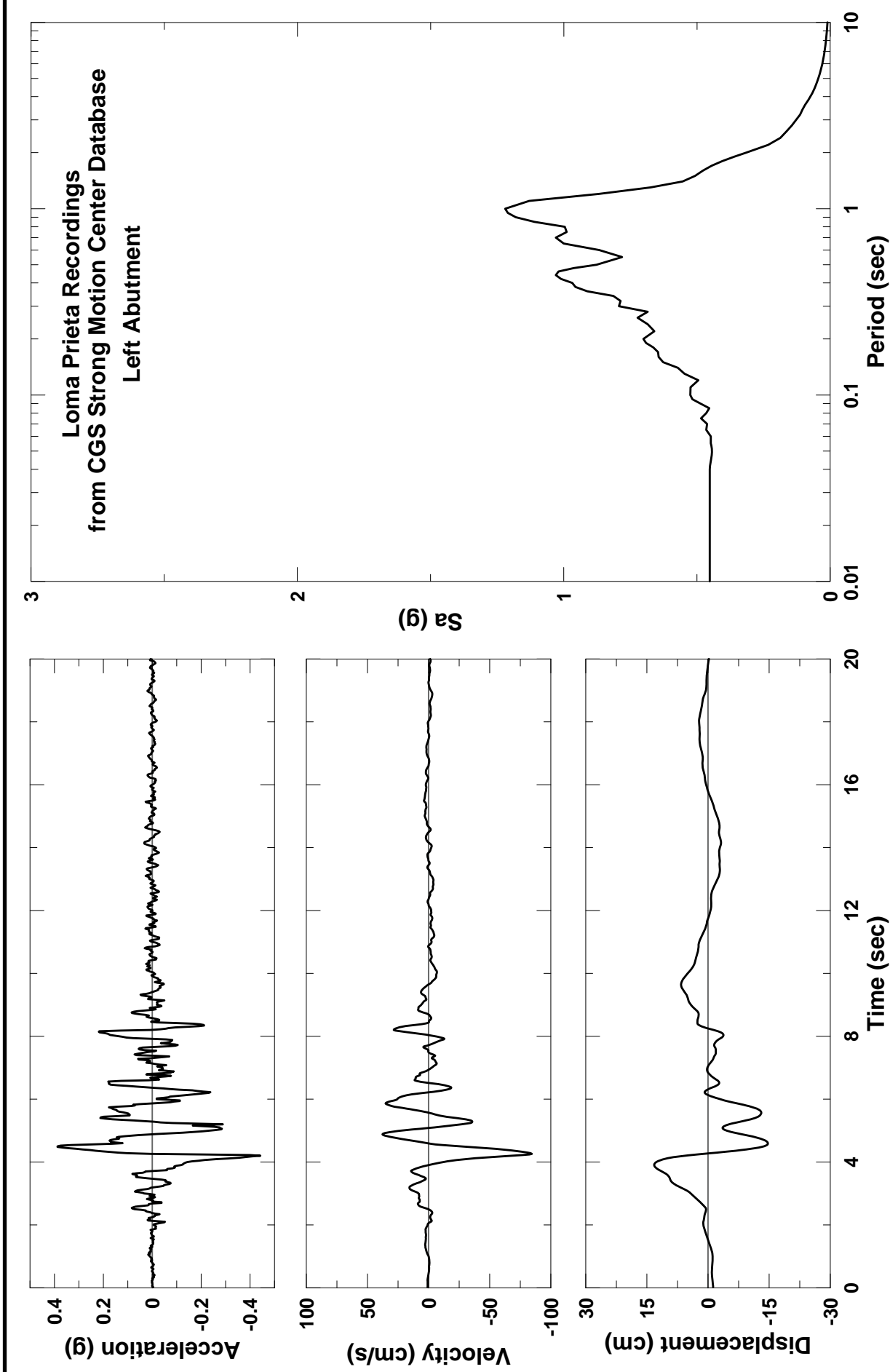
Pore Pressure
(ksf)

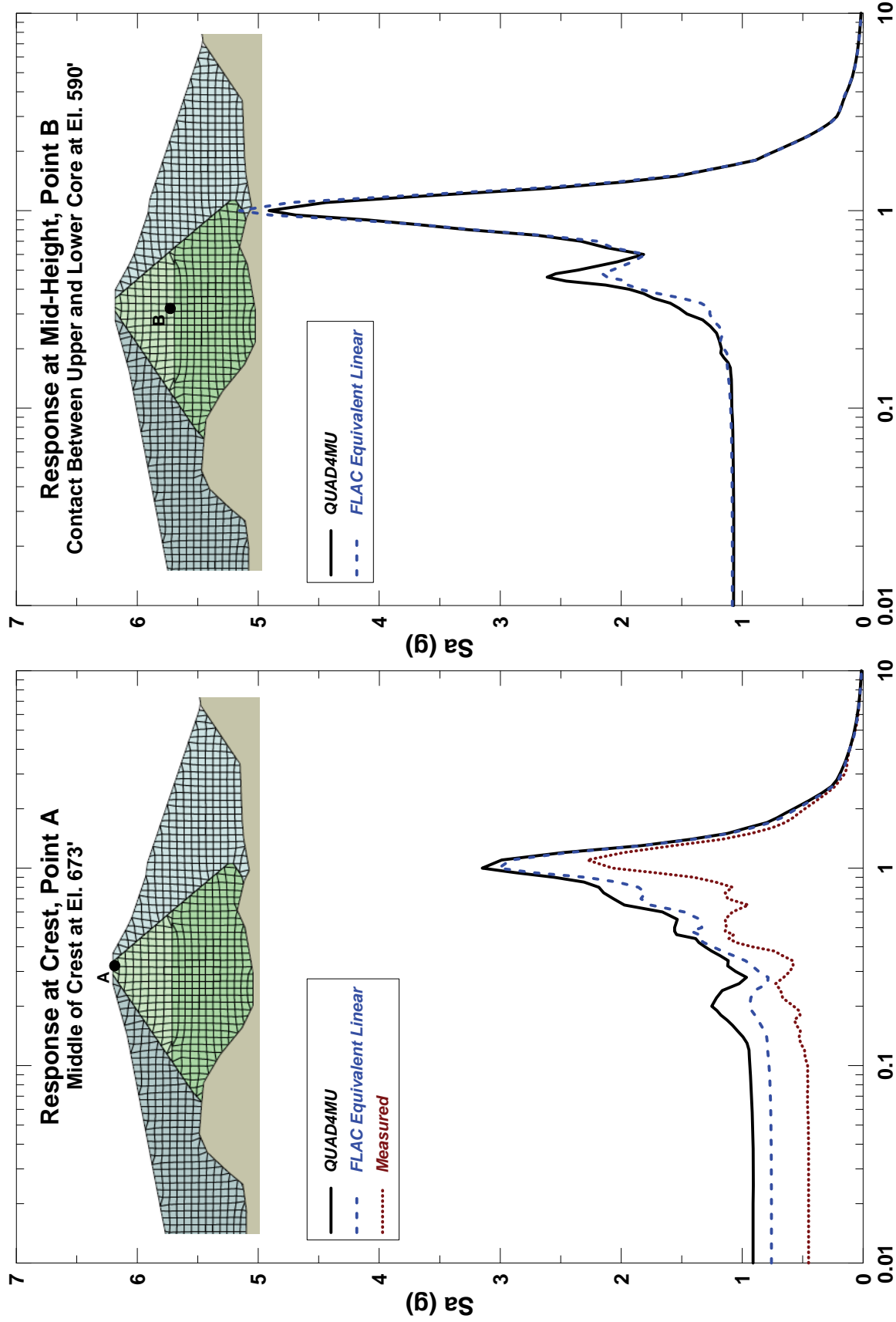


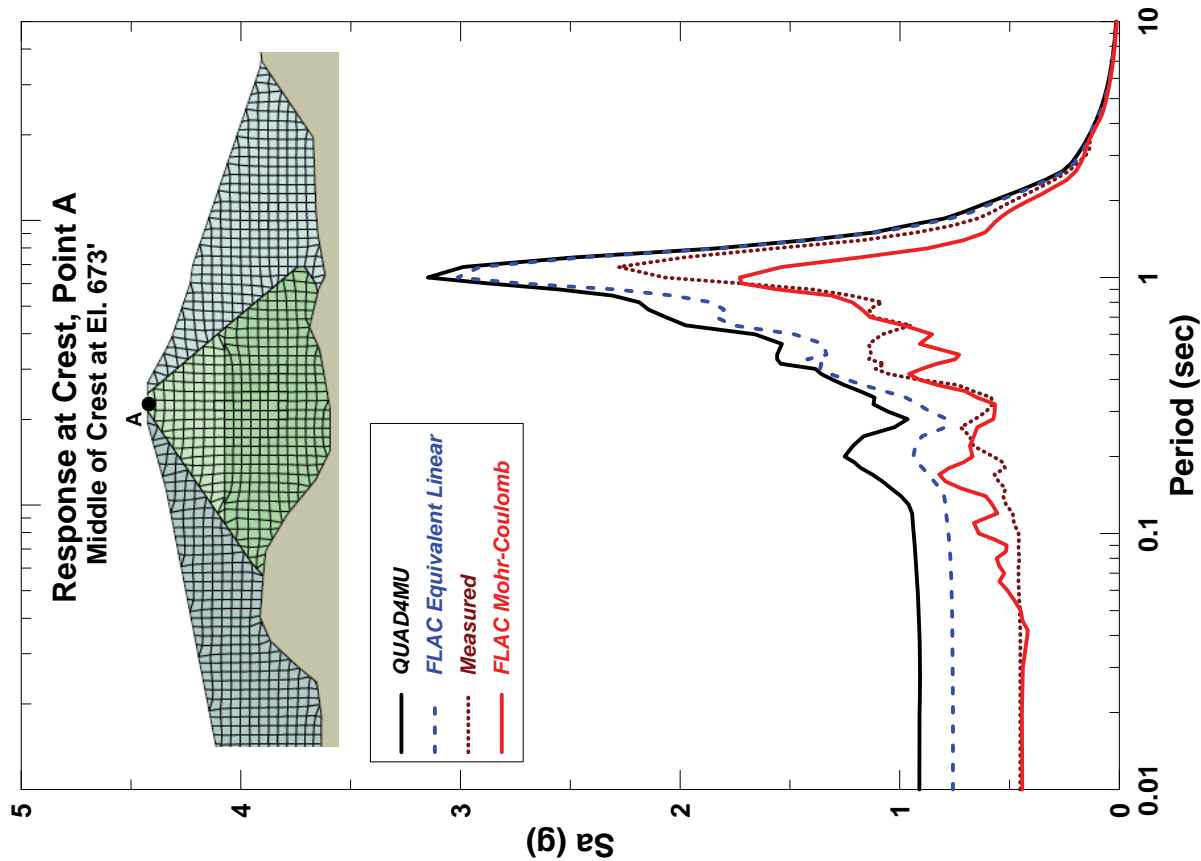
PORE PRESSURES AT FULL RESERVOIR
LEVEL - LENIHAN DAM
SEISMIC STABILITY EVALUATIONS (SSE2)

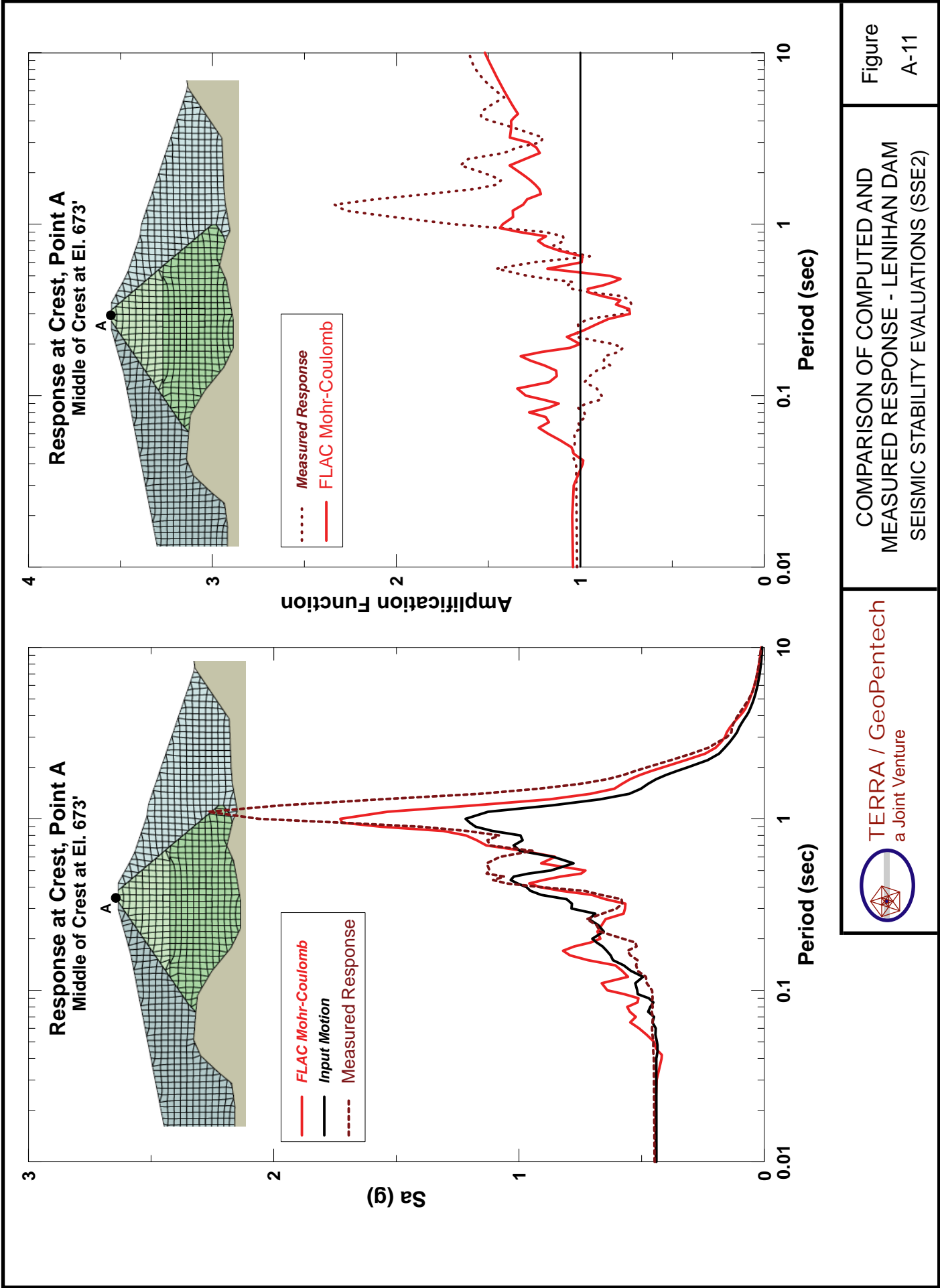
Figure
A-6



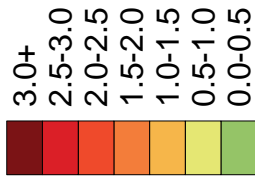








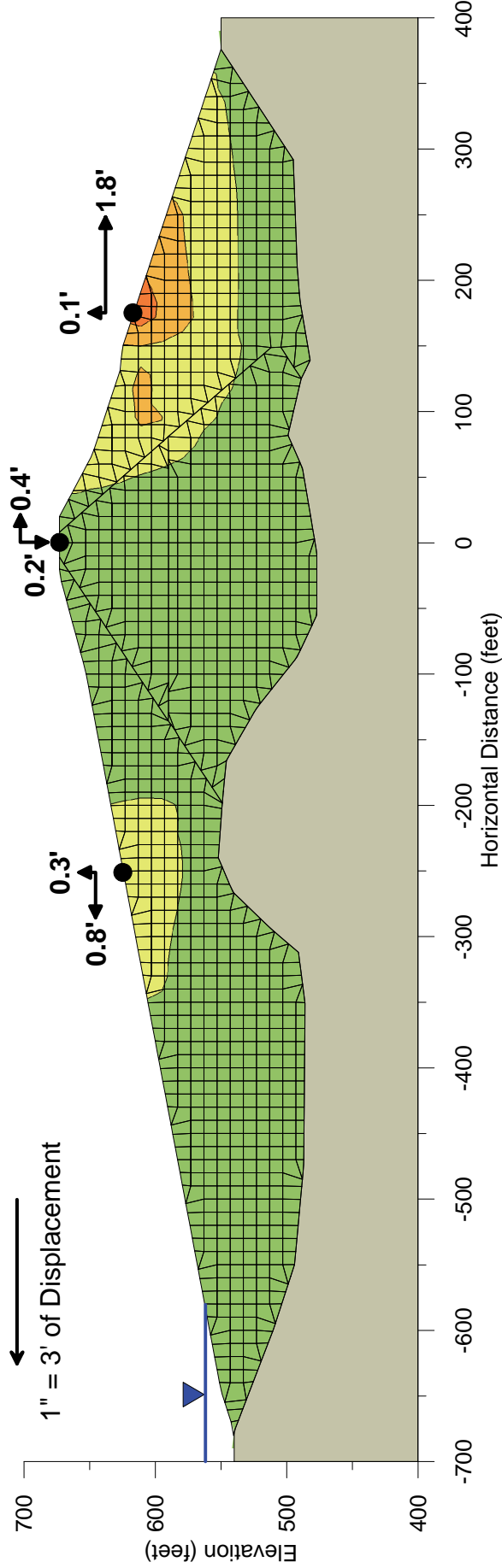
Displacement Scale (ft)



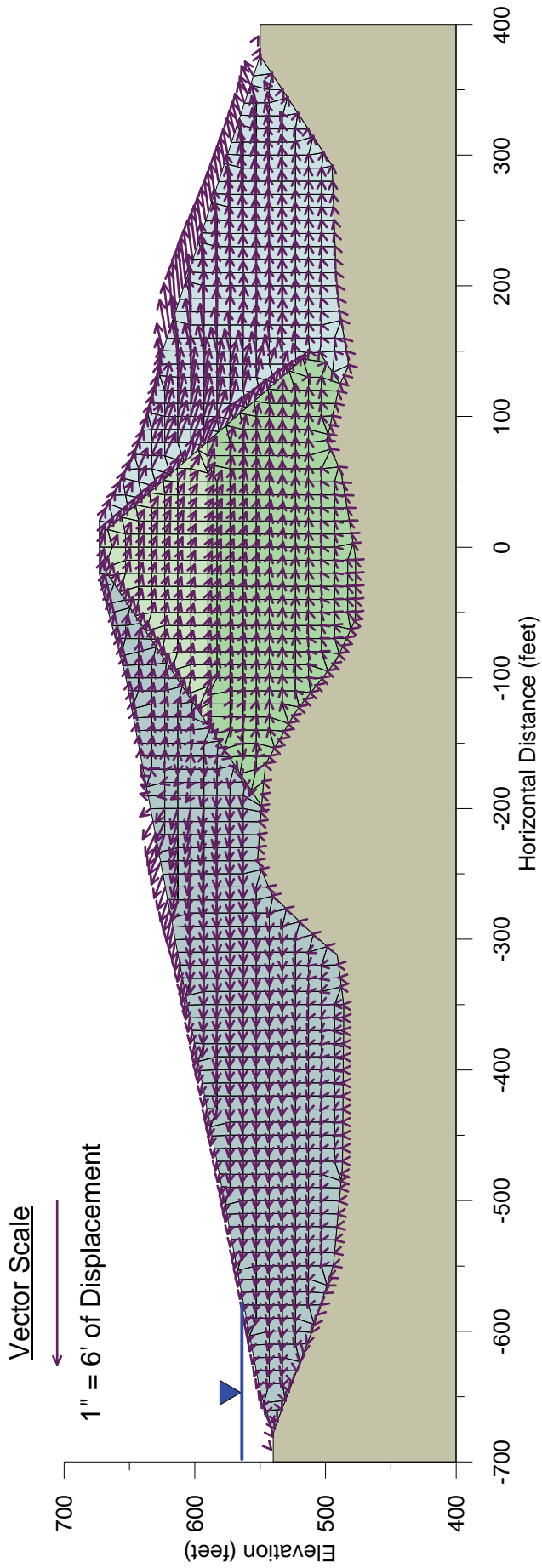
Vector Scale



1" = 3' of Displacement



Note: Permanent seismic displacement at the end of shaking, values in feet.

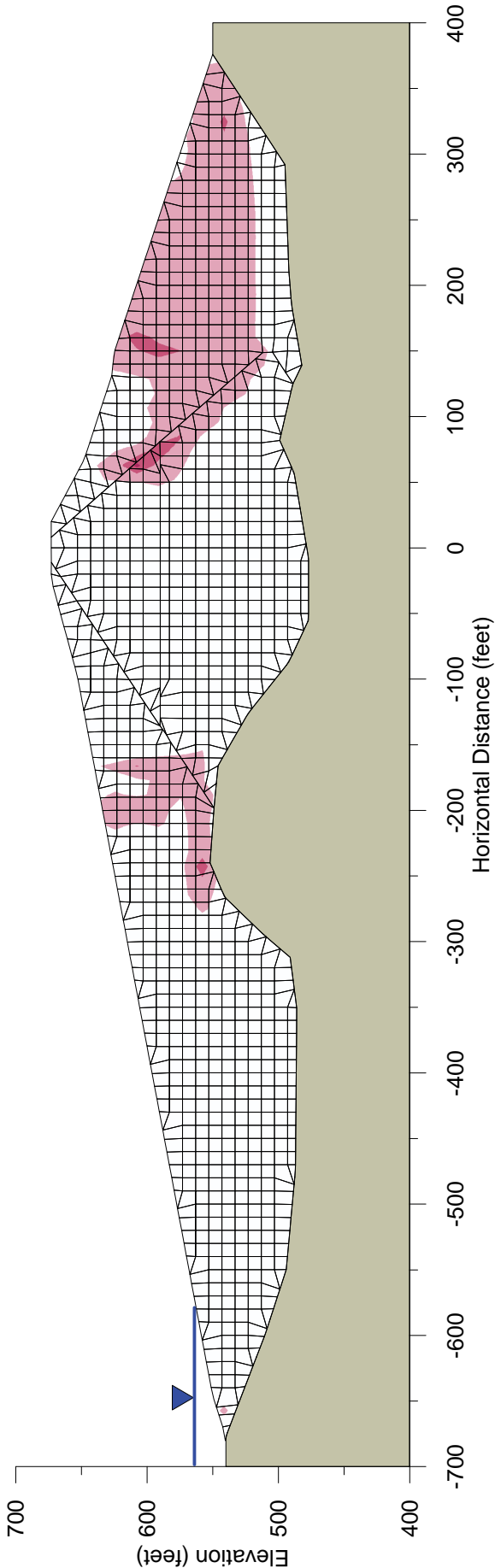
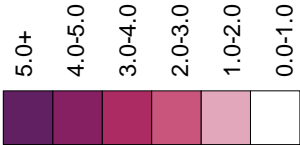


Note: Permanent seismic displacement at the end of shaking.



LOMA PRIETA EVENT - DISPLACEMENT
VECTORS - LENIHAN DAM
SEISMIC STABILITY EVALUATIONS (SSE2)

Shear Strain Scale (%)



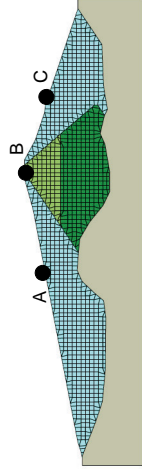
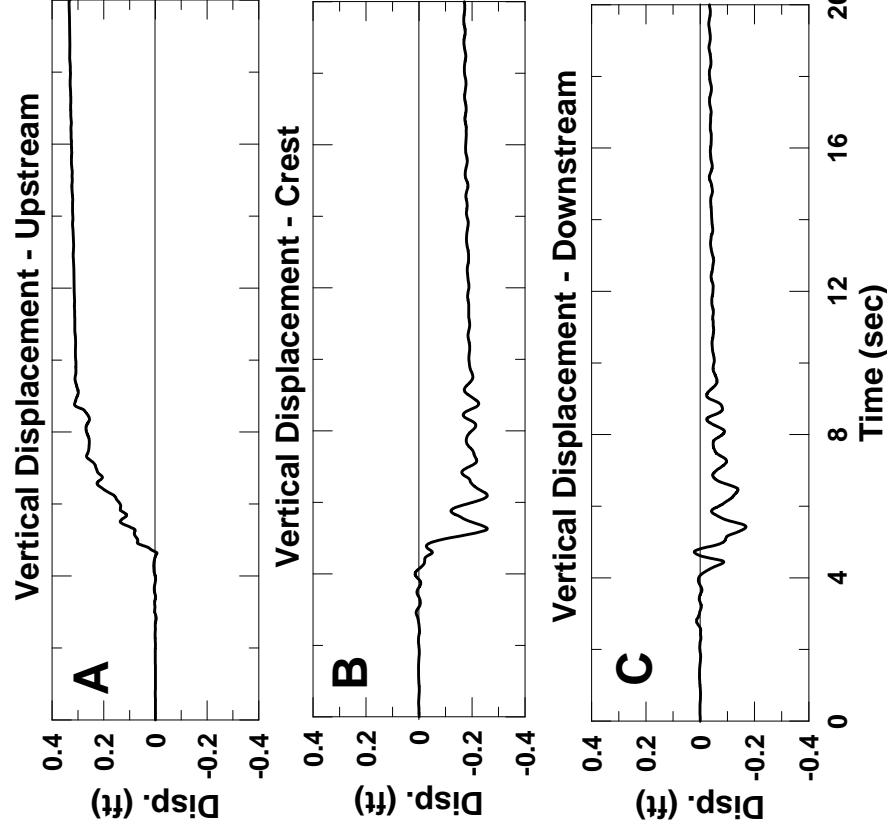
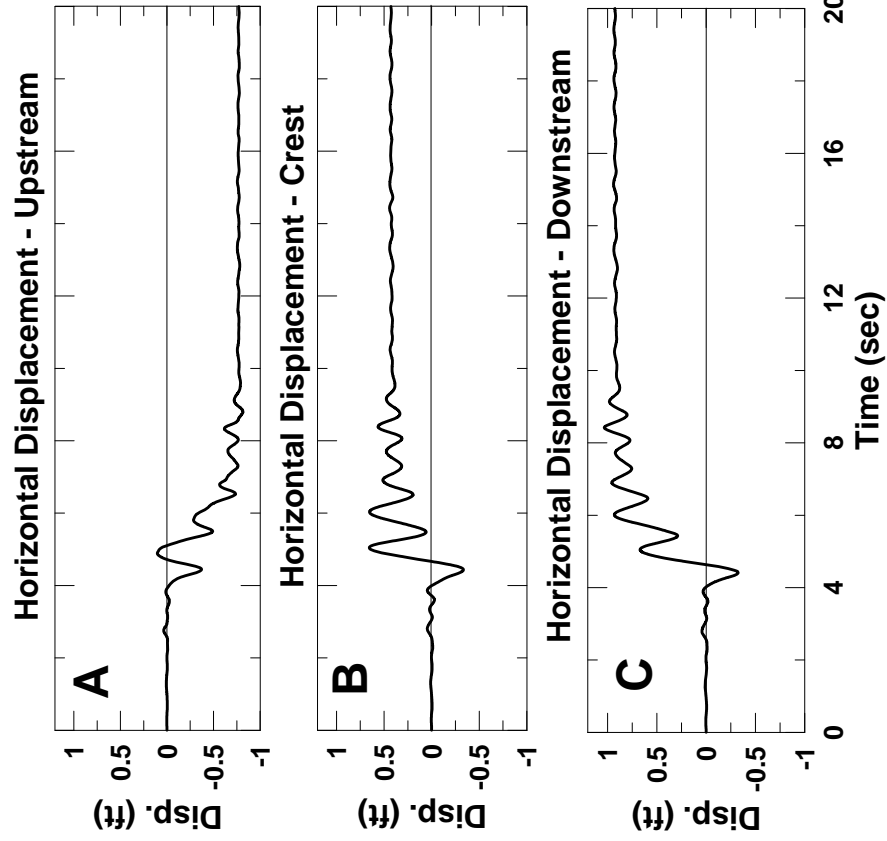
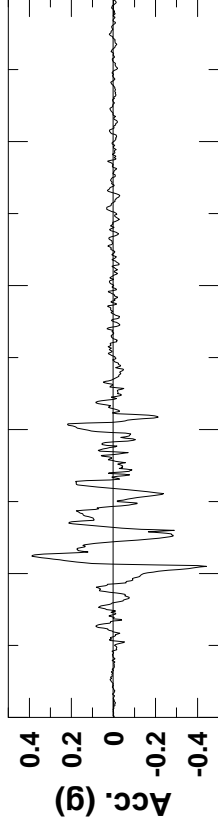
Note: Shear strain at the end of shaking.

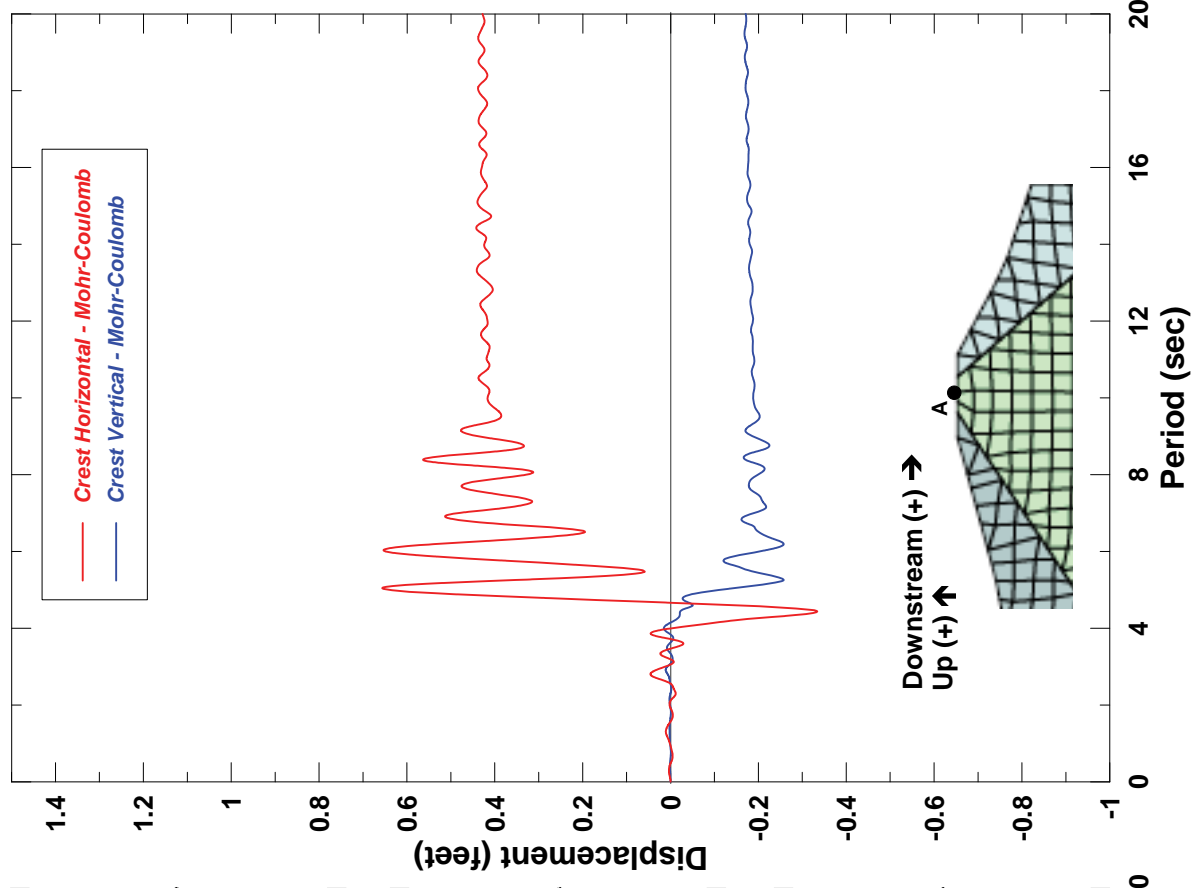
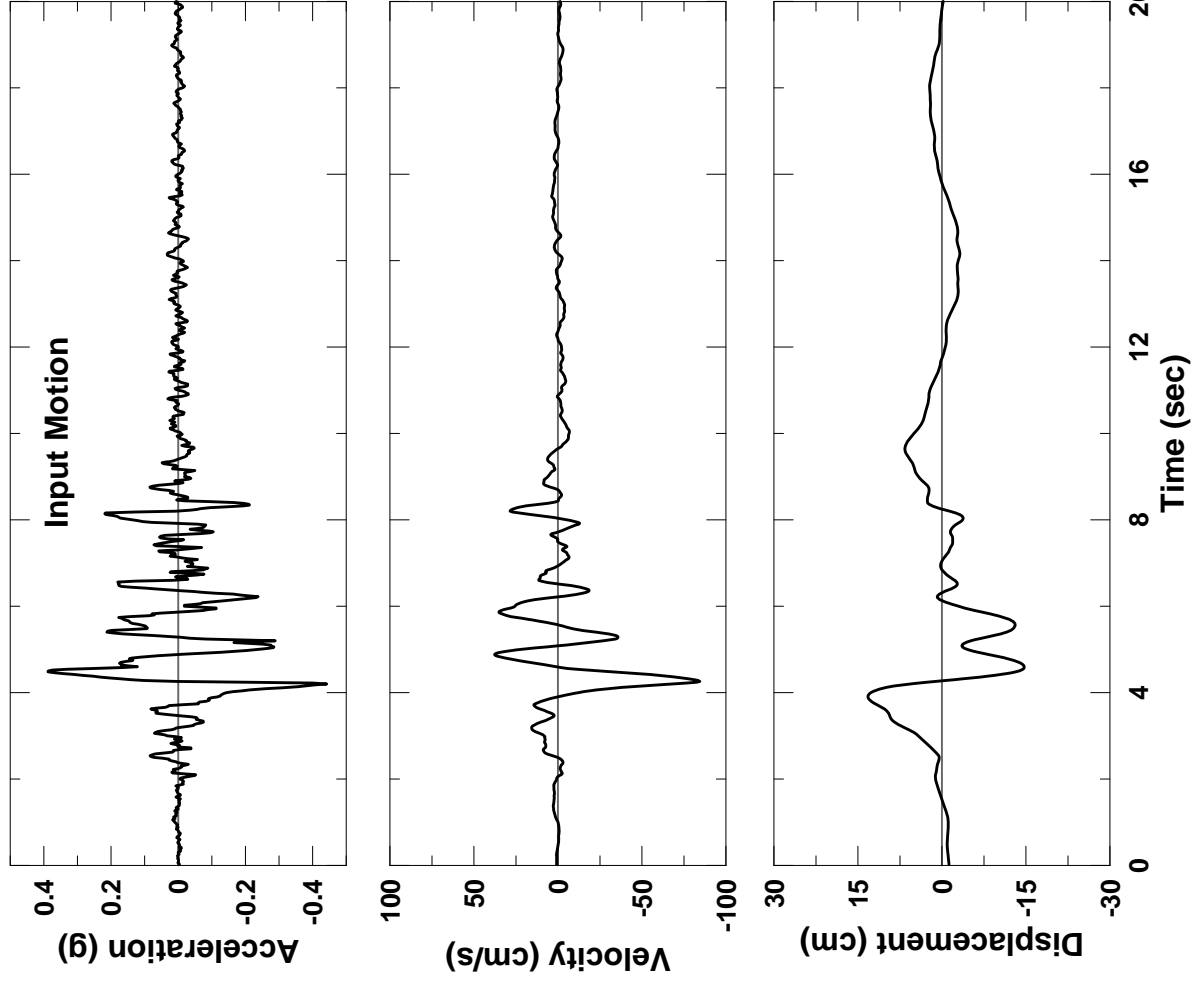


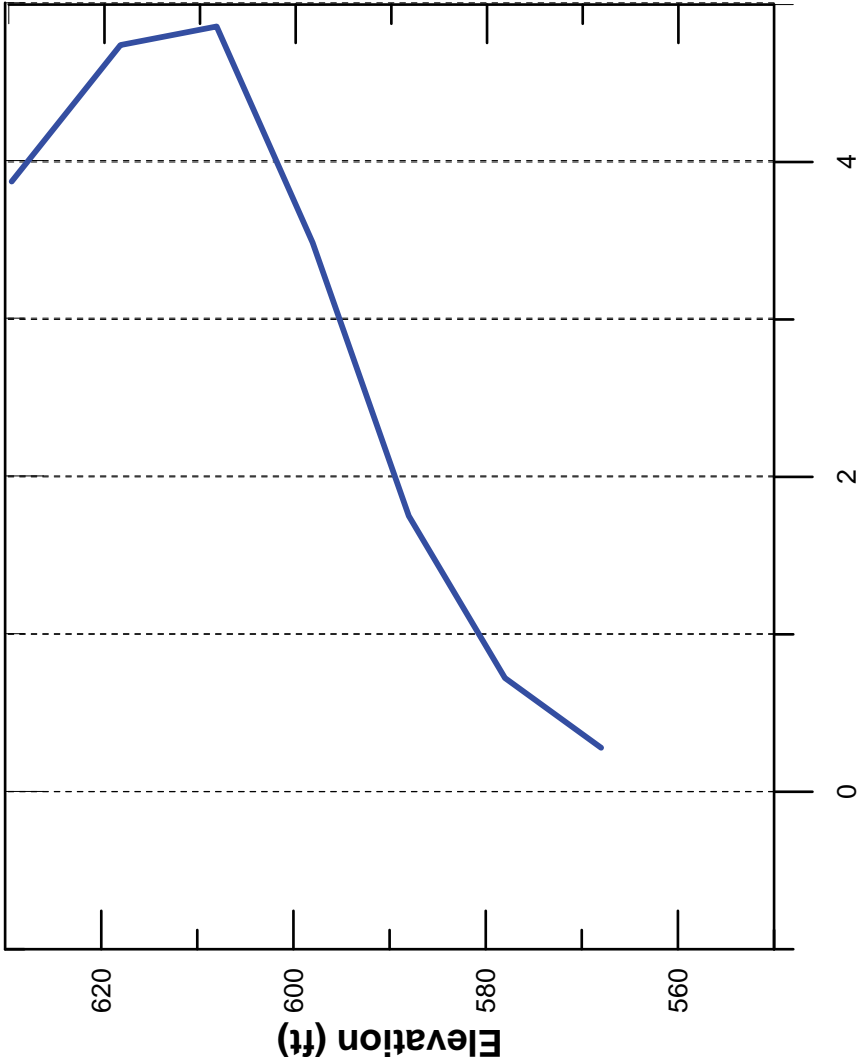
LOMA PRIETA EVENT - SHEAR STRAIN
CONTOURS - LENIHAN DAM
SEISMIC STABILITY EVALUATIONS (SSE2)

Figure
A-14

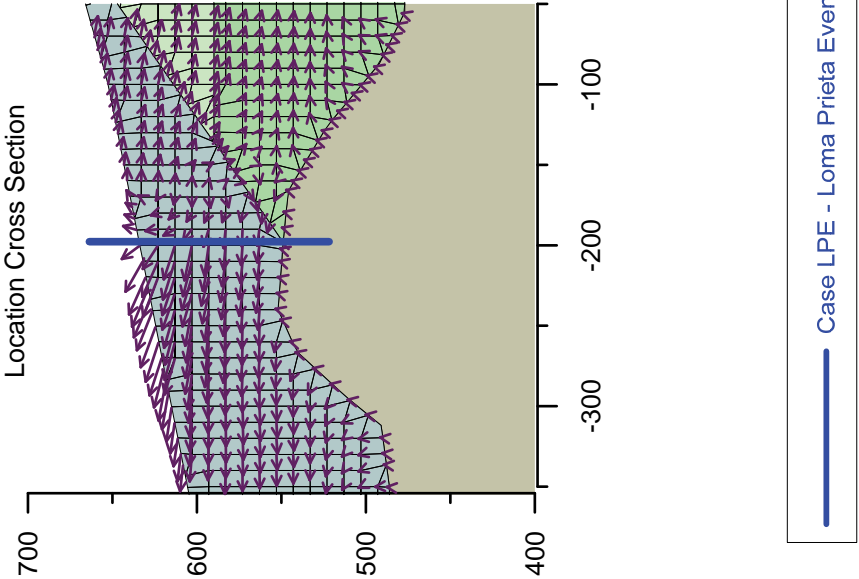
Loma Prieta Event







Change in Horizontal Length of the Zone Due to Shaking (%)
(+) = Stretch (-)=Compression



APPENDIX B

The following six MCE-evaluation ground motions were selected and were used in developing time histories that are compatible with the specified response spectral values.

1. Earthquake Records for Stanford-Monte Vista Event
 - a. Kobe Earthquake, Nish-Akashi Station, 1/16/1995
 - b. Loma Prieta Earthquake, LGPC Station, 10/18/1989
 - c. Northridge Earthquake, Sylmar-Olive View Med. FF Station, 1/17/1994
2. Earthquake Records for San Andreas Vista Event
 - a. Chi-Chi Earthquake, TCU065 Station, 9/20/1999
 - b. Landers Earthquake, Lucerne Station, 6/28/1992
 - c. Manjil Earthquake, Abbar Station, 11/03/1990

The analyses were performed considering normal and negative polarities for all six ground motions. The results of these analyses are summarized in Table B-1 in terms of crest, as well as upstream and downstream horizontal and vertical displacements.

As shown on Table B-1, the calculated horizontal crest deformations range from 0.1 to 1.1 feet downstream and the calculated vertical settlements range from 0.1 to 0.3 feet. At mid-height of the upstream shell the calculated horizontal displacements range from 0.5 feet downstream to 1.1 feet upstream, and the calculated vertical displacements range from 0.2 to 0.7 feet up (i.e. heave). At mid-height of the downstream shell the calculated horizontal displacements range from 0.7 to 2.8 feet downstream, and the calculated vertical displacements range from 0.1 to 0.4 feet up.

For each ground motion, the critical case between the normal and negative polarities was selected and the case identifier was assigned to the critical polarity (i.e. SAx, and SMVx for San Andreas, and Stanford-Monte Vista events, respectively). The critical case between the two polarities was chosen based on the magnitude of the calculated crest displacements.

The results of the critical cases identified in Table B-1 are summarized graphically in groups of five figures showing: (a) the comparison of QUAD4MU and FLAC spectra; (b) seismic displacement contours; (c) seismic displacement vectors; (d) computed shear strain contours; and (e) computed displacement time histories. The earthquake cases and results for parameters (a) through (e) are listed below with corresponding figure numbers where the results are shown.

Case	Comparison of QUAD4MU and FLAC spectra	Seismic displacement contours	Seismic displacement vectors	Computed shear strains contours	Computed displacement time histories
SA1 - Chi Chi	Fig. B-1A	Fig. B-1B	Fig. B-1C	Fig. B-1D	Fig. B-1E
SA2 - Landers	Fig. B-2A	Fig. B-2B	Fig. B-2C	Fig. B-2D	Fig. B-2E
SA3 - Manjil	Fig. B-3A	Fig. B-3B	Fig. B-3C	Fig. B-3D	Fig. B-3E
SMV1 - Kobe	Fig. B-4A	Fig. B-4B	Fig. B-4C	Fig. B-4D	Fig. B-4E
SMV2 - Loma Prieta	Fig. B-5A	Fig. B-5B	Fig. B-5C	Fig. B-5D	Fig. B-5E
SMV3 - Northridge	Fig. B-6A	Fig. B-6B	Fig. B-6C	Fig. B-6D	Fig. B-6E

As an example, the results for Landers case SA2 are summarized in Figures B-2A through B-2E. Figure B-2A shows a reasonable match between the FLAC and QUAD4MU spectra while Figure B-2B shows the displacement contours and numerical displacements at the three locations tabulated in Table B-1. The displacement vectors are shown on Figure B-2C and contours of induced shear strains are shown on Figure B-2D. Finally, the deformation time histories at the three points identified in Table B-1 are presented in Figure B-2E. The conclusions that are derived from these sets of graphical results are discussed in Sections 5 and 6 of the report.

List of Figures

- B-1A Case SA1-Chi Chi, FLAC & QUAD4MU Response Spectra
- B-1B Case SA1-Chi Chi, Displacement Contours
- B-1C Case SA1-Chi Chi, Displacement Vectors
- B-1D Case SA1-Chi Chi, Shear Strain Contours
- B-1E Case SA1-Chi Chi, Deformation Time History
- B-2A Case SA2-Landers, FLAC & QUAD4MU Response Spectra
- B-2B Case SA2-Landers, Displacement Contours
- B-2C Case SA2-Landers, Displacement Vectors
- B-2D Case SA2-Landers, Shear Strain Contours
- B-2E Case SA3-Manjil, Deformation Time History
- B-3A Case SA3-Manjil, FLAC & QUAD4MU Response Spectra
- B-3B Case SA3-Manjil, Displacement Contours
- B-3C Case SA3-Manjil, Displacement Vectors
- B-3D Case SA3-Manjil, Shear Strain Contours
- B-3E Case SA3-Manjil, Deformation Time History
- B-4A Case SMV1-Kobe, FLAC & QUAD4MU Response Spectra
- B-4B Case SMV1-Kobe, Displacement Contours
- B-4C Case SMV1-Kobe, Displacement Vectors
- B-4D Case SMV1-Kobe, Shear Strain Contours
- B-4E Case SMV1-Kobe, Deformation Time History
- B-5A Case SMV2-Loma Prieta, FLAC & QUAD4MU Response Spectra
- B-5B Case SMV2-Loma Prieta, Displacement Contours
- B-5C Case SMV2-Loma Prieta, Displacement Vectors
- B-5D Case SMV2-Loma Prieta, Shear Strain Contours

- B-5E Case SMV2-Loma Prieta, Deformation Time History
- B-6A SMV3-Northridge, FLAC & QUAD4MU Response Spectra
- B-6B SMV3-Northridge, Displacement Contours
- B-6C SMV3-Northridge, Displacement Vectors
- B-6D SMV3-Northridge, Shear Strain Contours
- B-6E SMV3-Northridge, Deformation Time History

TABLE B-1
SUMMARY OF CALCULATED DEFORMATIONS

Case ⁽¹⁾	Input GM	Polarity	Crest Displacement ⁽²⁾		Upstream Slope ⁽³⁾		Downstream Slope ⁽³⁾		Critical ⁽⁴⁾
			Horiz (ft)	Vert (ft)	Horiz (ft)	Vert (ft)	Horiz (ft)	Vert (ft)	
SA1	Chi Chi Scaled Input Motion	Normal	0.8	-0.2	-0.4	0.7	2.8	0.3	Yes
	Chi Chi Scaled Input Motion	Negative	0.4	-0.2	-1.1	0.5	2.6	0.4	No
	Landers Scaled Input Motion	Normal	0.1	-0.2	-0.7	0.2	0.7	0.1	No
SA2	Landers Scaled Input Motion	Negative	1.1	-0.3	0.4	0.3	1.5	0.1	Yes
	Manjil Scaled Input Motion	Normal	0.4	-0.1	-0.5	0.4	1.5	0.1	No
SA3	Manjil Scaled Input Motion	Negative	0.4	-0.1	-0.7	0.4	1.5	0.1	Yes
SMV1	Kobe Scaled Input Motion	Normal	0.7	-0.2	-0.3	0.5	2.0	0.2	Yes
	Kobe Scaled Input Motion	Negative	0.4	-0.1	-0.9	0.4	1.7	0.2	No
	Loma Prieta Scaled Input Motion	Normal	0.2	-0.1	-0.7	0.4	1.3	0.2	No
SMV2	Loma Prieta Scaled Input Motion	Negative	0.6	-0.2	-0.5	0.4	1.5	0.2	Yes
SMV3	Northridge Scaled Input Motion	Normal	0.9	-0.2	0.5	0.3	1.7	0.1	Yes
	Northridge Scaled Input Motion	Negative	0.1	0.1	-0.8	0.2	0.8	0.2	No

Notes:

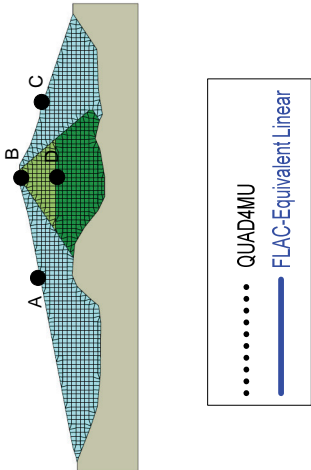
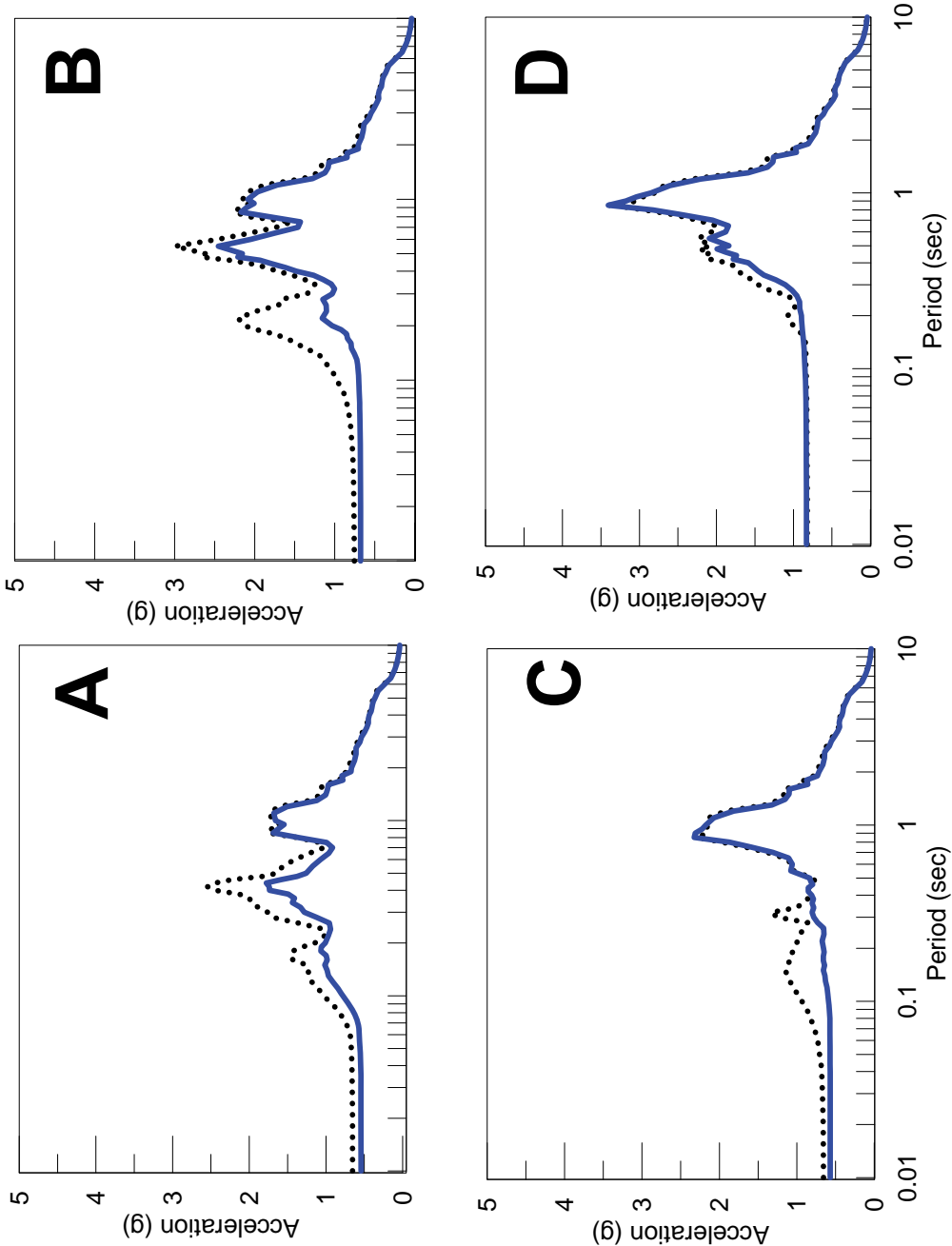
⁽¹⁾ Only the critical case between normal and negative polarity is assigned a Case Number.

⁽²⁾ Negative vertical displacement indicates settlement.

⁽³⁾ Positive horizontal displacement indicated movement towards downstream.

⁽⁴⁾ The critical case between the two polarities was chosen based on the magnitude of the calculated crest displacements.

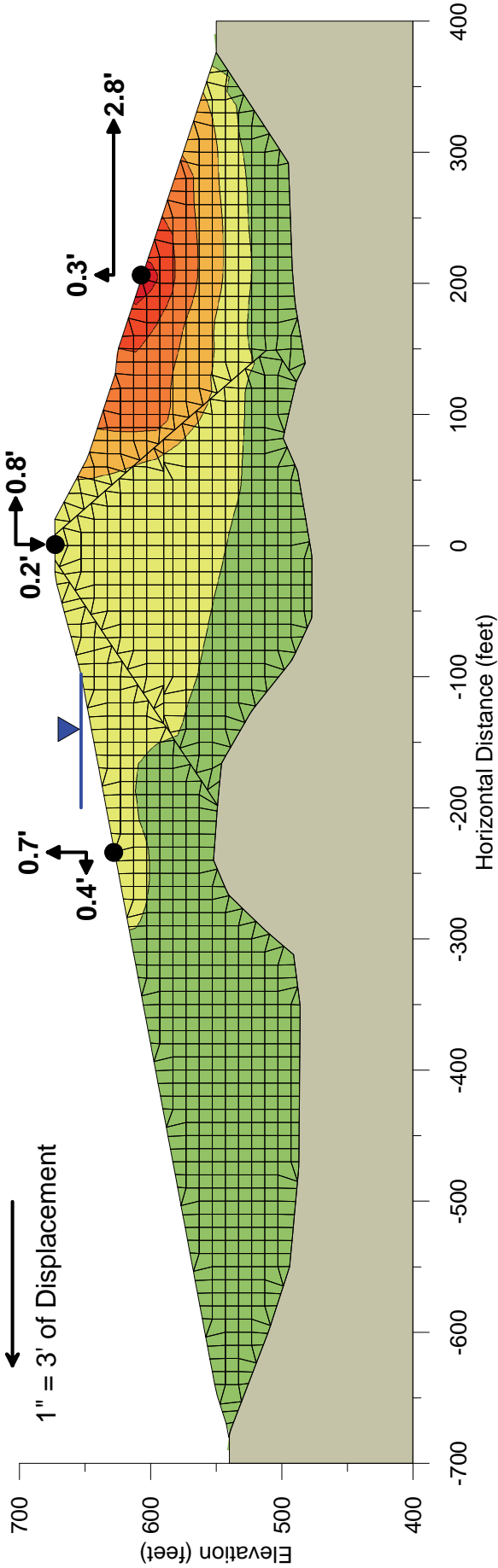
FIGURES



Displacement Scale (ft)



Vector Scale



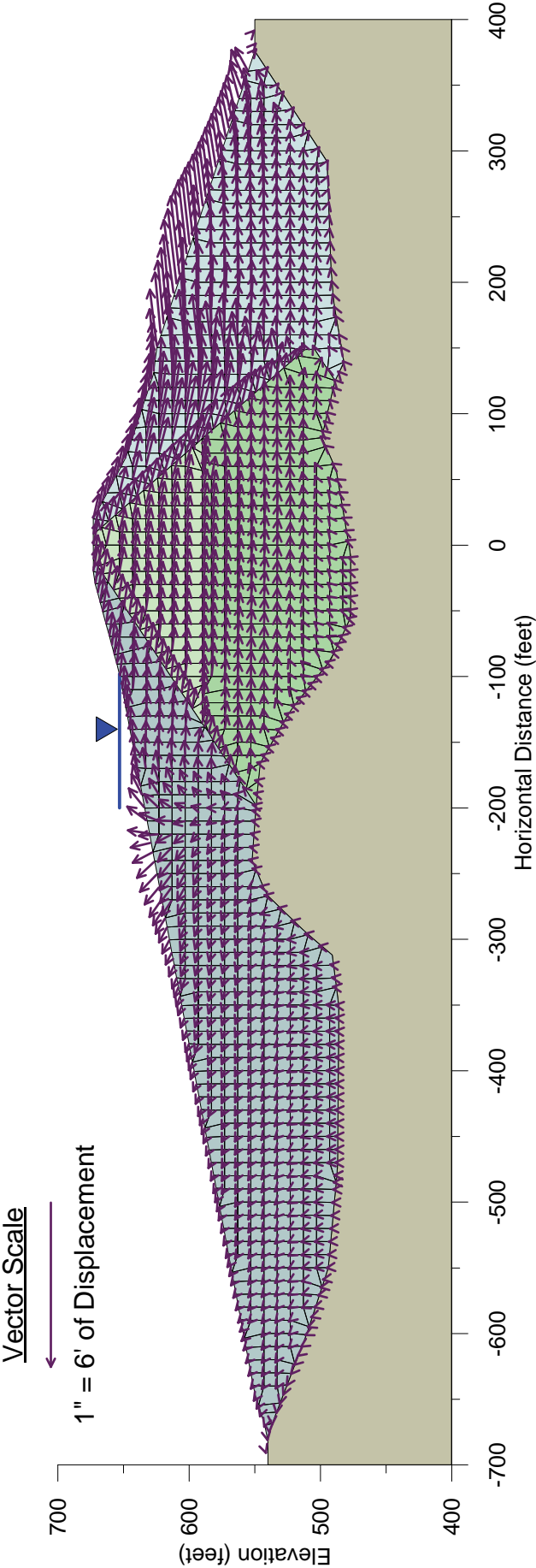
Note: Permanent seismic displacement at the end of shaking, values in feet.



TERRA / GeoPentech
a Joint Venture

CASE SA1 - CHI CHI, DISPLACEMENT
CONTOURS - LENIHAN DAM
SEISMIC STABILITY EVALUATIONS (SSE2)

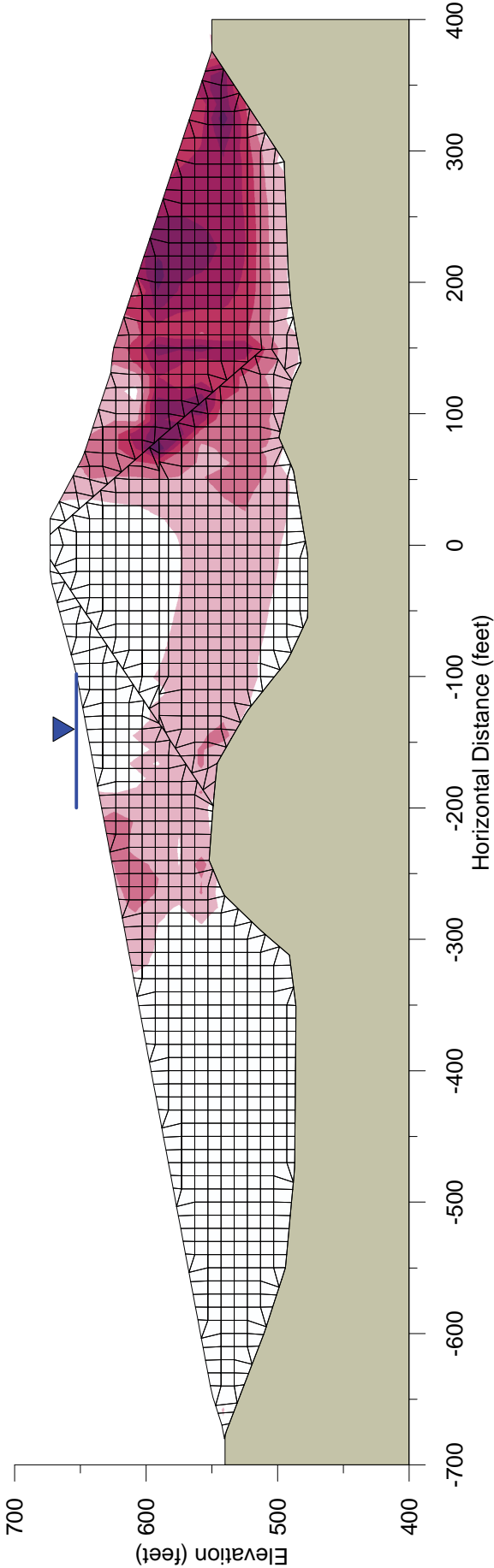
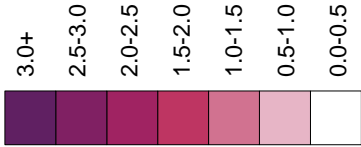
Figure
B-1B



Note: Permanent seismic displacement at the end of shaking.

<div data-bbox="1409 974 1490 1457"><div data-bbox="1419 974 1481 1339">TERRA / GeoPentech a Joint Venture</div></div>	<div data-bbox="1398 315 1511 890">CASE SA1 - CHI CHI, DISPLACEMENT VECTORS - LENIHAN DAM SEISMIC STABILITY EVALUATIONS (SSE2)</div>	<div data-bbox="1409 121 1500 210">Figure B-1C</div>
---	--	--

Shear Strain Scale (%)



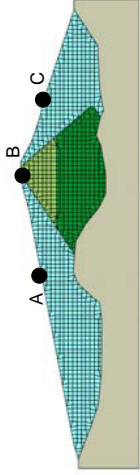
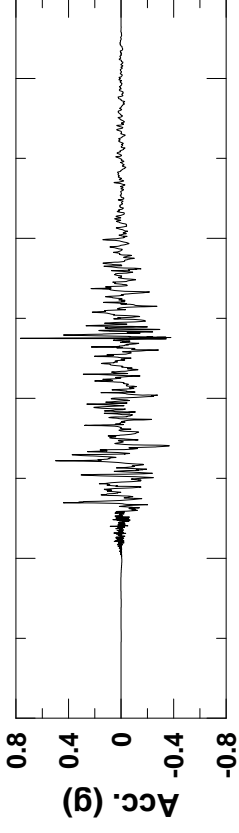
Note: Shear strain at the end of shaking.



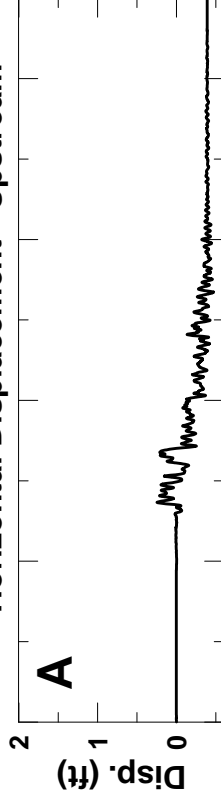
CASE SA1 - CHI CHI, SHEAR STRAIN
CONTOURS - LENIHAN DAM
SEISMIC STABILITY EVALUATIONS (SSE2)

Figure
B-1D

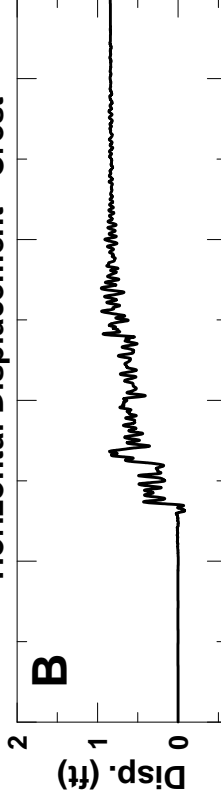
Chi Chi Evaluation Motion



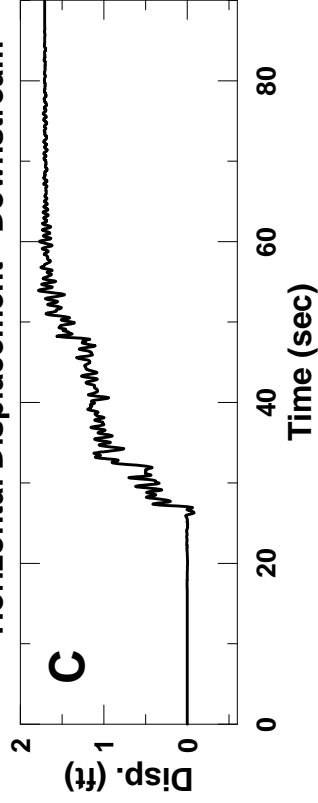
Horizontal Displacement - Upstream



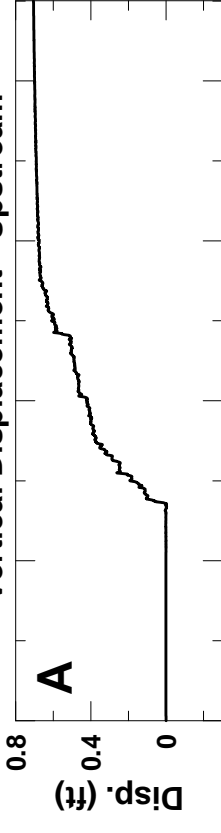
Horizontal Displacement - Crest



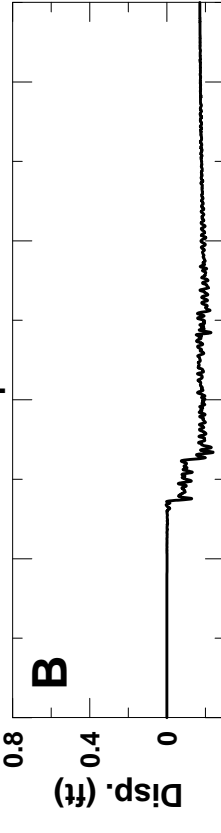
Horizontal Displacement - Downstream



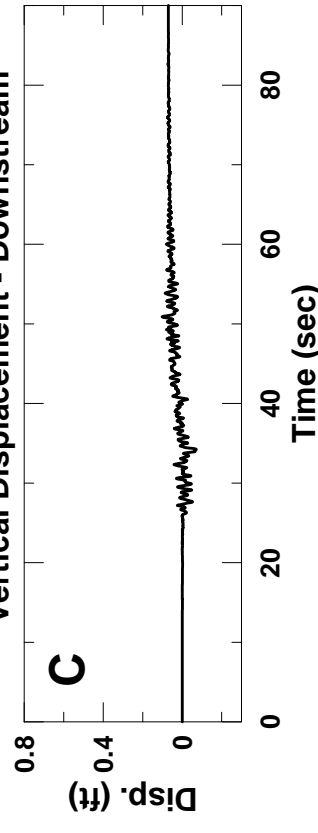
Vertical Displacement - Upstream

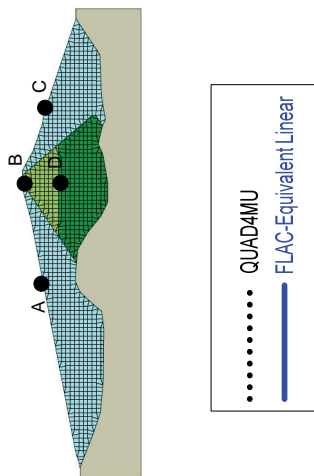
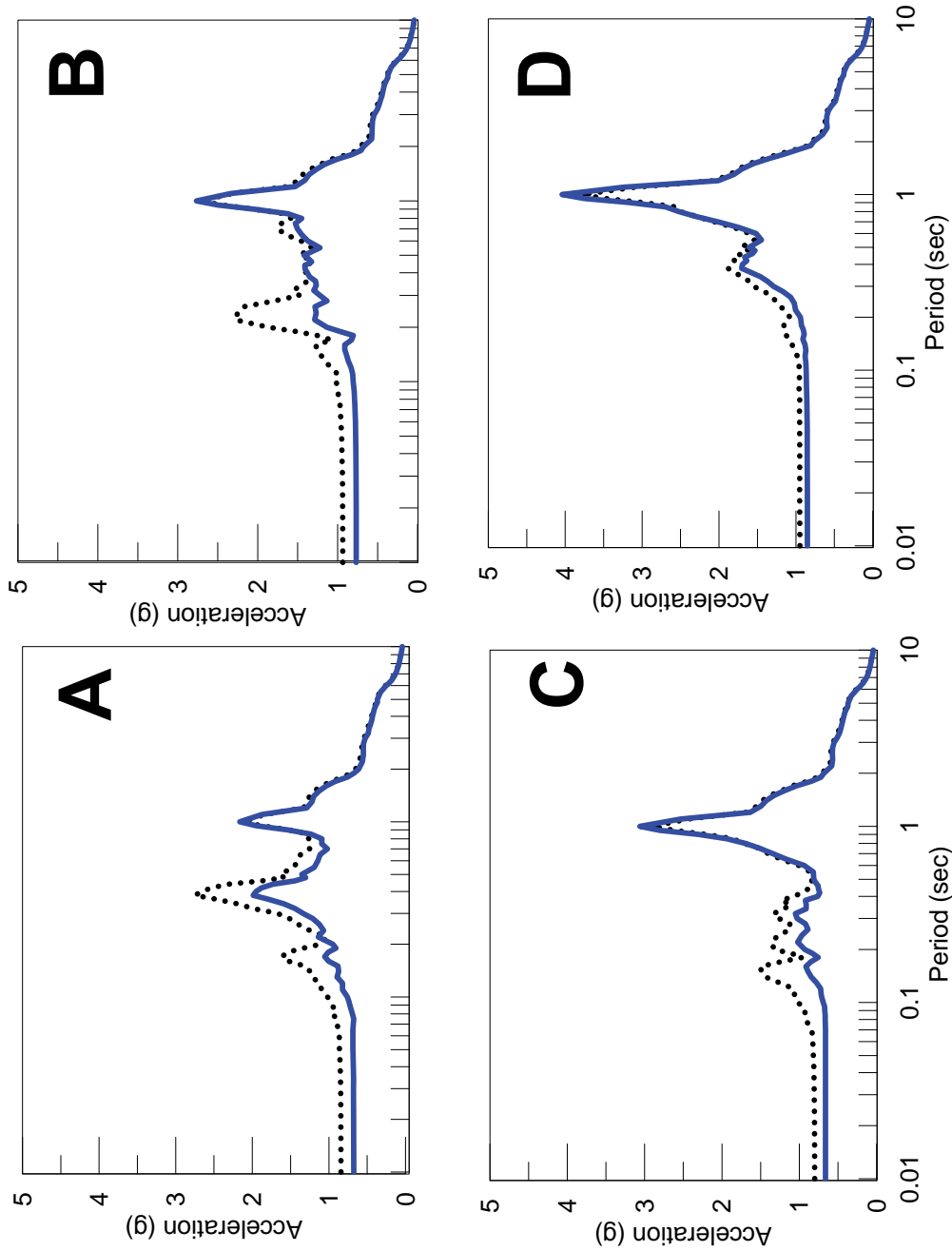


Vertical Displacement - Crest

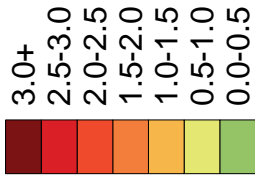


Vertical Displacement - Downstream

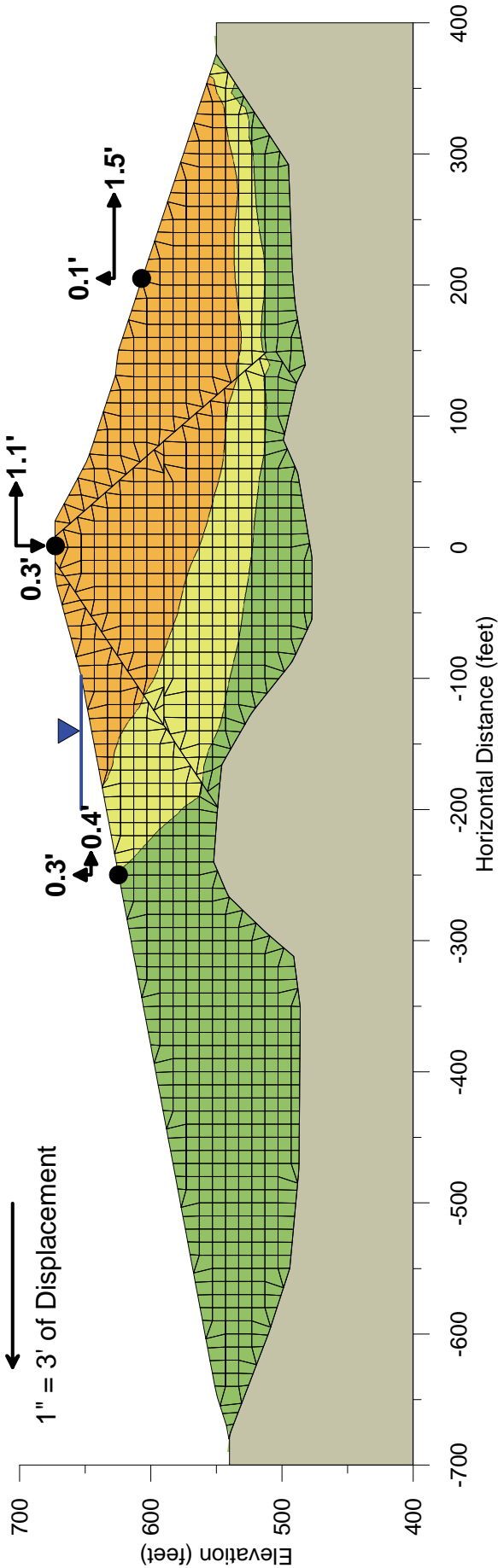
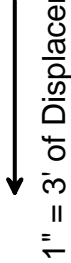




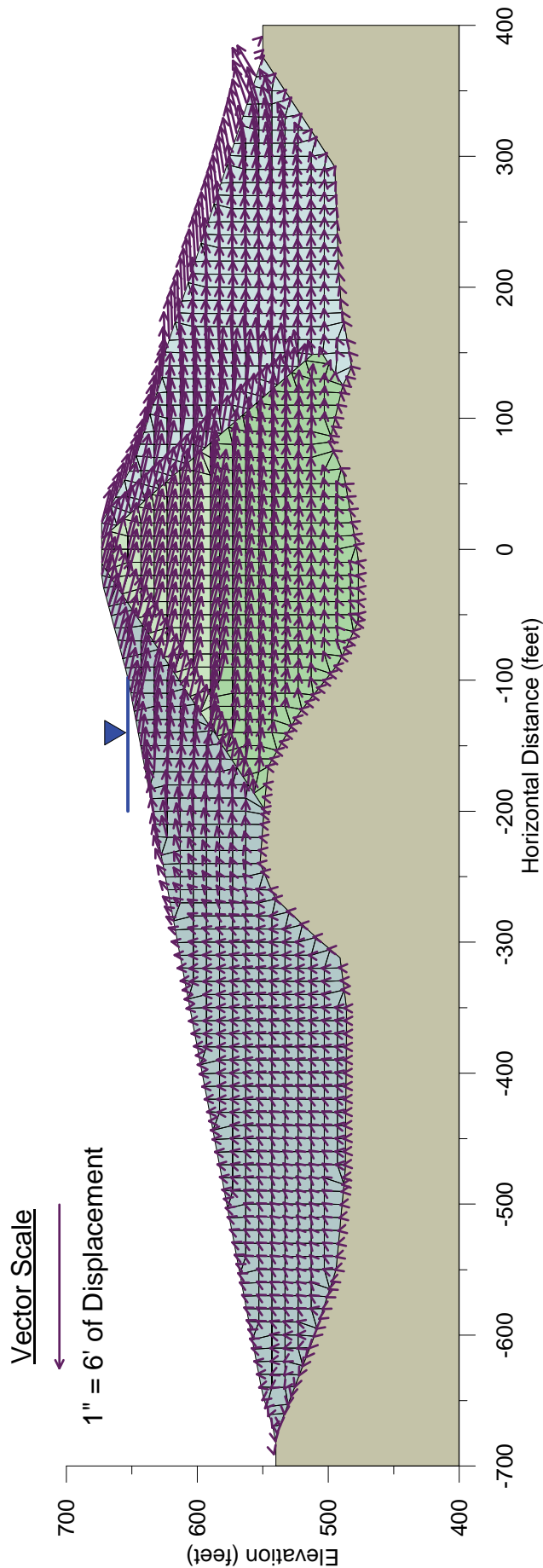
Displacement Scale (ft)



Vector Scale

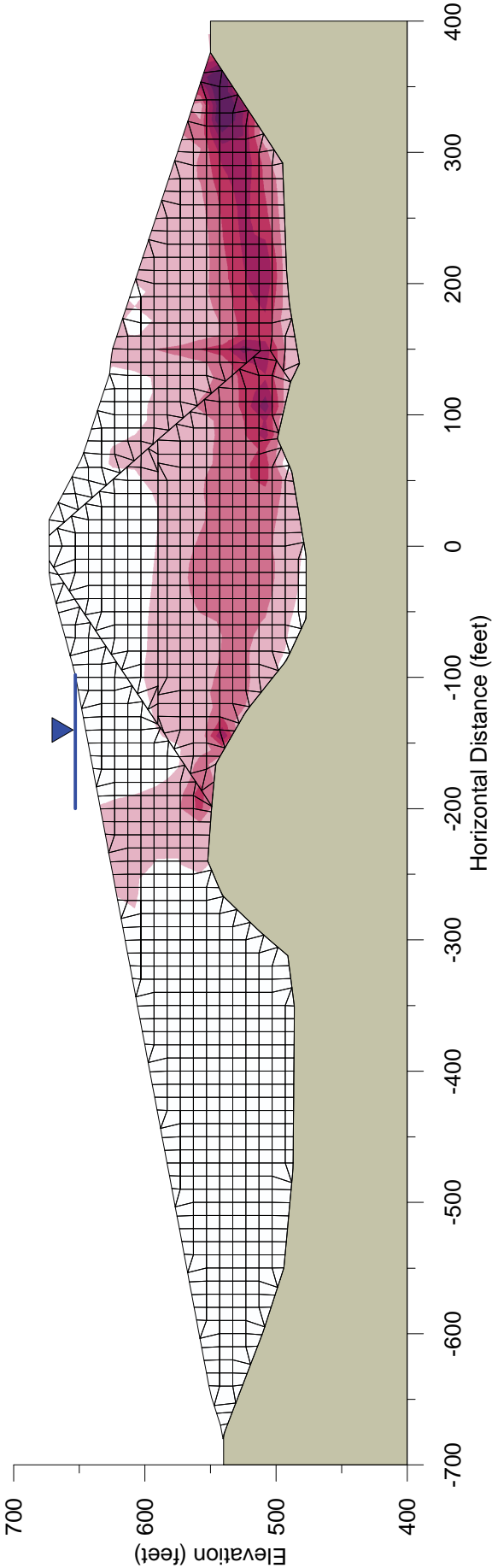
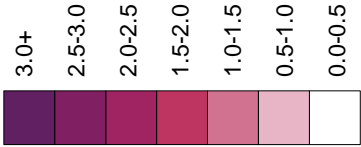


Note: Permanent seismic displacement at the end of shaking, values in feet.



Note: Permanent seismic displacement at the end of shaking.

Shear Strain Scale (%)



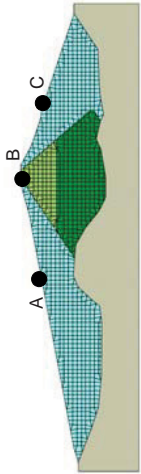
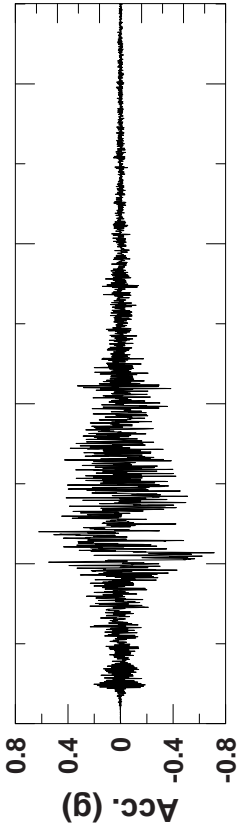
Note: Shear strain at the end of shaking.



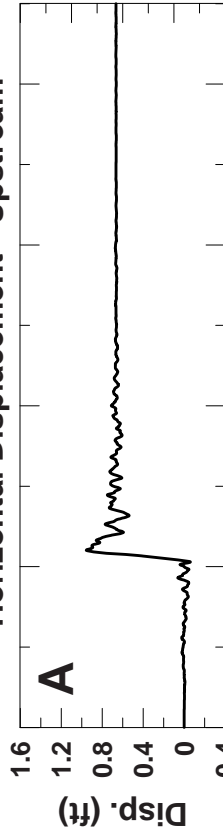
CASE SA2 - LANDERS, SHEAR STRAIN
CONTOURS - LENIHAN DAM
SEISMIC STABILITY EVALUATIONS (SSE2)

Figure
B-2D

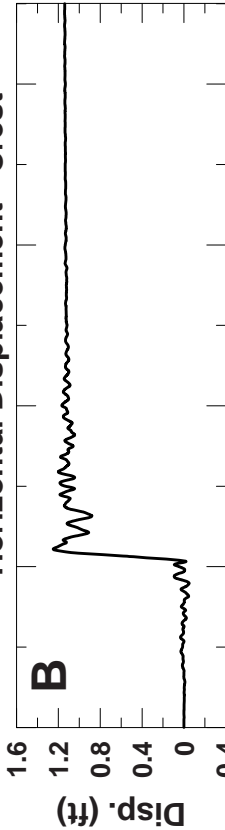
Landers Evaluation Motion



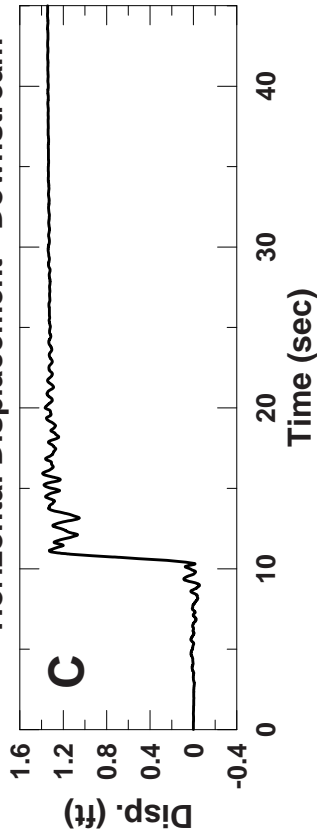
Horizontal Displacement - Upstream



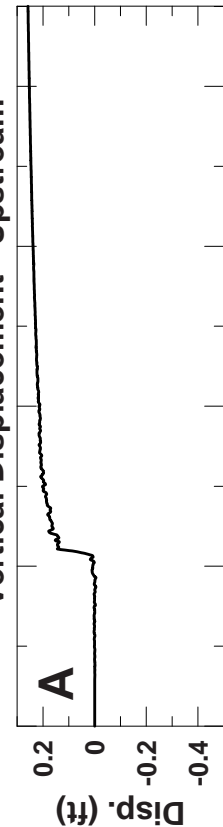
Horizontal Displacement - Crest



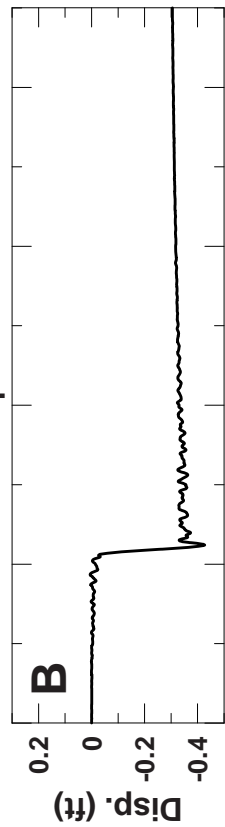
Horizontal Displacement - Downstream



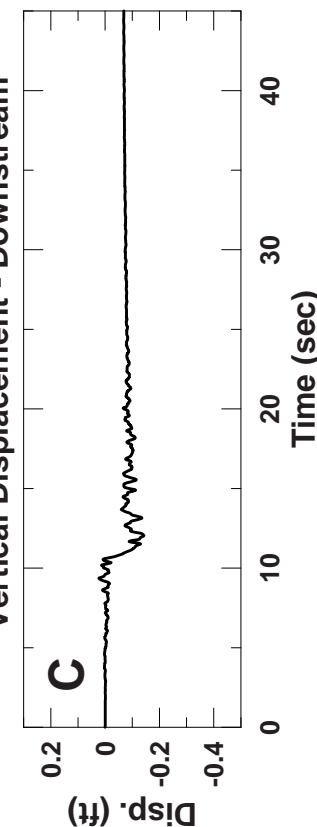
Vertical Displacement - Upstream

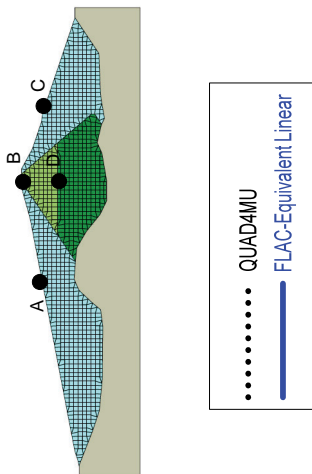
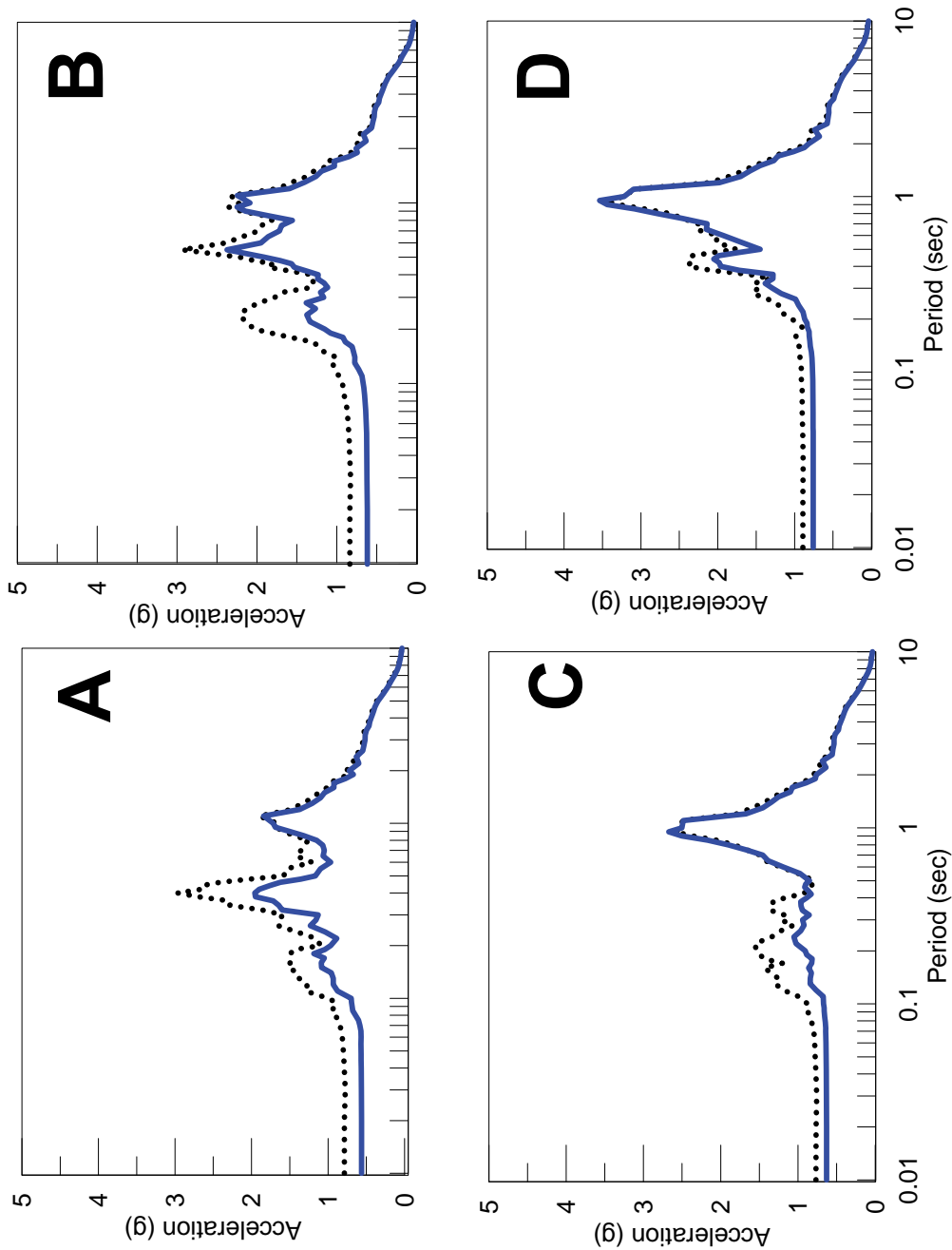


Vertical Displacement - Crest



Vertical Displacement - Downstream





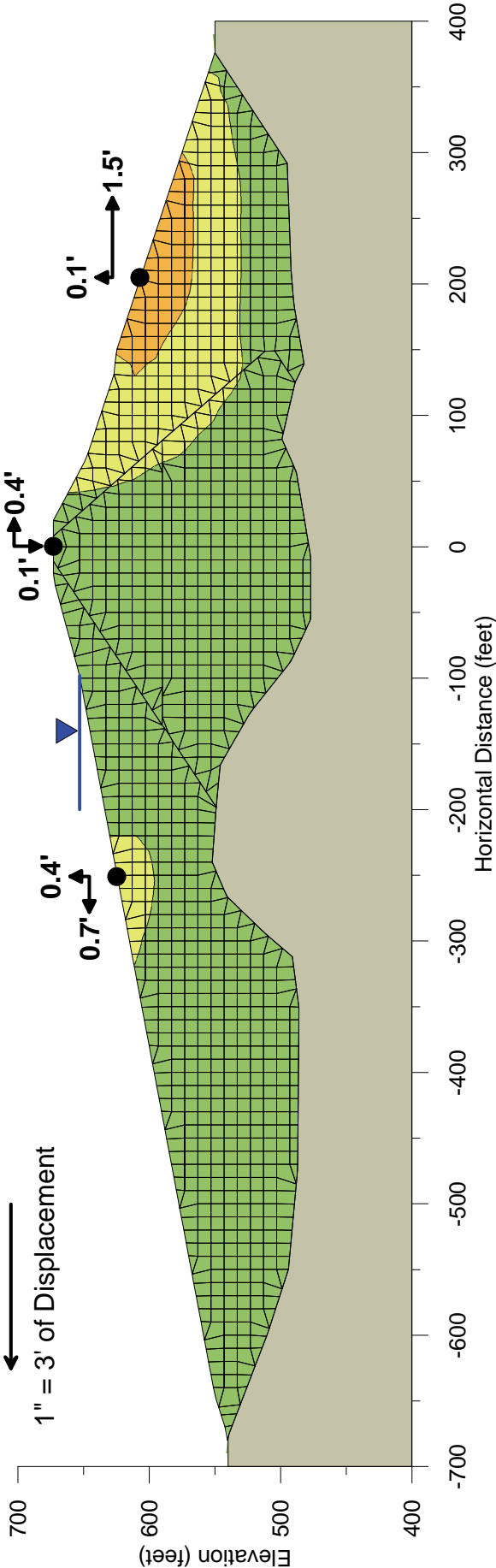
Displacement Scale (ft)



Vector Scale



1" = 3' of Displacement

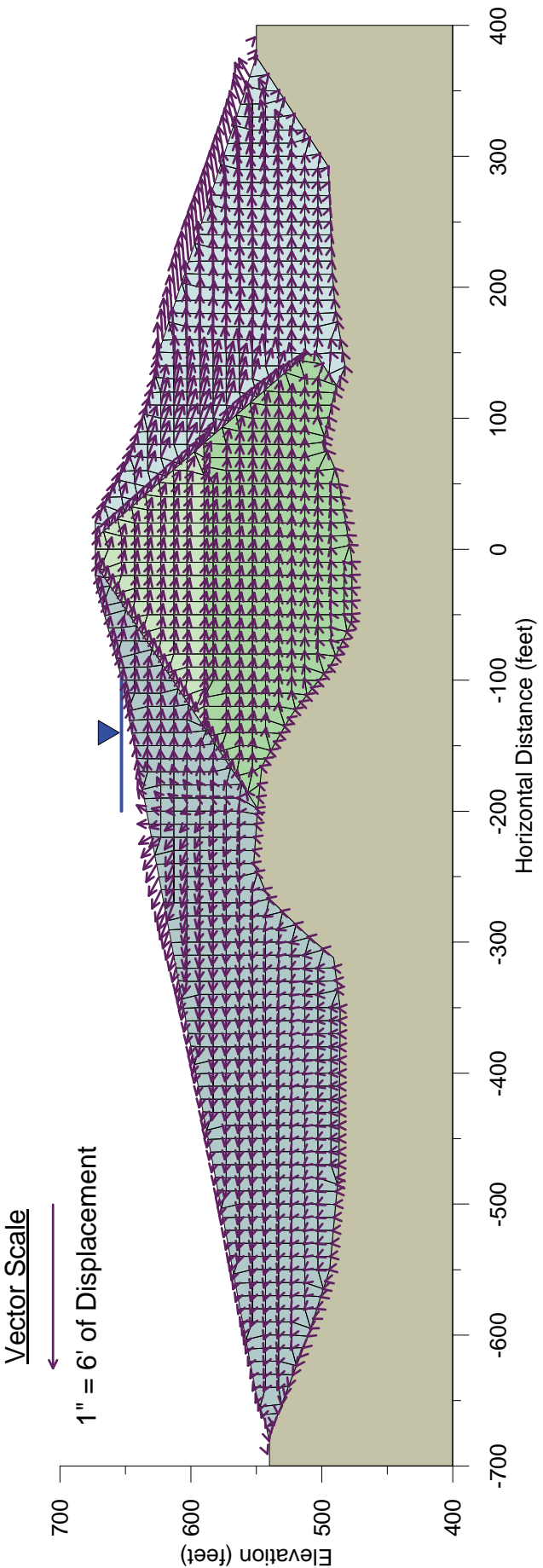


Note: Permanent seismic displacement at the end of shaking, values in feet.



CASE SA3 - MANJIL, DISPLACEMENT
CONTOURS - LENIHAN DAM
SEISMIC STABILITY EVALUATIONS (SSE2)

Figure
B-3B



Note: Permanent seismic displacement at the end of shaking.

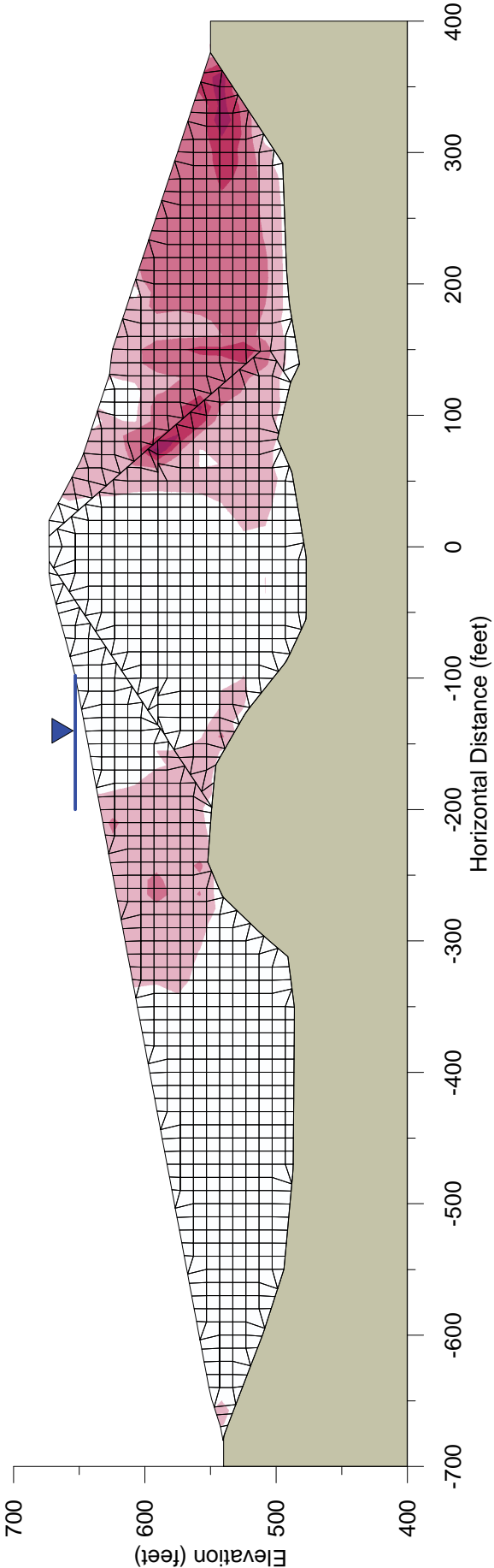
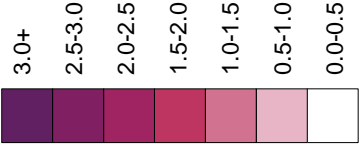


TERRA / GeoPentech
a Joint Venture

CASE SA3 - MANJIL, DISPLACEMENT
VECTORS - LENIHAN DAM
SEISMIC STABILITY EVALUATIONS (SSE2)

Figure
B-3C

Shear Strain Scale (%)



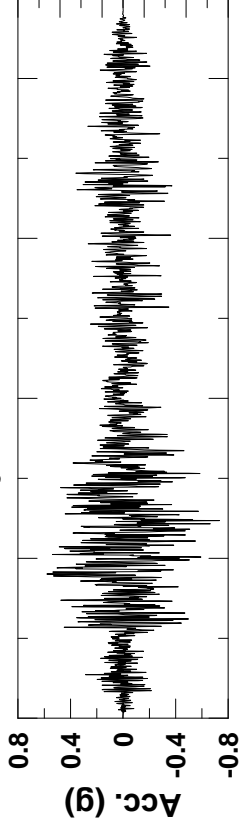
Note: Shear strain at the end of shaking.



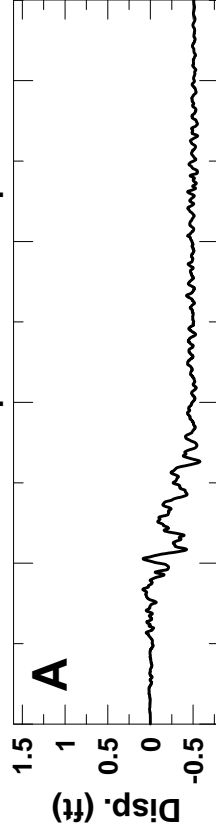
CASE SA3 - MANJIL, SHEAR STRAIN
CONTOURS - LENIHAN DAM
SEISMIC STABILITY EVALUATIONS (SSE2)

Figure
B-3D

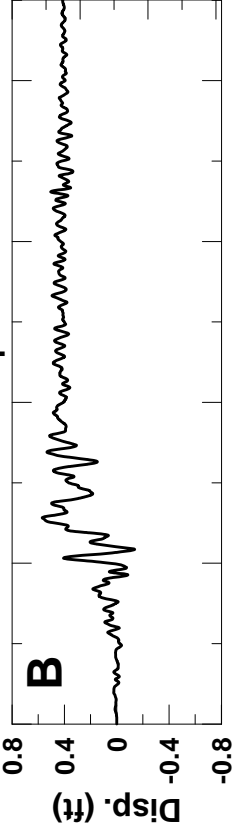
Manjil Evaluation Motion



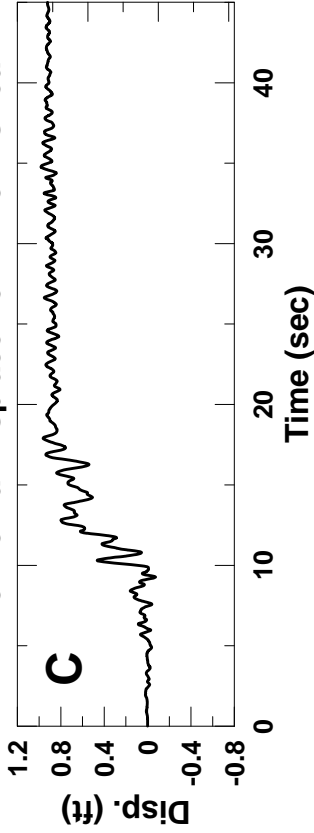
Horizontal Displacement - Upstream



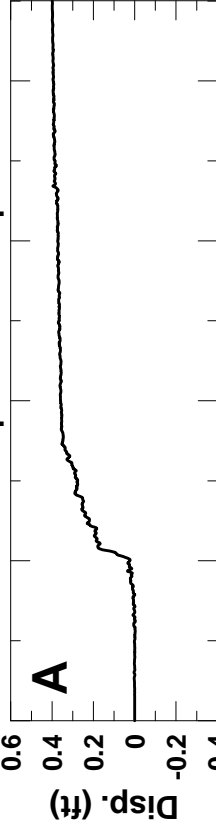
Horizontal Displacement - Crest



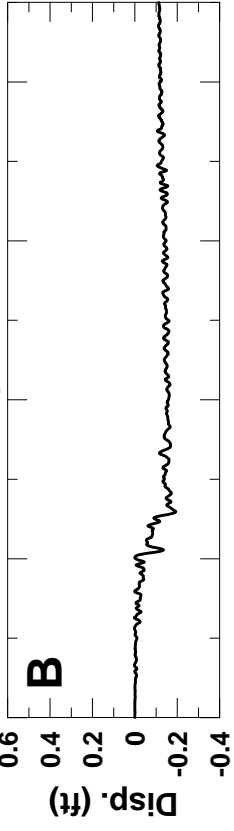
Horizontal Displacement - Downstream



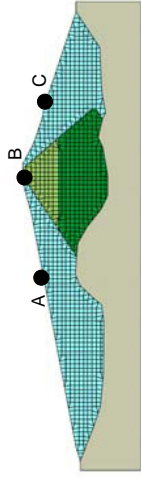
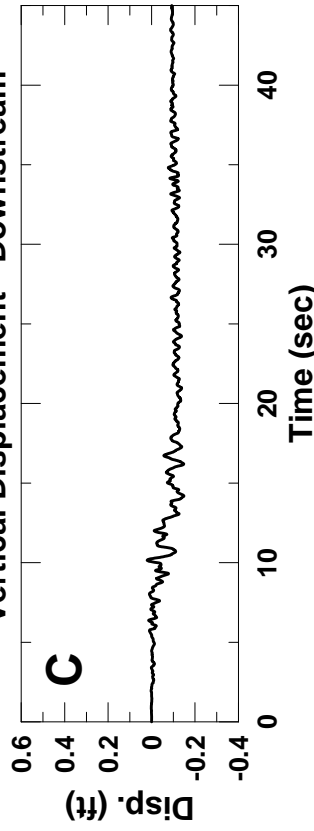
Vertical Displacement - Upstream

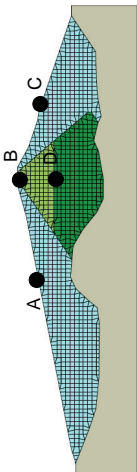
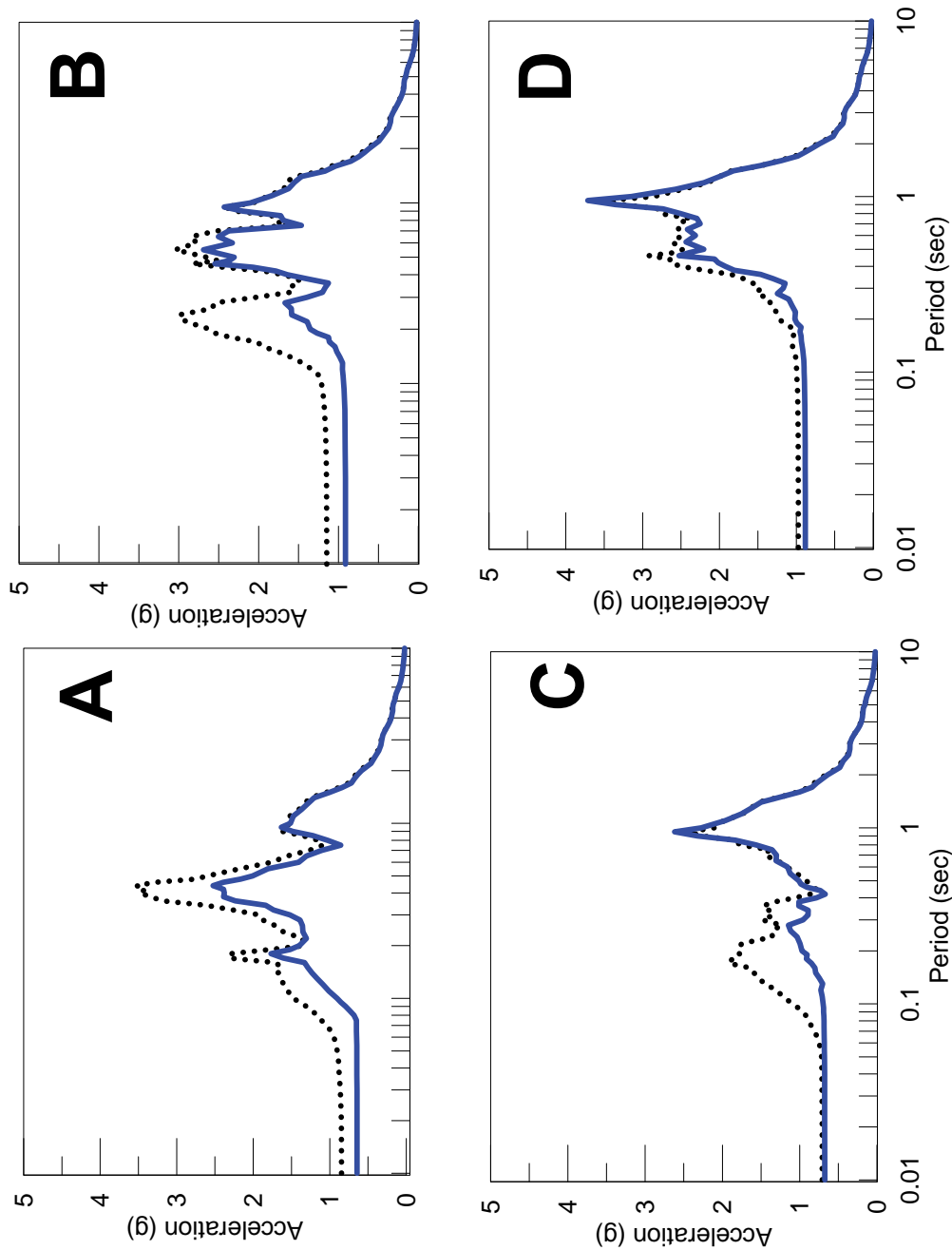


Vertical Displacement - Crest

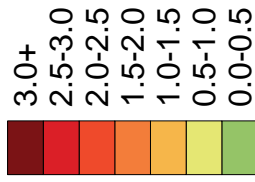


Vertical Displacement - Downstream





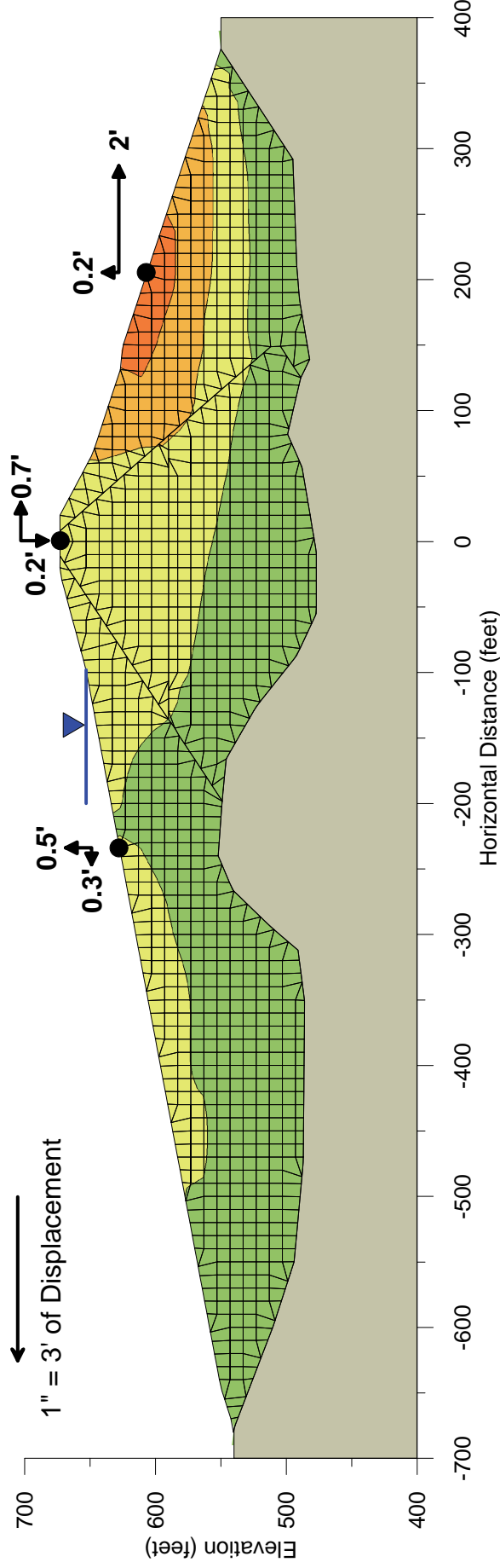
Displacement Scale (ft)



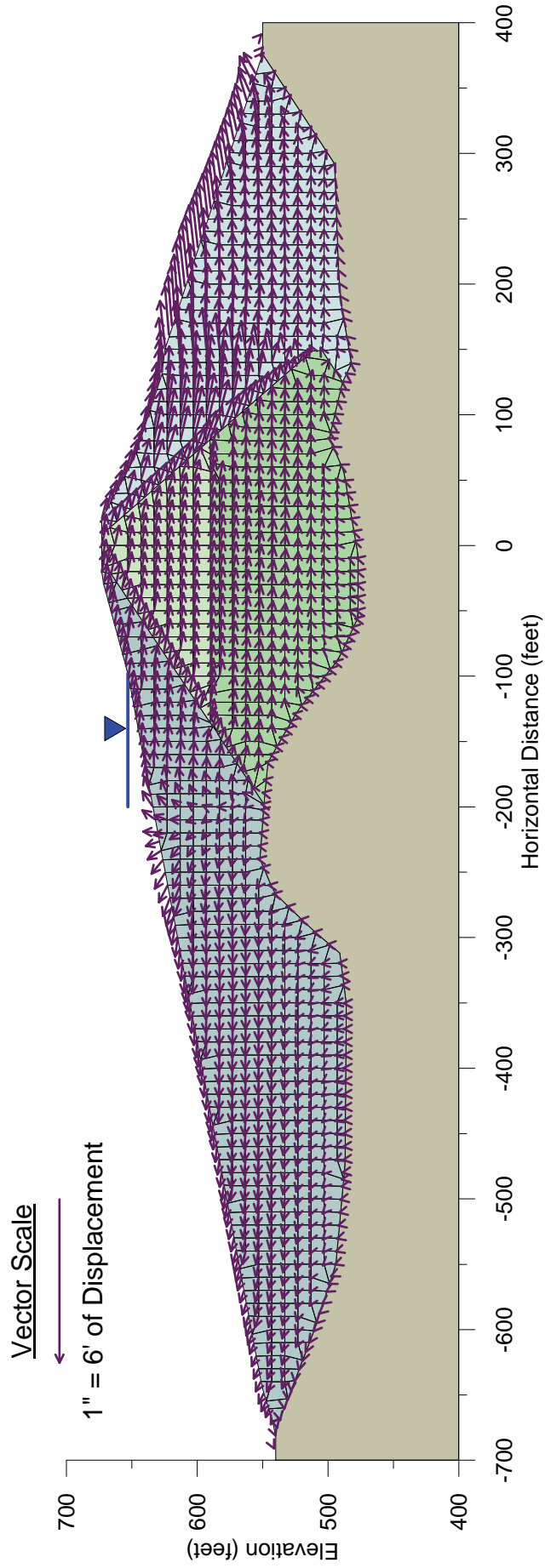
Vector Scale



1" = 3' of Displacement



Note: Permanent seismic displacement at the end of shaking, values in feet.



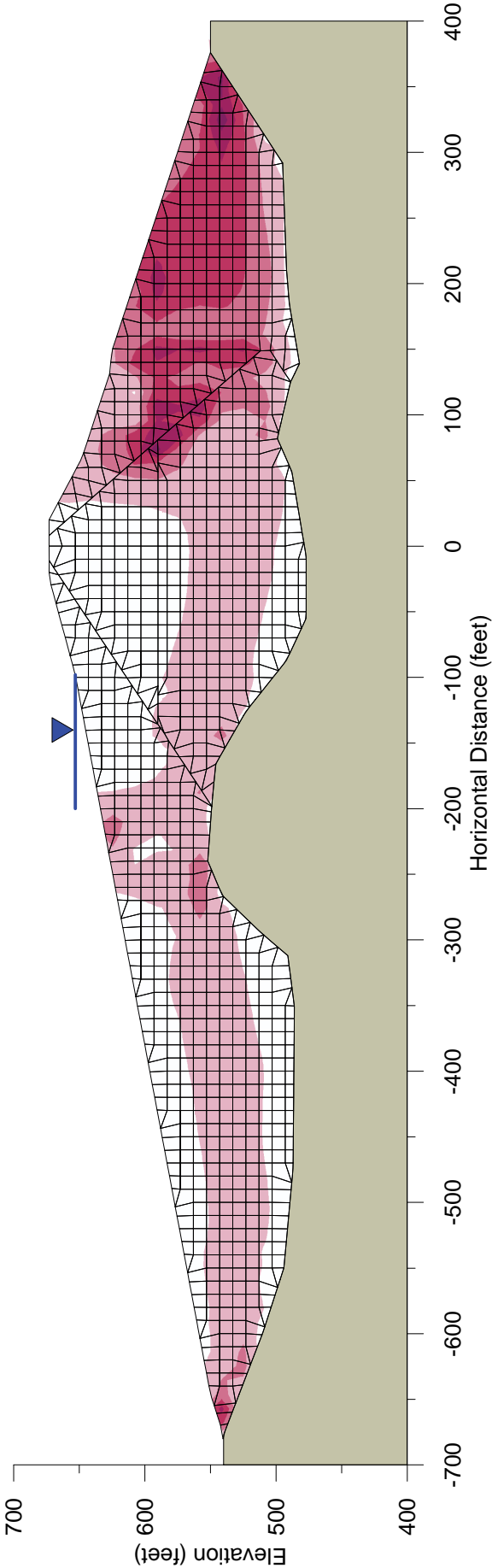
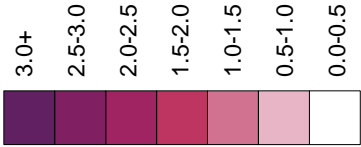
Note: Permanent seismic displacement at the end of shaking.



CASE SMV1 - KOBE, DISPLACEMENT
VECTORS - LENIHAN DAM
SEISMIC STABILITY EVALUATIONS (SSE2)

Figure
B-4C

Shear Strain Scale (%)



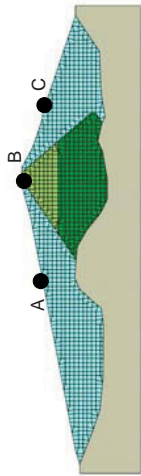
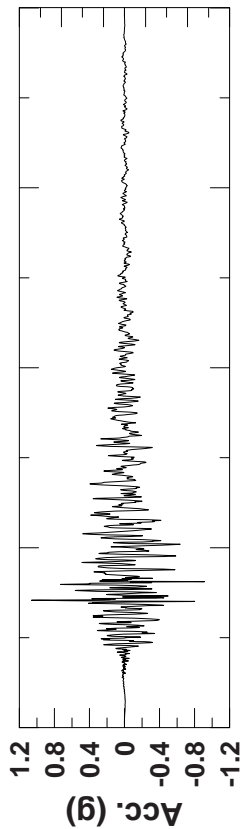
Note: Shear strain at the end of shaking.



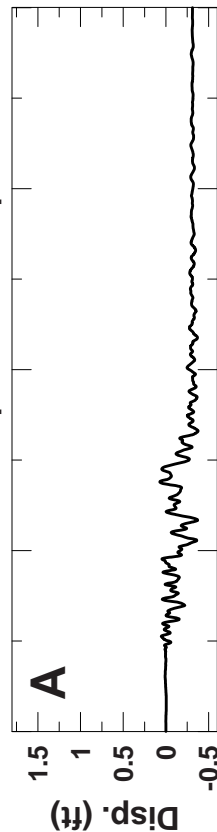
CASE SMV1 - KOBE, SHEAR STRAIN
CONTOURS - LENIHAN DAM
SEISMIC STABILITY EVALUATIONS (SSE2)

Figure
B-4D

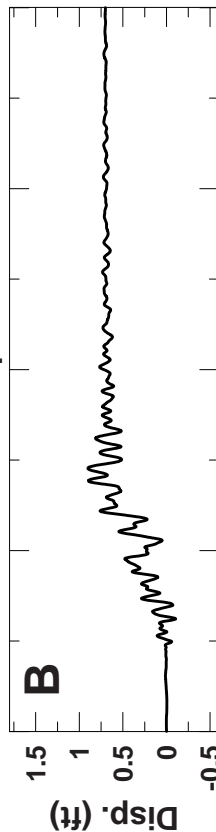
Kobe Evaluation Motion



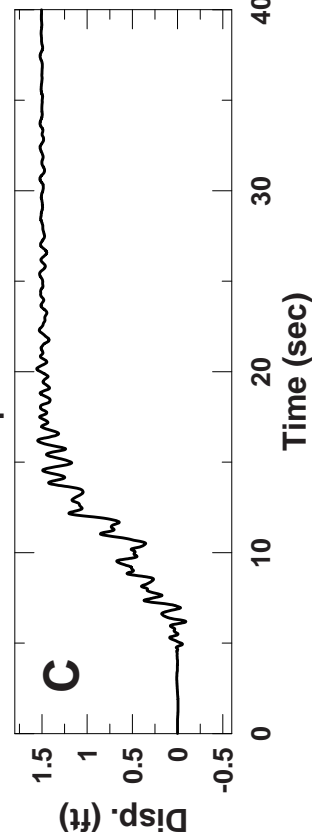
Horizontal Displacement - Upstream



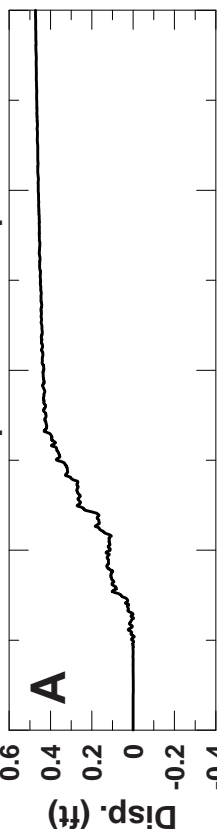
Horizontal Displacement - Crest



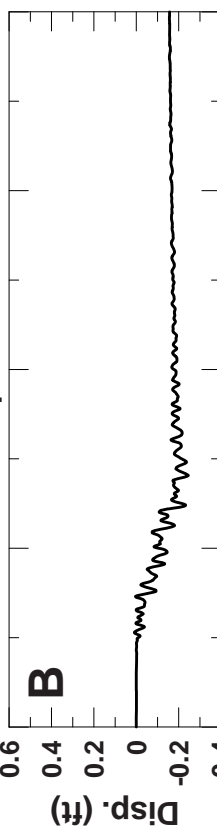
Horizontal Displacement - Downstream



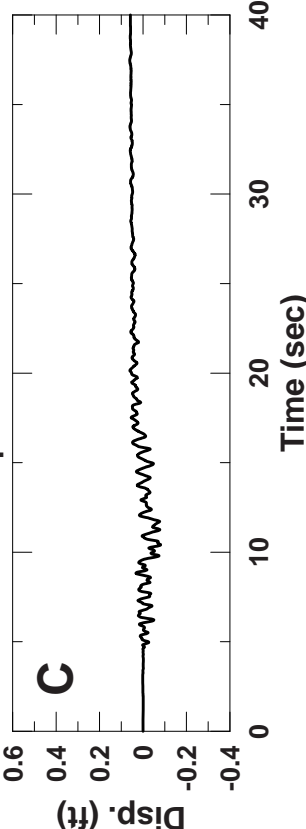
Vertical Displacement - Upstream

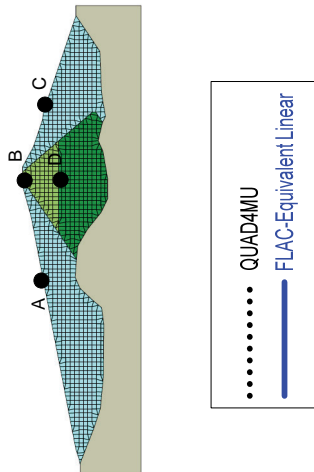
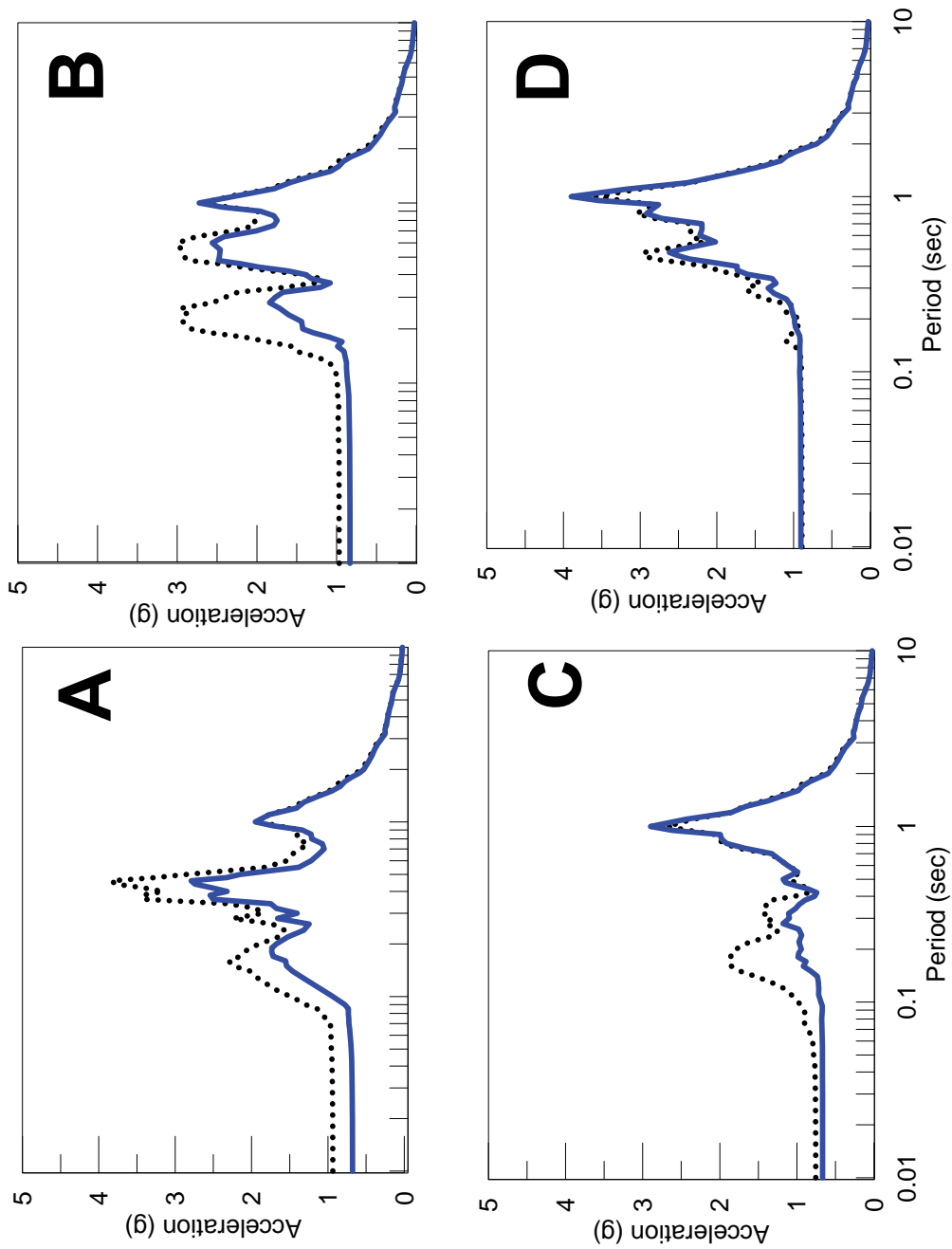


Vertical Displacement - Crest



Vertical Displacement - Downstream





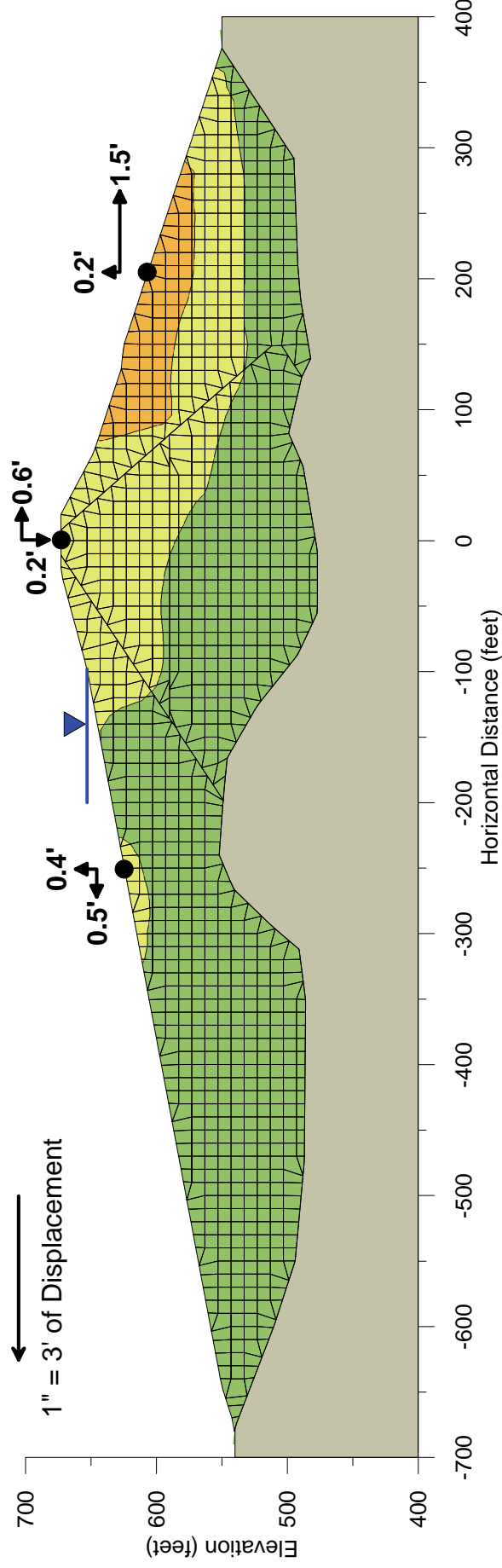
Displacement Scale (ft)



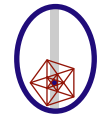
Vector Scale



1" = 3' of Displacement



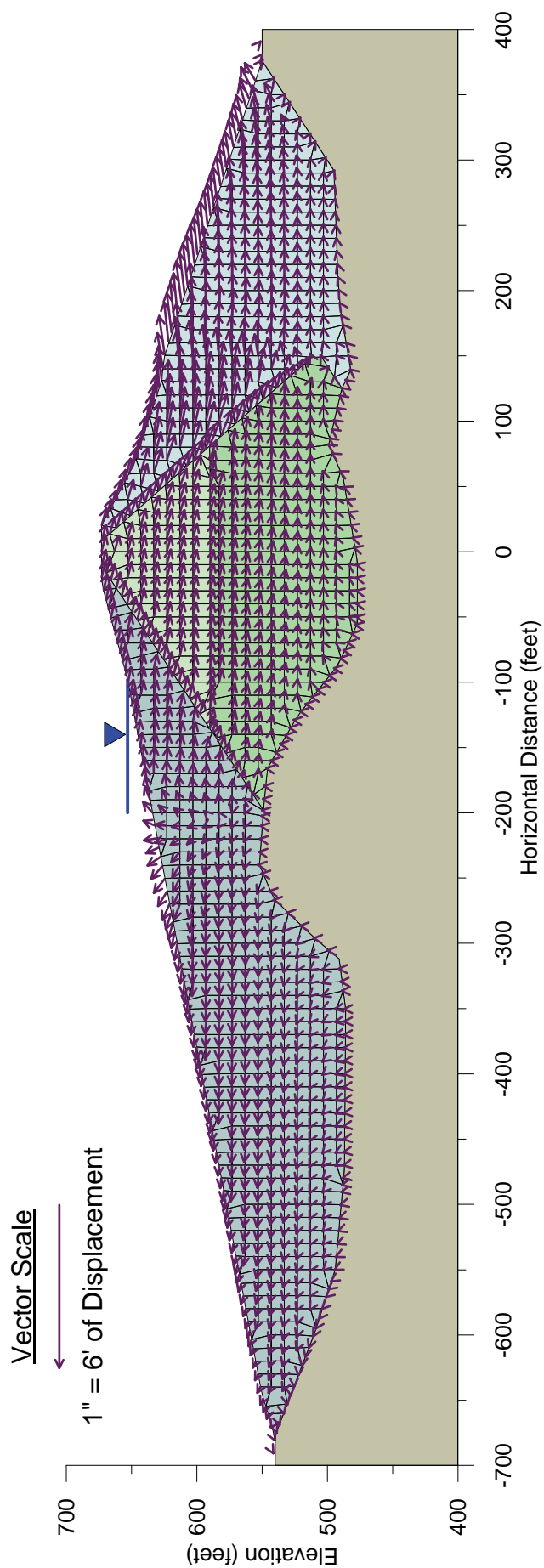
Note: Permanent seismic displacement at the end of shaking, values in feet.



TERRA / GeoPentech
a Joint Venture

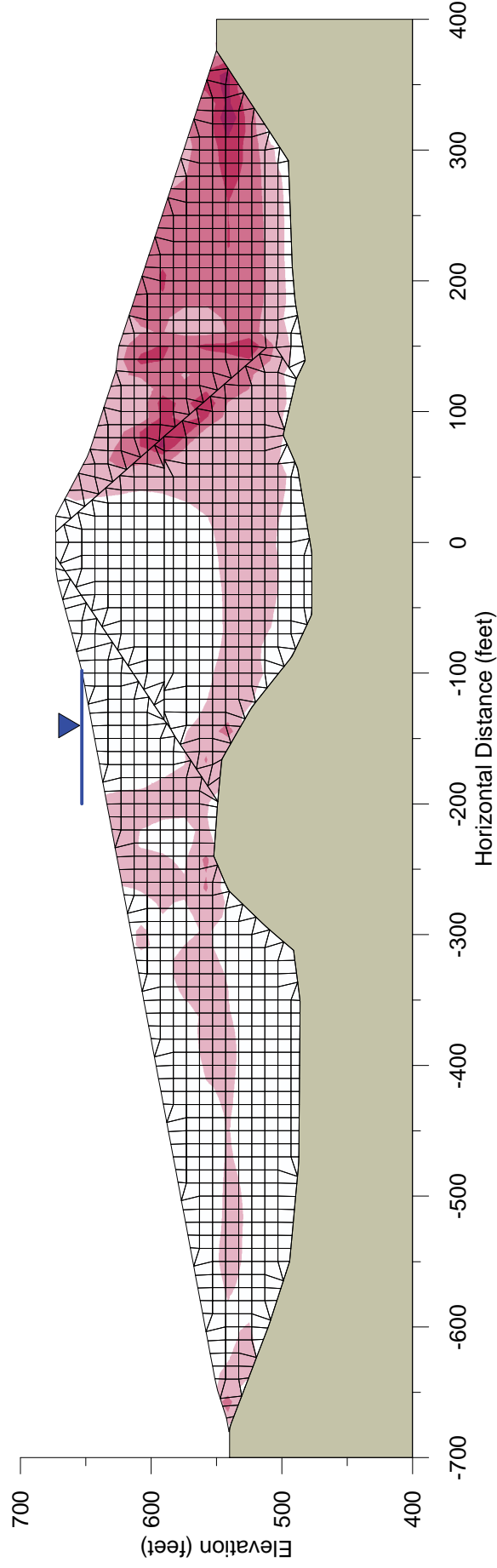
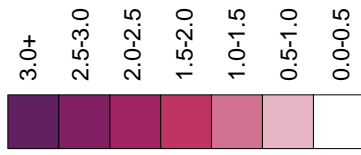
CASE SMV2 - LOMA PRIETA, DISPLACEMENT
CONTOURS - LENIHAN DAM
SEISMIC STABILITY EVALUATIONS (SSE2)

Figure
B-5B



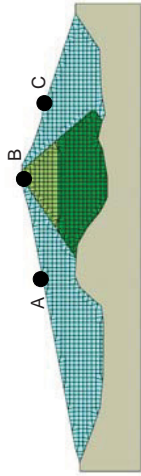
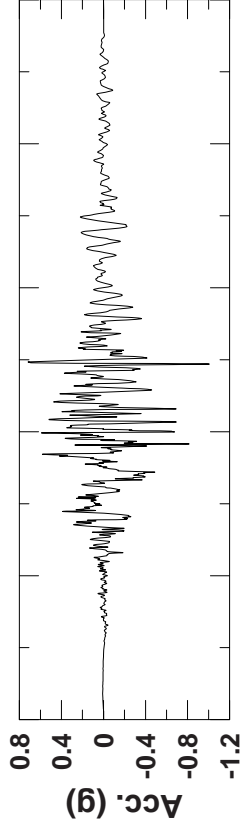
Note: Permanent seismic displacement at the end of shaking.

Shear Strain Scale (%)

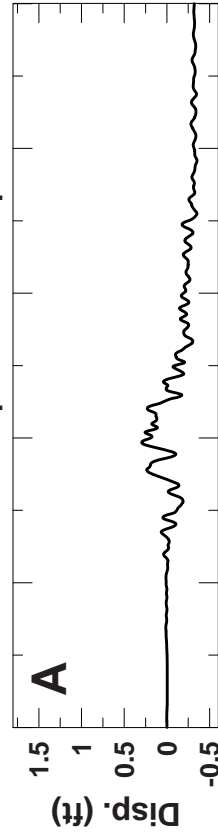


Note: Shear strain at the end of shaking.

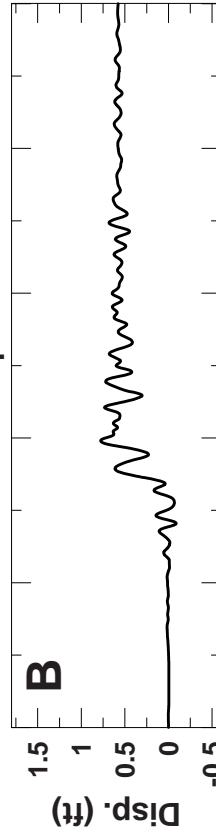
Loma Prieta Evaluation Motion



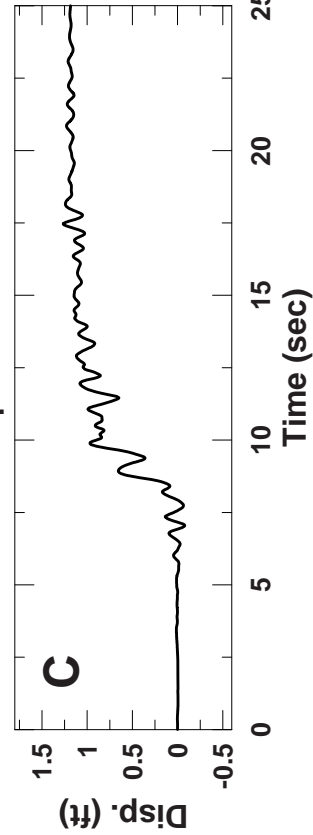
Horizontal Displacement - Upstream



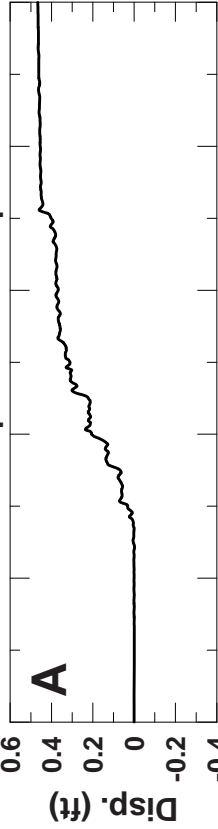
Horizontal Displacement - Crest



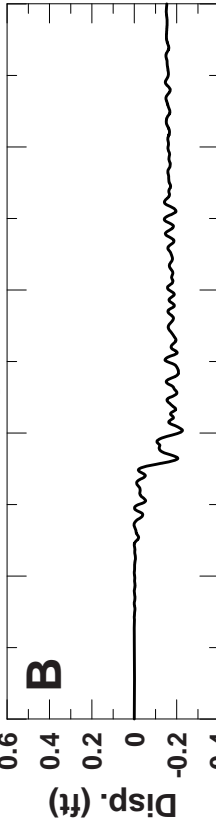
Horizontal Displacement - Downstream



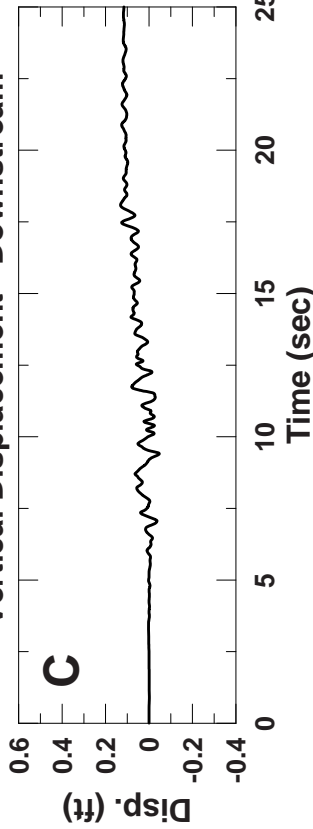
Vertical Displacement - Upstream

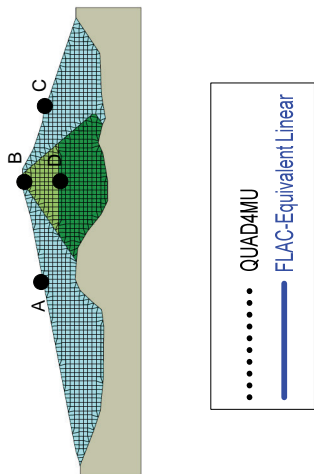
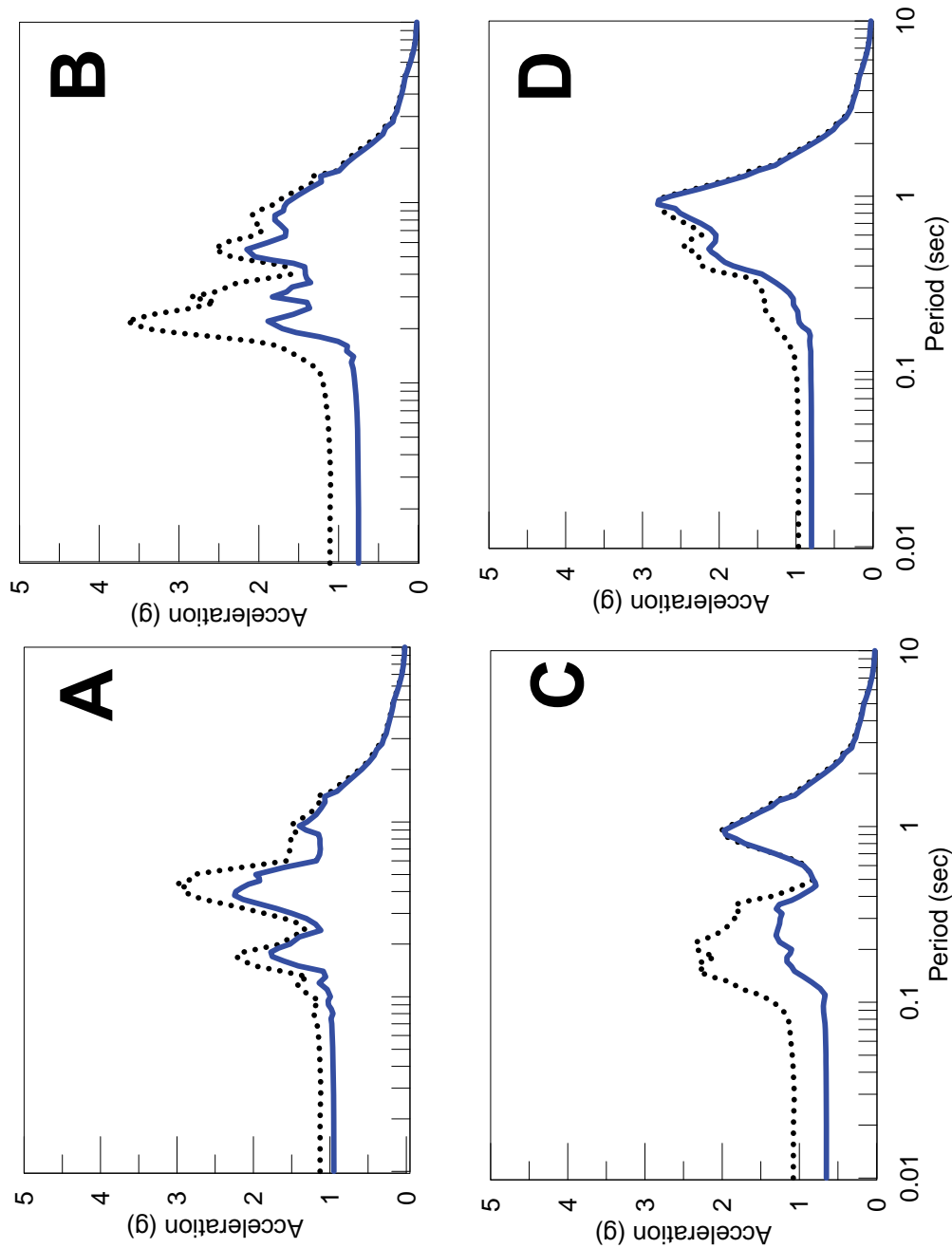


Vertical Displacement - Crest

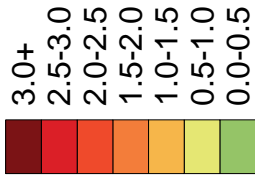


Vertical Displacement - Downstream





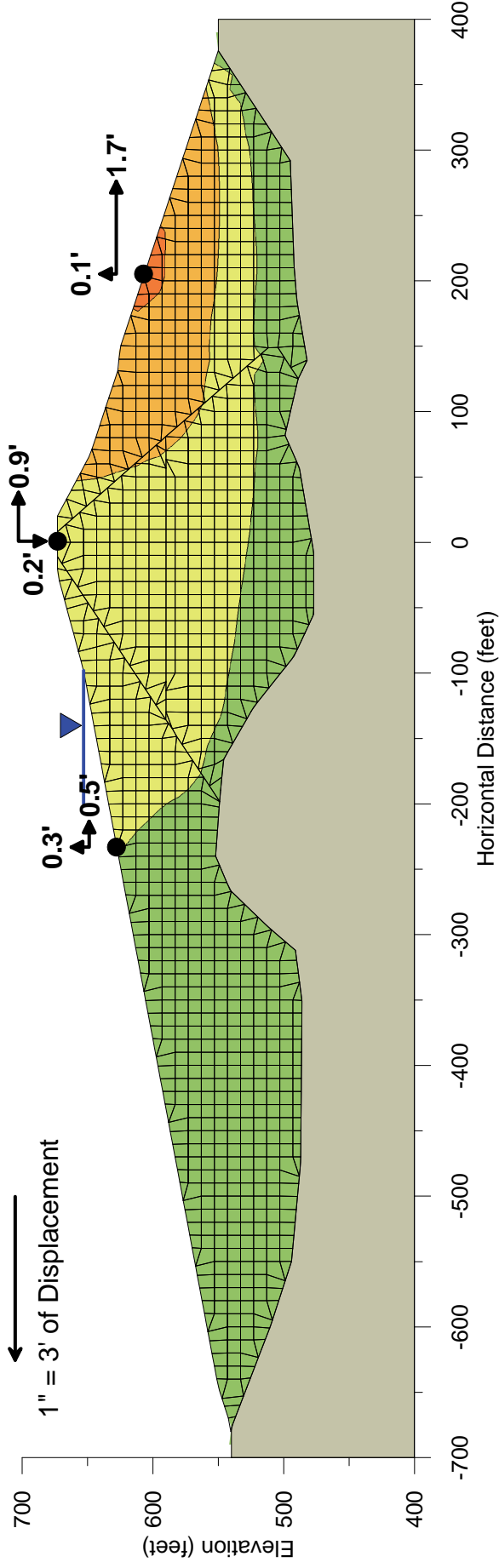
Displacement Scale (ft)



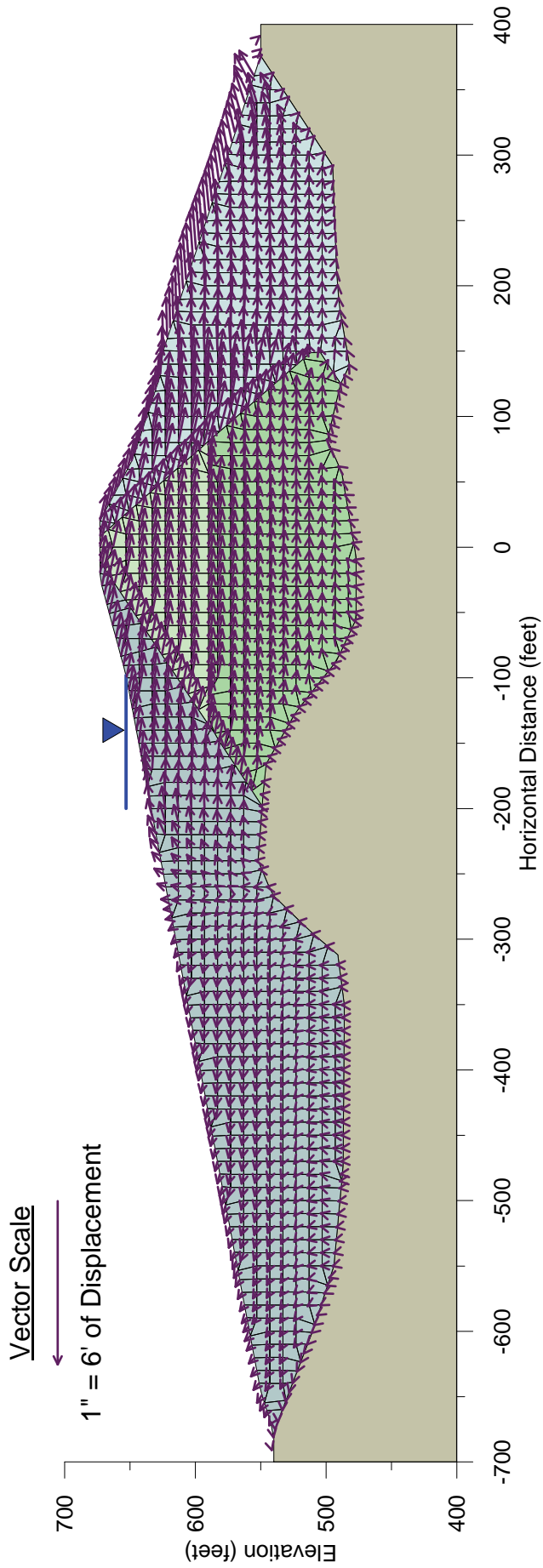
Vector Scale



1" = 3' of Displacement



Note: Permanent seismic displacement at the end of shaking, values in feet.



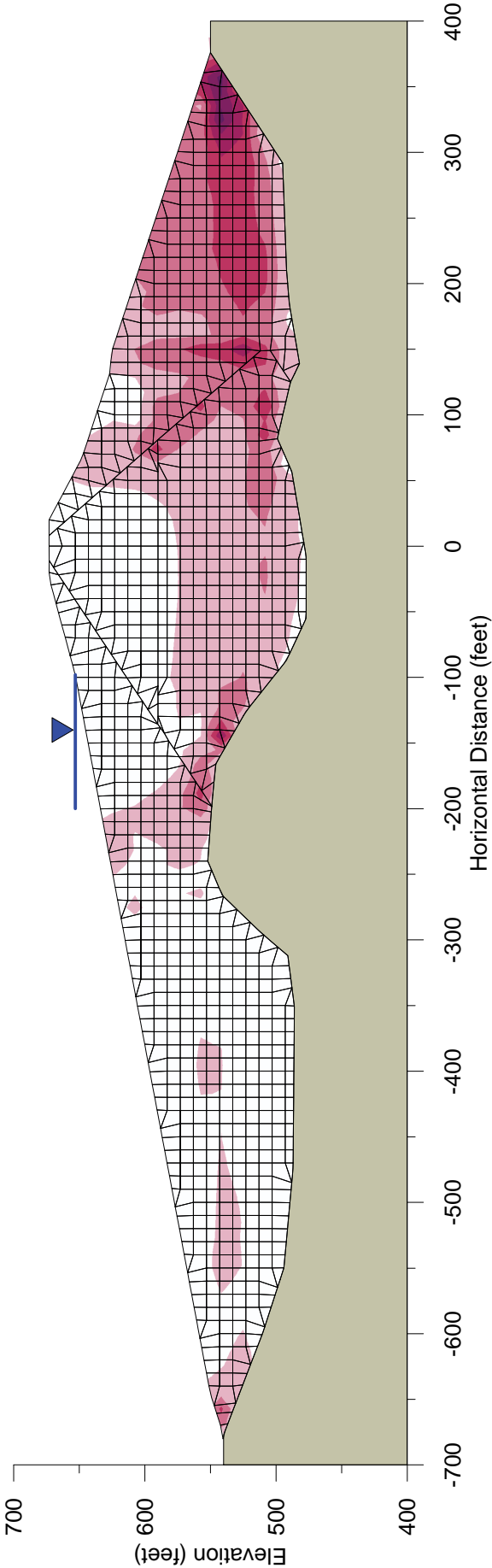
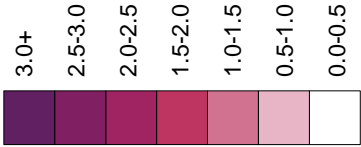
Note: Permanent seismic displacement at the end of shaking.



CASE SMV3 - NORTHRIDGE, DISPLACEMENT
VECTORS - LENIHAN DAM
SEISMIC STABILITY EVALUATIONS (SSE2)

Figure
B-6C

Shear Strain Scale (%)

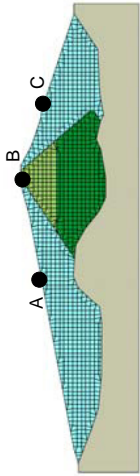


Note: Shear strain at the end of shaking.

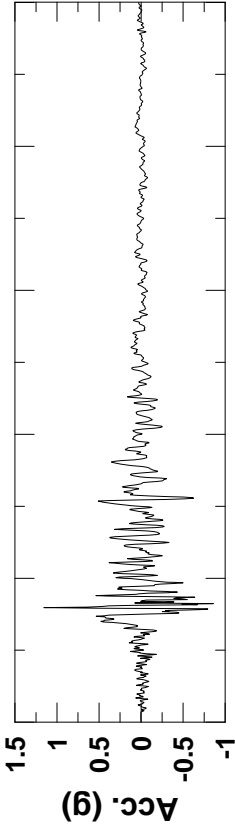


CASE SMV2 - NORTHRIDGE, SHEAR STRAIN
CONTOURS - LENIHAN DAM
SEISMIC STABILITY EVALUATIONS (SSE2)

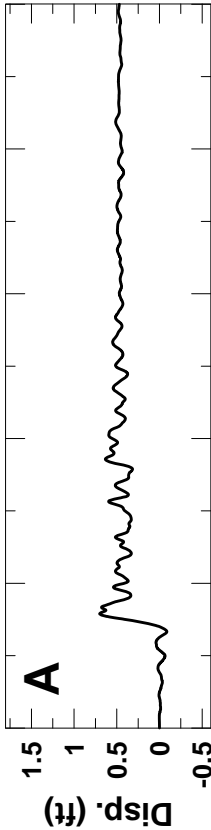
Figure
B-6D



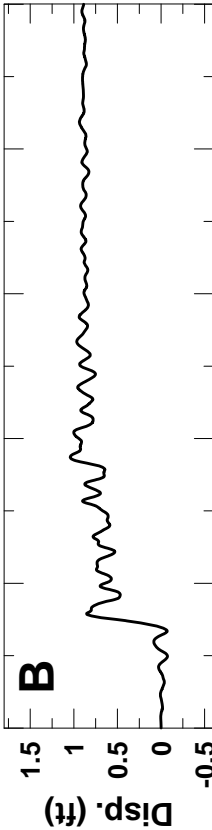
Northridge Evaluation Motion



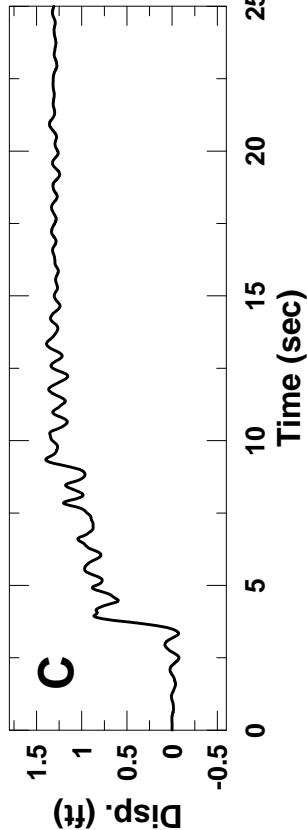
Horizontal Displacement - Upstream



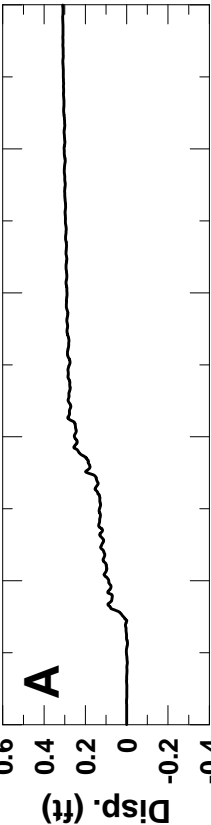
Horizontal Displacement - Crest



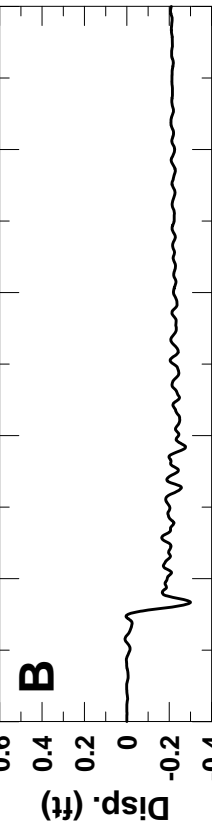
Horizontal Displacement - Downstream



Vertical Displacement - Upstream



Vertical Displacement - Crest



Vertical Displacement - Downstream

